Trafic de la protéine prion dans les cellules MDCK polarisées

Alexander Arkhiipenko Arkhipenko

Université Paris-Saclay & Institut Pasteur

ÉCOLE DOCTORALE: Structure et dynamique des systèmes vivants

ED n°577 DISCIPLINE: Biologie Cellulaire

NNT : 2015SACLS228

Trafic de la protéine prion PrP dans les cellules polarisées MDCK

Présentée par Arkhipenko Alexander

Pour obtenir le grade de

Docteur de l'Université Paris-Saclay

Soutenance le 9 décembre 2015 à l'Institut Pasteur devant le jury composé de:

Dr. Capy Pierre, professeur, Université Paris-Sud	Président
Dr. Echard Arnaud, DR, Institut Pasteur-CNRS	Rapporteur
Dr. Béringue Vincent, DR2, INRA	Rapporteur
Dr. Le Bivic André, DR, IBDM	Examinateur
Dr. Zurzolo Chiara, DR, Institut Pasteur	Directrice de these
Dr. Lebreton Stéphanie, CR, Institut Pasteur	Directrice de these

PrP traffic in polarized MDCK cells

Cette thèse est dédiée à Paul Tempelaere

Remerciements

Je voudrais remercier le jury de ma thèse, Messieurs Béringue, Echard, Le Bivic et Capy pour la discussion animée, ouverte et passionnante. Les heures de discussion avec vous étaient un véritable plaisir et un des meilleurs moments de ma thèse.

Je tiens à remercier en particulier ma directrice, Stéphanie LEBRETON, qui est une merveilleuse personne, qui m'a encouragé et qui m'a aidé à m'orienter pendant cette courte thèse. Je la remercie pour son professionnalisme, sa politesse, son sourire, son écoute ainsi que pour son attention toujours respectueuse. Stéphanie est une excellente chercheuse, qui connait son sujet, toutes les difficultés techniques et qui est ouverte pour explorer des nouveaux horizons, elle a sauvé ma thèse et ma reconnaissance pour elle est sans limite. Dès la première semaine de mon travail sous la direction de Stéphanie j'ai commencé à produire des résultats intéressants et solides. Grâce à Stéphanie, dans un délai d'un an, j'ai écrit un article qui est « accepté avec modification » dans le journal PLOS ONE et en un an et demi j'ai défendu ma thèse.

Une grande partie du succès de cette thèse est dû à mes tutrices : Marie-Isabelle Thoulouse (tutrice pour l'école doctorale) Suzana Celli et Monica Sala de l'équipe tutorat de l'Institut Pasteur. Je tiens surtout à remercier Monica qui m'a encouragé et qui m'a donné des forces pour aller jusqu'au bout de ma thèse. C'était un véritable plaisir d'échanger avec Monica, son approche positive et enthousiaste m'a stimulé pour avancer.

Je tiens à remercier Kerstin Klinkert pour son aide avec les cultures tridimensionnelles, grâce à Kerstin j'ai pu mettre au point une culture des kystes MDCK pour étudier le tri des protéines à l'ancre GPI dans 3 dimensions.

En liaison avec mon article je tiens à remercier Sylvie Syan qui a fait les dernières manipes pour publier notre travail. Qui travail de bonne humeur ? Qui est remplie d'énergie ? C'est Sylvie, un véritable miracle de laboratoire. Où puise-t-elle cette énergie ? Je ne le sais pas mais je remercie Sylvie d'avoir partagé avec moi sa joie et son enthousiasme.

Soraya Victoria, I was happy to work with you, I enjoyed your company around a cup of tea as much as in P3 around prion infected brain homogenate. Your experience with your own PhD and your support were very valuable for me. I have learnt from you how to be patient and how to behave decently in the most unpleasant circumstances. A special thank you for your outstanding English and for all the proof-readings you did for me, I hope that my writing skills did improve thanks to you.

Chères Elise et Saïda, ou plutôt Docteurs Delage et Abounit, j'ai adoré de travailler avec vous ! Vous avez ramené au laboratoire de la bonne humeur et de l'humour au quotidien. Quand vous rigoliez ensemble les vitres tremblaient, c'était génial. Dr. Delage, je vais garder un très bon souvenir d'une explication détaillée (dessinée au tableau) d'un phénomène physique

émergeant de l'accumulation de lipides. Saïda, ma véritable sœur de thèse, nous nous connaissons depuis 5 ans et je suis ravi que nous soyons restés amis au cours de ces 3 ans ensemble côte-à-côte, malgré toutes les tentations de nous nous opposer, tu m'as beaucoup aidé à arriver au grade de docteur.

Je veux remercier les secrétaires de mon unité et du département pour leur compréhension, leur aide avec les dossiers administratifs et tous les papiers qu'un étranger doit renouveler régulièrement. Merci, Olga, Isabelle, Jamila et Régine, c'était un plaisir de travailler avec vous !

Je tiens à remercier mes collègues et mes anciens collègues pour la bonne ambiance de travail et leur aide au quotidien : Seng chouchou, Gianni, Philippe, Zeina, Odile, Yuan Lou, Jessica, Frida, Nathalie, Suzanna, Rharaf, Mathieu et Gabriela.

Une partie très importante de mon parcours à l'Institut Pasteur fut l'enseignement dispensé au nouveau cours « iGEM-Pasteur ». Ce fut une expérience inoubliable et un défi que de mettre en place un nouveau cours au sein du centre d'enseignement, ainsi que d'aider les étudiants à construire leur propre projet et les préparer à le défendre à Boston. Je remercie l'équipe des étudiants « iGEM-Pasteur 2015 » et les encadrants du projet, en particulier Deshmukh, Claudia et Caroline avec qui j'ai beaucoup interagi lors du projet.

On n'est rien sans amis ; je dois beaucoup aux gens qui tout au long de ma thèse sont restés avec moi, qui me réconfortaient quand les manipes ne marchaient pas et quand la plupart de mes idées ont été publiées quand je n'étais qu'en première année de thèse. Mes chers amis avec qui j'ai partagé le peu de temps libre que j'avais. Merci Aména, Marc, Chiara, Dragos et Elena, Ann, Raphael, Nicolas, Ibailla, Tobi, Luciano, Asia, Basha, Eszter et Gabor et, bien sûr, Johannes et Ygrène. Je tiens à remercier en particulier Aména qui m'a convaincu de célébrer ma thèse et qui a joué le rôle moteur dans l'organisation du pot de thèse.

За дружескую поддержку благодарю Марию и Катю, Юлю, Лёшу, Нину, Женю, Арсения, Вову и Диму и, конечно, Аню. Благодарю Максима и Игумена Евмения за поддержку в самые трудные моменты! Otdel,noe spasibo Sasha I Ilie za podderzhky v rabote I cennie soveti!

Pour conclure la partie « remerciements » je remercie celui à qui ma thèse est dédiée, celui qui a donné le sens à mon travail, celui qui est tout pour moi, Paul. Je t'aime.

Janvier 2016

Table of content

Summary

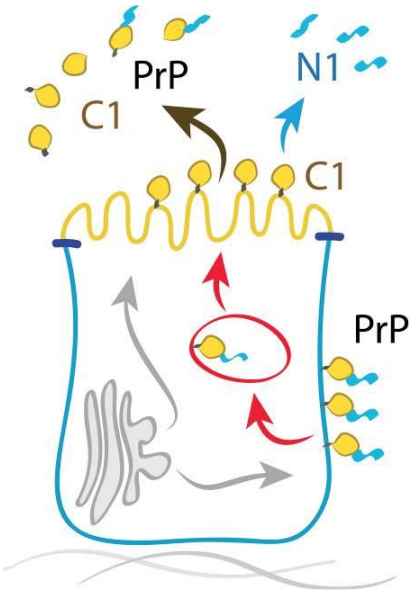

The Prion Protein (PrP) is an ubiquitously expressed glycosylated membrane protein attached to the external leaflet of the plasma membrane via a glycosylphosphatidylinositol anchor (GPI). While the misfolded PrP^{Sc} scrapie isoform is the infectious agent of "prion diseases" the cellular isoform (PrP^{C}) is an enigmatic protein with unclear function. Prion protein has received considerable attention due to its central role in the development of Transmissible Spongiform Encephalopathies (TSEs) known as "prion diseases", in animals and humans. Understanding the trafficking, the processing and the degradation of PrP is of fundamental importance in order to unravel the mechanism of PrP^{Sc} mediated pathogenesis, its spreading and cytotoxicity. The available data regarding PrP trafficking are contradictory. To investigate PrP trafficking and sorting we used polarized MDCK cells (two-dimensional and tree-dimensional cultures) where the intracellular traffic of GPI-anchored proteins (GPI-APs) is well characterized. GPI-APs that are sorted in the Trans Golgi Network follow a direct route from the Golgi apparatus to the apical plasma membrane. The exception to direct apical sorting of native GPI-APs in MDCK cells is represented by the Prion Protein. Of interest, PrP localization in polarized MDCK cells is controversial and its mechanism of trafficking is not clear.

We found that full-length PrP and its cleavage fragments are segregated in different domains of the plasma membrane in polarized cells in both 2D and 3D cultures and that the C1/PrP full-length ratio increases upon MDCK polarization. We revealed that differently from other GPI-APs, PrP undergoes basolateral-to-apical transcytosis in fully polarized MDCK cells and is α-cleaved during its transport to the apical surface.

This study not only reconciles and explains the different findings in the previous literature but also provides a better picture of PrP trafficking and processing, which has been shown to have major implications for its role in prion disease.

Résumé en français

La Protéine Prion (PrP) est une glycoprotéine ubiquitaire attachée au feuillet externe de la membrane plasmique par une ancre glycosylphosphatidylinositole (GPI). PrP est l'agent infectieux responsable de la maladie Creutzfeld-Jacob ou « maladie de la vache folle ». Cette protéine existe sous sa forme cellulaire mais également sous sa forme infectieuse, nommée PrP^{Sc} (Scrapie). Alors que la fonction de PrP^{Sc} est établie au cours de la pathogenèse, la fonction de la protéine cellulaire est beaucoup plus énigmatique notamment chez les mammifères. Il est clairement admis que la forme infectieuse découle d'un changement de conformation de la forme cellulaire. Ainsi afin de mieux appréhender le rôle de la protéine prion dans les cellules saines mais également lors de la pathogenèse il apparaît essentiel d'étudier le trafic de cette protéine. La protéine prion est exprimée partout dans le corps et elle est enrichie dans les cellules neuronales qui sont comme les cellules épithéliales des cellules polarisées.

J'ai au cours de ma thèse étudié le trafic de la protéine prion dans les cellules polarisées MDCK. MDCK est la lignée épithéliale sur laquelle nous avons la plus grande connaissance. Dans mon travail j'ai utilisé des cellules MDCK polarisées classiquement en culture bidimensionnelle (2D) mais également en culture tridimensionnelle (3D) où les cellules forment des kystes, structures hautement polarisées, physiologiquement proches de l'épithélium *in vivo*. Il apparaît que dans les cellules MDCK polarisées sur filtre (en 2D) la localisation de la PrP est controversée.

Nous avons trouvé que, contrairement à la majorité des protéines à ancre GPI, la PrP suit la voie de transcytose. La PrP qui se retrouve à la membrane baso-latérale est transcytosée vers la membrane apicale. De plus la PrP envoyée à la surface apicale est clivée (clivage alpha) générant deux fragments distincts : le fragment C1, pourvu de l'ancre GPI qui reste associé à la surface apicale et le fragment soluble N1 qui est sécrété dans le milieu de culture des cellules MDCK cultivées en 2D ou dans le lumen des cellules MDCK cultivées en 3D.

Mon travail permet de mieux comprendre les études réalisées auparavant mais surtout révèle l'existence d'un mécanisme de transcytose de la protéine prion dans les cellules épithéliales. Cette information est essentielle et nous permet de supposer que ce mécanisme pourrait être également utilisé par les cellules neuronales.

List of abbreviations

A: alanine

aa: amino acid

AP: adaptor protein

Aβ: amyloid-beta

BSE: bovine spongiform encephalopathy

CD: cluster of designation

CHO: chinese hamster ovary

CJD: Creutzfeldt-Jakob disease

CNS: central nervous system

CREB: cyclic adenosine monophosphate response element-binding protein

CWD: chronic wasting disease

D: aspartic acid

DAF: decay accelerating factor

DC: dendritic cell

DLG1: discs large

DNA: deoxyribonucleic acid

DPP: dipeptidyl peptidase

DRM: detergent resistant membrane

E: glutamic acid

ECL: enchanced chemiluminescence

ECM: extracellular matrix

EPP: epithelial polarity programme

ER: endoplasmic reticulum

FFI: fatal familial insomnia

FR: folate receptor

FRAP: fluorescence recovery after photo bleaching

FRT: fisher rat thyroid

G: glycine

GFP: green fluorescent protein

GP: glycoprotein

GPI-APs: GPI-anchored proteins

GPI: glycosyl phosphatidyl inositol

GPIsp: GPI-addition signal peptide

GRAF: GTP^{ase} regulator associated with focal adhesion kinase

GSS: Gerstmann-Sträussler-Scheinker syndrome

GSL: glycosphingolipides

GTP^{ase}: guanosine-5'-triphosphate hydrolase

H: histidine

HA: hemagglutinin

HMW: high molecular weight

IF: immunofluorescence

IHC: immunohistochemistry

K: lysine

kDa: kilodalton

Ld: liquid disordered state

LGL: lethal giant larvae

Lo: liquid ordered state

LRP1: low-density lipoprotein receptor-related protein 1

M: molar

MDCK: Madin-Darby canine kidney

mRNA: messenger RNA

N: asparagine

NADPH: nicotinamide adenine dinucleotide phosphate

NCAM: neural cell adhesion molecule

nm: nanometer

ORF: open reading frame

P: proline

P75NTR: neurotrophin receptor p75

PALS: protein associated with lin seven

PAR: partitioning defective

PATJ: PALS1-associated tight-junction protein

PI-PLC: phosphatidylinositol-specific phospholipase C

PI3K: phosphoinositide 3-kinase

PIP: phosphoinositol-phosphates

PK: proteinase K

PK: proteinase K

PLAP: placental alkaline phosphatase

PNG^{ase}: peptide-N-glycosidase F

prion: proteinaceous infectious particles

PRNP: prion gene

PrP: prion protein

PrP^{C} : cellular prion protein

PrP^{Sc}: scrapie (i.e. infectious) prion protein

Q: glutamine

R: arginine

RNA: ribonucleic acid

SDS: sodium dodecyl sulfate

SI: sucrase isomaltase

SL: sphingolipides

STI-1: stress inducible protein 1

T: threonine

TfR: transferrine receptor

TGN: trans golgi network

Thy-1: thymocyte differentiation antigen 1

TM: transmembrane

TNT: tunneling nanotubes

TSE: transmissible spongiform encephalopathy

V: valine

VSV: vesicular stomatitis virus

VSVG: envelope glycoprotein G of the vesicular stomatitis virus

W: tryptophan

WB: western blot

Introduction

1 Cell polarity

Cell polarity is a spatial asymmetry in shape, structure, and function of cells. It is a fundamental property of prokaryotic and eukaryotic cells. Polarity is necessary for coordination of proliferation, differentiation, morphogenesis, motility and signaling processes. Polarized cells are highly organized; they usually possess plasma membrane domains that differ in proteins and lipids composition and in functions. These specialized plasma membrane domains determine cell orientation and function (Mellman & Nelson 2008).

Cell polarity can be permanent or temporary. Permanently polarized cells include neuronal (Fig. 1A) and epithelial cells (Fig. 1B). Transient polarity is a feature of activated and migrating immune cells, migrating glial and fibroblastic cells (Fig.1C), and some dividing cells (Fig. 1D).

The main purpose of polarized organization is to assure a proper function. For example polarization allows (I) fibroblastic cells to migrate in a given direction, (II) neurons to rapidly transduce an electric signal or (III) epithelial cells to control the exchange between two different environments (Mostov et al. 2003; Rodriguez-Boulan, Kreitzer & Musch 2005; Takano et al. 2015; Overeem et al. 2015).

How cells establish and maintain their polarity is still an open question in biology. Cell polarity is governed by interconnected regulations between signaling cascades, that controls membrane trafficking, proteins and lipid sorting, and cytoskeleton organization and dynamics (Mostov et al. 2003; Rodriguez-Boulan, Kreitzer & Musch 2005; Takano et al. 2015; Overeem et al. 2015).

Cell polarity is of fundamental importance in cell physiology and is altered in case of many human diseases. For instance alterations in the polarity regulators, markedly influence cell identity, leading to dysplasia (Goldenring 2013), loss of cellular polarity is critical in human cancer (Aparicio et al. 2015). Thus, a fundamental question in cell biology is to understand how cells establish and maintain their polarity.

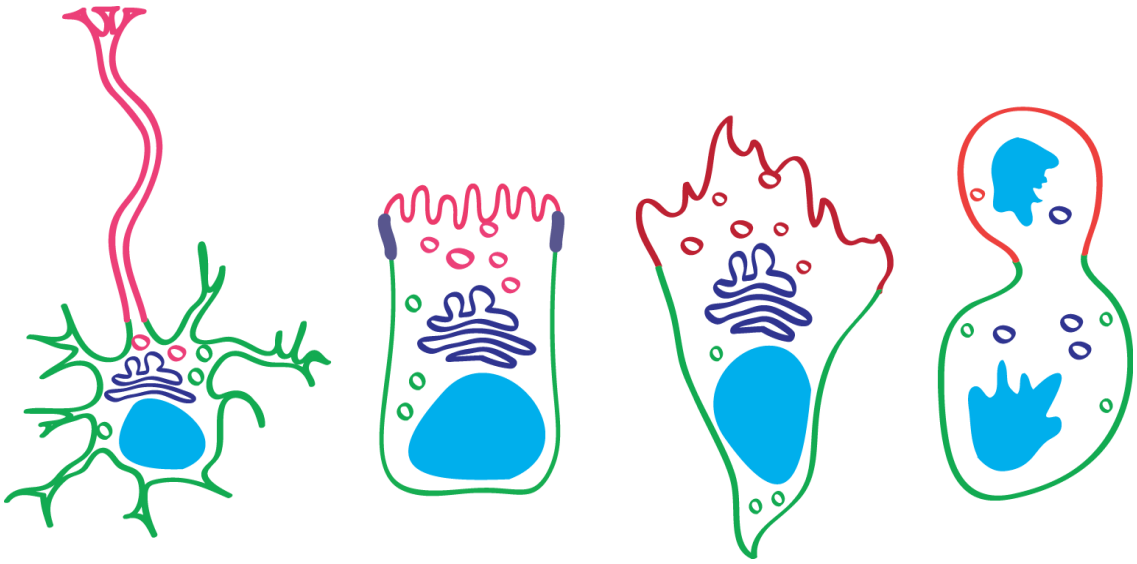

(a) Neuron (b) Epithelial cell (c) Migrating fibroblast (d) Asymmetric cell division

Figure 1. Examples of polarized cells. *Spatially and functionally restricted sub-compartments underlie the function of neurons (a) and epithelial cells (b). The spatial and temporal restriction of morphogen- and cytokine-receptor interactions directs cell migration during embryonic development and immune surveillance (c), while the asymmetric distribution of cell fate determinants enables asymmetric cell division and lead to the differentiation (d). Adapted from (Rodriguez-Boulan, Kreitzer & Musch 2005; Tahirovic & Bradke 2009; Neumüller & Knoblich 2009; Kadir et al. 2011).*

1.1 Polarized epithelia

One of the most abundant cell types in animals is epithelial cells. Hydra, as example of the simplest eumetazoan, consist essentially of two epithelial layers. In more complex animals, epithelial tissues line organs through the whole body (O'Brien et al. 2002). In the tissue, several epithelial cells form sheets held together through several intercellular interactions. There are two kinds of epithelial tissues: protective epithelium delimiting the body and internal organs, and glandular epithelium executing secretory function. Epithelial sheets can be composed by one-cell layer in the case of simple epithelia, or of many cells on top of each other for stratified epithelia.

Internal epithelial organs typically contain two types of building blocks: cysts and tubules (Fig. 2). Cysts (Fig. 2b top), also known as acini in the mammary gland, alveoli in the lung and follicles in the thyroid, are spherical monolayers of cells that enclose a central lumen. Tubules (Fig. 2b

bottom) are also lumen-enclosing monolayers, but are cylindrical instead of spherical. Combination of cysts and tubules can produce complex structures (Fig. 3a) such as the vertebrate lung — a network of branching bronchiolar tubules that terminates in alveolar cysts (O'Brien et al. 2002).

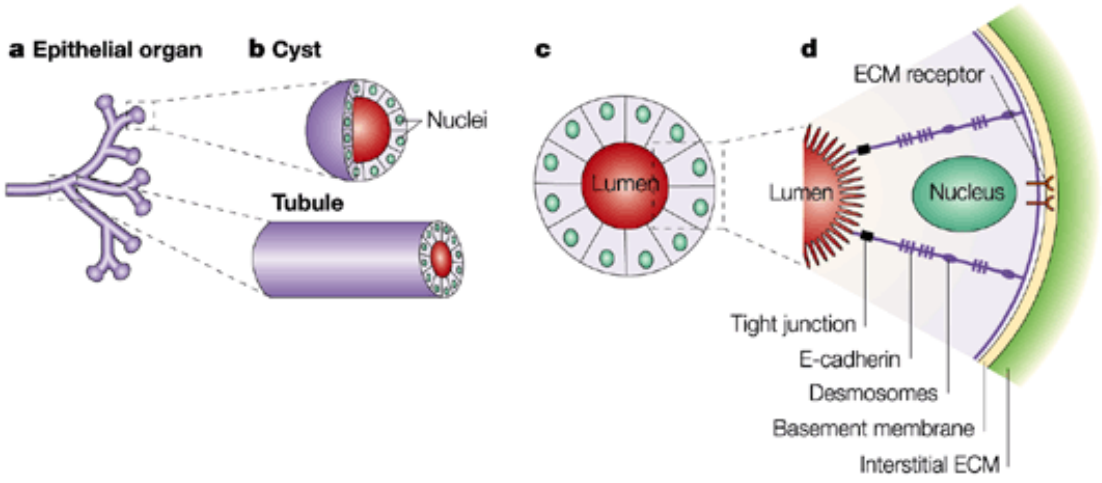

Figure 2. Epithelial organs organization. *Internal epithelial organs (a) consist of two basic building blocks: cysts and tubules (b). In cross section (c), these building blocks are lumen-enclosing monolayers of polarized cells. Each cell in the monolayer has a free apical membrane that faces the lumen, a lateral membrane domain that faces neighbouring cells, and a basal membrane domain that faces the basal lamina, a specialized extracellular matrix (d). Cells attach to ECM through integrin and non-integrin receptors and bind to neighbouring cells through tight junctions, desmosomes and homotypic E-cadherin interactions (d). Tight junctions also demarcate the boundary between the apical and lateral surfaces. From (O'Brien et al. 2002).*

Polarized epithelial cells are characterized by an asymmetric plasma membrane with an apical and basolateral domains (Fig. 3).

The apical domain of epithelial cells is usually in contact with the external surface of an organism or with the body cavities, while the basolateral surface faces basement membrane and adjacent cells. Interactions between adjacent cells are either simple mechanical adhesion via tight junctions, adherent junctions and desmosomes or metabolic cooperation via gap junctions (Citi et al. 2014). The apical and basolateral domains have distinct morphologies, and it is the apical domain that executes the specialized function (such as barrier, secretion,

absorption etc.). For example, the apical plasma membrane in enterocytes is characterized by a brush border, composed of microvilli, which play a role in the increment of the cell surface, and improve the absorption and exchange properties of the tissue. In general, the apical and basolateral domains are composed of different proteins and lipids (Rodriguez-Boulan & Macara 2014). For example, depending on the cell function the apical plasma membrane can be enriched in intestinal hydrolases, ion channels, transporters, whereas the basolateral domain in all epithelial cell types faces neighbouring cells and basal lamina, and therefore is enriched in E-cadherin and integrins, which play a role in the formation of cell/cell or cell/ECM contacts. Lipids such as cholesterol and sphingolipids are enriched in the apical domain, whereas phosphotidylcholine is enriched in the basolateral domain (van Meer & Simons 1988; Apodaca et al. 2012).

1.2 Molecular mechanisms underlying epithelial polarization

The overall process through which the network of epithelial polarity proteins and lipids mediate the organization of a polarized epithelial cell is called the epithelial polarity program (EPP). Cell polarity involves the spatiotemporal coordination of many processes such as signaling cascades, proteins and lipid sorting, trafficking and endocytosis as well as cytoskeletal dynamics (Mostov et al. 2003; Rodriguez-Boulan, Kreitzer & Musch 2005; Takano et al. 2015; Overeem et al. 2015).

The first step of polarization is the response to extracellular cues, it involves cell–matrix and cell–cell recognition (Manninen 2015). This step is determining how to orientate the cell and where to form the apical surface. The second step of apical-basal polarization is cytoskeleton rearrangement and the establishment of an apical–basal axis and intercellular junctions. Polarization requires the establishment of polarized trafficking machinery.

Studies on model organisms such as yeast, worms and flies have led to the identification of core protein complexes that regulate various aspects of EPP. Three major polarity complexes (Fig. 3), the PAR (PAR3-PAR6-aPKC), Crumbs (Crumbs3-PALS1-PATj) and Scribble (Scribble-DLG1-LGL1/2) have been shown to be involved in the epithelial polarization and also in asymmetric cell division (Overeem et al. 2015; Rodriguez-Boulan & Macara 2014; Assemat et al. 2008). These complexes distribute asymmetrically in the cells, promoting the establishment of apical and basolateral membrane domains.

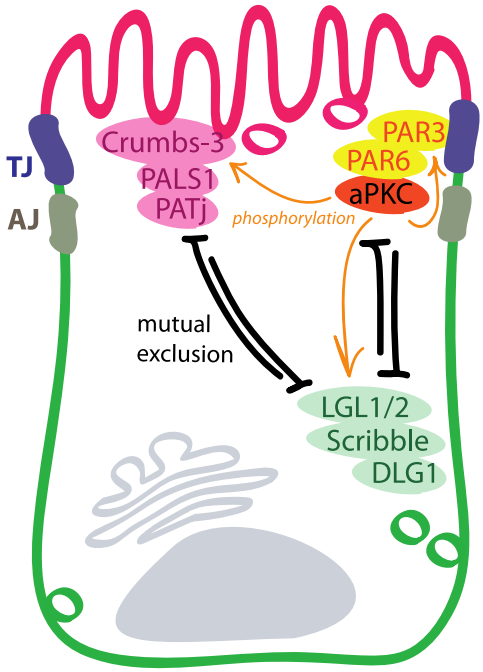

Figure 3. Polarity proteins of the PAR3, Crumbs and Scribble complexes. *Three conserved protein complexes — the partitioning defective (PAR), Crumbs and Scribble complexes — control many polarization processes. Two PDZ-domain proteins PAR-3 and PAR-6 which, together with the Ser/Thr kinase atypical protein kinase C (aPKC), constitute the PAR complex. The Crumbs complex comprises the transmembrane protein Crumbs and the cytoplasmic scaffolding molecules PALS1 ((protein associated with LIN-7)-1) and PATJ (PALS1-associated tight-junction protein). Cytoplasmic proteins Scribble, Discs large (DLG) and Lethal giant larvae (LGL) are involved in neuronal synapse formation or function. Scribble-complex proteins are considered as tumor suppressors. In polarized mammalian epithelial cells, the PAR3 and Crumbs-3 complexes localize predominantly to tight junctions, whereas components of the Scribble complex show basolateral localization. Several molecular interactions between the three complexes have been identified. Mutual exclusion of the Scribble complex and the apical junctional complexes controls apico–basal polarity TJ – tight junctions; AJ - adherent junctions. Adapted from (Iden & Collard 2008).*

In epithelial cells the PAR and Crumbs complexes localize at the apical surface were they are leading the establishment of the apical domain and in the assembly of tight junctions. Moreover, in MDCK cells these complexes play an important role in the biogenesis of the primary cilium (Fan et al. 2004; Sfakianos et al. 2007). The primary cilium is a solitary organelle that emanates from the cell surface of most mammalian cell types during growth arrest, primary cilia are key coordinators of signaling pathways during development and in tissue homeostasis (Satir et al. 2010). Opposite, the Scribble complex, localized at the basolateral membrane, is involved in the basolateral exclusion of apical proteins (Rodriguez-Boulan & Macara 2014). Additionally, polarity complexes are involved in the rearrangement of microtubule cytoskeleton and phosphoinositol phosphate synthesis (Bryant & Mostov 2008).

Along with the protein complexes, phosphoinositol-phosphates (PIPs) are involved in the regulation of cell polarity. In particular $PI(3,4,5)P_3$ and $PI(4,5)P_2$ seem to play an important role in the establishment of cell polarity. $PI(4,5)P_2$ is transformed to $PI(3,4,5)P_3$ by PI3-kinases (PI3K), and inversely $PI(3,4,5)P_3$ is transformed to $PI(4,5)P_2$ by a 3-phosphatase (PTEN). In polarized MDCK cells it was shown that $PI(3,4,5)P_3$ localizes exclusively at the basolateral surface, whereas $PI(4,5)P_2$ localizes mainly at the apical surface (Nelson 2009).

The asymmetric distribution of these two phosphoinositol-phosphates is regulated by specific recruitment of kinases PI3K to the basolateral domain and exclusion of the phosphatase PTEN from the basolateral domain and it's enrichment at the apical domain (Rodriguez-Boulan & Macara 2014). The $PI(4,5)P_2$ has been shown to be involved in the endocytosis by modulating the activity of AP-2 and Epsin involved in the assembly of clathrin-coated vesicles. Whereas, $PI(3,4,5)P_3$ regulates transcytosis of basolateral membrane components. Interestingly, it was shown that the presence of $PI(3,4,5)P_3$ is able to transform an apical membrane into a basolateral membrane by bringing the orchestra of basolateral proteins (Gassama-Diagne et al. 2006). In addition, evidences suggest that phosphoinositides can control the activity of PAR complex, thereby regulate the epithelial polarity (Gassama-Diagne & Payrastre 2009).

The cell polarity is maintained during the lifetime of an epithelium by constant plasma membrane turnover of lipids and proteins. A continuous sorting of newly synthesized molecules and recycling of membrane components are required to maintain the molecular asymmetry at the cell surface (Rodriguez-Boulan & Macara 2014).

1.3 Polarized protein sorting

Epithelial polarity is established and then maintained thanks to a polarized sorting and trafficking of lipids and proteins as well as the polarized endocytosis. Polarized cells must specifically address plasma membrane proteins and lipids to the apical and basolateral domains (Yeaman et al. 1999; Mostov 2003; Rodriguez-Boulan, Kreitzer & Musch 2005). Polarized sorting of proteins relies on the recognition of intrinsic signal by cellular sorting machineries.

1.4 Basolateral sorting signals

Early works on protein trafficking proposed that basolateral delivery was a default mechanism, not requiring any signals (Simons & Wandinger-Ness 1990). Later works identified discrete basolateral sorting signal in the cytoplasmic domain of the proteins playing an important role in both biosynthetic and recycling trafficking (Hunziker et al. 1991; Brewer & Roth 1991). Nowadays basolateral sorting signals are relatively well identified; the most common signals are recapitulated in the table 1.

Basolateral signals are found in the primary structure of the proteins, as specific amminoacidic sequences located in the cytoplasmic tail of cargo proteins. There are two most common types of basolateral signals: tyrosine- and di-leucine-based (Mellman & Nelson 2008; Edeling et al. 2006; Bonifacino & Traub 2003; Rodriguez-Boulan, Kreitzer & Müsch 2005; Stoops & Caplan 2014). In 2010, Weise and colleagues identified two basolateral targeting signals in the surface glycoproteins of the Nipah virus, involving tyrosine 525 in the F protein and a di-tyrosine motif at position 28/29 in the G protein (Weise et al. 2010). There are also basolateral signals constituted of a single leucine patch as in CD147 (Deora et al. 2004) or other sequences as identified in neural cell adhesion molecule (Le Gall et al. 1997), pIgR (Aroeti & Mostov 1994), epidermal growth-factor receptor (He et al. 2002), epidermal growth-factor receptor 2 (Dillon et al. 2002) and transforming growth factor β (Dempsey et al. 2003). Most likely, other basolateral sorting signals remain to be identified and characterized.

Table 1. Signals and mechanisms for sorting to the basolateral membrane

Sorting Signal	Protein	Presumed Sorting Mechanism	References
Tyrosine-based	Low-density lipoprotein receptor	Recycling, but not delivery, is μ1b-dependent	(Matter et al. 1992; Gan et al. 2002)
	Vesicular stomatitus virus G protein	μ1b-dependent	(Thomas et al. 1993; Folsch 2003)
	lgp120	μ3a-dependent	(Hunziker et al. 1991; Stephens & Banting 1998)
Dileucine	Fc receptor FcRII-B2	μ1b-independent	(Hunziker & Fumey 1994; Matter et al. 1994; Roush et al. 1998)
	Mannose 6-phosphate receptor	μ1b-independent	(Johnson & Kornfeld 1992; Distel et al. 1998)
	E-cadherin	Rab11-mediated	(Lock 2005; Miranda et al. 2001)
Monoleucine	Stem cell factor	?	(Wehrle-Haller & Imhof 2001)
	CD147	Clathrin-mediated; μ1b-dependent	(Deora et al. 2005)
	Amphiregulin	Recycling, but not delivery, is μ1b-dependent	(Gephart et al. 2011)

Table from (Stoops & Caplan 2014).

How do basolateral sorting signals specify the destination of a protein? Many basolateral proteins contain the di-hydrophobic-based or the tyrosine-based sorting signals resembling the clathrin-dependent endocytosis motifs (Stoops & Caplan 2014). Therefore the original hypothesis proposed that a clathrin-dependent machinery is also recruited to sort proteins to the basolateral membrane thus involving specific clathrin adaptor proteins (AP) involved in cargo recognition (Bonifacino 2014; Folsch et al. 1999). AP are hetero tetrameric complexes

composed by two large subunits (γ/α/δ/ε/ζ/β1-5), one medium-sized subunit (μ1–5) and one small-sized subunit (σ1–5). Five AP complexes have been identified to date: AP-1, AP-2, AP-3, AP-4 and AP-5 (Park & Guo 2014). While APs have a recognized role in clathrin mediated endocytosis, AP-1B has a well-characterized role in basolateral sorting (Gonzalez & Rodriguez-Boulan 2009). Interestingly, AP-1B differs from the ubiquitous adaptor AP-1A only by a medium subunit μ1B (Ohno et al. 1999; Cao et al. 2012; Nakatsu et al. 2014). It was also shown that AP-4 is involved in the basolateral sorting. Knockdown of the medium subunit of the AP-4 complex resulted in the missorting of LDL receptor in MDCK cells (Simmen et al. 2002). Intriguingly while AP-1B participates in the basolateral sorting on a clathrin dependent manner, AP-4 is involved in basolateral sorting independently of clathrin. Further investigation is required to understand the role of other APs in the basolateral sorting.

1.5 Apical sorting signals

The question of delivery of proteins to the apical surfaces of epithelial cells is more complex than in case of basolateral sorting. In contrast to the basolateral sorting signals, apical sorting signals are of variable nature including peptide sequences and post-translational modifications (Stoops & Caplan 2014; Weisz & Rodriguez-Boulan 2009), such as lipid and sugar moieties, and they can be localized in the extracellular, transmembrane or intracellular domains of the cargo proteins (Weisz & Rodriguez-Boulan 2009). Known apical signals and mechanisms of sorting are recapitulated in the table 2.

Originally one of the first apical signals described was the glycosylphosphotidylinositol (GPI) anchor. It was shown that addition of a GPI-anchor to the ectodomain of a basolateral (herpes simplex glycoprotein D) or a secretory (human growth hormone) protein resulted in its apical sorting (Lisanti et al. 1989; Lisanti et al. 1988; Brown et al. 1989). GPI-anchored proteins and the role of the GPI anchor in apical sorting are described in greater details later in the introduction (GPI-anchored proteins, page 29).

Table 2. Signals and mechanisms for sorting to the apical membrane

Sorting Signal	Protein	Presumed Sorting Mechanism	References
GPI-anchor	Decay accelerating factor	Lipid raft–associated	(Lisanti et al. 1989; Paladino et al. 2002)
	PLAP	Lipid raft–associated	(Paladino et al. 2004)
N-Glycans	Clusterin (gp80)	Raft-independent	(Urban et al. 1987; Graichen et al. 1996)
	gp114	Galectin-3–mediated, raft-independent	(Le Bivic et al. 1993; Delacour et al. 2006)
	Growth hormone	Galectins 3 & 4 independent	(Scheiffele et al. 1995)
	Erythropoietin	Cholesterol-dependent	(Kitagawa et al. 1994; Maruyama et al. 2005)
	Endolyn	Raft-independent	(Ihrke et al. 2001)
O-Glycans	p75 neurotrophin receptor	Galectin-3–mediated, raft-independent	(Yeaman 1997; Delacour et al. 2006)
	Lactase phlorizin hydrolase	Galectin-3–mediated, raft-independent	(Delacour et al. 2006)
	MUC1	Raft-independent	(Mattila et al. 2009; Huet et al. 1998; Kinlough et al. 2006)
	Podocalyxin	Transient lipid raft association	(Yu et al. 2007)
	Dipeptidyl peptidase IV	Lipid raft–associated	(Naim et al. 1999; Slimane et al. 2000)
	Sucrase isomaltase	Lipid raft–associated	(Naim et al. 1999; Alfalah et al. 1999)
Transmembrane domain	Neuraminidase	Lipid raft–associated	(Kundu et al. 1996; Barman & Nayak 2000)
	Influenza hemagglutinin	Lipid raft–associated	(Lin et al. 1998; Scheiffele et al. 1997)
	Respiratory syncytial virus F protein	Lipid raft–associated	(Brock et al. 2005; Brown et al. 2004)
	Sucrase isomaltase	Lipid raft–associated	(Jacob et al. 2000)
	H,K-ATPase	Raft-independent	(Dunbar et al. 2000)

Table modified from (Stoops & Caplan 2014). For more details on apical sorting signals please refer to (Weisz & Rodriguez-Boulan 2009).

Although there are contradictory data that could result from the protein specificity and from cellular context, good candidates for apical sorting signals are *N*- and *O*-glycans (J. H. Benting et al. 1999; Alfalah et al. 1999; Jacob et al. 2000; Yeaman et al. 1997). Inhibition of *N*-glycosylation, is leading to the mistargeting of apical gp80 and gp114 in MDCK cells (Le Bivic et al. 1993; Urban et al. 1987). Furthermore, recombinant addition of *N*-glycosylation chains to rat growth hormone (rGH) led to its apical localization (Scheiffele et al. 1995). *N*-glycans have been shown to play a role in the apical delivery of endolyn (Ihrke et al. 2001), the glycine transporters (Martínez-Maza et al. 2001) and dipeptidase (Pang et al. 2004). In contrast to aforementioned data in some systems (Delacour et al. 2006) N-glycosylation does not affect apical localyzation of p75NTR (Yeaman et al. 1997) or hepatitis B surface antigen (HBAgs) and Oesteopontin (Marzolo et al. 1997; Trischler et al. 2001). An article from our laboratory is showing that N-glycosylation plays a role in the apical delivery only in a particular cellular context; N-glycosylation is an apical signal in FRT cells, but not in MDCK. Interestingly prion protein is N-glycosylated but nevertheless is not delivered to the apical membrane neither in FRT nor in MDCK (Sarnataro et al. 2002).

O-linked glycosyl chains may also acts as an apical sorting signal. P75NTR and the hydrolase sucrase isomaltase (SI) contains heavily *O*-glycosylated stalk domains in close proximity to the membrane and deletion of these domains induced mistargeting of both p75NTR and SI from the apical to basolateral domain of plasma membrane (Yeaman et al. 1997; Jacob et al. 2000).

Another group of apical signals are encoded by transmembrane domains. In case of influenza virus neuraminidase (NA), it was shown that apical signals residing in the transmembrane domain mediate the association of the proteins with lipid rafts (Kundu et al. 1996; Barman & Nayak 2000; Delacour et al. 2006).

In addition, a putative apical sorting signal was found in the cytoplasmic tail of rhodopsin (Tai et al. 2001; Chuang & Sung 1998), Na-dependent bile acid transporter (Sun et al. 1998), megalin (Takeda et al. 2003). These studies indicate that cytoplasmic sorting machinery analogous to the one described for basolateral proteins might also exists for apically targeted proteins.

1.6 Trafficking routes in polarized cells

Polarity is maintained by the selective traffic of *de novo* synthesized proteins and by the selective polarized endocytosis and recycling. In general, membrane proteins are synthesized and modified in the ER and then are sorted and further maturate within the Golgi apparatus to their proper destination (Mellman & Nelson 2008; Goldenring 2013; Rindler et al. 1984; Fuller et al. 1985; Griffiths & Simons 1986; Muñiz & Zurzolo 2014; Rodriguez-Boulan, Kreitzer & Musch 2005). There are several trafficking roads for newly synthesized secretory membrane proteins. In the simplest case, membrane proteins leave TGN in vesicles and are sorted to the apical or basolateral membranes directly (Fig. 4a). Several studies have shown that the biosynthetic route of several membrane proteins includes a post-TGN transit through RE (Ang et al. 2004; Lock 2005; Cancino et al. 2007; Cresawn et al. 2007; Gravotta et al. 2007).

Once protein is located on the plasma membrane, endocytosis can relocate proteins into the cell. Proteins undergoing endocytosis can be additionally sorted in recycling endosomes, like Transferrin receptor (TfR) (Matter & Mellman 1994; Mostov & Cardone 1995; Odorizzi & Trowbridge 1997).

Upon endocytosis the eventual fate of a protein is decided along several distinct pathways. Some internalized proteins are recycled to the same membrane from where they were endocytosed (Fig. 4b). Other proteins are targeted for degradation through the lysosomes (Fig. 4c). This mechanism, for example, provides a pathway for the internalization of nutrients (Fuller & Simons 1986; Wang et al. 2000) as well as the transmission of signals into the cytoplasm or the termination of that signal (for example, internalization of epidermal growth factor receptor (EGFR)), (Kostaras et al. 2012; Balaji et al. 2012; Goh et al. 2010). Importantly the choice of endocytic pathway is greatly influenced by the protein concentration on the membrane and on the presence of the ligand. Some proteins will be recycled back to the Golgi apparatus (Fig. 4d), a mechanism that can potentially account for the repair of damaged receptors (Derby et al. 2007).

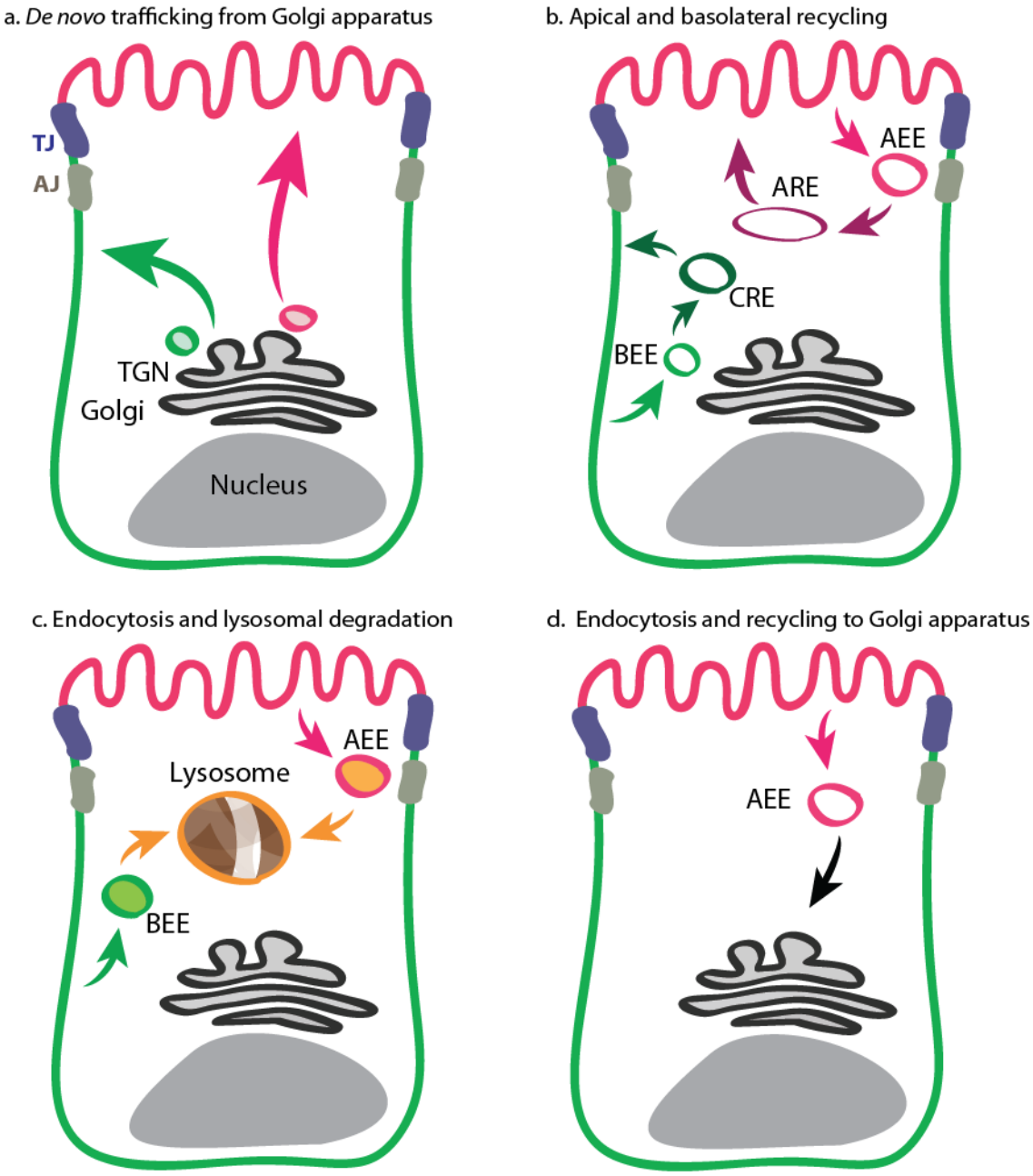

Figure 4. Paradigms for trafficking in polarized epithelial cells. *a. De novo trafficking from the Golgi apparatus. b. Endocytosis and recycling inside of to the same membrane domain. c. Endocytosis leading to degradation in the lysosome d. Endocytosis and trafficking back to the Golgi apparatus. All of these pathways may be operating in polarized epithelial cells. AEE, apical early endosome; ARE, apical recycling endosome; BEE, basolateral early endosome; CRE, common recycling endosome. Adapted from (Goldenring 2013).*

Studies on the LDLR (Matter et al. 1993) and polymeric immunoglobulin receptor (pIgR) (Aroeti & Mostov 1994) led to the concept that the same sorting motifs are used both at the TGN and recycling endosomes. However, the TfR seems to use distinct motifs at these two distinct locations (Odorizzi & Trowbridge 1997). The sorting machinery of the TGN can discriminate between different basolateral sorting signals *in vitro* (Musch et al. 1996) and *in vivo* (Soza et al. 2004) and could in principle also discriminate between basolateral and recycling motifs.

1.7 Transcytosis, indirect sorting mechanism

Finally, in polarized epithelial cells, internalized proteins may be transcytosed to the opposite side. The transcytotic pathways account for the exchange of nutrients and crucial proteins: for example, apical to basolateral transport of maternal immunoglobulin G (IgG) proteins in the neonatal gut (Tzaban et al. 2009), and basolateral to apical transport of immunoglobulin A (IgA) proteins in many epithelia (Apodaca et al. 1994; Casanova et al. 1999).

Depending on the cell type this mechanism is rare as in case of polarized MDCK cells or frequent as in case of hepatocytes. The most extensively studied pathway for regulated apical delivery in polarized MDCK cells is transcytosis of pIgR (Fig. 5) (Mostov et al. 2000; Rojas & Apodaca 2002). In the absence of pIgA, pIgR is largely recycled to the basolateral surface. However, binding of pIgA stimulates transcytosis approximately threefold (Giffroy et al. 1998). This stimulation involves two signaling pathways: first, binding of pIgA results in activation of the Src family non-receptor tyrosine kinase, $p62^{Yes}$, which in turn causes elevation of intracellular free calcium and thereby stimulates transcytosis (Luton et al. 1999; Mostov et al. 2000); second, pIgR associates directly with the low-molecular-weight GTPase, rab3b (van IJzendoorn et al. 2002), which normally exists in an active GTP-bound state. This promotes recycling of the pIgR to the basolateral surface. Binding of pIgA stimulates GTP hydrolysis on rab3b and dissociation of rab3b from pIgR, resulting in transcytosis.

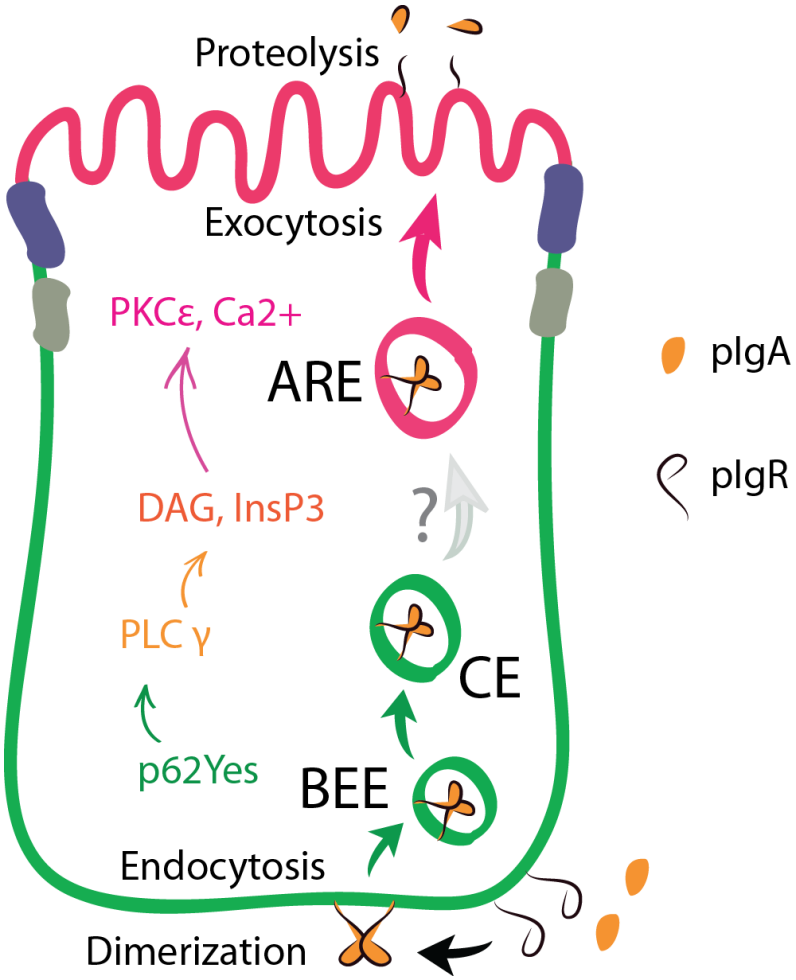

Figure 5. Regulated transcytosis. Exemple of pIgR. *Binding of pIgA to the pIgR causes dimerization of the pIgR and activation of p62Yes, probably at the basolateral cell surface (green) or in BEE. In turn, p62Yes activates phospholipase C (PLC-γ), which produces diacylglycerol (DAG) and inositol 1,4,5-trisphosphate (InsP3), although it is not clear where this occurs. Finally, protein kinase C (PKCε) is activated and levels of free calcium increase, both of which promote delivery from the ARE to the apical surface. After the pIgR reaches the apical surface, its extracellular ligand-binding domain is proteolytically cleaved and released with pIgA into secretions. Modified from (Mostov et al. 2003).*

1.8 Model system to study cell polarity - MDCK cells

One of the fundamental questions is how epithelial cells establish and maintain their polarity. The analysis of these processes could be addressed with establishment of Madin-Darby canine kidney (MDCK) cell line, that was firstly characterized in 1966 (Gaush et al. 1966). MDCK cells develop a tight epithelial monolayer when they were plated on a permeable substratum (Leighton et al. 1970; Misfeldt et al. 1976). A key step in the study of polarized epithelia using MDCK was made by Rodrigez-Boulan and colleagues, when they showed that influenza virus assembles from apical surface and vesicular stomatitis virus (VSV) assembles from the basolateral surface of MDCK cells guided by the polarized distribution of their envelope glycoproteins influenza hemagglutinin (HA) and VSVG protein (VSVG) (Rodriguez Boulan & Sabatini 1978; Rodriguez Boulan & Pendergast 1980; Rodriguez-Boulan, Kreitzer & Musch 2005). The MDCK cells in short time became a popular model cell system to study the polarized protein targeting.

HA and VSVG provided the first evidence of polarized biosynthetic routes and sorting at the Golgi complex and they are still widely used as apical and basolateral markers (Rodriguez Boulan & Sabatini 1978; Rodriguez Boulan & Pendergast 1980; Rodriguez-Boulan, Kreitzer & Musch 2005). The studies of viral proteins traffic in MDCK lead to the discovery of Trans Golgi Network (TGN) (Griffiths & Simons 1986) as a major sorting compartment in the biosynthetic route (Rodriguez-Boulan, Kreitzer & Musch 2005; Matlin & Simons 1984; Misek et al. 1984; Rindler et al. 1984). Several laboratories were able to directly monitor the traffic of chimeric proteins fused to Green-fluorescent protein (GFP) from the TGN up to the plasma membrane (Polishchuk et al. 2004; Kreitzer et al. 2003; Paladino et al. 2006; Hua et al. 2006).

The most common polarization protocol is to plate cells on top of the Transwell^{TM} filter (Hanzel et al. 1991) (Fig. 6 left). Interestingly MDCK cells are also able to establish tree-dimensional (3D) cyst (O'Brien et al. 2002), providing a physiological model recapitulating numerous features of an *in vivo* epithelia in 3D system (Debnath & Brugge 2005) (Fig. 6 right).

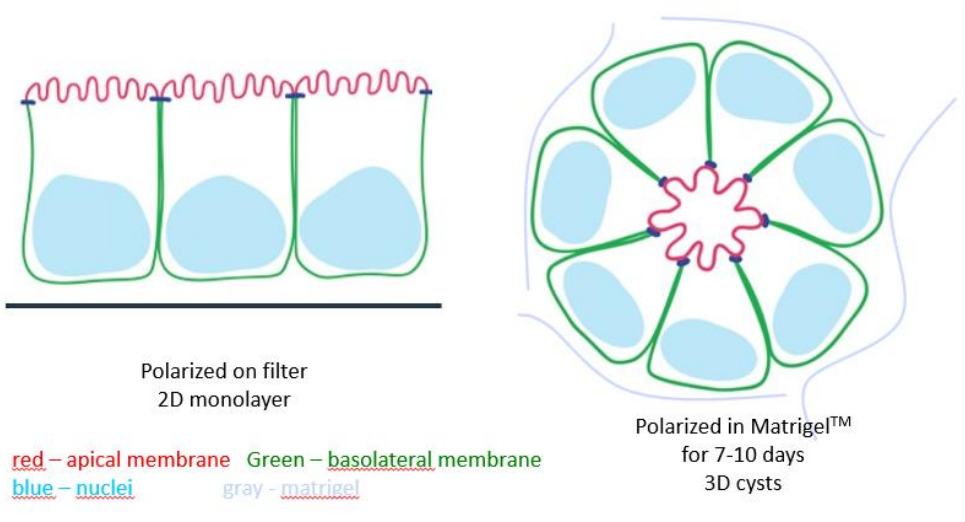

Figure 6. Schematic of MDCK monolayer and cyst. *MDCK plated on a permeable filter form 2D monolayer. While MDCK cells are plated in or on top of Matrigel™ or another ECM they form 3D cyst.*

3D culture is a powerful tool to investigate the molecular signals that specify epithelial architecture. The ability of MDCK cells to reproduce a tissue-like organization when grown inside a 3D extracellular matrix (ECM) is impressive. MDCK cells form cysts when embedded in Matrigel™ or collagen type I matrix (Fig. 6 right). Like simple epithelial tissues, MDCK cysts are polarized monolayers that enclose a lumen and are encircled by a basement membrane. Moreover, these cysts develop branching tubules when exposed to mesenchymally derived hepatocyte growth factor (HGF) (Montesano, Schaller, et al. 1991; Montesano, Matsumoto, et al. 1991) a response that is reminiscent of the epithelial–mesenchymal interactions that stimulate tubulogenesis *in vivo*.

Cells cultured as 3D models exhibit features that are closer to the complex *in vivo* conditions (Vinci et al. 2012; Ravi et al. 2015).

Where and how the variety of sorting signals is decoded in MDCK cells?

In MDCK cells newly synthesized apical and basolateral membrane proteins segregate first at the TGN (Rodriguez-Boulan, Kreitzer & Musch 2005) (Fig. 4a). Several membrane proteins leaving the Golgi apparatus may traverse RE compartments before arrival to the cell surface.

This pathway has been better documented for basolateral proteins (Ang et al. 2004; Lock 2005; Cancino et al. 2007; Cresawn et al. 2007; Gravotta et al. 2007; Paladino et al. 2015). For some basolateral proteins, such as the transferrin receptor (TfR) and VSVG protein, biosynthetic trafficking through RE seems to be an obligate station (Cancino et al. 2007). Some apical proteins may also pass through endosomal intermediates as shown in case of endolin (Cresawn et al. 2007). Once at the plasma membrane, proteins internalized from each cell surface domain can be recycled back to the same domain or transported by transcytosis to the opposite pole (Matter et al. 1993; Aroeti & Mostov 1994; Matter & Mellman 1994; Mostov & Cardone 1995; Odorizzi & Trowbridge 1997). Indeed, in case of basolateral proteins they are also endocytic proteins that recycle several times without losing polarity (Rodriguez-Boulan, Kreitzer & Musch 2005), indicating that they are sorted first during their biosynthetic trafficking and then several times during recycling (Matter et al. 1993; Gan et al. 2002; Marzolo et al. 2003; Cancino et al. 2007; Gravotta et al. 2007).

2 GPI-anchored proteins

As mentioned before, originally it was postulated that the GPI-anchor was acting like an apical targeting signal. GPI-APs are luminal secretory proteins that are attached by a post-translational glycolipid modification, the GPI anchor, to the external leaflet of the plasma membrane (Muñiz & Zurzolo 2014; Paladino et al. 2015). GPI-anchored proteins (GPI-APs) were identified more than 2 decades ago; they are widely expressed from yeast to humans and more than hundreds GPI-APs have been characterized to date (Nosjean et al. 1997). Indeed it is an extremely diverse group of proteins that play important roles in signal transduction, immune response, pathobiology of trypanosomal parasites and in prion disease pathogenesis (Nosjean et al. 1997; Muñiz & Zurzolo 2014; Chesebro et al. 2005).

Among the multiple functions of GPI-anchored proteins are hydrolytic enzymes, adhesion molecules, complement regulatory proteins, receptors, protozoan coat proteins, and prion proteins. While many GPI-APs have been characterized, the only confirmed biological function of the GPI anchor itself is to fix the protein in the outer leaflet of the cellular membrane (Low 1989; Low & Saltiel 1988). Of note in mammals, alternative mRNA splicing may lead to the expression of transmembrane and/or soluble and GPI-anchored forms of the same gene product. These variants may be developmentally regulated. For example, neural cell adhesion molecule (NCAM) exists in GPI-anchored and soluble forms when expressed in muscle and in GPI-anchored and transmembrane forms when expressed in brain (Schor et al. 2013; Mukasa et al. 1995).

The GPI-anchor is a glycolipid structure that is added post-translationally to the C-terminus of many eukaryotic proteins (Nosjean et al. 1997; Ferguson 1999; Homans et al. 1988; Ferguson et al. 1985). Unlike simple lipid modifications, the GPI anchor has a complex structure that includes a phosphoethanolamine linker, glycan core, and phospholipid tail (Fig. 7) (Paulick & Bertozzi 2008; Ferguson et al. 2009).

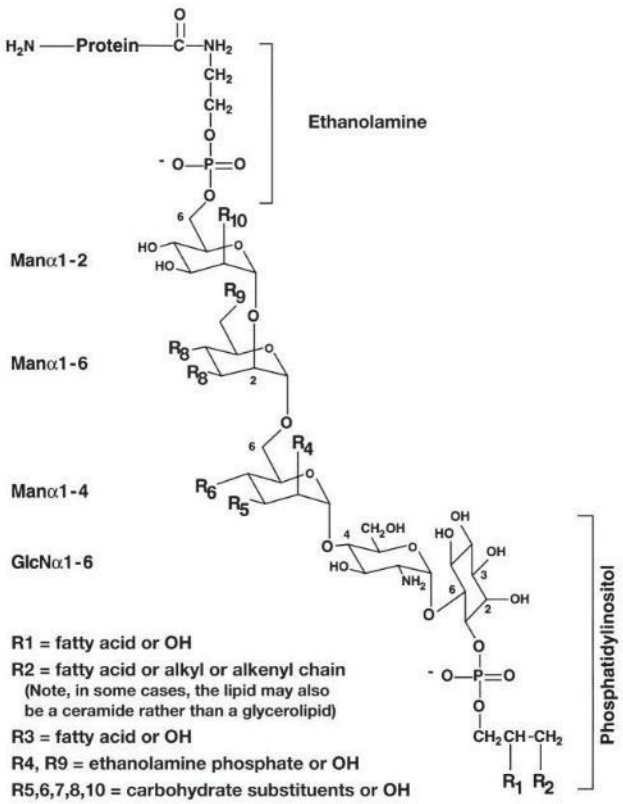

Figure 7. General structure of GPI-anchors. All GPI-anchors share a common core. Heterogeneity in GPI anchors is derived from various substitutions of this core structure and is represented as R groups. R1 may be a long-chain fatty acyl chain or OH and R2 may be a long-chain fatty acyl, alkyl, or alkenyl chain. In some cases the lipid is a ceramide rather than a glycerolipid. R3 is most often a palmitate group attached to C-2 of the inositol ring and, when present, renders anchors resistant to PI-PLC. R4 and R9 can be OH or additional ethanolamine phosphate groups that are not attached to protein. R5, R6, R7, R8 and R10 can be OH or monosaccharide or oligosaccharide side-chain attachment points (Ferguson et al. 2009).

The first structure of a GPI-anchor was published by Ferguson and colleagues in 1988. To determine the exact structure of the VSG anchor from *T. brucei* authors combined NMR spectroscopy, mass spectrometry, chemical modification, and exoglycosidase digestions (Ferguson et al. 1988).

The C-terminus of a GPI-anchored protein is linked through a phosphoethanolamine bridge to the highly conserved core glycan, mannose(α1−2)-mannose(α1−6)-mannose(α1−4)-glucosamine(α1−6)-*myo*-inositol (Fig. 9). A phospholipid tail attaches the GPI-anchor to the cell membrane. The glycan core can be variously modified with side chains, such as a

phosphoethanolamine group, mannose, galactose, sialic acid, *N*-acetylgalactosamine-containing polysaccharides or other sugars (Ferguson et al. 1988; Homans et al. 1988; Ikezawa 2002; Deeg et al. 1992; Brewis et al. 1995; Nakano et al. 1994; Mukasa et al. 1995; Fontaine et al. 2003; Oxley & Bacic 1999; McConville & Ferguson 1993). The most common side chain attached to the first mannose residue is another mannose. Depending on the origin, the lipid anchor of the phosphoinositol ring is a diacylglycerol, an alkylacylglycerol, or a ceramide. The lipid species vary in length, ranging from 14 to 28 carbons, and can be either saturated or unsaturated (Macrae et al. 2005). Many GPI anchors also contain an additional fatty acid, such as palmitic acid, on the 2-hydroxyl of the inositol ring. This extra fatty acid renders the GPI anchor resistant to cleavage by PI-PLC (McConville & Ferguson 1993).

2.1 GPI-anchor biosynthesis

How GPI-anchor is attached to the protein?

A typical GPI-AP protopeptite is translocated into the ER by a classical signal peptide located at the N terminus of the protein. In addition at the C terminus, it contains a signal peptide fragment cleaved at the ω-site for addition of a preformed GPI anchor, spacer and hydrophobic regions (Fig. 8). The biosynthesis of GPI anchors occurs in three stages: (1) preassembly of a GPI precursor in the ER membrane, (2) cleavage of a carboxy-terminal GPI-addition signal peptide coupled with attachment of the GPI to newly synthesized protein in the lumen of the ER, and (3) lipid remodeling and/or carbohydrateside-chain modifications in the ER and the Golgi (Muñiz & Zurzolo 2014; Chatterjee & Mayor 2001).

The carboxy-terminal GPI-addition signal peptide (GPIsp) has three domains: (1) three relatively small amino acids located at ω, ω + 1, ω + 2, where ω is the amino acid attached to the GPI anchor and where ω + 1 and ω + 2 are the first two residues of the cleaved peptide; (2) a relatively polar domain of typically five to ten residues; and (3) a hydrophobic domain of typically 15–20 hydrophobic amino acids (Fig. 8).

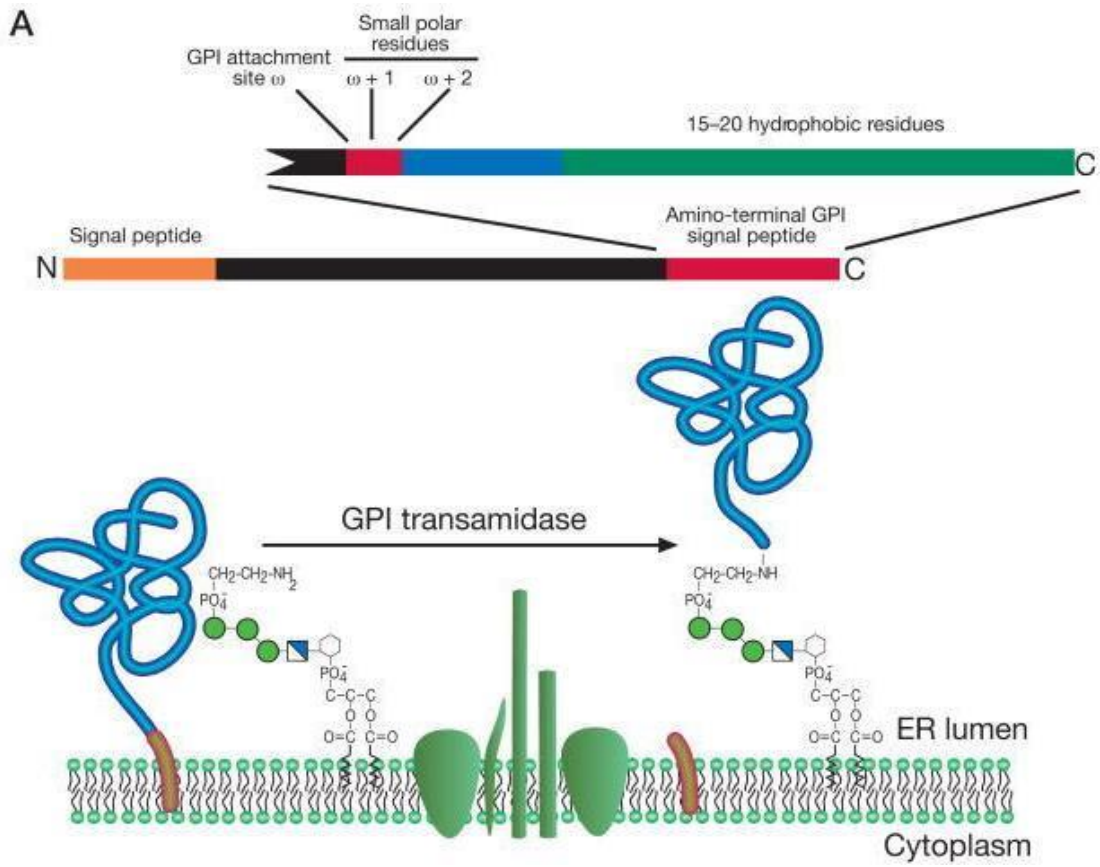

Figure 8. Attachment of GPI-anchor to the peptide. *Features of GPI-anchored proteins and their processing by GPI transamidase. GPI-anchored proteins have an amino-terminal signal peptide and a carboxy-terminal GPI-addition signal peptide (top) that is removed and directly replaced by a GPI precursor (bottom). From (Chatterjee & Mayor 2001).*

2.2 Sorting of GPI-AP

As mentioned already, the GPI-anchor was the first apical sorting signal that was described. Pioneering work demonstrated in 1989 that GPI-APs localize on the apical membrane in MDCK cells and the addition of a GPI-anchor to the ectodomain of a basolateral protein (herpes simplex glycoprotein D) resulted in its apical sorting (Brown et al. 1989; Lisanti et al. 1989). It was further shown that GPI-APs traffic directly to the apical membrane (Lisanti et al. 1990; Paladino et al. 2006; Hua et al. 2006). Early hypothesis link apical sorting of GPI with their inclusion into lipid micro-domains, so called rafts, that might act as apical sorting platforms at the level of the TGN (Simons & Ikonen 1997).

2.3 Lipid raft concept

Lipid rafts as membrane microdomains enriched in cholesterol and sphingolipids, is a concept developed in 1997 by Simons and Ikonen to describe the relative organization of lipids and proteins at the plasma membrane (Simons & Ikonen 1997) (Fig. 9). Lipid rafts were originally characterized biochemically and were isolated as Detergent Resistant Membrane (DRM) fraction (Rajendran & Simons 2005). In this microdomains cholesterol and sphingolipids have a critical role in the segregation of different types of proteins such as GPI-APs, certain transmembrane proteins, and acylated proteins (Simons & Ikonen, 1997). The raft concept improved our understanding of membrane organization; it shed light on protein mobility and activity regulation inside of lipid bilayer. Raft domains regulate many cellular processes such as protein sorting, endocytosis, virus and bacterial infection, and cell signaling (Harder & Sangani 2009; Parton & Richards 2003; Pike 2003; Simons & Gerl 2010; Simons & Toomre 2000). Following the first biochemical detergent extraction, which cannot represent lipid domains but simply describe the biochemical properties of proteins and lipids, biophysical studies in model membranes have generated an enormous body of literature to better characterize these domains *in vitro* (Brown 2006; Sonnino & Prinetti 2013).

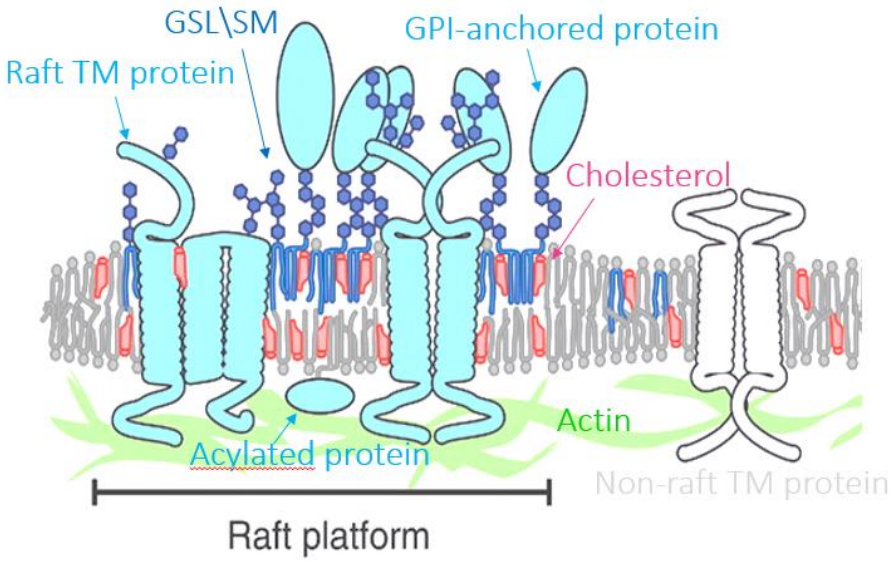

Figure 9. Lipid raft concept. *Rafts are membrane microdomanes enriched in cholesterol and sphingolipides (Simons & Ikonen 1997). Rafts are involved in: endocytosis, signalling, viral, bacterial infections and protein sorting. The lipid density of a raft affects the function of embedded proteins, suggesting that the cell membrane might play an active role in regulating protein function. Picture modified from (Lingwood & Simons 2010).*

Because the size of rafts is below the classical optical resolution of fluorescence microscopy, biophysical techniques with exquisite sensitivity have been developed and used to better understand the nature of lipid micro-domains and how proteins are organized within this domain. Thanks to the improvement of many biophysical approaches in 2015, including SPT, FRET, N&B, FCS, FRAP, and super-resolution microscopy, recent evidence support the fact that the plasma membrane is organized in microdomains enriched in cholesterol and sphingolipids, segregating lipids and proteins and that this contributes to the regulation of their functions (Paladino et al. 2014; Paladino et al. 2015).

2.4 GPI-AP are associated with lipid rafts

GPI-APs associate with DRMs in TGN, it was shown that GPI-APs acquire resistance to detergent extraction during their transport through the Golgi (Maeda et al. 2007; Fujita & Kinoshita 2012), and co-migrate with glycosphingolipids and cholesterol on sucrose density gradients (Brown & Rose 1992; Zurzolo et al. 1994). In different epithelial cell lines some GPI-APs are sorted basolaterally while still associated with DRMs (Zurzolo et al. 1993; Paladino et al. 2004; J. Benting et al. 1999; Sarnataro et al. 2002), indicating that association with DRM is not sufficient for apical sorting and pushing for the formulation of alternative hypothesis (Fig. 10).

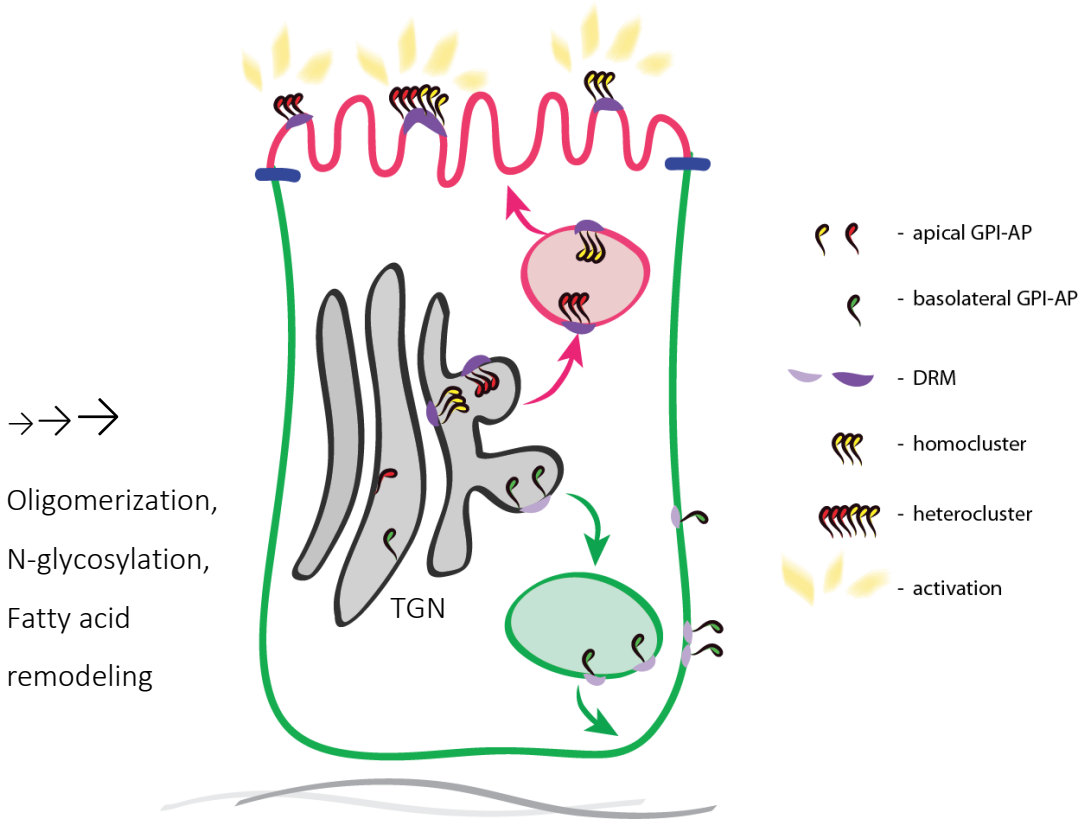

Figure 1O. GPI-AP sorting upon TGN exit in polarized epithelial cells. *A schematic model for the sorting mechanism of GPI-APs at the TGN in polarized epithelial cells. Upon GPI-lipid remodeling with saturated fatty acid chains in the Golgi, GPI-APs can be segregated from other proteins into sphingolipids and cholesterol-enriched domains. Further segregation would then occur as consequence of the oligomerization process that might involve putative luminal receptors binding either the ectodomain or the lipid anchor. Vesicle formation and budding might derive from the coalescence of lipid domains that are driven by the protein oligomerization. On the apical membrane GPI-APs form heteroclusters. Importantly oligomerisation of GPI-APs was shown to contribute to their activity (Paladino et al. 2014). Note that the mechanism of basolateral sorting is not detailed for clarity.*

Work from our and other laboratories has unraveled the mechanism of apical sorting of GPI-AP showing that both association of GPI-APs with detergent resistant membranes (DRMs) and clustering in high molecular weight (HMW) clusters in the Golgi are necessary (Paladino et al. 2014; Paladino et al. 2004; Schuck & Simons 2004) (Fig. 11). Indeed we have demonstrated that

the ability to form high-molecular-weight complexes or clusters at the Golgi is a specific property of apical GPI-APs compared to basolateral ones and is required for apical sorting (Paladino et al. 2004; Paladino et al. 2014) (Fig. 10; Fig. 11).

Furthermore, oligomerization appears to be an essential step for GPI-AP apical sorting in different epithelial cells, as its impairment results in their miss-sorting to the basolateral domain (Paladino et al. 2007; Paladino et al. 2004; Imjeti et al. 2011). Oligomerization might promote apical sorting by increasing the affinity of apical GPI-APs for rafts (Paladino et al. 2015), as previously suggested in the case of cluster induced sorting of GPI-APs in early endosomes (Fivaz et al. 2002; Howes et al. 2010). There is a hypothesis, that a growing bud of clustering GPI-APs could facilitate protein sorting by recruiting curvature-preferring proteins into the lipid raft platform, further increasing the propensity to generate curvature in a feedback loop (van Meer & Vaz 2005; Tian & Baumgart 2009; Huttner & Zimmerberg 2001; McMahon & Gallop 2005; Kuzmin et al. 2005). Thus, the mechanism of oligomerization of GPI-APs could have a double role: first, it would enable GPI-APs to be segregated from the remainder of the proteins in Golgi membranes and, second, it would drive the budding of an apical vesicle, inducing coalescence of “raft-like” domains (Muñiz & Zurzolo 2014).

Interestingly, recent data from our lab have shown that oligomerization plays an important role not only in GPI-AP trafficking, but also in the modulation of their biological activity. Upon clustering in the Golgi and sorting to the apical membrane GPI-APs become fully functional and achieve their catalytic activity (Paladino et al. 2014), (Fig. 10; Fig. 11).

What is promoting GPI-APs oligomerization in the Golgi and subsequent apical transport? It was shown in MDCK that clustering is cholesterol dependent (Paladino et al. 2007; Lebreton et al. 2008). One of hypothesis of apical GPI-APs sorting is linked to the N-glycosylation (see above in “apical sorting signals”). Our laboratory has shown that in some epithelial cells (FRT) N-glycosylation is necessary for the apical sorting, but this mechanism isn’t active in other epithelial cell line, notably MDCK (Imjeti et al. 2011)

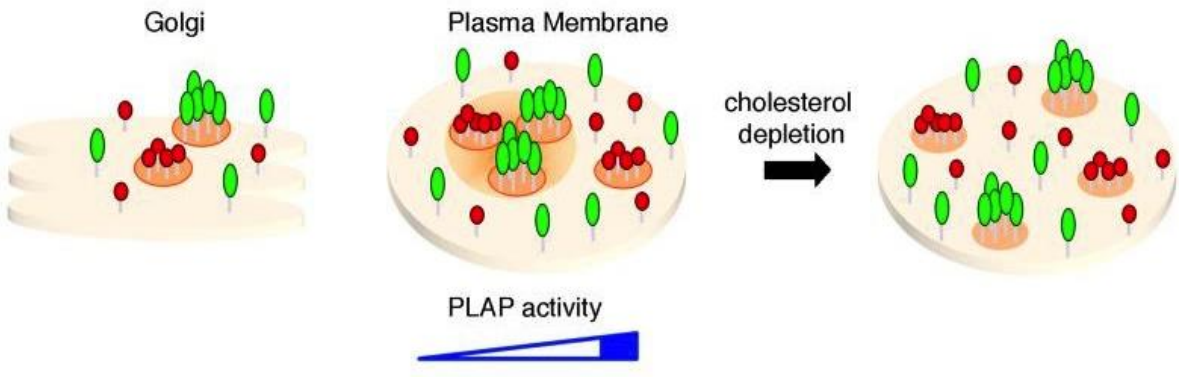

Figure 11. Model of GPI-APs organization in MDCK cells. Apical GPI-APs form clusters in TGN, this clusters are small and they are composed of one species of GPI-APs (homocluster). Once exported to the apical membrane homoclusters associate together in bigger structures, composed of many different GPI-APs species (heterocluster), which are cholesterol dependent. Basolateral GPI-APs do not form clusters (not shown here). Clustering was shown to be crucial for GPI-AP functioning and activity. Adapted from (Paladino et al. 2014).

Another question is whether oligomerization is sufficient, or there are supplementary mechanisms, that result in the sorting of GPI-APs into apically delivered vesicles (Paladino et al. 2004; Paladino et al. 2007). Morphological studies indicate that GPI-APs are segregated from transmembrane proteins in the TGN, from where they exit in distinct vesicles (Keller et al. 2001; Guerriero et al. 2008; Lebreton et al. 2008). In addition, it has been reported that GPI-AP-carrying vesicles emerge from large Golgi domains with a spherical appearance, in contrast to the elongated Golgi extensions from which basolateral carriers appear to arise (Luini et al. 2005). The process of carrier generation probably does not rely exclusively on lipid clustering. Membrane-bending factors such as BAR-domain-containing proteins (Overath & Engstler 2004) or the insertion of a small amphipathic or hydrophobic wedge to induce membrane asymmetry and curvature (McMahon & Gallop 2005) are likely to be required (Muñiz & Zurzolo 2014).

It is also unclear whether specific cargo receptors and coat proteins on the cytosolic side are required for the formation of vesicles that contain raft components, including GPI-APs. GPI-AP oligomerization and, consequently, raft clustering could be promoted by a variety of raft-associated proteins (Schuck & Simons 2004). For instance, the protein VIP17/MAL has been shown to be required for the apical delivery of some, but not all GPI-APs (Cheong et al. 1999; Martin-Belmonte et al. 2000). Other factors, including caveolins, flotillins and stomatin, and

raft-associated oligomerizing proteins have also been hypothesized to promote GPI-AP clustering proteins (Schuck & Simons 2004; Muñiz & Zurzolo 2014).

The one exception to direct apical sorting of GPI-APs in MDCK cells for a native GPI-AP is the Prion Protein (Sarnataro et al. 2002).

2.5 GPI-AP endocytosis

GPI-APs undergo clathrin- and caveolin- independent endocytosis through morphologically identified clathrin-independent carriers (CLICs) (Sabharanjak et al. 2002; Nichols et al. 2001; Sharma et al. 2002; Howes et al. 2010; Maeda & Kinoshita 2011; Fujita & Kinoshita 2012). GPI-APs are considered to enter early endosomal organelles referred to as GPI-enriched early endosomal compartments (GEECs) that also include fluid-phase markers. Dominant-negative mutants of Arf1 and Cdc42 have been shown to perturb endocytosis of GPI-APs into GEECs (Kumari & Mayor 2008; Fujita & Kinoshita 2012). In contrast to clathrin-coated pits GPI-APs are generally taken up slowly with a half-time in the order of minutes to hours and are retained in the endosomes longer than clathrin-mediated endocytic proteins in cholesterol- and sphingolipid-dependent manners (Chatterjee 2001; Mayor et al. 1998). The rho-GAP domain containing protein GRAF1 was identified as a necessary element of CLIC/GEECs structures and therefore GPI-APs internalization (Lundmark et al. 2008).

3 Prion Protein

I have studied a particular GPI-AP – the Prion Protein (PrP). Its trafficking in polarized cells is exceptional; moreover, dysfunctions of PrP traffic may lead to the development of neurodegeneration.

PrP is a ubiquitously expressed GPI-AP that exists in 2 forms, cellular and pathological. While the misfolded PrP^{Sc}, or Scrapie, isoform is the infectious agent of prion diseases, while the cellular isoform (PrP^{C}) is an enigmatic protein of controversial function.

3.1 PrP expression and structure

Prion protein, also known as CD230 (cluster of designation 230), is encoded by a conserved single-copy gene (*PRNP)*, which is positioned on the short arm of chromosome 20 in humans. The human *PRNP* comprises two exons separated by a single intron with the entire open reading frame (ORF) located in exon two (Puckett et al. 1991). The *Prnp* of mice, sheep and cattle contains three exons with the protein coding sequence located in the third exon (Carlson et al. 1994; Basler et al. 1986). The prion protein gene is highly conserved across species. In mammals, the DNA sequence of the ORF encoding PrP generally exhibits around 90% similarity (Schätzl et al. 1995; Wopfner et al. 1999). PrP is ubiquitously expressed, with an enrichment in nervous and immune systems (Kretzschmar et al. 1986; Ford et al. 2002).

PrP contains several distinct domains, including an N-terminal signal peptide, an octapeptide repeat (OR) region, a central hydrophobic region, and a C-terminal hydrophobic portion that functions as a signal for addition of a GPI anchor (Fig. 12).

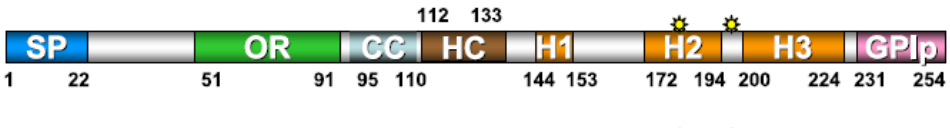

Figure 12. Linear representation of translated sequence of the prion protein. *Amino acid numeration is for mouse PrP. Signal peptide (SP) and GPI anchor signaling peptide (GPIp) are removed during post-translational PrP processing. Octapeptide repeat domain (OR) and charged cluster (CC) constitute the N-terminal part of PrP; hydrophobic core (HC) and α-helix domains (H1, H2, H3) form a C-terminal part. Adapted from (Linden et al. 2008).*

The mature prion protein can be divided in two parts, a flexible and unstructured N-terminal region and a C-terminal globular region arranged in three α-helices interspersed with an antiparallel β-sheet (Fig. 13).

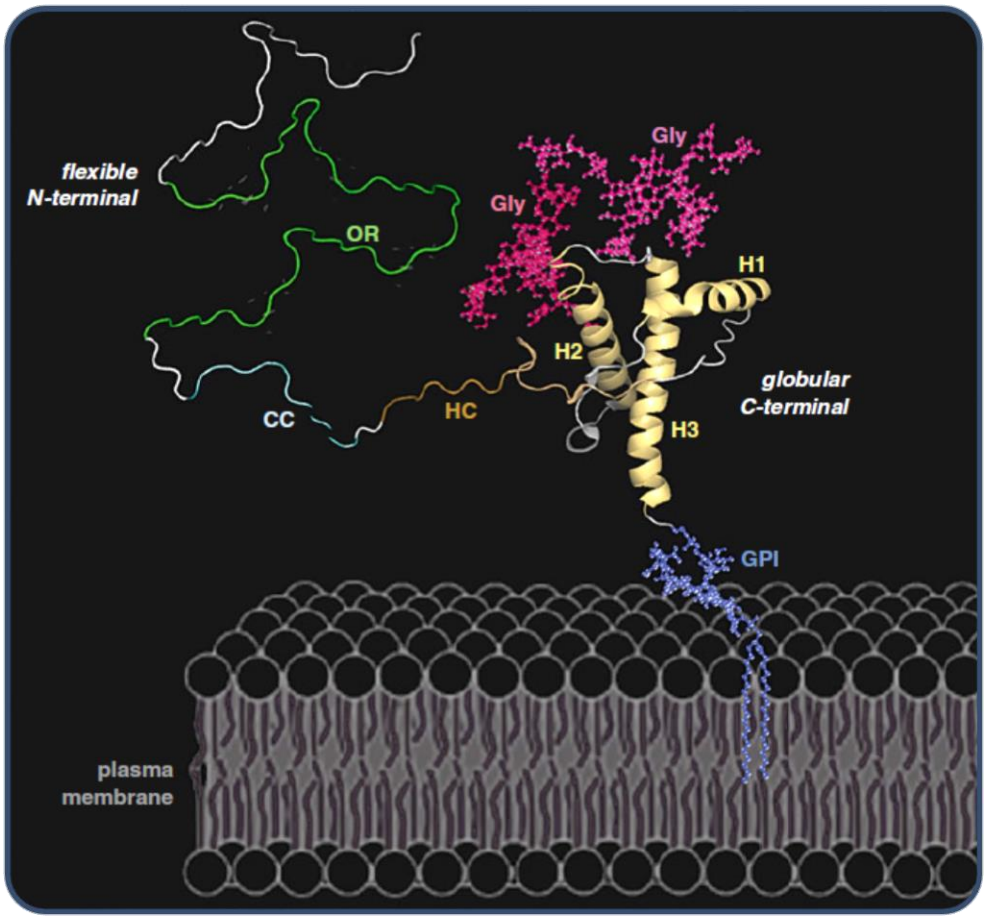

Figure 13. The three-dimensional representation of PrP at approximate scale. Globular C-terminal domain contain three α-helices and a short anti-parallel β-sheet, this structure drawing is based on mouse PrP121-231 structure. Flexible N-terminal tail is unstructured and was freely drawn by R. Linden, V. Martins and M. Prado according to the amino acid number (Choi 2012).

PrP is a GPI-AP and therefore, like other GPI-AP it is attached to the outer leaflet of the cell membrane and the whole protein epitope is exposed to the extracellular space. Like other GPI-AP PrP is synthesized in the ER and follows the exocytic pathway to reach the cell surface. But PrP is in several ways an exceptional GPI-AP. First of all, differently from other GPI-APs the anchor of PrP contain N-acetylneuraminic acid, that is the predominant sialic acid found in mammalian cells (Stahl et al. 1992) (Fig. 14). Interestingly, there is a hypothesis, that the prion

toxicity is linked to the presence of sialic acid in the GPI-anchor. It was proposed that the aggregation of PrP^{Sc}, or the cross-linkage of PrP^{C}, causes the clustering of sialic acid-containing GPI anchors at high densities, resulting in altered membrane composition, the pathological activation of cPLA2, and synapse damage (Bate & Williams 2012). Of note, these effects were not seen after cross-linkage of Thy-1.

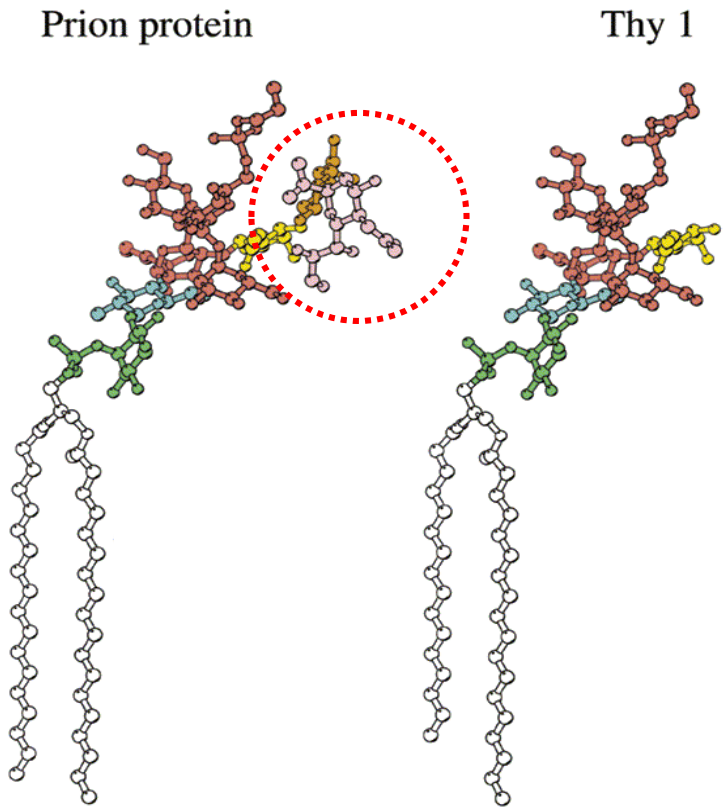

Figure 14. GPI-anchor of PrP. *Comparison of the GPI anchors from the prion protein (left) and a neuronal GPI-AP Thy-1 (right). Sugar residues are coloured as follows: green, inositol; blue, glucosamine; brown, mannose; yellow, N-acetylgalactosamine; orange, galactose; and pink, N-acetylneuraminic (sialic) acid, also surrounded by a red circle. Adapted from (Rudd et al. 2001).*

Furthermore, PrP in mammals appears to use a particular set of cofactors for its biosynthesis. Indeed in a screening for the factors essential for proper GPI synthesis and traffic it was shown that in case of PrP there are several co-factors (SEC62 and SEC63), that are not essential for other GPI. Also PrP do not use several cofactors essential for other GPI-APs synthesis and traffic (PIGN, PIGF, PGAP2, SPPL3). Nevertheless over 23 cofactors are overlapping between PrP and other GPI-APs (Davis et al. 2015).

PrP has 2 N-glycosylation sites therefore PrP exists as di-, mono-, or unglycosylated forms with respective molecular weights of around 34, 28 and 26 kb (Russelakis-Carneiro et al. 2002). The N-linked oligosaccharide chains added initially in ER are modified in the Golgi to yield a complex chain that is resistant to endoglycosidase H (Caughey 1991; Caughey et al. 1989) but can be cleaved off by Peptide-N-glycosidase F (PNG^{ase} F), giving rise to a 26 kDa full length PrP. PNGase F treatment of a cell lysate is a helpful tool, allowing to identify the size of PrP, PrP mutants and cleavage fragments (Fig. 15).

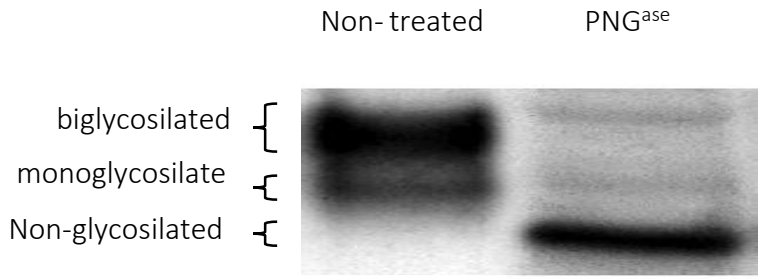

Figure 15. Glycosylation of PrP monitored by Western blot. *Example of PrP western blot; on the left the three differently glycosylated moieties of PrP^C (non-, mono-, and diglycosylated) and on the right deglycosylated PrP after treatment with PNG^{ase} F.*

As for all glycoproteins the glycosylation patterns may affect PrP trafficking. Neurons from transgenic mice producing only non-glycosylated PrP mutant are showing altered trafficking with PrP accumulation in the Golgi (Cancellotti et al. 2005). Nevertheless this transgenic mice don't exhibit any pathological signs, suggesting that trapping of PrP in the Golgi does not contribute to the neurodegeneration.

3.2 PrP function(s)

The physiological role of PrP^C still remains highly uncertain despite more than two decades of research and numerous proposed functions (Martins et al. 2010).

Knockout approach does not give clear-cut answer of PrP function(s). There is no lethal and no major phenotype in mice (Mallucci et al. 2002) but diverse subtle phenotypes such as mild cognitive and behavioral deficits (Büeler et al. 1992), altered circadian rhythms (Tobler et al. 1996), altered olfaction (Le Pichon et al. 2009), abnormalities in neuronal electrical activity (Collinge et al. 1994), defective proliferation and differentiation of neural precursor cells (Steele et al. 2006) and hematopoietic stem cells (Zhang et al. 2006), increased sensitivity to hypoxia, ischemia, and seizures (Spudich et al. 2005), enhanced resistance to microbial infections (Watarai et al. 2003) and myelin maintenance defects (Bremer et al. 2010).

Contrary to mammals, in zebrafish knockdown of *PrP* led to severe biological phenotypes: gastrulation arrest and malformations of the brain and the eyes (Málaga-Trillo et al. 2009; Malaga-Trillo & Sempou 2009; Nourizadeh-Lillabadi et al. 2010). It was postulated that this severe phenotype was linked to PrP function in cell-to-cell interactions, and in E-caderins trafficking; but most likely in mammals, these PrP functions are redundant with other cellular proteins (Petit et al. 2013).

Interestingly, accumulating evidences suggest that PrP plays a role of a receptor and is involved in signal transduction. Early work by Mouillet-Richard and colleagues showed that engagement of PrP by antibodies leads to activation of the soluble tyrosine kinase Fyn. Subsequently they have shown that PrP clustering activates NADPH oxydase, ERK1/2 kinase and leads to CREB-dependent gene regulation. Based on that Dr. Mouillet-Richard and Dr. Schneider continuously publish new details of signal transduction through prion protein (Kellermann et al. 2002; Loubet et al. 2012; Mouillet-Richard et al. 2005; Pietri et al. 2006; Pradines et al. 2013). Martins, Prado and Linden groups also demonstrated a PrP mediated signal transduction through cyclic AMP/protein kinase A and MAP kinase pathways (Chiarini et al. 2002). They work led to the identification of Hop/STI1 as a physiological binding partner of PrP and the mapping of their cognate binding domains (Americo et al. 2007; Arruda-Carvalho et al. 2007; Zanata et al. 2002).

A striking discovery was made by Strittmatter laboratory in 2009: it was shown that PrP is directly involved in Alzheimer disease and act as a receptor for amyloid-β (Aβ) (Laurén et al.

2009). Later on it was further shown that PrP-dependent signaling of Aβ actually overlaps with the signaling of STI1, PrP^{Sc} and PrP-antibodies. Among molecules involved in Aβ signaling and previously shown to be PrP partners are NCAM and Fyn kinase (Santuccione et al. 2005; Um et al. 2012); mGluR1 and mGluR5 (Santos et al. 2013; Rodríguez et al. 2006; Um et al. 2012; Beraldo et al. 2011); LRP1 (Rushworth et al. 2013; Hooper et al. 2008). It is important to mention that Aβ is inducing Tau phosphorylation through Fyn kinase on a PrP dependent manner, thus pointing towards the relevance of PrP in the Alzheimer disease (Larson et al. 2012).

3.3 Prion disorders

Because PrP is involved in human and animal diseases, this protein has been extensively studied. Prusiner discovered the prion protein in 1998 while he was looking for the infectious pathogen involved in the transmissible spongiform encephalopathies (TSEs). TSE are severe, incurable fatal neurodegenerative diseases. Nowadays it is widely accepted that the PrP protein plays a central role in prion diseases called Creutzfeldt-Jakob disease (CJD) in humans and bovine spongiform encephalopathy (BSE) and chronic wasting disease (CWD) in animals (Blattler 2002; Mastrianni 2010). Like most neurodegenerative disorders, prion diseases are mainly sporadic although a small percentage (about 10% in human) is inherited (Prusiner 1994). Differently from other neurodegenerative disorders, prion diseases are infectious. Transmission of the pathology can occur between individuals and across species through exposure to the infectious prions (e.g; contaminated bovine meat or medical material), raising new variant CJD (vCJD/nvCJD) (Aguzzi & Calella 2009). Prion diseases were presented by rare and isolated cases until the advent of the Bovine Spongiform Encephalopathy (BSE) epidemic, also known as „Mad Cow Disease“, in the 1980s mainly in the United Kingdom. This pathogen has non-conventional features, and could not be shown to associate with any form of nucleic acid and therefore does not fit into any viral model (Chatigny & Prusiner 1980). In 1982 Prusiner has developed a new concept of “prion”, an acronym of “proteinaceous infectious particles” and in 1997 he received the Nobel Prize for this work.

3.4 Prion conversion: PrP^{C} to PrP^{Sc}

Nowadays it is widely accepted that the infectious agent consists of proteinaceous aggregates, called "prions", that derive from the conformational change of the native PrP^{C} into its pathological counterpart, PrP^{Sc} (Prusiner 1998), (Fig. 16). The molecular mechanism underlying prion infectivity is the ability of prions to self-propagate via conversion of endogenous PrP^{C} into pathological PrP^{Sc}. When PrP^{C} is converted to PrP^{Sc}, it undergoes a major biochemical alteration from an α-helical to a ß-sheet conformation (S B Prusiner 1998). PrP^{C} is easily hydrolyzed by proteinase K (PK) digestion, while similar treatment on PrP^{Sc} leaves a PK-resistant core termed PrP27-30 (Prusiner et al. 1988).

Conversion of PrP^{C} in PrP^{Sc} was reproduced in a cell-free system in presence of purified constituents revealing that PrP^{Sc} derived from specific PrP^{C}-PrP^{Sc} interactions (Kocisko et al. 1994; Ryou & Mays 2008; Benetti & Legname 2009; Legname et al. 2004).

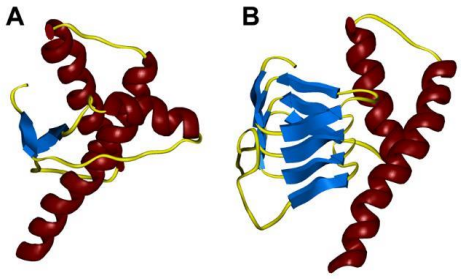

Picture 16. Model of the structure of PrP^{C} (depicted in A) and PrP^{Sc} (depicted in B). *The PrP^{Sc} is suggested to be enriched in parallel left-handed β-helical structures. Modified from (Wille et al. 2002).*

Today there are 2 different models proposed to explain the propagation of PrP^{Sc} by the conversion of PrP^{C} (Fig. 17). In the first one named "refolding" or "template-directed" model (Fig. 17 A) PrP^{Sc} is a template or a matrix for the conversion of PrP^{C} into new PrP^{Sc} monomers (Hsiao & Prusiner 1991). While in the second model (Fig. 17 B) called the "seeded nucleation model" PrP can spontaneously adopt different folding conformations PrP^{C} or PrP^{Sc} that are energetically equivalent (Harper & Lansbury 1997).

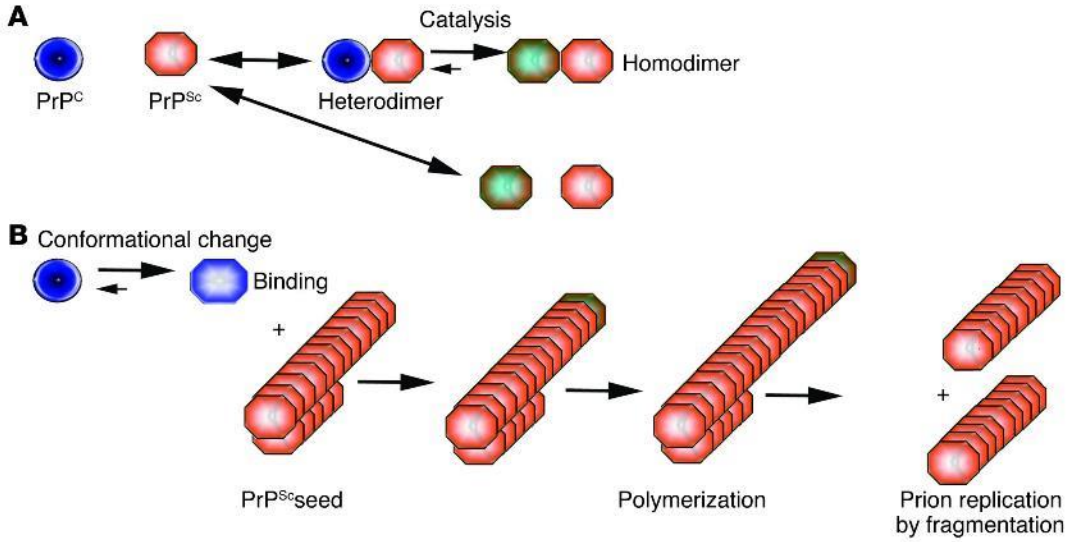

Figure 17. Models of PrP^C to PrP^{Sc} conversion. (A) The heterodimer model proposes that upon infection, the PrP^{Sc} (red) starts a catalytic cascade using endogenous PrP^C (blue) or a partially unfolded intermediate arising from stochastic fluctuations in PrP^C conformations as a substrate, converting it by a conformational change into a new β-sheet–rich protein. The newly formed PrP^{Sc} (green-black) will in turn convert new PrP^C molecules. This model in literature is sometimes called "template-directed refolding model" or "template assistance" (B) The noncatalytic nucleated polymerization model proposes that the conformational change of PrP^C into PrP^{Sc} is thermodynamically controlled: the conversion of PrP^C to PrP^{Sc} is a reversible process but at equilibrium strongly favors the conformation of PrP^C. Converted PrP^{Sc} is established only when it adds onto a fibril-like seed or aggregate of PrP^{Sc}. Once a seed is present, further monomer addition is accelerated, therefore this model is also called the "seeded nucleation" or "nucleation-polymerization model". From (Aguzzi & Miele 2004).

3.5 Site of conversion

It is proposed that prion conversion occurs either at the plasma membrane (Godsave et al. 2013; Rouvinski et al. 2014; Goold et al. 2011) or in the endo-lysosomal pathway where PrP^{C} traffic (Borchelt et al., 1992; Caughey et al., 1991; Magalhaes et al., 2005). In addition it was postulated that the conversion could occur in the TGN (Beranger et al. 2001). Evidences from our laboratory indicate that conversion might occur in the endocytic recycling compartment (Marijanovic et al. 2009). While recent data postulate the involvement of the multivesicular body (Yim et al. 2015).

3.6 Prion propagation

In order to propagate in the infected organism PrP^{Sc} needs to spread between cells. It was shown from our group that cell-to-cell contact greatly increases PrP^{Sc} propagation and a fast spreading of PrP could be mediated by Tunneling nanotubes (TNT), cytoplasmic bridges connecting neighboring cells (Gousset et al. 2009). Other evidences suggest that prions could be spread by exosomes (Fevrier et al. 2004; Fevrier et al. 2005). While exosomal localization of Prions is clear, the mechanism of cell-to-cell transmission in vivo is still a challenging question.

Interestingly, prion propagation and prion toxicity are two distinct processes (Aguzzi & Falsig 2012; Sandberg et al. 2011; Mallucci et al. 2003). It was reported that selective depletion of neuronal PrP^{C} in infected mice is sufficient to prevent neuronal loss and stop the progression of the disease, despite the continuing accumulation of PrP^{Sc} (Mallucci et al. 2003). Thus, accumulation and propagation of PrP^{Sc} is neither toxic nor pathogenic by itself, but absolutely requires the presence of PrP^{C} on the neuronal surface to trigger prion neurotoxicity (Fig. 18).

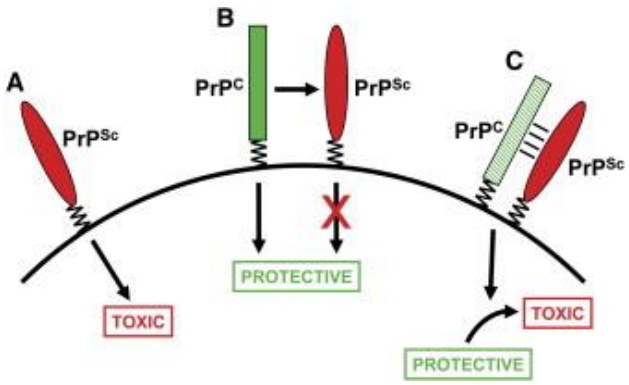

Figure 18. Models for the cellular toxicity of PrP^{Sc}

(A) Toxic gain-of-function mechanism. PrP^{Sc} possesses a novel neurotoxic activity that is independent of the normal function of PrP^{C}. (B) Loss-of-function mechanism. PrP^{C} possesses a normal, physiological activity, in this case neuroprotection, that is lost upon conversion to PrP^{Sc}. (C) Subversion-of-function mechanism. The normal, neuroprotective activity of PrP^{C} is subverted by binding to PrP^{Sc}. Signaling properties of PrP change and a neurotoxic rather than a neuroprotective signal is delivered. In the absence of the GPI anchor attachment of PrP^{C} to the membrane, no signal would be delivered and disease would not occur, as was observed in the study of (Chesebro et al. 2005). Adapted from (Harris & True 2006).

3.7 Trafficking & processing of PrP^{C}

In polarized neurons it was reported that PrP, like other GPI-APs is sequestered to the axolemma of polarized hippocampal neurons and this polarized distribution depends on cholesterol-sphingomielin enriched lipid rafts (Galvan et al. 2005).

Nevertheless the majority of the articles investigating PrP trafficking were made in non-polarized neuronal cells and primary neurons at different polarity stages (Fig. 19). As for many GPI-APs PrP traffic starts with the translocation from the cytosol to the ER, then passage to the Golgi and final arrival to the plasma membrane. Then PrP^{C} unlike other GPI-APs, is internalized in clathrin-coated vesicles (Shyng et al. 1993; Sunyach et al. 2003; Lakhan et al. 2009; Taylor 2005; Taylor & Hooper 2006; Magalhães et al. 2002; Linden et al. 2008). Raft-associated PrP^{C} is sequestered by clathrin-coated pits via the interaction of N-terminal domain of PrP with transmembrane LRP1 protein. Therefore PrP undergoes constitutive clathrin-dependent endocytosis by its engaging with an integral membrane protein (Sunyach et al. 2003; Shyng et al. 1993; Lakhan et al. 2009a; Taylor 2005; Taylor & Hooper 2006; Magalhães et al. 2002; Linden

et al. 2008; Shyng et al. 1995; Lee et al. 2001; Nunziante et al. 2003; Hooper et al. 2008; Taylor & Hooper 2007; Gauczynski et al. 2006; Gauczynski et al. 2001).

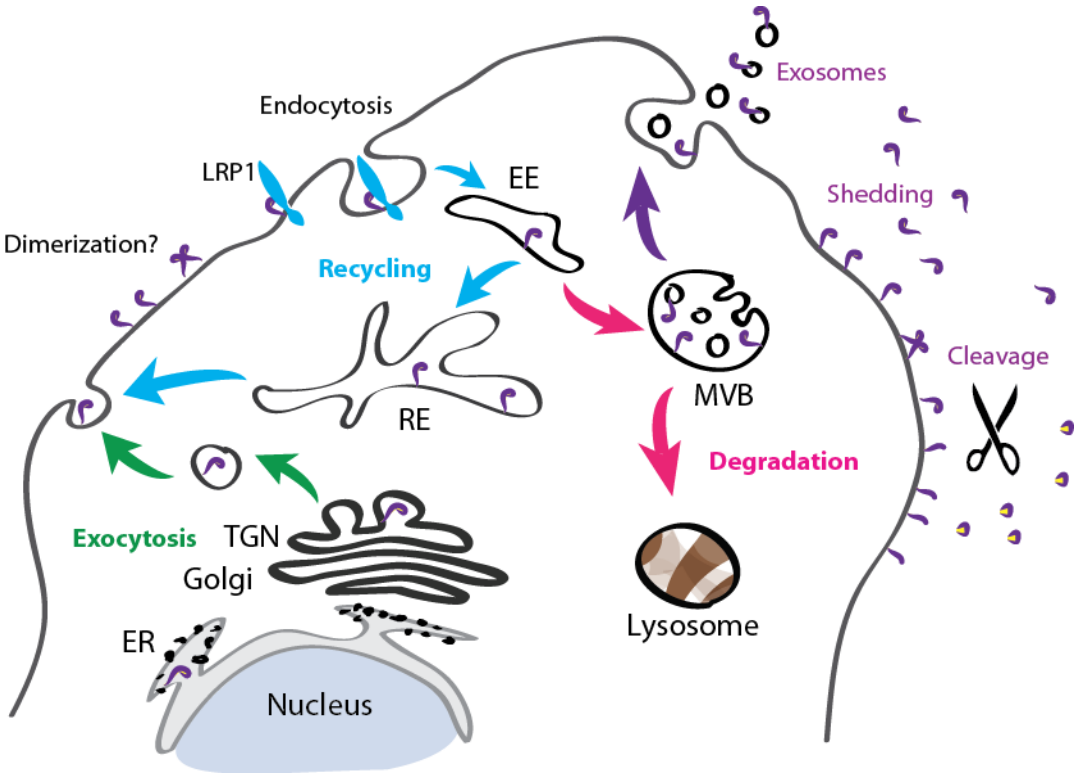

Figure 19. PrP trafficking. *The major vesicular systems involved in the exocytosis is depicted in green, the recycling of PrP is depicted in blue, and lysosomal in red. Secretion of PrP-containing exosomes, shedding and cleavage are indicated in purple. MVB, multivesicular bodies; TGN, trans-Golgi network; RE, recycling endosome; EE, early endosome; ER, endoplasmic reticulum; LRP1, lipoprotein receptor-related protein 1.*

There is a striking impact of PrP trafficking on neurodegeneration. PrP mutant (cyPrP, aa 23-230) having defective entry to the ER leads to the cytosolic accumulation of PrP bearing GPI-signal peptide and devoid of GPI-anchor, causing severe ataxia and cerebellar degeneration in transgenic mice (Drisaldi et al., 2003; Ma et al., 2002). Perturbing proteasome activity (due to cellular stress for example) or inducing ER-stress promotes the accumulation of cytosolic forms of PrP wt that are reported be toxic in neuronal cells (Orsi et al. 2006). It is puzzling that at the same time it was reported in human primary neurons that PrP^{C} accumulation in the cytosol is not toxic, moreover, PrP relocalization to the cytosol contribute to the cytoprotective, Bax-related antiapoptotic function (Roucou et al. 2003).

In addition to the GPI-anchored PrP in the ER there are two transmembrane forms of PrP: C-terminal form (^{Ctm}PrP) and N-terminal form (^{Ntm}PrP). The ^{Ctm}PrP that is favored by certain mutation was suggested to be toxic, and cause neurodegeneration (Hegde et al. 1998; Stewart et al. 2005). Proper association with DRM can be altered by the mutations and also lead to the neurodegeneration (Schiff et al. 2008; Hegde et al. 1998; Goldfarb et al. 1991). Degradation of N-terminal signal peptide is also necessary; point mutations in the GPIsp, M232R/T and P238S, which inhibit proteasomal degradation of the signal peptide (Guizzunti & Zurzolo 2014) are responsible for genetic forms of prion disorders (Guizzunti & Zurzolo 2014; Hoque et al. 1996; Windl et al. 1999).

Finally internalization of PrP seems to be crucial for its cytoprotective PrP function (Americo et al. 2007). In physiological conditions STI1 binding as well as extracellular copper ions induce endocytosis of PrP^{C} to intracellular organelles and to the Golgi (Brown & Harris 2003; Lee et al. 2001; Pauly & Harris 1998). Vice-versa in Alzheimer disease amyloid-beta was reported to bind PrP and retain it on the cell surface (Caetano et al. 2011) from where it would transduce a cytotoxic signal (Laurén et al. 2009).

3.8 PrP & transcytosis

Cellular prion protein as well as its Scrapie isoform were both shown to be able to undertake a transcytotic pathway. While Scrapie prion is using transcytotic road to penetrate the body through the M-cells of the intestinal tract (Kujala et al. 2011; Miyazawa et al. 2010; Heppner et al. 2001), the cellular PrP mediate or at least facilitate amyloid-β transcytosis through the Blood-Brain Barrier (BBB) (Pflanzner et al. 2012). Aβ transcytosis is reduced by genetic knockout of PrP or after addition of a competing PrP antibody in the BBB model (Pflanzner et al. 2012).

It is worth mentioning that the bacteria *Brucella abortus* uses PrP on the surface of M-cells as the receptor for the invasion (Nakato et al. 2012).

Several groups, working on PrP physiology share the idea that PrP is a receptor and also a co-receptor for many molecules (Linden et al. 2012). Taking into account the capacity of PrP to participate in transcytosis it is attractive to suppose that PrP can function as an “extracellular scaffold protein”. It is interesting to hypothesize that PrP is able not only to bind a broad range

of partners (Linden et al. 2008) but also to guide this molecules through the endocytic and/or transcytotic road from one membrane compartment to another.

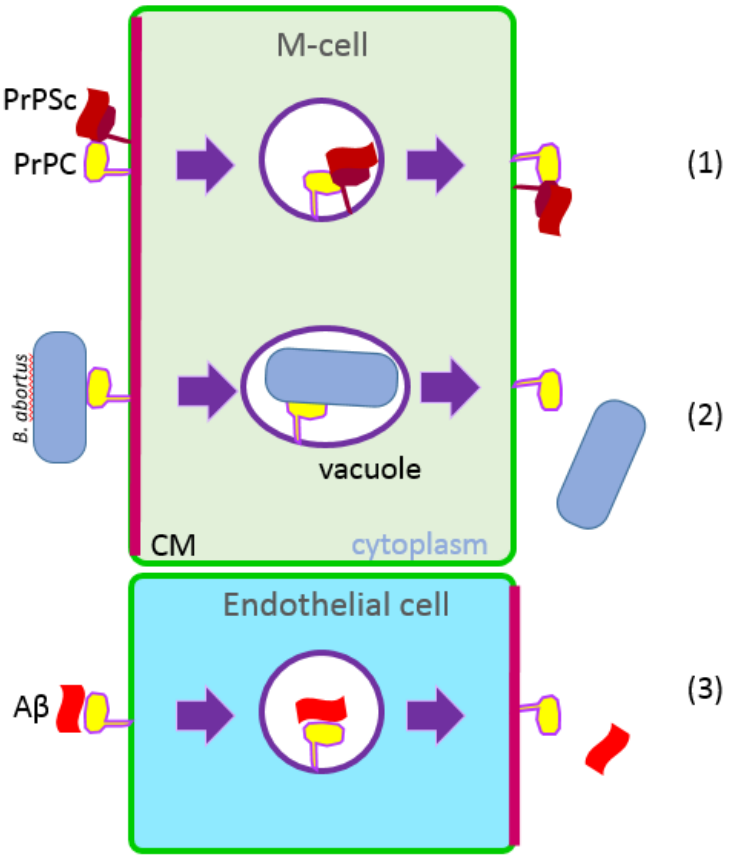

Figure 20. PrP is involved in transcytosis of PrP^{Sc}, B. abortus and amyloid-β. *(1) PrP^{Sc} is using transcytotic road to penetrate the body through the gut (Kujala et al. 2011; Miyazawa et al. 2010; Heppner et al. 2001). (2) Brucella abortus uses PrP^{C} as the receptor for the invasion (Nakato et al. 2012). (3) PrP^{C} mediates or at least facilitates Aβ transcytosis through the Blood-Brain Barrier (Pflanzner et al. 2012).*

3.9 PrP secretion and degradation

An important issue refers to the fate of PrP. While cycling between plasma membrane and recycling compartment at each round of internalization small fraction of endocytosed PrP is degraded by lysosomes, but large fractions return to the cell surface (Shyng et al. 1993). In addition to classical lysosomal degradation there are at least three more ways PrP can disappear from the cell membrane: secretion in exosomes, shedding and cleavage.

3.10 Exosomes

Work, originally intended to understand the intercellular transfer of PrP^{Sc}, has led to evidence that part of the recycled PrP may be secreted to the extracellular medium associated with exosomes (Fevrier et al. 2005; Robertson et al. 2006; Fevrier et al. 2004). Exosomes are single membrane vesicular structures around 50 to 100 nm in diameter, deriving from the multivesicular bodies (MVBs) formed within the endosomal system (Hurley 2015).

Exosome secretion into the extracellular matrix occurs upon fusion of MBVs with the cell membrane thus releasing their internal exosomes outside the cell. Exosomes have been associated with transfer of wide variety of signals between cells (Schneider & Simons 2013; Milane et al. 2015). Recent study by Chivet and colleagues has emphasized the specificity of exosomal signaling (Chivet et al. 2014). In fact, exosomes covered by cellular PrP may allow cellular interactions, such as cell-cell signaling transduction. Regarding the relevance of exosomes for the prion infection: Vella and colleagues found that exosomes from infected cells could also produce prion disease when inoculated into mice (Vella et al. 2007).

3.11 Shedding

PrP undergoes shedding, meaning the detachment of the protein from the cell surface leading to its diffusion into the extracellular space. A secreted form of full length PrP was first found in early nineties in both the medium of cultured cells and the human cerebrospinal fluid (Borchelt et al. 1993; Harris et al. 1993). Soluble PrP is present in the medium of multiple cultured cells and in blood (Borchelt et al. 1993; Li et al. 2003; Borchelt 1990; Caughey et al. 1989; Parkin et al. 2004; Perini et al. 1996; MacGregor et al. 1999; Parizek et al. 2001). However, the exact mechanism(s) by which soluble PrP is shed from cells is still not clear. In SHY5 cell line PrP detaches from the membrane devoided of GPI-anchor and as GPI-anchored form suggesting that both phospholipases and proteases contribute to its shedding (Parkin et al. 2004; Taylor et al. 2009; Zhao et al. 2006). As for proteolytic shedding it is most likely due to the metalloprotease ADAM10 (Altmeppen et al. 2015; Cissé et al. 2005; Jiménez-Huete et al. 1998; Heiseke et al. 2008; Altmeppen et al. 2011). Regarding the role in prion infection, in mice model lack of ADAM10 reduces disease incubation time and increases PrP^{Sc} formation, suggesting a protective role of ADAM10 mediated shedding in prion infection.

3.12 PrP cleavages

PrP is subjected to two well characterized (α and β) and one recently discovered (γ) cleavages (McMahon et al. 2001; McDonald et al. 2014; Liang & Kong 2012; Chen et al. 1995; Harris et al. 1993; Lewis et al. 2015). The most common is the α-cleavage that occurs between the amino acid residues 110 and 111 (mouse) generating a 11-kDa soluble N-terminal fragment called N1 and a 18-kDa GPI-anchored C-terminal fragment called C1 (Liang & Kong 2012; Harris et al. 1993), (Fig. 20).

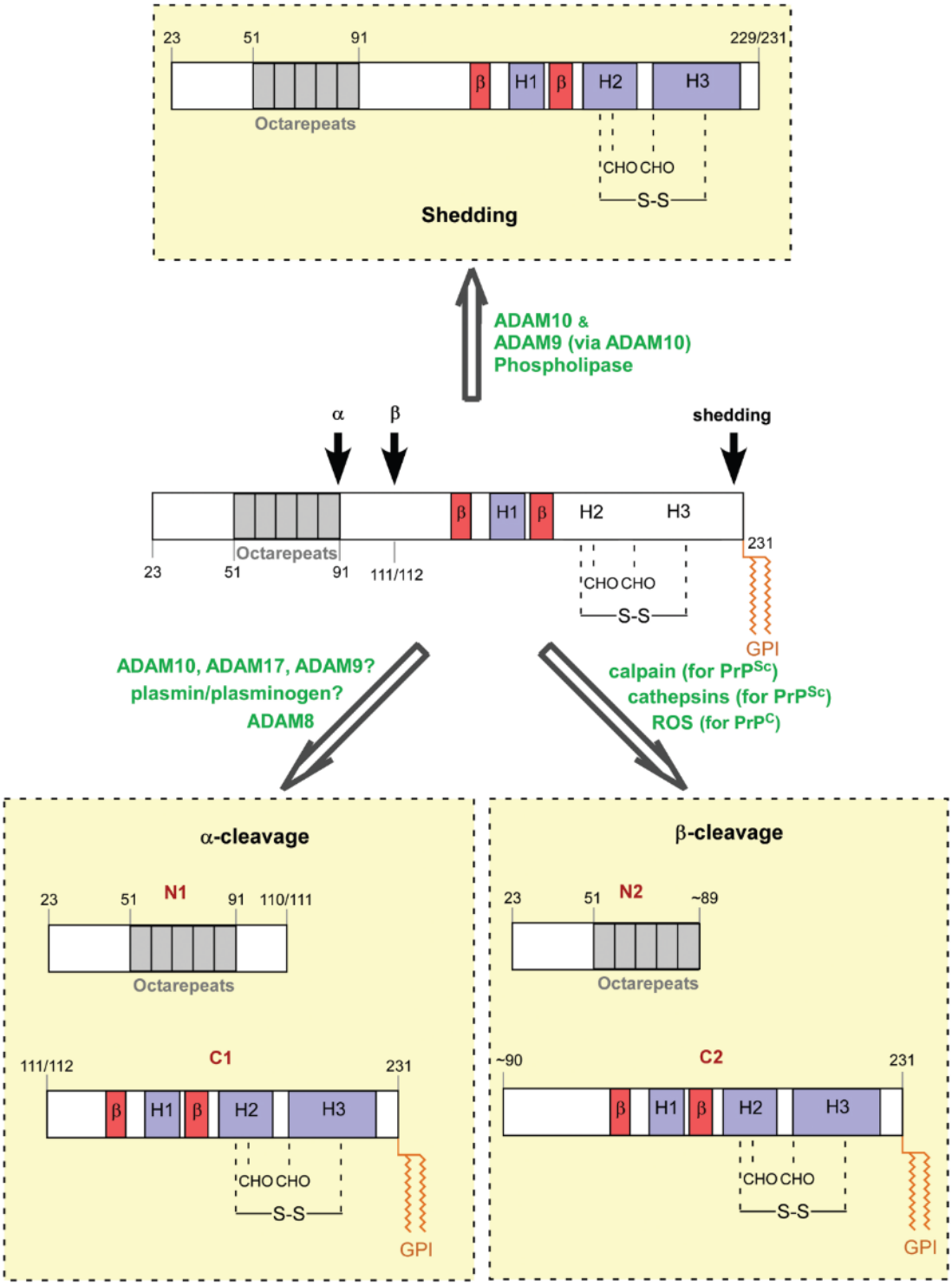

Figure 20. Schematic diagram of PrP processing. *PrP is known to undergo α-cleavage, β-cleavage, and shedding. The amino acid numbering is based on human PrP. CHO- N-glycans; -S-S - disulfide bridge; ROS - reactive oxygen species. The enzymes/factors potentially involved in the cleavage are in green, question marks are marking contradictory data. From (Liang & Kong 2012).*

3.13 Physiological α-cleavage

α-cleavage is the most common physiological PrP processing; C1 fragment is found in the healthy brain with some inter-individual variability (Chen et al. 1995). The overall function of the α-cleavage is still elusive, on one hand it can be a mechanism depleting PrP full-length and thereby limiting its activity, and on the other hand PrP cleavage can be a mechanism of functional molecule generation. PrP cleavage fragments received considerable attention and they were shown to be biologically active and several functions have been described (Liang & Kong 2012; Turnbaugh et al. 2011; Guillot-Sestier & Checler 2012).

The N1 fragment has an anti-apoptotic, neuroprotective function (Turnbaugh et al. 2011; Guillot-Sestier et al. 2009). It has also been suggested that the N1 fragment could interfere with Aβ associated toxicity by direct binding to soluble oligomeric Aβ peptides (Fluharty et al. 2013; Chen et al. 2010; Guillot-Sestier et al. 2012). Interestingly Aβ induces α-cleavage and produced N1-fragment mediates neutralization of amorphous Aβ aggregates (Béland et al. 2014).

While N1 is soluble, C1 accumulates at the cell surface (Shyng et al. 1995). C1 inherits from PrP full-length not only the GPI anchor, but also N-glycosylation sites, making C1 migration pattern in Western Blot as complex as PrP pattern itself. On its own C1 has been shown to interfere with prion infection (Westergard et al. 2011).

Interestingly when expressed in transgenic mice, PrP mutants bearing large deletions around the α-cleavage site induced a rapid lethal phenotype directly connected to a complete inhibition of the α-cleavage (Li et al. 2007; Baumann et al. 2007).

Where does the α-cleavage occur?

The cellular site where α-cleavage occurs as well as the enzyme(s) responsible for this cleavage are highly debated. On one hand Aguzzi's laboratory claims that PrP is most likely cleaved on the plasma membrane (Bremer et al. 2010; Oliveira-Martins et al. 2010) but other laboratories

accumulated data suggesting that endosomal/lysosomal compartments and late compartments of the secretory pathway could be the site of PrP^C cleavage (Walmsley *et al.*, 2009; Tveit *et al.*, 2005; Taraboulos *et al.*, 1995; Shyng *et al.*, 1993).

What is the enzyme(s) responsible for a-cleavage?

The most discussed enzyme family, related to PrP cleavage is ADAM (a disintegrin and metalloproteinase) enzymes. Unfortunately there is no consensus in the scientific community about the PrP α-cleavage so far, each enzyme is surrounded by a cloud of contradictory data (Liang & Kong 2012).

It has been suggested that ADAM10 and TACE (ADAM17) are involved in the α-cleavage of PrP (Vincent et al. 2001; Jiménez-Huete et al. 1998; Laffont-Proust et al. 2005; Taylor et al. 2009), but opposite data have also been reported (Altmeppen et al. 2013; Altmeppen et al. 2011; Endres et al. 2009; Vincent et al. 2001; Jiménez-Huete et al. 1998). Further investigations are needed to determine the role of ADAM10 and ADAM17 in PrP cleavage.

In a recent publication, ADAM8 was shown to directly cleave PrP in the skeletal muscle (Liang et al. 2012) as well as *in vitro* (McDonald et al. 2014).

For a very long time an accurate *in vitro* study was missing (Linden et al. 2008; Liang & Kong 2012). Last year two *in vitro* studies addressing PrP cleavage were published (Kojima et al. 2014; McDonald et al. 2014). McDonald and colleagues have shown that ADAM8 in cell free system cleaves mouse PrP at K109*H110 the previously proposed location of α-cleavage. Upon the addition of Cu^{2+} and Zn^{2+} ADAM8 changed the cleavage pattern to β-cleavage at the octapeptide repeat region. ADAM10 and ADAM17 have been validated for α-cleavage, in addition there is a novel cleavage site for both ADAM10 and ADAM17: A119*V120. In addition

McDonald and colleagues showed that ADAM10 is responsible for the PrP shedding by cleaveing PrP near the C terminus (Fig. 21).

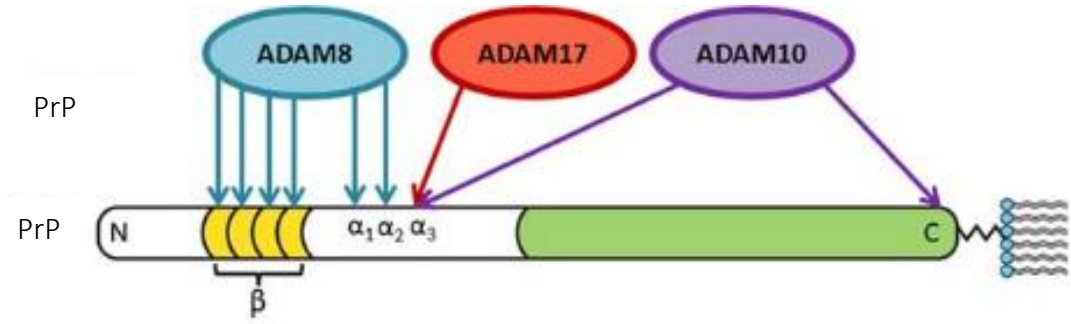

Figure 21. Schematics of PrP cleavage, reported by McDonald and colleagues. *Plasma membrane and the GPI-anchor on the right, ocapeptide repeats (yellow) on the left. Cleavage is depicted as a flash, pointing at the cleavage site. Adapted from (McDonald et al. 2014).*

PrP cleavage is more complex than previously thought; the physiological cleavage *in vivo* is far from being clear.

3.14 Pathological β-cleavage

The second well-studied cleavage event is the β-cleavage. Upon this process PrP is cleaved around the end of the octapeptide repeat region (around aa 80-100) to generate C2 and N2 fragments (Mangé et al. 2004; Jiménez-Huete et al. 1998; Pan et al. 1992; Taraboulos et al. 1992). This proteolytic processing was mostly reported in the context of prion infected models, although this process can also be detected in non-infected conditions (McMahon et al. 2001; Yadavalli et al. 2004; Dron et al. 2010; Liang & Kong 2012), (Fig. 20).

What is the enzyme(s) responsible for β*-cleavage?*

Calpain (Yadavalli et al. 2004) and cathepsin (Dron et al. 2010) are the enzymes responsible for the β-cleavage when the main substrate is prion PrP^{Sc}. On the contrary, when cellular PrP is the substrate of the β-cleavage the main actors are reaction oxygen species (ROS) (McMahon et al. 2001; Watt et al. 2005).

β-cleavage does not appear to have any role in the cell physiology of PrP^C as well as for the disease development (Guillot-Sestier et al. 2009; Sunyach et al. 2007).

3.15 γ-cleavage

A new PrP cleavage was described this year by Lewis and colleagues, they have named it γ-cleavage and the resulting PrP fragments were named N3 and C3 (Fig. 22).

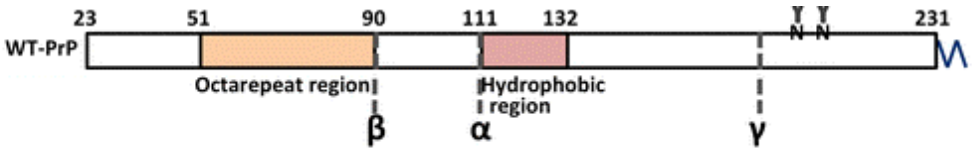

Figure 22. New γ-cleavage site. *N-terminal part, containing octarepeats is marked in orange, central hydrophobic region in red, GPI-anchor in blue. α,β and γ cleavage sites are indicated. Of note the site of proteolytic shedding, situated next to GPI-anchor is not indicated. Adapted from (Lewis et al. 2015).*

Only specific distal C-terminal anti-PrP antibodies can detect C3, therefore this fragment was not described before, C3 is not recognized by the majority of PrP antibodies. Of interest a small GPI-anchored C-terminal fragment of the same size of C3 was found in several cell lines and, more important, in the postmortem brain lysate of individuals diagnosed with CJD (Lewis et al. 2015).

What is the enzyme(s) responsible for β*-cleavage?*

Candidates for the enzyme performing γ-cleavage are matrix metalloproteases as shown by an inhibitor array (same family as for α-cleavage). As C3 fragment was found mostly in the cell lines and in brains of human suffering from sporadic CJD the question of functionality and relevance for the prion disease remains to be elucidated (Lewis et al. 2015).

Dissecting the intracellular trafficking of the PrP cleavage fragments, as well as of the full-length, is of major relevance for the PrP functions and most likely for the pathogenesis of the prion diseases.

3.16 PrP traffic in MDCK cells.

MDCK do not express endogenous PrP, therefore a transfection of cDNA encoding for PrP under a strong promoter is necessary. MDCK expressing PrP wt was used by many laboratories to study polarized PrP traffic.

The Prion Protein is the only native GPI-AP that was shown not to be apically sorted when transfected in MDCK cells. In 2002 work from our laboratory showed that mouse PrP^C localizes on the basolateral membrane of fully polarized MDCK and FRT cells grown on filters (Sarnataro et al. 2002). Several groups have later addressed the distribution and intracellular trafficking of PrP in polarized MDCK cells (Uelhoff et al. 2005; De Keukeleire et al. 2007; Christensen & Harris 2009; Puig et al. 2011) and obtained contradictory results (Fig. 23).

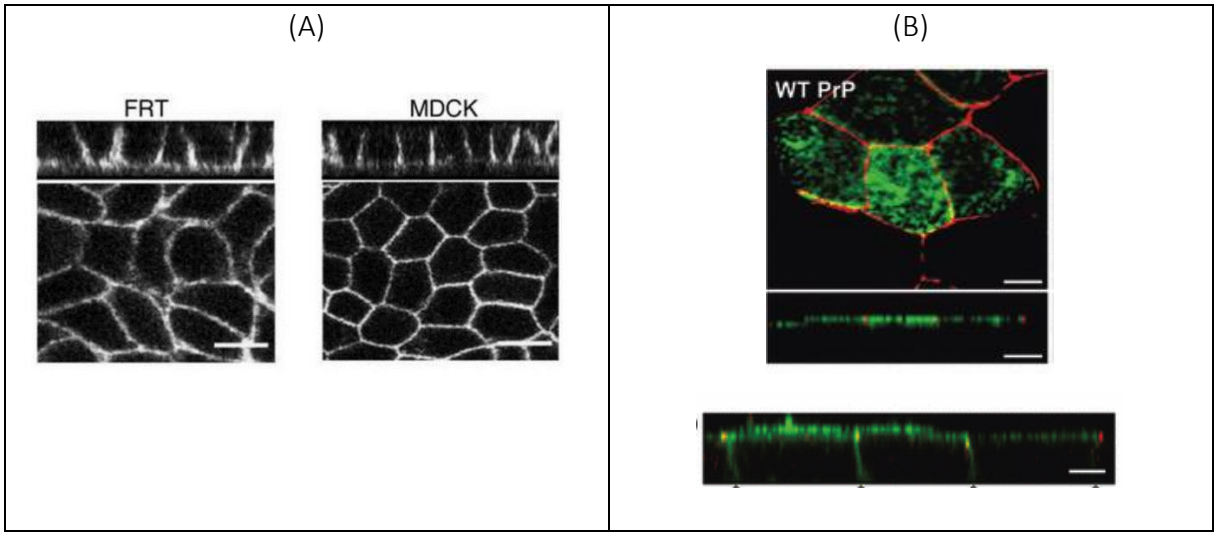

Figure 23. Contradictory PrP localization in MDCK cells. *(A) Basolateral localization initially found by Sarnataro and coworkers; PrP is revealed by SAF32 (Sarnataro et al. 2002). (B) Apical localization found by Christensen and Harris; PrP is revealed by 3F4 - in green; ZO1 in red (Christensen & Harris 2009).*

While De Keukeleire and collaborators (De Keukeleire et al. 2007) as well as Christensen and Harris (Christensen & Harris 2009) have found PrP at the apical membrane of MDCK cells, Uelhoff and colleagues (Uelhoff et al. 2005) confirmed our findings showing a basolateral localization of PrP^C. The reason for these opposite results has never been explained. The two major differences in these studies are in the PrP sequence and the anti-PrP antibodies used. While De Keukeleire worked with human PrP, the other studies have employed mouse PrP. In addition, Christensen and Harris have used the C-terminal PrP antibody SA65, while our laboratory used the N-terminal antibody SAF32. Uelhoff and colleagues introduced into mouse PrP a 3F4 tag and used 3F4 antibody, recognizing the region of the α-cleavage (aa 108-111 in mouse PrP), also at the N terminal. PrP at steady state undergoes extensive proteolytic modification, called α-cleavage (Liang & Kong 2012), differential α-cleavage could also explain the contradictory localization of PrP in polarized MDCK cells. Of note, none of these publications took into account the posttranslational proteolytic processing of PrP. However, bovine GFP-PrP construct was shown to be cleaved and shed in the apical media in MDCK cells (Tveit et al. 2005).

The aim of my PhD

In the field of prion disease, many open questions are linked to the trafficking of PrP. The localization of this protein is debated in polarized MDCK cells. Indeed, differently from all native GPI-APs PrP is basolateral in MDCK cells. A pioneering study from our laboratory showed that PrP is sorted to both the apical and the basolateral surfaces, but then it is unstable on the apical membrane. Furthermore, later works addressing PrP localization in the polarized MDCK cell model brought even more confusion as some researchers found PrP residing in the apical membrane (De Keukeleire et al. 2007; Christensen & Harris 2009).

Taking into account the importance of studying PrP metabolism for its role in pathogenesis I decided to investigate PrP trafficking in MDCK cells both in 2D and in 3D systems in order to explain the discrepancy of the literature on PrP sorting. Importantly 3D system recapitulates many physiological features and allows a more accurate study.

Material and Methods

Reagents and antibodies

Cell culture media were purchased from Sigma-Aldrich (St. Louis, MO). Antibodies were purchased as follows: polyclonal α-GFP and monoclonal α-GFP from Invitrogen (Eugene, OR), SAF32 and SHA31 from Bertin pharma, France. The monoclonal antibody GP135 developed by Ojakian, G.K. was obtained from the Developmental Studies Hybridoma Bank, created by the NICHD of the NIH and maintained at The University of Iowa, Department of Biology, Iowa City, IA 52242. Matrigel was purchased from Corning (France), Phalloidine-Alexa647 from Thermo; all other reagents were purchased from Sigma-Aldrich.

Cell culture

MDCK cells were grown in DMEM containing 5% fetal bovine serum and 1% penicillin/streptomycin (Invitrogen). MDCK cells stably expressing mouse PrP was obtained previously (Sarnataro et al. 2002). 3D cyst formation was performed as described in (Jung et al. 2013). Briefly, 8 well chambers and pipet tips were cooled down, chambers were coated with 15 µl Matrigel™ freshly melted on ice. The gel coating was solidified 15 min at 37°C. Low density cell suspension (20 000 cells per ml of media) was prepared in DMEM containing 1% penicillin/streptomycin, 5% FBS, 2% Matrigel. 200 µl of cell suspension was plated in each well. Media containing 2% Matrigel was changed every 3 days.

Deglycosylation assay and Western Blotting

For deglycosylation, cells were lysed in NP-40 lysis buffer (25mM Tris pH 7.5, 150 mM NaCl, 1% NP-40), protein concentration in the cell lysate was quantified with Pierce BCA Protein Assay Kit (Thermo scientific). 40 µg of protein was treated with 50 units of PNG^{ase} (New England Biolabs, MA) at 37°C for 1h with agitation. Samples were mixed with SDS-loading dye and run on a 4-12% Criterion™ XT Bis-Tris Gel (Biorad). Western blots were carried out with SHA31 antibody (1:10000), SAF32 (1:2000). Peroxidase-conjugated secondary antibodies to mouse

were used (GE Healthcare) and blots were revealed with ECL 2 Western Blot detection reagent (Thermo).

Immunofluorescence

MDCK cells, grown either on coverslips, on transwell filters, or in Matrigel™ were washed with phosphate-buffered saline containing $CaCl_2$ and $MgCl_2$, fixed with 2% paraformaldehyde for 30min at room temperature, washed with 50 mM NH_4Cl and saturated in non-permeabiling buffer (PBS, 10% Goat Serum) or permeabilizing buffer (PBS, 0.5% Triton X-100, 0.04% Tween 20, 10% Goat Serum). Primary antibodies used in immunofluorescence SHA31 (1:500), SAF32 (1:200), GP135 (1:750) were detected with Alexa-488 or Alexa-546 conjugated secondary antibodies (1:500). Phalloidin-Alexa647 (1:100) was used to stain actin. The images were acquired using a laser scanning confocal microscope (LSM 700; Zeiss) equipped with a Plan Apo 63× oil immersion (NA 1.4) objective lens.

Antibody transcytosis assay

For the transcytosis assay in 2D cells grown on polycarbonate filters for 5 days were incubated 3h on ice with primary anti-PrP antibodies SHA31 (1:500) and SAF32 (1:200) in basolateral media. Cells were then washed 3 times with cold DMEM and incubated at 37°C for 3 hours. Cells were fixed with 2% PFA, and an Immunofluorescence was performed with appropriate Alexa-labeled secondary antibody.

For the transcytosis assay in 3D MDCK cysts grown in Matrigel for 5-10 days were incubated 3h or overnight at 37°C with primary anti-PrP antibodies SHA31 (1:500) and SAF32 (1:100) in the growth media. Incubation at 4°C for 3h was used as a control condition.

Colocalization assay

After fixation and immunofluorescence Z-stack images were acquired using a Zeiss LSM700 confocal microscope with a 63x oil plan apochromat objective (NA 1.4) to eliminate chromatic

aberration. Colocalization analysis was performed using the Coloc 2 plugin on ImageJ software (Schneider et al. 2012) (http://fiji.sc/Coloc_2).

Biotinylation and Streptavidin Precipitation

Biotinylation was performed according to the standard protocol (Le Bivic et al. 1990; Hanzel et al. 1991) with modifications. Biotinylation of monolayers on Transwells with S-NHS-biotin was carried out twice in a row for 20 min at 4°C with 0.5 ml for the apical chamber and 1 ml for the basolateral chamber. Free biotin was blocked with 50 mM NH4CI in PBS containing $MgCl_2$ and $CaCl_2$. After washes 0,5 ml of DMEM was placed in apical and basolateral chambers and cells were incubated 3h at 37°C. Media was harvested; centrifuged 5 min 5000 rpm to remove cell debris, supernatants were supplied with 150 mM of NaCl and protease inhibitors. Media were incubated for 12 h with Streptavidin-sepharose (GE). After incubation, the beads were washed (PBS, 150mM NaCl, 0,2% BSA) 3 times in a row for 1 h at 4°C. After washes beads were treated with PNG^{ase} and subjected to Western Blot.

Primary cultures

Cerebellar granular neurons and cerebellar astrocytes (CA) were isolated from 4-6 day-old C57BL/6J pups. Pups were euthanized in accordance with regulations set down by the French Government. Cerebella were isolated, meninges removed and washed twice in PBS. After Trypsin-EDTA treatment for 10 minutes at 37°C followed by trypsin inactivation with FBS, 10^5 units/ml of DNase I (Sigma Aldrich) were added and the solution triturated with a 5 ml pipette until the cell suspension was completely dissociated. After gentle centrifugation (700 rpm, 7 minutes no brake), the supernatant was removed and 5 ml of complete neuronal medium (DMEM-Glutamax, 10% FBS, B27 supplement, N2 supplement, 20mM KCl and 1% Pen-strep) was added to the pellet. Cells were plated at a density of 150000-cells per 12 mm coverslip. For cerebellar astrocytes, the procedure was identical. The day after plating, CA cultures were vigorously shaken to remove debris and other types of glia. Plating and maintenance was carried out using DMEM-Glutamax, 10% Horse serum and 1% Pen-strep as the culture medium.

Proteinase K resistance assays and western blots.

For western blots to determine infection of primary cultures, cells were lysed in 25mM Tris pH 7.5 buffer containing 1% TritonX-100 and 1% β-octyl glucoside. 50μg of protein was treated with 3.75 μg/ml of proteinase K at 37°C for 30 minutes and methanol-precipitated prior to resuspension in SDS-loading dye and running on a 12% Tris-Glycine gel. Western blots were carried out with Sha31 antibody (SPIBio, mouse anti-PrP, 1:5000), β3-tubulin (Sigma Aldrich, mouse 1:5000), a-tubulin (Sigma-aldrich, mouse 1:10000), GFAP (Dako, rabbit 1:5000). Peroxidase-conjugated secondary antibodies to mouse or rabbit were used (GE Healthcare) and blots were revealed with ECL Western Blot detection reagent (Amersham).

Statistical analyses

All graphs show the mean +/- S.E.M. from at least 3 independent experiments. Mann–Whitney U test was used to evaluate the significance of nonparametric data. Paired two-tailed t test was used for the apical vs basolateral signal distribution *$p < 0.05$, ** $p< 0.01$

Summary of the results

In order to study PrP localization and intracellular trafficking in fully polarized MDCK cells, we have used both C-terminal (SHA31) and N-terminal (SAF32) antibodies

We have found that N-terminal antibody recognizing PrP full-length and the soluble N1 fragment, stains intracellular vesicles and the basolateral membrane in agreement with previous findings (Sarnataro et al. 2002; Uelhoff et al. 2005; Puig et al. 2011). Surprisingly, when using the C-terminal antibody, which recognizes PrP full-length and membrane-anchored C1 fragment we observed a clear apical signal, as shown before by Christensen and Harris (Christensen & Harris 2009). The apical signal that is revealed exclusively by C-terminal antibody (and not recognized by N-terminal antibody) represents the C1 cleavage fragment. Therefore, the reason of discrepancy of earlier data in the literature is in the use of different PrP antibodies, recognizing full-length PrP and N1 fragment or full-length PrP and C1 fragment. By using both types of antibodies we have reproduced both the basolateral localization of full-length PrP and apical localization of C1 and explained earlier findings.

Next, to investigate and characterize PrP trafficking in fully polarized conditions we successfully used 3D polarization protocol. At first when we compared 3D and 2D immunofluorescence data obtained with an N-terminal antibody we found strikingly different pictures: in 2D we observed a basolateral PrP localization like previously reported (Sarnataro et al. 2002), while in 3D we observed a vast majority of the signal trapped in the apical lumen, indicating apical secretion. Further investigation, using biochemical approach showed that PrP is secreted from the apical membrane in 2D cultures, like in 3D. Therefore, the only difference between 2D and 3D system, explained by the simple geometry of the system, is the accumulation of apically secreted proteins in the lumen of the cysts (Fig. 24).

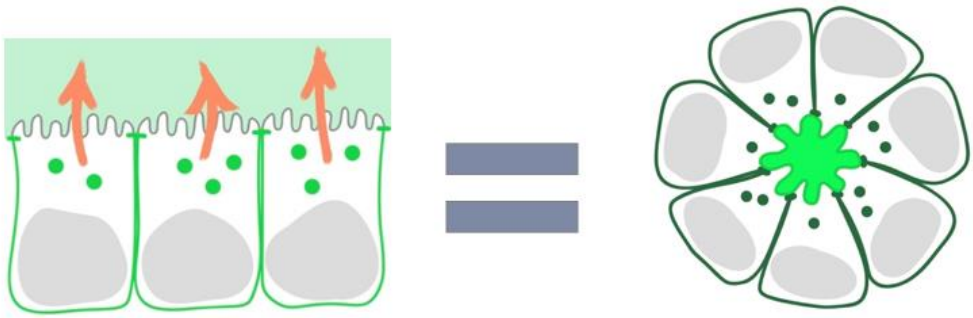

Figure 24. Schematic showing the equality of 2D and 3D culture systems for PrP trafficking. Apically secreted proteins are diluted in the apical culture media and therefore are not detectable in immunofluorescence, while in 3D apically secreted protein are trapped in the isolated lumen and stay visible in the immunofluorescence.

Furthermore, using a biochemical approach we have shown that in fully polarized cells in 2D most of PrP is present as a C1 cleavage fragment (ratio 5 to 1). The presence of cleavage fragments in the media revealed that secretion of PrP and its cleavage fragments is polarized: PrP FL, N1 and C1 are secreted apically while only C1 is found in the basolateral media. Therefore, PrP addressed to the apical membrane is cleaved and shed to the apical media in 2D or to the apical lumen in 3D. We noticed that during cell polarization there is a progressive enrichment of the C1 fragment on the apical membrane over the full-length, at the same time N1 production gradually decreases, therefore a relative increase in C1 could be due to the overall decrease of C1 degradation in polarized cells.

PrP full-length is basolateral and C1 is apical, but what is the mechanism responsible for the different localization of PrP FL and its cleavage fragment? We hypothesized that the mechanism re-localizing PrP to the apical membrane is basolateral-to-apical transcytosis. To monitor transcytosis we have used N-terminal and C-terminal antibodies that can cluster PrP on the basolateral membrane, therefore mimicking a ligand binding. We also investigated ligand independent “steady state” PrP transcytosis using selective biotinylation assay. We found that, unlike other GPI-APs, PrP undergoes basolateral-to-apical transcytosis in both 2D and 3D cultures of polarized MDCK cells.

Our data are consistent with PrP full-length being endocytosed from the basolateral membrane and undergoing α-cleavage either inside the intracellular vesicular compartment on its way to the apical surface or at the apical surface.

As we mentioned in the introduction (3.8 PrP & transcytosis) PrP was reported to play a role of a guide, brining amyloid-β, PrP^{Sc} aggregates and even a bacteria *Brucella abortus* from one membrane compartment to another. A recent article by Pflanzner and colleagues has shown that amyloid-β (1-40) transcytosis through the blood-brain barrier depends on PrP (Pflanzner et al. 2012). In our work, we show for the first time that PrP itself undergoes transcytosis, unraveling the ability of PrP to naturally travel from basolateral to apical membrane in ligand independent way. In addition, our work showing the transcytosis of antibodies-bound PrP is confirming the possibility that PrP can play the role of a guide for its natural ligands and other PrP-interacting molecules.

The impact of our study is further enhanced by the recent publication of Zhao and colleagues, they have shown that a key PrP interactor LRP1 (Taylor & Hooper 2007; Rushworth et al. 2013) binds and leads Aβ into transcytosis and clearance by endothelial cells, composing BBB (Zhao et al. 2015).

To summarize the data of PrP in polarized MDCK cells we propose the following model:

- At first a similar amount of PrP is sorted at the level of TGN to apical and basolateral membranes
- Upon the traffic to the apical membrane PrP undergoes α-cleavage
- Basolaterally sorted PrP reaches the cell membrane intact
- While transcytosed from the basolateral to the apical membrane PrP is cleaved
- Part of PrP full length reaching the apical surface is shed to the media, soluble N1 fragment is secreted to the apical media, C1 fragment is stabilized on the apical surface, and part of it is shed to the apical media.

First author paper submitted to PLOS ONE

PrP^C undergoes basal to apical transcytosis in polarized epithelial MDCK cells.

Alexander Arkhipenko, Sylvie Syan, Stéphanie Lebreton¶ and Chiara Zurzolo¶*

Unité de Trafic Membranaire et Pathogénèse, Institut Pasteur, 25-28 rue du docteur Roux, 75015 Paris, France

¶ These authors contributed equally to this work.

* Corresponding author

E-mail: zurzolo@pasteur.fr

Abstract

The Prion Protein (PrP) is an ubiquitously expressed glycosylated membrane protein attached to the external leaflet of the plasma membrane via a glycosylphosphatidylinositol anchor (GPI). While the misfolded PrP^{Sc} scrapie isoform is the infectious agent of prion disease the cellular isoform (PrP^{C}) is an enigmatic protein with unclear function. Of interest PrP localization in polarized MDCK cells is highly controversial and its mechanism of trafficking is not clear. As PrP trafficking is of fundamental relevance for its role in the pathogenesis of prion diseases, here we have investigated PrP traffic in MDCK cells polarized on filters and in three-dimensional MDCK cysts, a more physiological model of polarized epithelia. We found that differently from other GPI-APs PrP undergoes basolateral-to-apical transcytosis and is α-cleaved during its transport to the apical surface.

Introduction

The cellular isoform of the prion protein (PrP^{C}) is a glycosylphosphatidylinositol-anchored protein (GPI-AP) ubiquitously expressed in different tissues, with high levels in the nervous and lymphoid tissues, and lower levels in muscles, heart, digestive tract and skin (S. B. Prusiner 1998). The physiological function of PrP^{C} is still elusive (Linden et al. 2008; Linden et al. 2012). Prion protein has received considerable attention due to its central role in the development of Transmissible Spongiform Encephalopathies (TSEs) known as “prion diseases”, in animals and humans (S. B. Prusiner 1998; Kretzschmar & Tatzelt 2013). In these neurodegenerative disorders, PrP^{C} converts into a pathological isoform, called PrP^{Sc} (where Sc stands for Scrapie). Understanding the trafficking, the processing and degradation of PrP is of fundamental importance in order to unravel the mechanism of PrP^{Sc} mediated pathogenesis, its spreading and cytotoxicity.

Here we focused on PrP trafficking as the few studies addressing this issue have produced contradictory results. As a model we have chosen Madin-Darby canine kidney (MDCK) cells stably transfected with the mouse PrP cDNA (Sarnataro et al. 2002). We have used this epithelial cell line because it is well characterized for intracellular trafficking and GPI-AP sorting

(Lisanti et al. 1989a; Brown et al. 1989; Paladino et al. 2004; Paladino et al. 2014; Muñiz & Zurzolo 2014; Paladino et al. 2002; Paladino et al. 2008). Pioneering work demonstrated that GPI-APs localize on the apical membrane in MDCK cells (Brown et al. 1989; Lisanti et al. 1989a; M P Lisanti et al. 1990) as well as in other epithelial cell lines (Muñiz & Zurzolo 2014; M P Lisanti et al. 1990). It was shown that GPI-APs which are preferentially sorted from the TGN to the apical surface follow a direct route from the Golgi apparatus to the plasma membrane (M. P. Lisanti et al. 1990). Later work from our and other laboratories has unravelled the mechanism of apical sorting of GPI-APs, demonstrating that both association of GPI-APs with detergent resistant membranes (DRMs) and cholesterol dependent clustering in high molecular weight (HMW) complexes in the Golgi are necessary for this process (Paladino et al. 2006a; Paladino et al. 2014; Deborah A. Brown & Rose 1992; Schuck & Simons 2006).

The one exception to direct apical sorting of native GPI-APs in MDCK cells is represented by the Prion Protein. In 2002 work from our laboratory showed that mouse PrP^C localizes on the basolateral membrane of fully polarized MDCK cells (Sarnataro et al. 2002). Several groups later addressed the distribution and intracellular trafficking of PrP in polarized MDCK cells (Uelhoff et al. 2005; De Keukeleire et al. 2007; Christensen & Harris 2009; Puig et al. 2011) and obtained contradictory results. While De Keukeleire and collaborators (De Keukeleire et al. 2007) as well as Christensen and Harris (Christensen & Harris 2009) found PrP at the apical membrane of MDCK cells, Uelhoff and colleagues (Uelhoff et al. 2005) confirmed our findings showing a basolateral localization of PrP^C. The reason for these opposite results has never been explained. The two major differences in these studies are in the PrP sequence and the anti-PrP antibodies used. While De Keukeleire worked with human PrP, the other studies employed mouse PrP. In addition, Christensen and Harris used the C-terminal PrP antibody SA65, while our laboratory used the N-terminal antibody SAF32. Uelhoff and colleagues introduced a 3F4 tag into the N terminal region of mouse PrP and used a 3F4 antibody, thereby also recognizing the region of the α-cleavage (aa 108-111 in mouse PrP). Of note, none of these publications took into account the posttranslational proteolytic processing of PrP. Because PrP at steady state undergoes extensive proteolytic modification, called α-cleavage (Liang & Kong 2012), differential α-cleavage could also explain the contradictory localisation of PrP in polarized MDCK cells.

In this work we addressed PrP trafficking in MDCK cells, taking into account its proteolytic processing. Furthermore we used MDCK cells polarized on filters and a more physiological 3D culture system of MDCK cells cysts embedded in matrigel. 3D MDCK cysts recapitulate numerous features of epithelial tissues *in vivo* (O'Brien et al. 2002; Debnath & Brugge 2005) and therefore provide a good model to study polarized protein trafficking under physiological conditions. We report here that full-length PrP and its cleavage fragments are segregated in different domains of the plasma membrane in polarized cells in both 2D and 3D cultures and that the C1/PrP full-length ratio increases upon MDCK polarization. We found that differently from other GPI-APs, PrP undergoes basolateral-to-apical transcytosis in fully polarized MDCK cells.

This study not only reconciles and explains the different findings in the previous literature but also provides a better picture of PrP trafficking and processing, which has been shown to have major implications for its role in prion disease (Campana et al. 2005; Senatore et al. 2013).

Material and Methods

Reagents and antibodies

Cell culture media were purchased from Sigma-Aldrich (St. Louis, MO). Antibodies were purchased as follows: polyclonal α-GFP and monoclonal α-GFP from Invitrogen (Eugene, OR), SAF32 and SHA31 from Bertin pharma, France. The monoclonal antibody developed by Ojakian, G.K. was obtained from the Developmental Studies Hybridoma Bank, created by the NICHD of the NIH and maintained at The University of Iowa, Department of Biology, Iowa City, IA 52242.

Matrigel was purchased from Corning (France), Phalloidine-Alexa647 from Thermo; all other reagents were purchased from Sigma-Aldrich.

Cell culture

MDCK cells were grown in DMEM containing 5% fetal bovine serum. MDCK cells stably expressing mouse PrP was obtained previously (Sarnataro et al. 2002). 3D cyst formation was performed as described in (Jung et al. 2013). Briefly, 8 well chambers and pipet tips were cooled down, chambers were coated with 15 µl Matrigel™ freshly melted on ice. The gel coating was solidified 15 min at 37°C. Low density cell suspension (20 000 cells per ml of media) was prepared in DMEM containing Penicillin/streptomycin 5ml (100x), 5% FBS, 2% Matrigel. 200 µl of cell suspension was plated in each well. Media containing 2% matrigel was changed every 3 days.

Deglycosylation assay and Western Blotting

For deglycosylation, cells were lysed in NP-40 lysis buffer (25mM Tris pH 7.5, 150 mM NaCl, 1% NP-40), protein concentration in the cell lysate was quantified with Pierce BCA Protein Assay Kit (Thermo scientific). 40 µg of protein was treated with 50 units of PNG^{ase} (New England Biolabs, MA) at 37°C for 1h with agitation. Samples were mixed with SDS-loading dye and run on a 4-12% Criterion™ XT Bis-Tris Gel (Biorad). Western blots were carried out with SHA31 antibody (1:10000), SAF32 (1:2000). Peroxidase-conjugated secondary antibodies to mouse were used (GE Healthcare) and blots were revealed with ECL 2 Western Blot detection reagent (Thermo).

Immunofluorescence

MDCK cells, grown either on coverslips, on transwell filters, or in Matrigel™ were washed with phosphate-buffered saline containing $CaCl_2$ and $MgCl_2$, fixed with 2% paraformaldehyde for 30min at room temperature, washed with 50 mM NH_4Cl and saturated in non-permeabiling buffer (PBS, 10% Goat Serum) or permeabilizing buffer (PBS, 0.5% Triton X-100, 0.04% Tween 20, 10% Goat Serum). Primary antibodies used in immunofluorescence SHA31 (1:500), SAF32 (1:200), GP135 (1:750) were detected with Alexa-488 or Alexa-546 conjugated secondary

antibodies (1:500). Phalloidin-Alexa647 (1:100) was used to stain actin. The images were acquired using a laser scanning confocal microscope (LSM 700; Zeiss) equipped with a Plan Apo 63× oil immersion (NA 1.4) objective lens.

Antibody transcytosis assay

For the transcytosis assay in 2D cells grown on polycarbonate filters for 5 days were incubated 3h on ice with primary anti-PrP antibodies SHA31 (1:500) and SAF32 (1:200) in basolateral media. Cells were then washed 3 times with cold DMEM and incubated at 37°C for 3 hours. Cells were fixed with 4% PFA, and an Immunofluorescence was performed with appropriate Alexa-labeled secondary antibody.

For the transcytosis assay in 3D MDCK cysts grown in Matrigel for 5-10 days were incubated 3h or overnight at 37°C with primary anti-PrP antibodies SHA31 (1:500) and SAF32 (1:100) in the growth media. Incubation at 4°C for 3h was used as a control condition.

Colocalization assay

After fixation and immunofluorescence Z-stack images were acquired using a Zeiss LSM700 confocal microscope with a 63x oil plan apochromat objective (NA 1.4) to eliminate chromatic aberration. Colocalization analysis was performed using the Coloc 2 plugin on ImageJ software (Schneider et al. 2012) (http://fiji.sc/Coloc_2).

Biotinylation and Streptavidin Precipitation

Biotinylation was performed according to the standard protocol (Le Bivic et al. 1990; Hanzel et al. 1991) with modifications. Biotinylation of monolayers on Transwells with s-NHS-biotin was carried out twice in a row for 20 min at 4°C with 0.5 ml for the apical chamber and 1 ml for the basolateral chamber. Free biotin was blocked with 50 mM NH4CI in PBS containing $MgCl_2$ and $CaCl_2$. After washes 0,5 ml of DMEM was placed in apical and basolateral chambers and cells were incubated 3h at 37°C. Media was harvested; centrifuged 5 min 5000 rpm to remove cell debris, supernatants were supplied with 150 mM of NaCl and protease inhibitors. Media were incubated for 12 h with Streptavidin-sepharose (GE). After incubation, the beads were washed

(PBS, 150mM NaCl, 0,2% BSA) 3 times in a row for 1 h at 4°C. After washes beads were treated with PNG^{ase} and subjected to Western Blot.

Statistical analyses

All graphs show the mean+/- S.E.M. from at least 3 independent experiments. Mann–Whitney U test was used to evaluate the significance of nonparametric data. Paired two-tailed t test was used for the apical vs basolateral signal distribution *$p < 0.05$, ** $p< 0.01$

Results

N and C terminal antibodies reveal different PrP localization in 2D and 3D polarized MDCK cultures.

Polarized epithelial Madin-Darby canine kidney (MDCK) cells were previously used to characterize the exocytic pathway of PrP (Uelhoff et al. 2005; De Keukeleire et al. 2007; Christensen & Harris 2009; Puig et al. 2011; Sarnataro et al. 2002). The localization and intracellular traffic of PrP in stably transfected MDCK cells is contradictory as some studies reported PrP to be apical (Christensen & Harris 2009; De Keukeleire et al. 2007) while others have shown PrP to be basolateral (Uelhoff et al. 2005; Puig et al. 2011; Sarnataro et al. 2002). Because in epithelial cells protein localization depends directly on the polarity state of the cells (Zurzolo et al. 1992) we decided to compare PrP localization in non-polarized, fully polarized two-dimensional (2D) MDCK cells grown on filter, as well as in more physiological polarized three-dimensional (3D) MDCK cysts growing in Matrigel™. We assessed PrP localization using 2 different PrP antibodies: C-terminal SHA31 (epitope 148–159) and N-terminal SAF32 (epitope 59–89) (Fig.1A). As expected, in non-polarized cells the PrP signal revealed with SHA31 and SAF32 antibodies co-localize (Fig. 1B) (Pearson's R coefficient for SAF32/SHA31 colocalization, R=0.9; Fig 1E), revealing an ubiquitous distribution of PrP at the cell surface. Surprisingly, in polarized cells grown on filters in 2D the SAF32 and SHA31 staining clearly segregate (Fig.1C) (Pearson's R drops to 0.3; Fig 1E). While SAF32 antibody reveals PrP staining mostly on the basolateral surface (65±2%), confirming our earlier results (Sarnataro et al. 2002); SHA31 antibody reveals PrP enrichment at the apical membrane (72±2%) (Fig 1F), as previously shown in similar conditions in polarized MDCK cells (Christensen & Harris 2009). Interestingly, in 3D cysts, SAF32 signal concentrates in the cyst lumen while SHA31 is enriched at the apical surface (66±2%), similar to 2D culture (Fig 1D and 1E; Pearson's R value in cysts is 0.63).

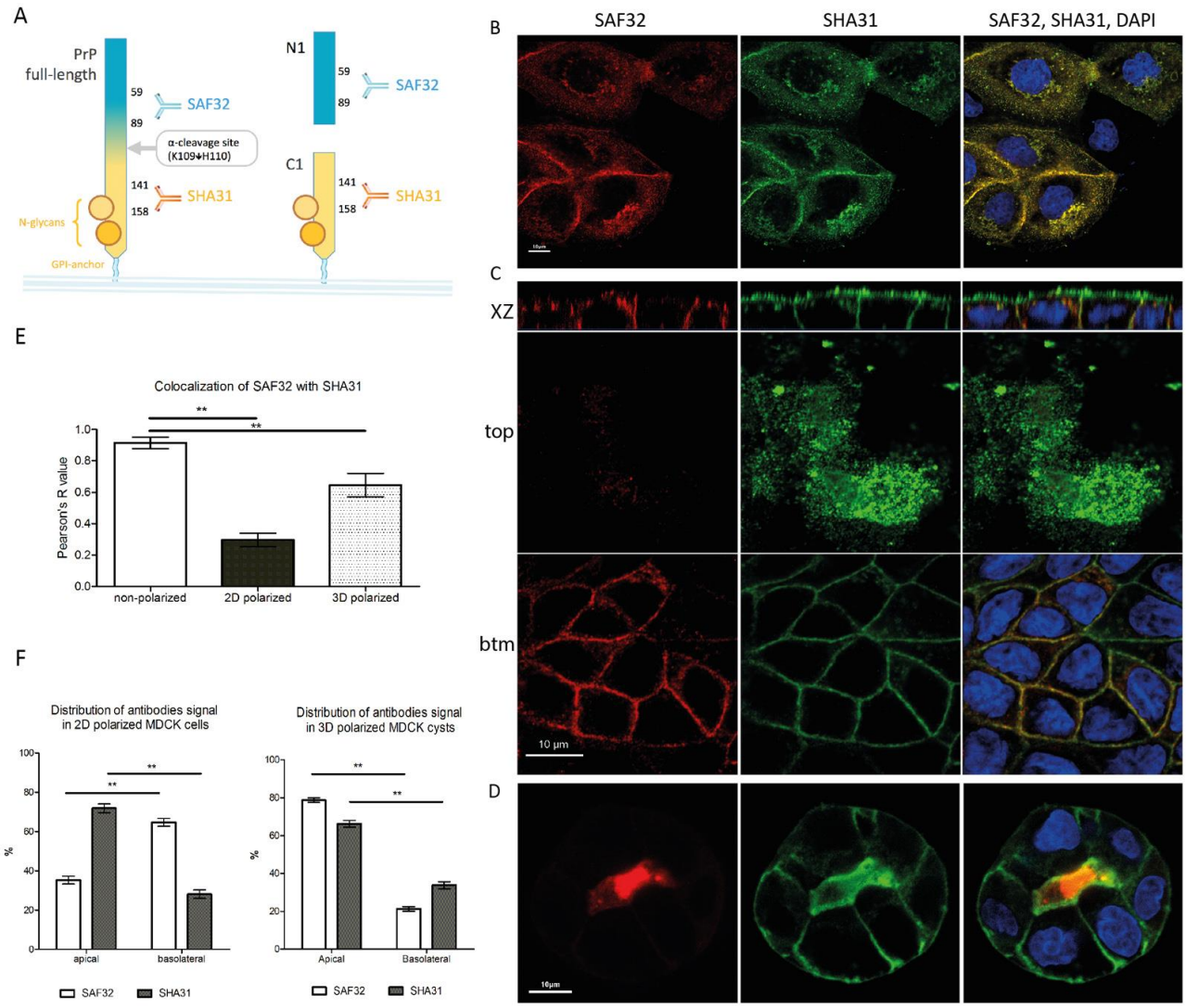

Fig 1. Different localization of PrP in nonpolarized, 2D and 3D polarized MDCK cells revealed by using different antibodies.

(A) *Schematic representation of mouse PrP α-cleavage and the antibodies used in this paper. The C-terminal part of PrP (orange) is membrane-attached via GPI-anchor; it has 2 independently occupied glycosylation sites (orange circles). Proteolytic α-cleavage occurs at the position 109*110. After the cleavage C1 fragment stays on the plasma membrane. C1 as well as PrP full-length is recognized by SHA31 antibody (orange). The N-terminal part (blue), becomes a soluble N1 fragment upon cleavage. N1 and PrP full-length are recognized by SAF32 antibody (blue).* ***(B), (C)*** *and* ***(D)*** *Immunofluorescent pictures of MDCK cells stably expressing PrP (MDCK PrPwt cells). Cells plated for 24 hours on plastic dish (B), 5 days on Transwell filters (C) or 5 days on top of Matrigel TM (D) were fixed and immunostained for PrP using SAF32 antibody (left column) and SHA31 antibody (middle column) and nuclei are stained with DAPI (right column). Scale bars 10 µm. In* ***(C)*** *serial confocal sections of 0,3 µm were collected from the top to the bottom of the cell monolayer.* ***(E)*** *Pearson's R values revealing SAF32 and SHA31 colocalization*

*in non-polarized, 2D and 3D polarized states. Mann-Whitney test was used for the statistical analysis (**p ≤ 0.01)* ***(F)*** *Quantification of apical vs. basolateral distribution of SAF32 and SHA31 in 2D polarized MDCK cells growing for 5 days on a Transwell™ filter (2D, left panel) and in 3D polarized MDCK cysts 5 days after plating on top of Matrigel™ (3D, right panel). These experiments were performed 3 independent times and a total of 60 cells were used for quantification. Paired t test was used for the statistical analysis (** P ≤ 0.01).*

C1 cleavage fragment accumulates during the establishment of monolayer polarity.

The immunofluorescence data show that the localization of PrP depends on the antibody epitope (Fig 1A). In order to explain the staining differences obtained with two different antibodies we hypothesize that PrP in MDCK cells is proteolytically processed and truncated fragments are sorted differently from PrP FL (full-length). Indeed SAF32 and SHA31 antibodies should recognize not only the full length PrP but also different cleavage products. The most common proteolytic processing of PrP are α and β cleavages (Liang & Kong 2012; Chen et al. 1995; Jiménez-Huete et al. 1998). α-cleavage has already been shown for ovine PrP expressed in MDCK cells (Tveit et al. 2005). In order to confirm the proteolytic processing of PrP in MDCK cells and to investigate the dynamics of cleavage during the polarization we compared by western blot the amount of PrP FL and PrP cleavage fragments in total cell lysate and in the culture media of MDCK cells during polarization (Fig 2). For the western blot from the whole cell lysate we used SHA31 antibody, as it recognizes both PrP full-length and the C1 fragment residing on the cell membranes (see schematic in Fig 1A) (Jiménez-Huete et al. 1998). PrP is a heavily glycosylated protein, which in SDS PAGE migrates as several bands (1 diglycosylated, 2 monoglycosylated and 1 non-glycosylated band) (S. B. Prusiner 1998). This makes biochemical distinction between PrP full-length and truncated fragments bearing sugars difficult. In order to clearly separate full-length and cleavage fragments we treated our samples with PNG^{ase} to deglycosylate PrP.

In order to elucidate the mechanism allowing the detection of PrP signal recognized by SHA31 at the apical surface of MDCK cells by immunofluorescence, we analyzed biochemically the presence and level of PrP FL and its cleavage fragments during polarity establishment (Fig. 2A). Cells were plated on 6-well filters at a density of 2 millions per well. Filters were lysed at day 0

(6 hours post plating), 1 and 3 days; cell lysate was PNG^{ase} treated, subjected to Western Blotting. We revealed using SHA31 antibody full length PrP around 27 kDa and a truncated PrP form around 15 kDa (Fig 2A), which corresponds to C1 fragment, the product of the α-cleavage (Liang & Kong 2012). Interestingly, while in non-polarized conditions (0 dpp) PrP FL and C1 are present in similar amounts, in fully polarized cells (3 dpp) C1 appears to be 5 times more abundant than full-length PrP (Fig 2B left). The ratio of C1 to PrP FL increases with monolayer maturation on filter. Interestingly the ratio of C1 to the total protein load (evaluated with coomassie blue) is stable over polarization, but PrP FL level constantly decreases though polarization (Fig 2A and 2B right).

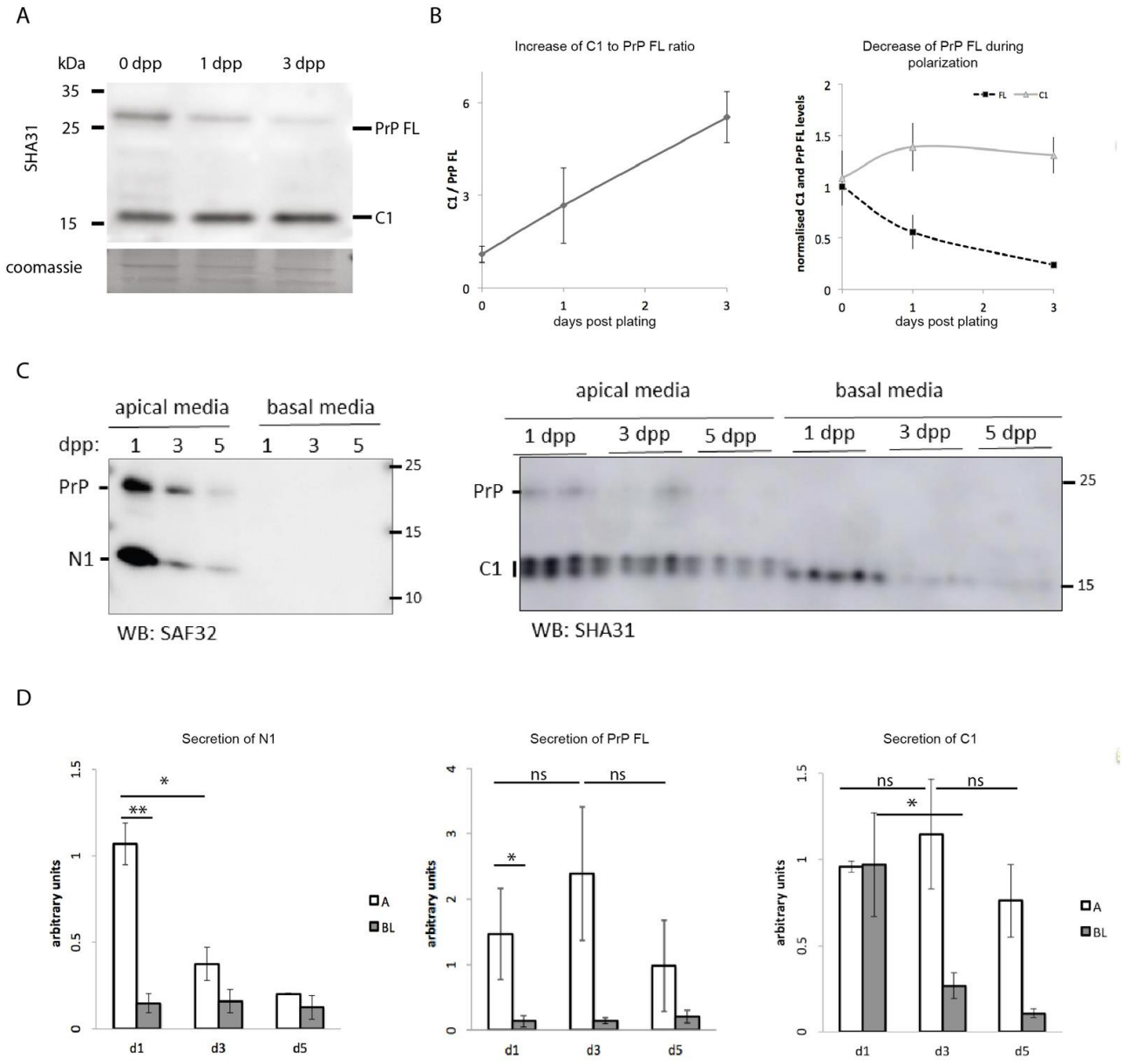

Fig 2. PrP cleavage through establishment of polarity in 2D MDCK cells.

*(A) MDCK PrP wt was plated in Transwell™ filters, then lysed at 6 hours (0 days), 1, and 3 days post plating. Cell lysates were PNG^ase treated and analyzed by western blot, revealed with SHA31 antibody. (B) Quantification of C1/PrP FL ratio through time is shown panel B left and normalization (using coomassie blue staining) of C1 and PrP levels with time is shown panel B right. 4 independent experiments were quantified. (C) MDCK cells were plated on Transwell™ filters for 5 days. At 1, 3 and 5 days post plating growth media was replaced by serum-free media for 3 h. This media was collected and secreted proteins were methanol precipitated from the apical or basolateral media. Media was subjected to PNG^ase treatment and western blotting with SAF32 antibody (left) and SHA31 antibody (right). Of note, we detect 2 different bands around 15 kDa in the apically secreted C1, while we detect a single band of C1 in the basolateral media. (D) Quantification of N1 (left panel), PrP FL (middle panel) and C1 (right panel) secretion. 3 independent experiments were quantified. Mann-Whitney test was used for the statistical analysis (*p ≤ 0.05; **p ≤ 0.01)*

N terminal cleavage fragments are apically secreted.

As C1 is a membrane-bound and relatively stable fragment (Liang & Kong 2012; Chen et al. 1995) in order to understand if α-cleavage increases along with the monolayer maturation process, we decided to monitor the kinetic of secretion of the soluble N1 fragment that directly reflects the occurrence of α-cleavage process. To this aim we analyzed PrP secretion in the filter culture medium during the establishment of the polarized monolayer. After 1, 3, and 5 days post plating cells were allowed to secrete in serum-free media for 3h. Proteins were methanol precipitated from the media and loaded on the gel or subjected to PNG^ase treatment, western blot and revealed with SHA31 or SAF32 (Fig. 2C). We found that PrP full-length and soluble N1 are secreted exclusively in the apical media throughout the process of monolayer maturation (Fig 2C left and 2D left and center). Interestingly, the larger amount of N1 secretion is at 1 day post plating (Fig 2D left). This might indicate that α-cleavage is most active in non-polarized conditions or in the beginning of polarity program activation. Alternatively if the cleavage occurs only at the apical surface one possible explanation is that in the 3 hour time slot more PrP goes directly to the forming apical surface in early polarity stages rather than in late polarity stages, suggesting that PrP trafficking changes during the establishment of the polarized phenotype. Consistently with apical alpha cleavage C1 is secreted in larger amounts into the apical media than into the basolateral one (Fig 2C right and 2D right). Basolateral secretion of C1 occurs mainly at 1dpp, and then it decreases dramatically (Fig 2D right), in agreement with

the apical enrichment of C1 during polarity establishment of the MDCK monolayer (Fig 1C and S1 Fig).

Next we decided to characterize the dynamics of PrP cleavage fragment, localization and secretion in 3D culture during cyst maturation. We analyzed PrP localization by immunofluorescence using SHA31 and SAF32 antibodies on 1, 2, 3 and 4 day-old cysts (Fig 3). At early time points (1 and 2dpp) SAF32 and SHA31 co-localize (R = 0,86 ± 0,06). At the earliest stage of 1 dpp, the apical membrane is not established yet and SAF32 and SHA31 distribution is similar to the non-polarized cells growing on coverslip. As soon as membrane polarity is established PrP is enriched on the apical membrane as revealed by both antibodies. In the 4-day old cysts SAF32 and SHA31 signals segregate from each other, Pearson's R decreases up to 0,67 ± 0,1. Specifically, we observed different dynamics for the two antibodies. While the signal from SAF32 was mainly in the lumen in 5 day-old cysts (Fig 1D), at day 2 we could find a staining on the basolateral surface, which progressively disappeared with time until day 4 when the entire signal was observed in the cyst lumen. On the contrary the distribution of SHA31 does not significantly change from day 2 to day 4, as it is enriched at the apical membrane from day 2 and its basolateral staining is stable with time (Fig 3).

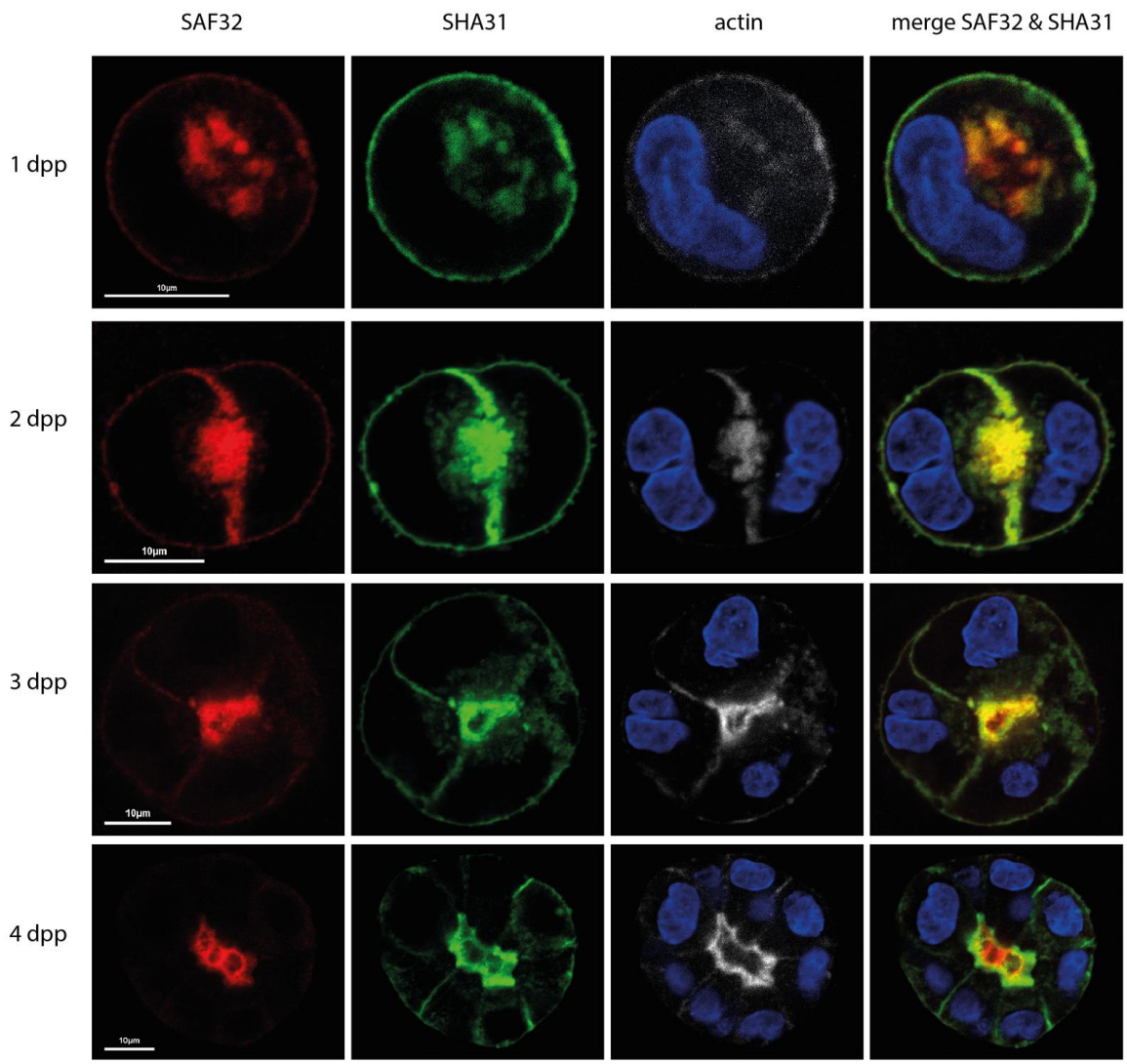

Fig 3. PrP distribution changes upon cyst maturation. *MDCK PrP wt cells were plated in 2% MatrigelTM, and then fixed at 1 day (1 dpp), 2 days (2 dpp), 3 days (3 dpp) and 4 days (4 dpp) post plating. Cyst were co-stained with SAF32 (red), SHA31 (green), phalloidin-Alexa-647 (white) and DAPI (blue). Scale bar 10 µm. Representative pictures of 3 experiments.*

PrP undergoes basolateral-to-apical transcytosis in fully polarized MDCK cells

The progressive enrichment of SAF32 signal in the apical lumen concomitant with its progressive disappearance from the basolateral membrane prompted us to investigate whether PrP undergoes basolateral to apical transcytosis that progressively increases with maturation of the epithelium.

To sustain this hypothesis we directly investigated the occurrence of basolateral-to-apical transcytosis in MDCK cells fully polarized in 2D and in 3D. To this aim, we first performed an antibody based transcytosis assay on MDCK cells grown on filters (Fig. 4). Polarized monolayers grown on filters for 5 days were incubated with SHA31 and SAF32 antibodies in the basolateral chamber for 2 hours at +4°C (to saturate basolateral PrP with antibodies). Then filters were washed and placed for 3h at +4°C (as a control condition) or at +37°C. After fixation cells were permeabilized and stained using fluorescently labelled secondary antibodies, and DAPI. As shown in figure 4 at +4°C both SHA31 and SAF32 staining are restricted to the basolateral membrane (Fig 4B left). After the incubation at 37°C SHA31 signal is significantly enriched on the apical membrane, 66±4% of SHA31 is detected at the apical surface (Fig 4B right), indicating occurrence of transcytosis. In the case of SAF32 we could not observe an apical signal. Instead after 3 hours of incubation with SAF32 antibody at 37°C, we monitored that SAF32 signal on the basolateral membrane becomes weaker compared to the signal at +4°C and is abundantly revealed in intracellular vesicles. These results are consistent with antibody internalization from the basolateral membrane and with the α-cleavage occurring on the apical surface or on the way to the apical surface, which would explain why we do not recover SAF32 signal on the apical surface.

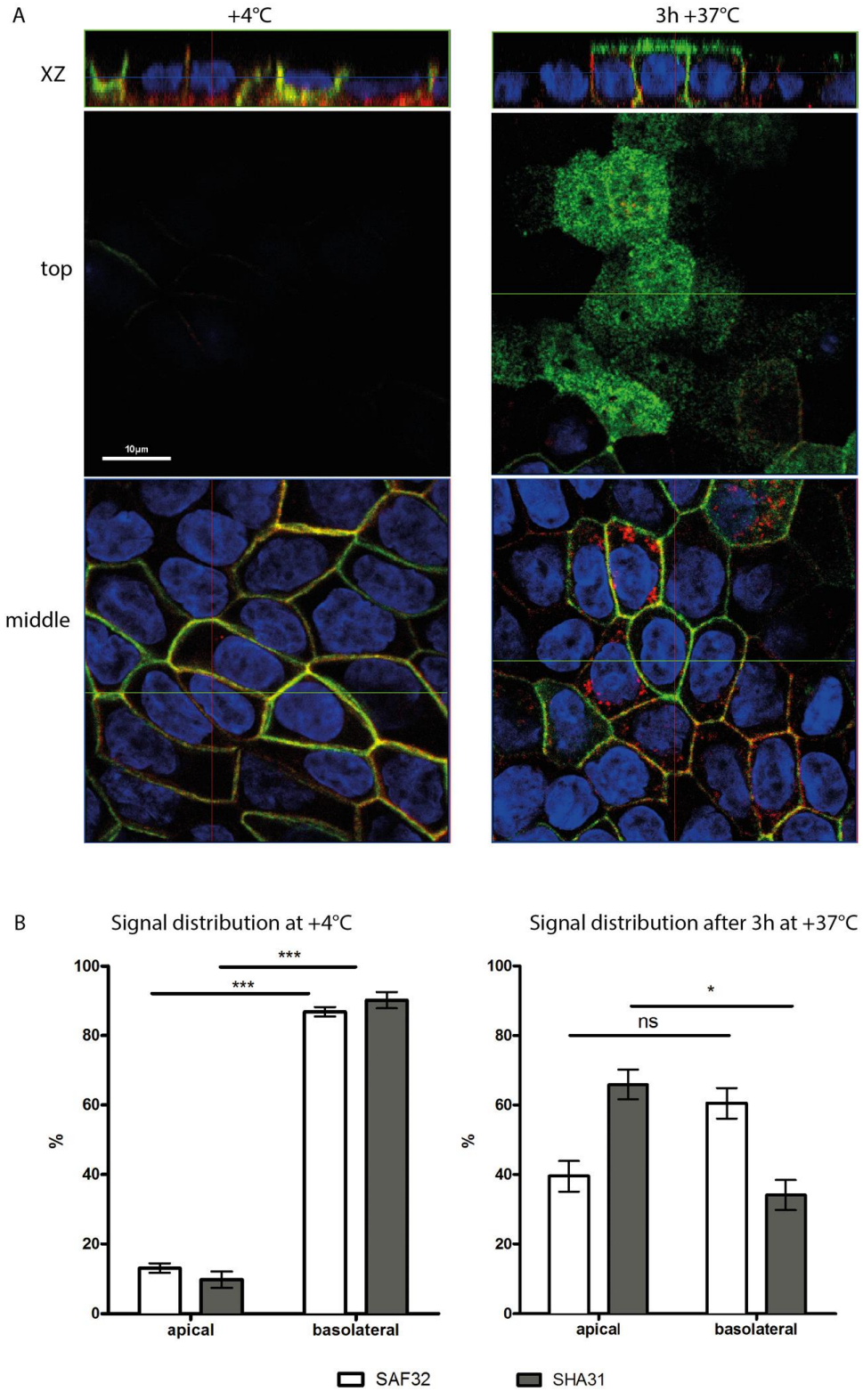

Figure 4

Fig 4. PrP wt undergoes basolateral to apical transcytosis in 2D polarized MDCK. (A)*. After 5 days of polarization MDCK cells were incubated with SHA31 (green) and SAF32 (red) antibodies in the basal media for 2 hours on ice, then filters were washed and incubated for +4°C as a control (left column) or*

for 3h at 37°C (right column). After fixation cells were permeabilized and stained with secondary antibodies and DAPI (blue). ***(B)****. Quantification of the apical vs basolateral antibody distribution for 3h of incubation at 4°C (left) or at 37°C (right) . Note that after the 3h of incubation SAF32 is present in intracellular sub-apical vesicles contributing to the quantification. The experiment was repeated 5 times, and a total of 100 cells were included in the analysis. Paired t test was used for statistical analysis (*P ≤ 0.05; ***P ≤ 0.001)*

To sustain these results, we investigated the occurrence of PrP transcytosis in fully polarized cysts in 3D culture. 5 to 10 days polarized cysts were incubated with the mix of SHA31 and SAF32 antibodies at 37°C for different times, while incubation at +4°C for 3h was used as a control. After fixation cysts were permeabilized and stained with secondary antibodies, Phalloidin-Alexa 647 conjugate and DAPI (Fig 5). We found that both antibodies were able to bind the basolateral surface, and progressively transcytose towards the apical membrane. However while SHA31 signal gradually enriches the apical rim of the apical lumen, SAF32 fluorescence is found mostly in the lumen where it accumulates with time (over-night incubation). These combined experiments show clearly that PrP undergoes basolateral to apical transcytosis and indicate that cleavage occurs before arrival to the apical membrane or at the apical surface.

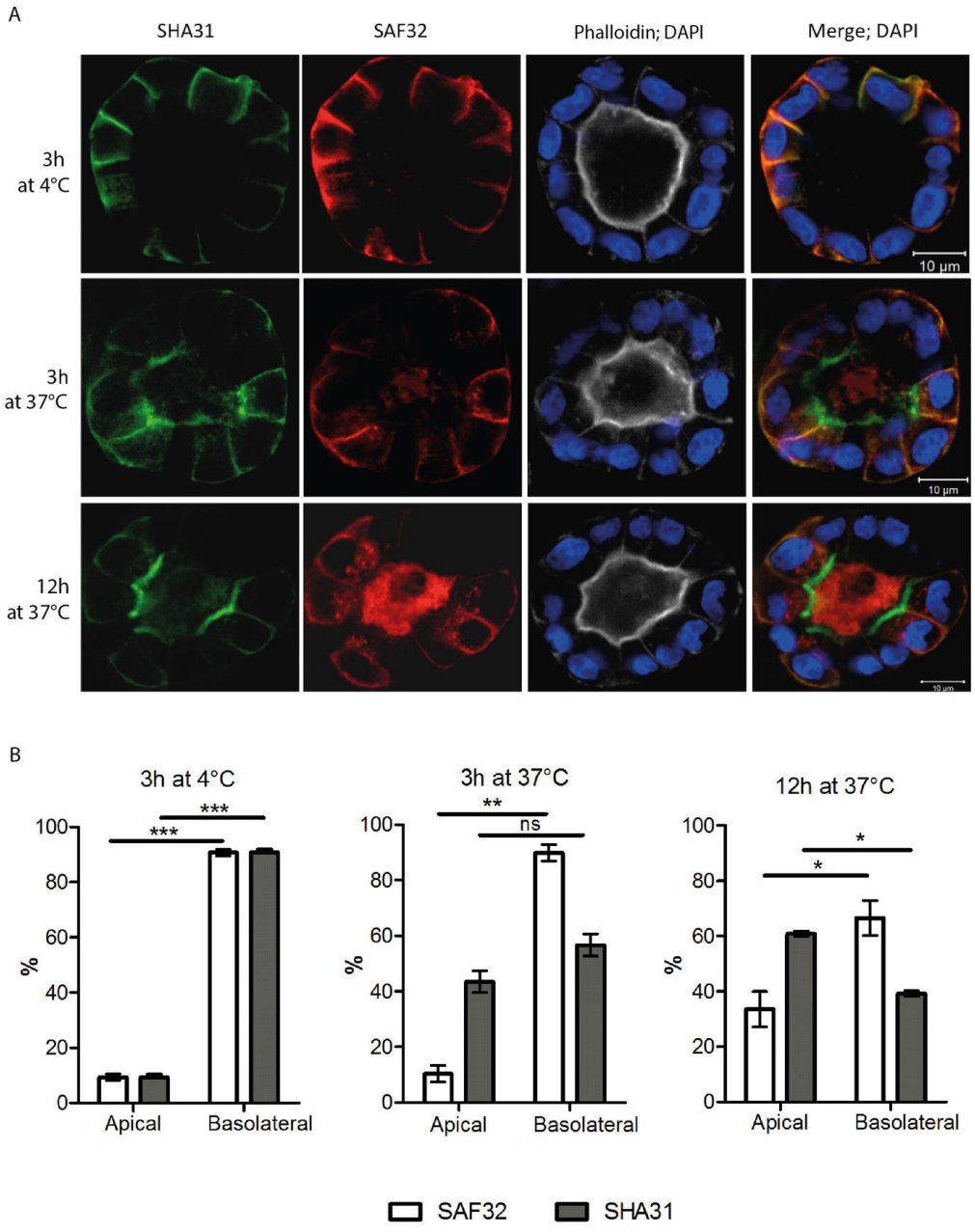

Fig 5. PrP wt undergoes basolateral to apical transcytosis in 3D polarized MDCK cysts. ***(A)*** *Fully polarized, mature cysts were incubated with the mix of SHA31 (green) and SAF32 (red) antibodies for the indicated time. Incubation at +4°C was used as a control. After fixation cysts were permeabilised and stained with secondary antibodies, phalloidin-Alexa647 (gray) and DAPI (blue).* ***(B)*** *Quantification of the apical vs basolateral antibody distribution in case of 3h of incubation at 4°C (left), 3h at 37°C (center) and overnight at 37°C (right) . Note that starting at 3h and especially after an overnight incubation SAF32 is present in intracellular vesicles and in the lumen, contributing to the quantification. The experiment was repeated 3 times, and a total of 120 cells were included in the*

*analysis. Paired t test was used for statistical analysis (*p ≤ 0.05; **p ≤ 0.01; *** p ≤ 0.001). Scale bar 10 µm.*

The remaining question is whether the antibody binding induces the observed transcytosis and whether PrP undergoes transcytosis in physiological conditions (ie.,in the absence of antibody). To answer to this question we used a biotinylation assay (Deora et al. 2006). MDCK cells were grown on filters for 5 days to reach the fully polarized state. Basolateral membrane was biotinylated on ice. After washes serum-free culture media was added and filters were placed at +4°C (as a control) or at 37°C for the transcytosis assay. At the end of 3h apical and basolateral media were recovered and biotinylated proteins were precipitated from the media by incubation with immobilized streptavidin. Recovered proteins were deglycosylated, run on SDS-PAGE and revealed by western blot with SHA31 antibody (Fig 6). We observed that PrP initially residing in basolateral membrane was recovered into the apical media. We also performed control experiments where we incubated the filters at +4°C instead of 37°C. In this condition, secretion of PrP was dramatically decreased (Fig 6 A). Additionally, all the PrP that was apically secreted at +4°C was not biotinylated (Fig 6B), confirming that apical secretion of PrP biotinylated on the basal membrane is an active process. We compared the amount of transcytosed and secreted PrP using as positive control the secretion of PrP after apical biotinylation. We found that 17±4% of secreted PrP comes from the basolateral membrane (Fig 6C). This data indicates that PrP undergoes transcytosis in steady state conditions.

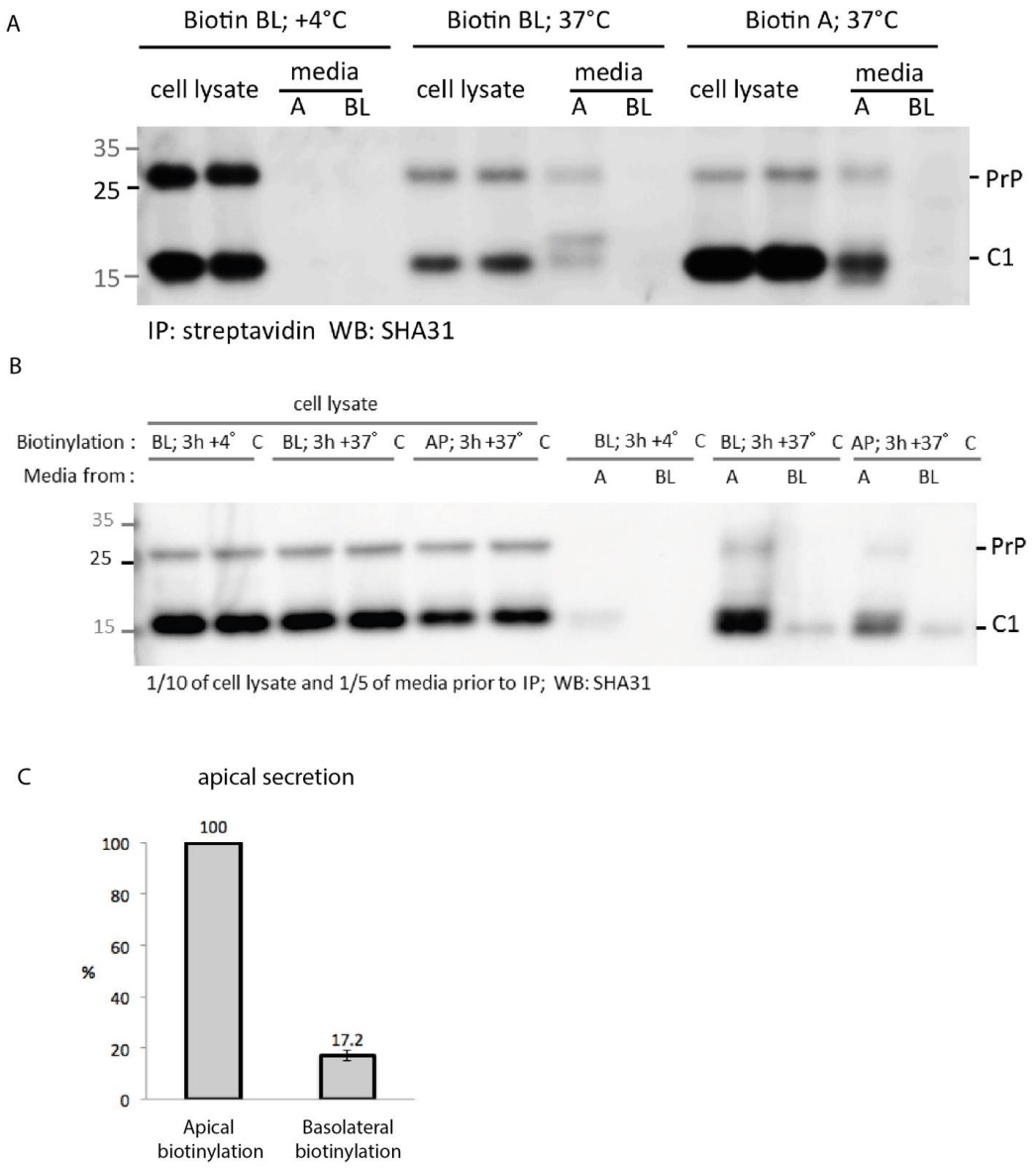

Fig 6. PrP follows transcytotic road at steady state (A) *After 5 days of polarization MDCK cells were biotinylated on the basolateral or apical membrane. After surface biotinylation cells were allowed to secrete in serum-free media for 3hours. Media was collected, immunoprecipitated PNG^{ase} treated and then analyzed by western blot using SHA31 antibody.* ***(B)*** *1/10 of cell lysate and 1/5 of media before the immunoprecipitation was deglycosylated and run on western blot.* ***(C)*** *Transcytosis quantification. The relative amount of PrP, biotinylated on the basolateral membrane and immunoprecipitated in the apical membrane was normalized to the amount of PrP biotinylated on the apical membrane and immunoprecipitated from the apical media. Quantification was done on 4 independent experiments.*

Discussion

In the present study we used both C-terminal (SHA31) and N-terminal (SAF32) antibodies to study PrP localization and intracellular trafficking in fully polarized MDCK cells. We observed that in polarized MDCK cells SAF32 antibody, which recognizes PrP FL and the soluble N1 fragment, stains intracellular vesicles and the basolateral membrane in agreement with our and other previous findings (Sarnataro et al. 2002; Uelhoff et al. 2005; Puig et al. 2011). On the other hand when using the SHA31 antibody, which recognizes PrP FL and membrane-anchored C1 fragment we obtained a clear apical signal for PrP, as shown before by Christensen and Harris (Christensen & Harris 2009). Apical SHA31 signal is most likely due to C1 cleavage fragment, which is not recognized by SAF32 antibody. We found that C1 segregates from PrP full length both in 2D and in 3D polarized cells. An advantage of 3D culture is the presence of the isolated apical lumen where we could detect an abundant signal of SAF32, probably coming from soluble N1 fragment. Thus using the two different N-terminal and C-terminal antibodies we could reconcile and explain the opposite results in the literature on PrP localization.

We next used a biochemical approach to confirm and study α-cleavage in MDCK cells (Fig 2). C1 is present both in non-polarized and polarized MDCK cells; interestingly, in polarized cells C1 is 5 times more abundant than PrP FL. Also by assessing the presence of cleavage fragments in the media we could show that secretion of PrP and its cleavage fragments is polarized: PrP FL, N1 and C1 are secreted apically while only C1 is found in the basolateral media. These data suggest that apically sorted PrP is both cleaved and secreted as full length into the apical media in MDCK cells. This is consistent with, and explains, our previous data (Sarnataro et al. 2002) showing that newly synthesized PrP is sorted to both apical and basolateral surfaces, but then, while the signal was stable on the basolateral membrane, it quickly disappeared from the apical surface (Sarnataro et al. 2002). This is sustained and explained by the fact that while the N-terminal antibody does not recognize the protein on the apical domain, this latter is recognized by the C terminal antibody (reacting against the C1 cleaved fragment on the apical surface). Consistently, the fact that SHA31 reveals high signal at the apical surface (Fig 1C, 1D, S1 Fig) indicates that there is a progressive enrichment of the C1 fragment on the apical membrane over the full-length.

Interestingly we note that while in the apical media we found 2 forms of C1 previously described as membrane anchored and devoid of GPI anchor C1 (Wik et al. 2012), in the basolateral media we revealed only one form of C1 fragment. It seems probable that, in MDCK cells as well as in BHK, (used by Wik and collaborators) (Wik et al. 2012) there are at least 2 mechanisms of shedding and release of PrP. The unidirectional secretion of PrP and several cleavage fragments in MDCK indicates that PrP cleavage in our model occurs either on the apical membrane or in an intracellular compartment on the way to the apical surface. This data are in agreement with what we have previously shown for PrP secretion, mainly occurring from the apical surface of FRT cells (Campana et al. 2007); It also agrees with the data of Tveit and collaborators showing that GFP-PrP and its cleavage fragments are secreted from the apical side of polarized MDCK (Tveit et al. 2005).

Next we investigated the dynamic of the secretion during the polarity establishment. We observed that C1/PrP FL ratio gradually increases throughout polarization, and the main reason is the decrease of PrP FL upon polarization (Figure 2D). Because the secretion of soluble N1 is maximal at early stages of polarization it is likely that alpha cleavage is not increasing through polarization. On the other hand a possible explanation is that the cleavage occurs only at the forming apical surface and in the 3 hour time slot of the experiment, more PrP goes directly to the apical surface in early polarity stages rather than in late polarity stages, suggesting that PrP trafficking changes during the establishment of the polarized phenotype. Supporting this hypothesis, an immunofluorescence of the early polarization stage unveils significant apical signal of PrP full-length detected by SAF32 antibody (S1 Fig). Further experiments will be required to investigate this mechanism.

PrP full-length is basolateral and C1 is apical, but how is this steady state distribution maintained? In 2002 Sarnataro and colleagues performed pulse-chase experiments and made an interesting conclusion: comparable amount of PrP full-length reaches the apical and the basolateral membranes simultaneously, but the protein is unstable on the apical surface and rapidly leaves it (Sarnataro et al. 2002). Our results with the two distinct antibodies allowed us to hypothesize that the mechanism re-localizing PrP FL to the apical membrane is the transcytosis.

As PrP is a non-conventional GPI-AP, showing features different from other GPI-APs (Davis et al. 2015), we investigated if PrP takes a transcytotic road in polarized MDCK cells. We found that in both 2D and 3D cultures of polarized MDCK cells PrP efficiently undergoes basolateral-to-apical transcytosis. To monitor transcytosis we have used N-terminal and C-terminal antibodies that can cluster PrP, therefore mimicking a ligand binding. In these conditions transcytosis of PrP is very efficient: at the end of 3 hours C-terminal antibody SHA31 from the basolateral membrane is significantly enriched in the apical membrane (Fig 4B). When we monitor transcytosis by SAF32 antibody we did not observe any significant apical enrichment, however we observe it enriched in intracellular vesicles. We hypothesize that SAF32 recognizes PrP in the intracellular vesicles but not at the apical surface because α-cleavage occurs, releasing the N-terminal fragment (containing the SA32 epitope) by secretion from the apical surface. Consistent with this hypothesis we can clearly see apical secretion of SAF32 in 3D polarized cells (Fig 5); thus most likely SAF32 luminal signal is due to the proteolytic removal of the epitope from the cell surface. Our data are consistent with PrP full-length being endocytosed from the basolateral membrane and undergoing α-cleavage either inside the intracellular vesicular compartment on its way to the apical surface or at the apical surface. It is also intriguing to investigate if ligand binding stimulates PrP transcytosis, making PrP behave like IgA receptor in MDCK cells (Apodaca et al. 1994). A recent article by Pflanzner and colleagues has shown that amyloid-β (1-40) transcytosis through the blood-brain barrier depends on PrP (Pflanzner et al. 2012). In our work we show that PrP itself undergoes transcytosis, therefore PrP can play the role of shuttle for its ligands and PrP-interacting molecules.

Our work showed that PrP in polarized cells is cleaved on its way to the apical membrane, and that it undergoes basal-to-apical transcytosis. To summarize the data of PrP in polarized MDCK cells we propose the following model (Fig 7): first, a similar amount of PrP is sorted in TGN to apical and basolateral membranes; 1. During the traffic to the apical surface a part of PrP molecules undergo α-cleavage; 2. Basolaterally sorted PrP reaches the cell membrane intact; 3. PrP is transcytosed from the basolateral to the apical membrane where part of PrP molecules are cleaved; 4. PrP full length reaching the apical surface is shed to the media, soluble N1

fragment is secreted to the apical media, C1 fragment is stabilized on the apical surface, and part of it is shed to the apical media.

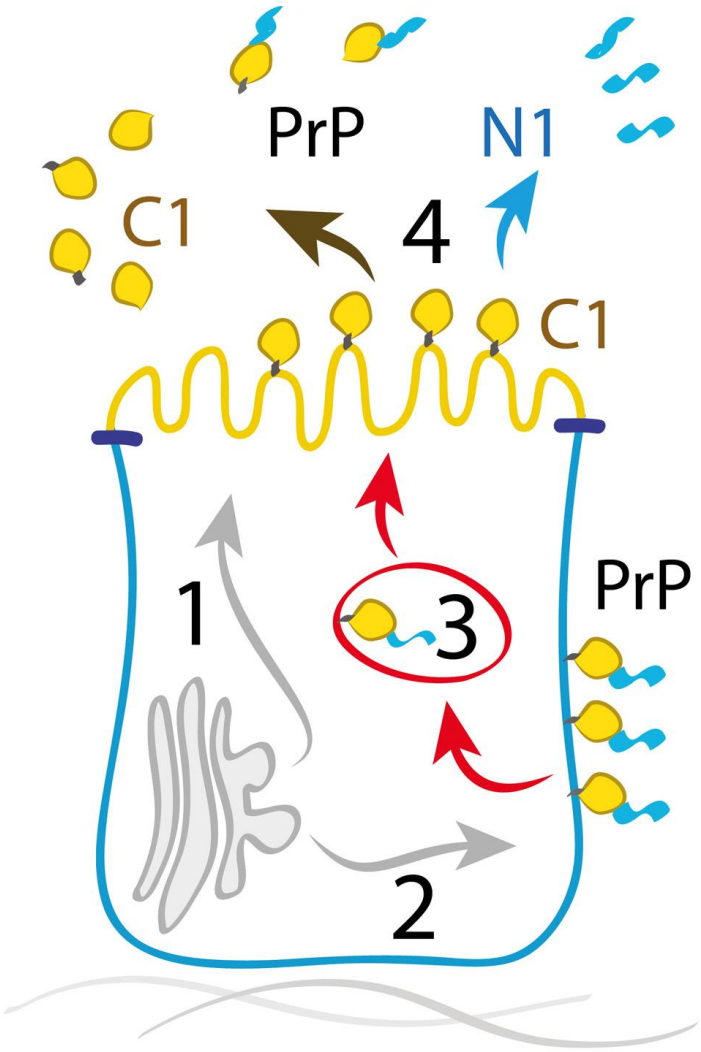

Fig 7. Model of PrP trafficking in MDCK cells. *In fully polarized epithelial cells PrP is exported from the Golgi to both apical and basolateral surfaces (40/60) (Sarnataro et al.; 2002). (1) Significant part of PrP sorted from TGN to the apical membrane undergoes the α-cleavage in the vesicular compartment or at the apical cell surface. (2) PrP sorted from TGN to the basolateral membrane stays intact. (3) Basolateral PrP is transcytosed and a part of it is cleaved on the way to the apical membrane. (4) Soluble N1 is released to the apical media; full-length PrP as well as C1 are shed from the apical media.*

Our findings are of fundamental importance for the GPI-AP trafficking in polarized cells. Further studies of PrP trafficking (eg., by using deletion mutants) will allow determining the PrP signal

responsible for the transcytotic route and to better characterize the underlying mechanisms. Both the N and C terminal region of PrP have been shown to be of importance in the prion disease pathogenesis (Senatore et al. 2013; Westergard et al. 2011; Chen et al. 1995; Guillot-Sestier et al. 2009); by shedding some light on the trafficking of PrP cleavage fragments,this study could help to explain their role in PrP^{Sc} formation, as for example in the case of the dominant negative effect observed for C1 fragment in this process (Westergard et al. 2011).

Acknowledgments

We thank Dr. G.S.Victoria for the manuscript reading and for her helpful advice. We thank K. Klinkert for the help with 3D cyst culture.

References are listed on the page 112 of the manuscript.

Supplementary figure

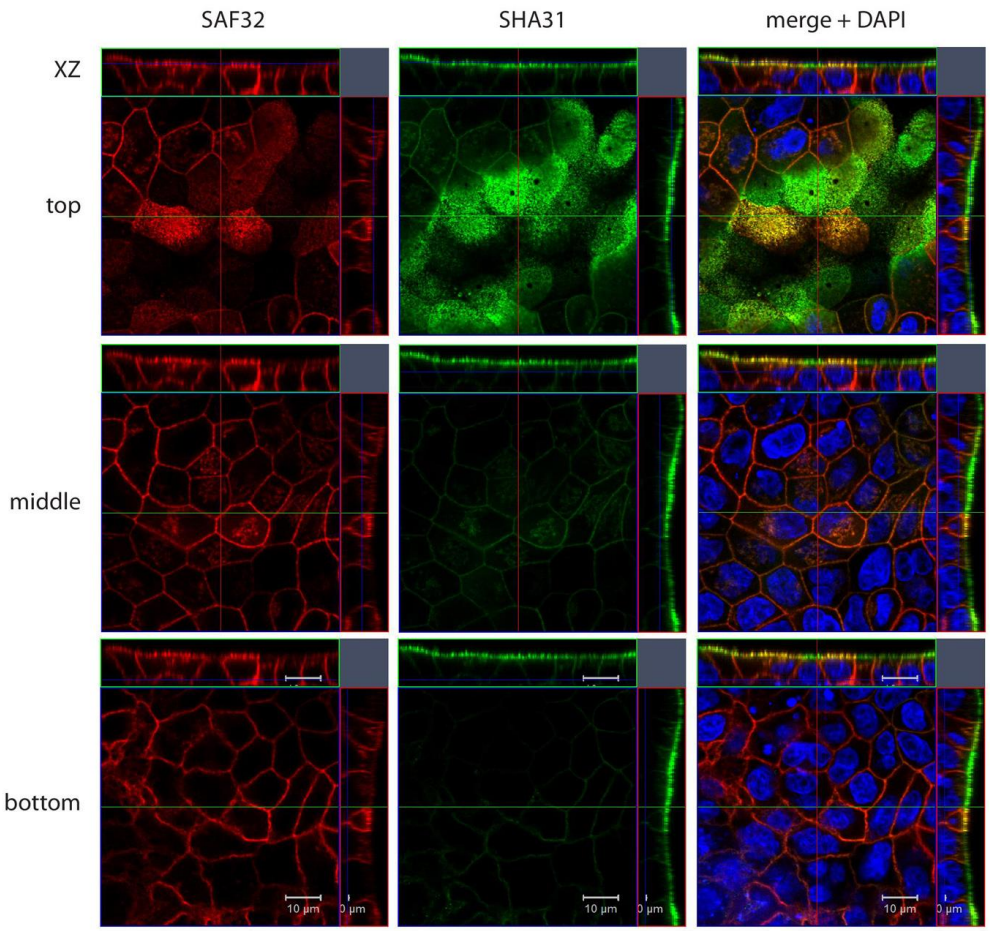

S1 Fig. Localization of PrP in early stage of polarization in 2D. *Immunofluorescent pictures of MDCK PrPwt cells plated for 24 hours on Transwell filters. Cells were fixed and immunostained for PrP using SAF32 antibody (left column) and SHA31 antibody (middle column) and nuclei are stained with DAPI (right column). Scale bars 10 µm. Serial confocal sections of 0,3 µm were collected from the top to the bottom of the cell monolayer.*

Conclusions

We can conclude from my work that:

1. PrP sorting in 2D and 3D systems is similar. 3D system provides an additional compartment – an apical lumen, where apically secreted PrP was trapped.
2. **Unlike other GPI-APs PrP undergoes basolateral-to-apical transcytosis in polarized MDCK cells.**
3. In fully polarized cells most of PrP is present as a C1 cleavage fragment on the apical surface. PrP addressed to the apical membrane is cleaved and shed to the apical media in 2D or to the apical lumen in 3D.
4. The reason of discrepancy of earlier published data resides in the use of different PrP antibodies, recognizing full-length PrP and N1 fragment or full-length PrP and C1 fragment. By using both types of antibodies I have reproduced basolateral localization of full-length PrP and apical localization of C1.

Our findings are of fundamental importance for the GPI-AP trafficking in polarized cells. Further studies of PrP trafficking (eg., by using deletion mutants) will allow determining the PrP signal responsible for the transcytotic route and to better characterize the underlying mechanisms. Both the N and C terminal region of PrP have been shown to be of importance in the prion disease pathogenesis (Senatore et al. 2013; Westergard et al. 2011; Chen et al. 1995; Guillot-Sestier et al. 2009); by shedding some light on the trafficking of PrP cleavage fragments,this study could help to explain their role in PrP^{Sc} formation, as for example in the case of the dominant negative effect observed for C1 fragment in this process (Westergard et al. 2011).

Discussion

This part of the manuscript is a continuation of the discussion started in the article.

I. Comparison of PrP trafficking in epithelial cells

As summarized in the introduction PrP was studied by multiples laboratories in MDCK cell model. This experimental model is widely accepted in the field of polarity and trafficking, however, MDCK is not the only available polarized cell line. Many diverse epithelial models are used in the research and their diversity is as high as the diversity of epithelial organs (thyroid glands, kidney, gut, ovary etc.) and animal model (human, mouse, rat, hamster, dog etc.). Localization and trafficking of protein is greatly diverse in different epithelial cells lines, reflecting the unique functions of each epithelial cell type (Cao et al. 2012). PrP was also investigated in a broad range or epithelial cell line, unraveling its possible functions in specific organs (Morel et al. 2004; Petit et al. 2013; Málaga-Trillo et al. 2009; Malaga-Trillo & Sempou 2009; Petit et al. 2012; Viegas et al. 2006; Solis et al. 2012).

The finding of our laboratory that PrP full-length is basolateral in MDCK cells as well as present work showing that PrP and its cleavage fragment localize in the opposite membrane compartments in MDCK cells, are conflicting with data, obtained in very similar kidney cell model Rov. Rov cells are derived from rabbit kidney (RK13) epithelial cells by transfection of a Tet-regulatable ovine PrP gene (Paquet et al. 2004). In Rov cells full-length ovine PrP is primarily expressed on the apical side. Paquet and colleagues further show that prion transmission to Rov cells is much more efficient if infectivity contacts the apical side. Why MDCK PrPwt and Rov cells sort PrP so differently? One possibility is that generations of these cell lines were associated with undesirable mutations altering protein trafficking. Alternatively because the sequences of PrP have different origins they might be differently sorted and/or processed.

the other possibility is that the sequence of PrP from different origin (mouse vs. ovine) is differently sorted and processed.

The possibility that ovine and murine PrP are differently processed should be carefully explored. GFP-tagged ovine PrP was shown earlier to undergo the alpha-cleavage at comparable rate in neuronal and epithelial cells such as murine neuroblastoma cells (N2a), human neuroblastoma cells (SH-SY5Y), MDCK and human colon cancer cells (LoVo) (Tveit et al. 2005). Tveit and colleagues also demonstrated that PrP full-length is predominantly apically secreted. In our

work, contrary to Tveit and colleagues we have used a native mouse PrP sequence. We have performed several experiment with GFP-PrP construct and we did not include this data to the manuscript, because we have found that GFP-PrP construct has an altered cleavage pattern and produce a multitude of C and N cleavage fragments, therefore is prone to generate artefacts.

Interestingly, in intestine cells, enterocytes, PrP has basolateral localization and was shown to co-localize with cell-to-cell junctional domain (Morel et al. 2004). Furthermore in these cells there is no difference between N- and C-terminal PrP antibody staining. In addition, the involvement of PrP in cell-cell junctions and barrier function was later shown in zebrafish and Drosophila S2 cells (Petit et al. 2013; Málaga-Trillo et al. 2009; Malaga-Trillo & Sempou 2009; Paquet et al. 2004). Possible involvement of PrP in cell-cell junctional connection of epithelial cells was confirmed by several laboratories in enterocytes (Petit et al. 2012), brain endothelial cells (Viegas et al. 2006) and a model human epithelial A431 cells originated from epidermoid carcinoma (Solis et al. 2012). In our hands only PrP full-length was localizing on the basolateral membrane, therefore it is still possible that in MDCK PrP full-length is involved in cell-cell contact. Of note in MDCK cells expressing GFP-PrP construct GFP signal highly co-localize with E-cadherine (data not shown) suggesting the function similar to the PrP in enterocytes.

The regulation of cell-cell contact by PrP is a promising pass, many laboratories found the interaction between PrP and cell adhesion molecules in neuronal and immune cells (Pantera et al. 2009; Loubet et al. 2012; Bodrikov et al. 2011; Schrock et al. 2009; Richardson & Fernandez-Borja 2016)

Even if MDCK express a negligible level of dog PrP and are refractory to Prion infection (Polymenidou et al. 2008) it is still a reliable model for prion protein trafficking. The final goal of our work in MDCK cells is not to characterize prion protein behavior, function or relevance of PrP cleavage in primary epithelial cells, but rather use MDCK model as a step on the way to characterize PrP processing in several types of neurons.

II. PrP localization in neurons

The pioneering work on hippocampal neurons, has characterized PrP as a resident of axonal membrane of fully developed, stage 5 of differentiation neurons (Galvan et al. 2005). Of note, to detect endogenous PrP Galan and colleagues used a C-terminal antibody Pom-1, therefore

PrP FL and C1 fragment were not distinguished. In a more complex system, in the mouse brain there is an important diversity of neuronal types, it was shown by the immunohistochemical staining of brain slices with N- and C-terminal PrP antibodies, that among brain regions the cerebellum has a highest level of C1 (Beringue 2003; Liu et al. 2001). A refined work from Aguzzi laboratory, has brought into light an importance of PrP full-length and PrP C1 cleavage fragment in peripheral sciatic nerve (Bremer et al. 2010). In a picture from their article (Fig A), we see that unlike total brain homogenate, the sciatic nerve protein extraction shows mostly C1 fragment. In mouse model where PrP expression was restricted to neurons Bremer and colleagues have shown that PrP in sciatic nerve is mostly present in the axon and not in the Shwann cells.

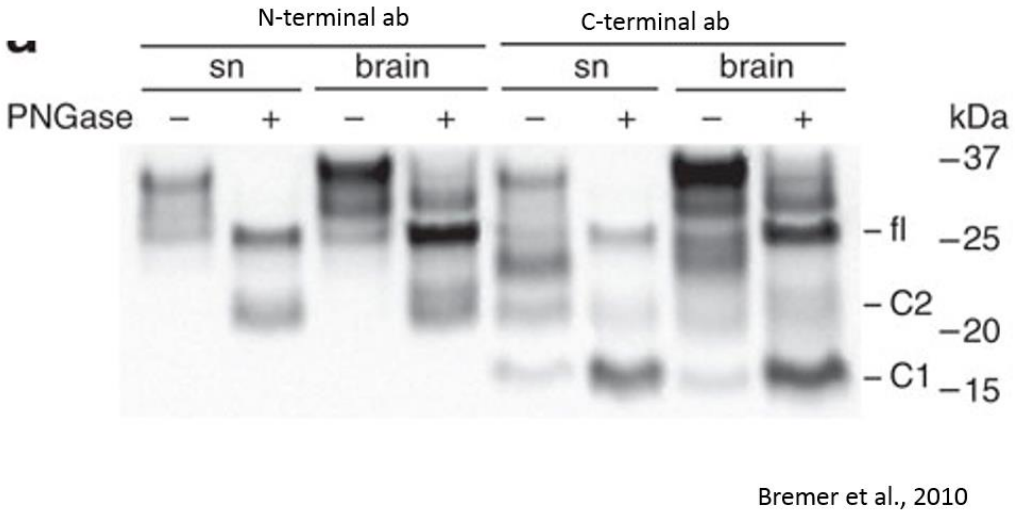

Figure A. PrP^C expression and proteolytic processing in sciatic nerves of wild-type mice*. Western blot analysis comparing PrP^C protein expression in the sciatic nerve with that in the brain of wild-type mice, using two different monoclonal antibodies, C-terminal POM1 and N-terminal POM3* (Bremer et al. 2010).

Strikingly the ratio of C1 to PrP FL in purely axonal membrane of sciatic nerve is very similar to what we have obtained in fully polarized MDCK cells. The apical membrane of MDCK cells, enriched in C1 cleavage fragment reflects the axonal membranes of sciatic nerve. What kind of neurons project through this nerve? The rat sciatic nerve originates from the spinal segments L4-L6, the entire sciatic nerve contains 6% of motor, 71% of sensory, and 23% of sympathetic axons (Schmalbruch 1986). Therefore, it is tempting to suppose that behavior of PrP in MDCK

cells is similar to sensory neurons. The logic continuation of our work in MDCK cells would be a validation of our data on PrP transcytosis in fully developed sensory neurons.

III. PrP α-cleavage in MDCK

Using the two different N-terminal and C-terminal antibodies, we could reconcile and explain the opposite results in the literature on PrP localization. We observed that in polarized MDCK cells N-terminal SAF32 stains intracellular vesicles and the basolateral membrane similar to previous findings (Sarnataro et al. 2002; Uelhoff et al. 2005; Puig et al. 2011). On the other hand when using the C-terminal SHA31 antibody we obtained a clear apical signal for PrP, as shown before by Christensen and Harris (Christensen & Harris 2009). In this work, we have shown that PrP in MDCK cells undergoes the α-cleavage, and resulting C1 fragment resides on the apical membrane. C1 is present both in non-polarized and polarized MDCK cells; interestingly, in polarized cells C1 is 5 times more abundant than PrP FL. Also by assessing the presence of cleavage fragments in the media, we could show that secretion of PrP and its cleavage fragments is polarized: PrP FL, N1 and C1 are secreted apically while only C1 is found in the basolateral media.

Interestingly in the apical media we found 2 forms of C1 (Figure B) previously described as membrane anchored and devoid of GPI anchor C1 (Wik et al. 2012), in the basolateral media we revealed only one form of C1 fragment. It seems possible that, in MDCK cells as well as in BHK, (used by Wik and collaborators) (Wik et al. 2012) there are at least 2 mechanisms of shedding and release of PrP.

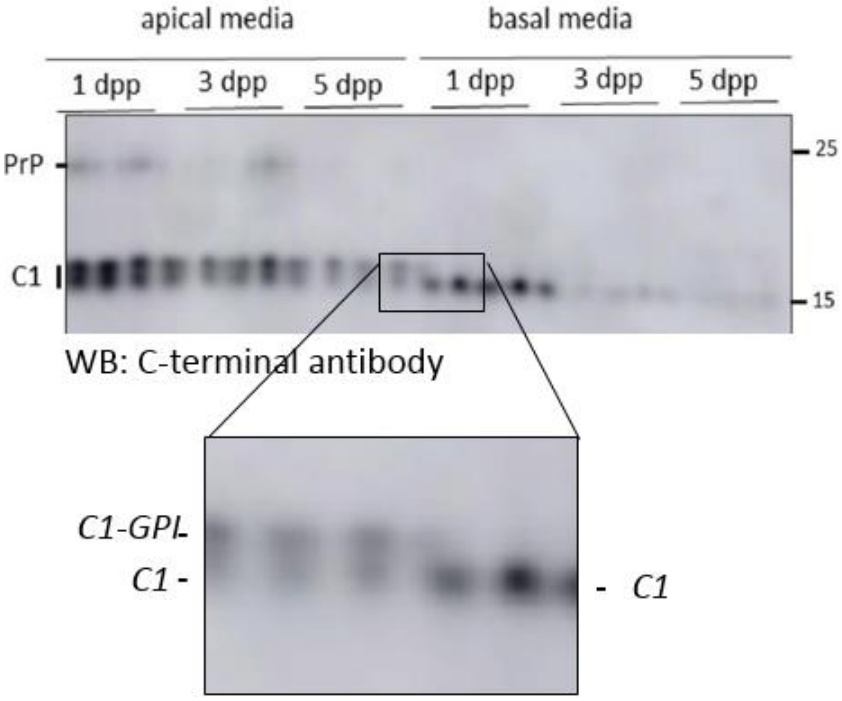

Figure B. Zoom on C1 secretion. Experiment described in the paper, page 80. Magnified region shows apically and basolaterally secreted C1, migrating as 2 separate bands C1 and C1-GPI in case of apical secretion.

Our discovery of spatial separation of mechanisms of PrP shedding opens a unique opportunity to characterize these mechanisms separately. Interestingly the vast majority of secreted PrP in MDCK is soluble and not associated with the exosomes (data not shown), therefore, most likely, there are only 3 mechanisms of PrP release in our system: proteolytic cleavage, proteolytic shedding and phospholipase-mediated shedding.

It was shown by Aguzzi laboratory that sequence variation do not dramatically affect cleavage, suggesting existence either sequence-independent PrP-ase or an activity of multiple enzymes with overlapping alpha-cleavage function, but different sequence specificity (Salamat et al. 2013; Oliveira-Martins et al. 2010). A recent finding by McDonald and colleagues is that there is at least 3 alpha-cleavage sites, producing C1 and N1 fragments, enhancing therefore the multiple enzymes and multiple cuts hypothesis (McDonald et al. 2014; McDonald & Millhauser). It would be important to see whether target genes for PrP cleavage, notably metalloproteases are expressed in MDCK and where they localize. One of the prominent target for PrP shedding and cleavage, ADAM10 is expressed and basolaterally localized in MDCK cells (Wild-Bode et al. 2006). Other ADAM proteins, notably ADAM8, 9 and 17 must be further investigated in polarized MDCK cells. Subsequent blocking of ADAM family enzymes by membrane-permeable

and non-permeable pan-inhibitors will also shed lite on the site of PrP cleavage.The unidirectional secretion of PrP and several cleavage fragments in MDCK indicates that PrP cleavage in our model occurs either on the apical membrane or in an intracellular compartment on the way to the apical surface.

IV. Transcytosis

How PrP and C1 distribution at steady state is maintained? Previously our laboratory has demonstrated that PrP FL is addressed to both basolateral and apical membranes, our present results show that further specificity of sorting is enhanced by the transcytosis. We found that in both 2D and 3D cultures of polarized MDCK cells PrP efficiently undergoes basolateral-to-apical transcytosis. To monitor transcytosis at steady state we have a biotinilation assay and to investigate ligand-dependent transcytosis we have used N-terminal and C-terminal antibodies that can cluster PrP, therefore mimicking a ligand binding. When we monitor transcytosis by SAF32 antibody we did not observe any significant apical enrichment, however we observe SAF32 in intracellular vesicles and in the lumen. Most likely SAF32 luminal signal is due to the cleavage of PrP and the liberation of SAF32 bound to its epitope on N1 fragment from the cell. Our data are consistent with PrP full-length being endocytosed from the basolateral membrane and undergoing α-cleavage during the transcytosis to the apical surface.

The main discovery of this work is that PrP undergoes basolateral-to-apical transcytosis in fully polarized MDCK cells. Transcytosis is not a common mechanism for MDCK cells (Apodaca et al. 2012). It is intriguing to investigate if ligand binding stimulates PrP transcytosis, making PrP behave like IgA receptor in MDCK cells (Apodaca et al. 1994). Our preliminary data (see "Perspectives") suggest that PrP transcytosis is further enhanced by ligand binding, in our case SAF32 antibody. It is tempting to investigate if HOP/STI-1 (Zanata et al. 2002) and Aβ (Laurén et al. 2009) undergo transcytosis in polarized MDCK PrP wt cell model.

MDCK cells were previously used as a transcytosis model, mimicking Aβ penetration of Blood-Brain-Barrier (Nazer et al. 2008; Tuma & Hubbard 2003). Nazer and colleagues did not detect significant transcytosis of Aβ trough MDCK monolayer; introduction of PrP in MDCK experimental model seems to be a promising pass.

MDCK cell model can serve for the dissection of PrP transcytosis signal. Deletion mutants (Solomon et al. 2011; Laurén et al. 2009; OliveirβMartins et al. 2010) and domain-swap approach (Puig et al. 2011) are accessible and widely used in prion field; careful study of mutants using N-terminal and C-terminal antibodies in combination with quantitative transcytosis assay can point out which part of PrP contains the signal for the transcytosis.

Perspectives

I. Investigation of cleavage

The α-cleavage of PrP^C may be a therapeutic target in prion disease (Campbell et al., 2013; Westergard, Turnbaugh, & Harris, 2011)

Sarnataro and colleagues (Sarnataro et al. 2002) showed that PrP is sent both to the apical and basolateral membranes in polarized MDCK cells. I furthermore found that part of basolateral PrP transcytoses from the basolateral to the apical surface. Interestingly PrP appears unstable at the apical membrane. The experiments performed during this thesis have shown that PrP sorted to the apical membrane, undergoes shedding and cleavage.

An open question is to determine where the α-cleavage occurs. In order to understand how transcytosis and cleavage are connected I am performing additional experiments, giving some preliminary data.

In the biotinilation assay (see article submitted) we used SHA31 antibody to reveal PrP, immunoprecipitated from the media. This antibody has exceptionally high affinity for PrP and gives a strong signal even with a small protein load. In the resulting western blot we observed PrP FL and PrP C1 fragment that were first exposed to biotin on the basolateral membrane and then translocated to the apical membrane and shed into the apical media. This data are sufficient to claim that PrP undergoes basal-to-apical transcytosis, but do not tell whether PrP was cleaved during the transcytosis. To see if PrP is cleaved during the passage from basal to the apical membrane we revealed PrP immunoprecipitated from the apical media with SAF32 antibody (Fig. A). In the apical media we detected biotinylated N1 fragment, as well PrP FL, confirming that transcytosis is coupled to α-cleavage. Interestingly in the positive control (apically biotinylated MDCK monolayer) in the apical media a high amount of biotinylated N1 and PrP FL was detected (Fig. A). These results suggest that a detectable portion of PrP is present on the apical membrane and rapidly undergoes cleavage and shedding.

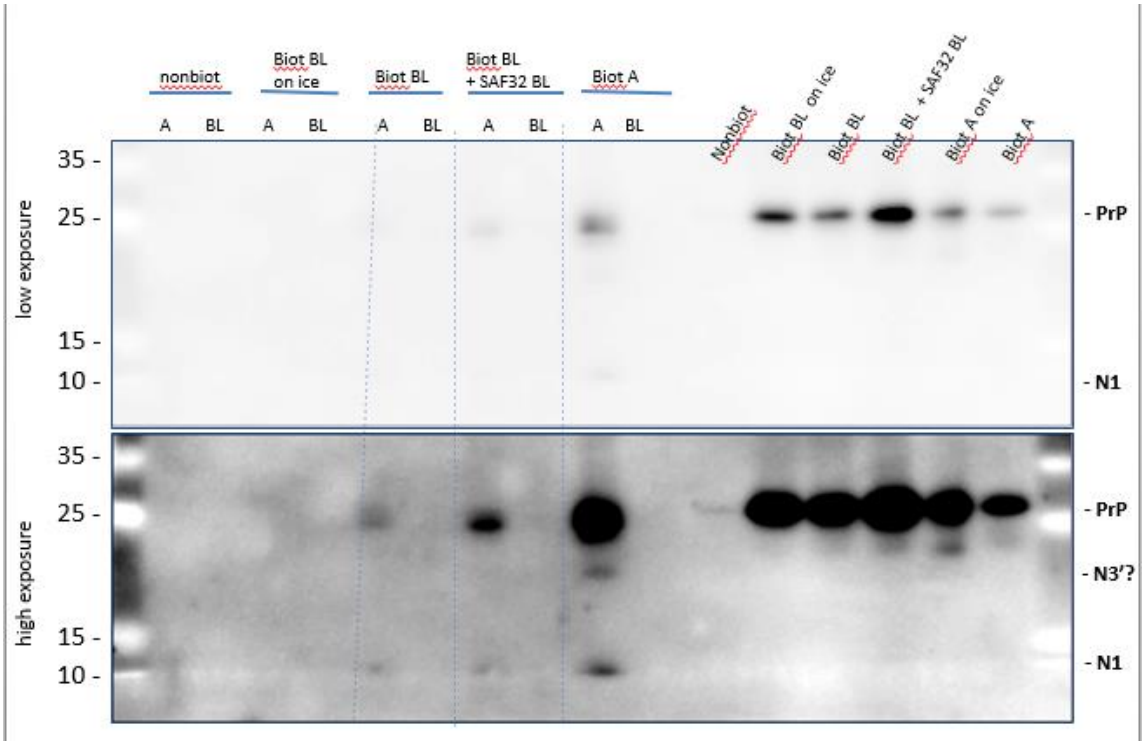

Figure A. PrP is cleaved while follows transcytotic road and after exposure to the apical surface. After 5 days of polarization MDCK cells were biotinylated on the basolateral or apical membrane. After surface biotinylation cells were allowed to secrete in serum-free media for 3 hours. Media was collected, immunoprecipitated PNG^{ase} treated and then analyzed by western blot using SAF32 antibody.

On the same western-blot we tested if treatment of cells with the anti-PrP antibody can enhance the PrP transcytosis. Antibody treatment was reported to enhance the endocytosis of GPI-APs (Lakhan et al. 2009) Before the biotinilation we saturated basolateral compartment of 3 filters with SAF32 and then proceed as described in M&M of the article. Our preliminary data support the hypothesis that antibody treatment stimulates PrP transcytosis.

PrP is permanently cycling between cell surface and recycling endosomes (Shyng et al. 1993). In our experiment α-cleavage can occur on the apical membrane but also inside of the apical recycling endosomes from were cleavage products are secreted apically.
Further experiments are necessary to find out the cellular compartment of α-cleavage. For example we can use protease inhibitors penetrating the cell (such as 1,10-Phenanthroline) or acting strictly on the surface (such as TAPI-2).

The question of cleavage site is not restricted to the recycling compartment and plasma membrane. PrP can also be cleaved during the initial export from TGN. When we looked at the maturation of the cell monolayer on filters, we noticed that PrP FL decreased during MDCK polarization. It is tempting to hypothesize that in polarized cells a functional form of PrP is a cleaved one. It will be interesting to reveal the direct export of cleavage fragments from TGN by performing the same pulls-chase experiment that was previously done by Sarnantaro (Sarnataro et al. 2002); but this time using both N-terminal and C-terminal antibodies. This experiment will allow us to understand whether the sorting machinery is sending C1 directly to the apical membrane from the TGN (like for all native GPI-APs) or if there is no cleavage upon direct trafficking from the Golgi and no specificity in initial export of PrP full-length from the Golgi (like shown by Sarnataro); therefore only following transcytosis and cleavage establish polarized non-symmetric distribution of PrP.

II. PrP transcytosis in neurons.

The neuron is a classic example of a polarized cell, usually characterized by a long, thin axon and thick, shorter dendrites. Neurons develop from epithelial cells and share with them a fundamental epithelial feature, notably polarization. We can do an approximation to some extend: the epithelial cell's basolateral surface is comparable to the somato-dendritic plasma, while the apical surface corresponds to the axonal plasma (Rodriguez-Boulan & Powell 1992; Winckler & Mellman 1999), (Fig. B). Polarized neurons maintain axonal and somatodendritic plasma membrane domains without an obvious physical barrier (Winckler et al. 1999). The establishment and maintenance of neuronal polarity are essential for the correct development and function of the nervous system and rely on the exquisite coordination between membrane transport and cytoskeletal dynamics.

Trafficking aspects are less known in neurons than in epithelial cells, even though they are considered to share elements of the sorting (Horton & Ehlers 2003; Silverman et al. 2005). Model molecule, that are used to study protein sorting are differentially delivered to axonal and dendritic membranes. For example in polarized hippocampal neurons viral

hemagglutinin (HA) and model GPI-anchored protein Thy-1 are specifically sorted to the axolemma (Ledesma 1998).

In fact there are several examples of apical and basolateral proteins sent, respectively, as axonal and somatodendritic proteins in neurons, and vice versa in epithelial cells (Dotti & Simons 1990; Bradke & Dotti 1998; Dotti et al. 1991; Pietrini et al. 1994). However, there are also examples that do not fit into this pattern. There is evidence suggesting that neurons cannot interpret certain sorting signals as epithelial cells do (Silverman et al. 2005).

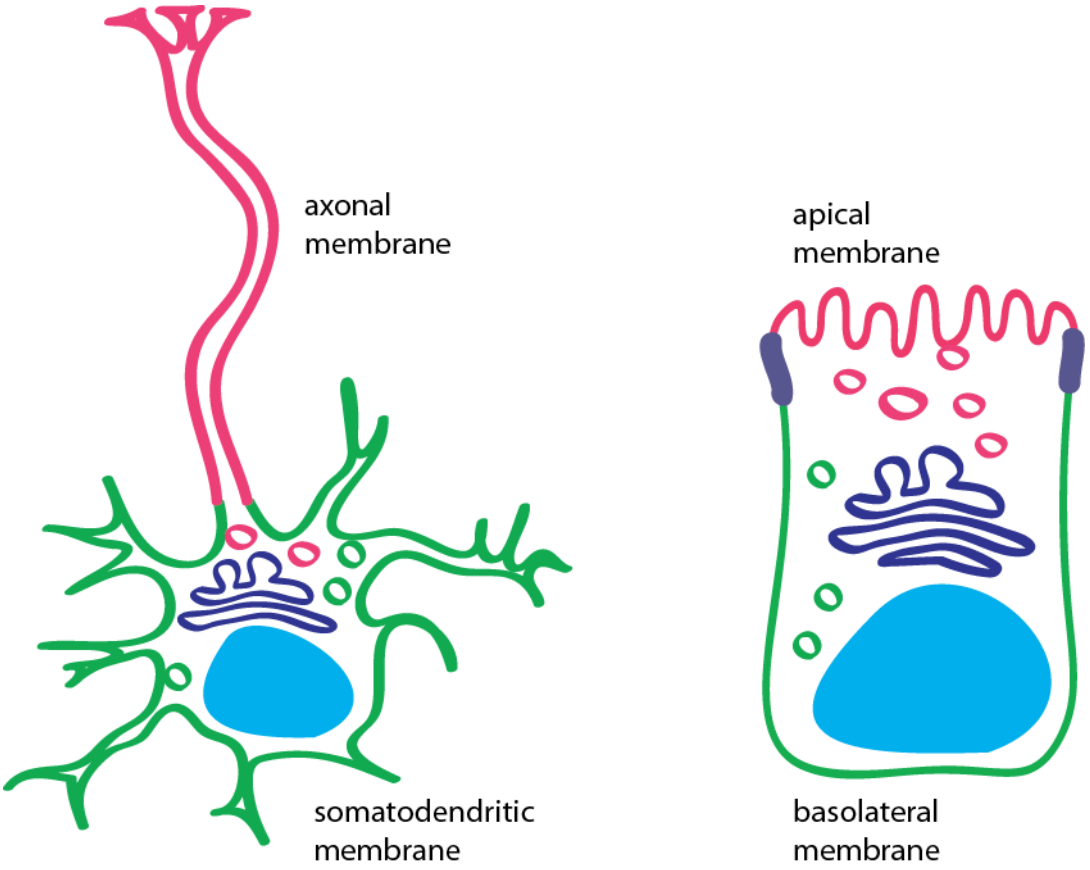

***Figure B. The epithelial blueprint of a neuron**. On the left schematics of a motoneuron showing the cell body and the nucleus. Dendrites (in green) emerge from the basolateral aspect of the neuron, the axon (in red) from the apical aspect. Schematic of an epithelial cell is shown on the right. Basolateral membrane (green) is distinct from the apical membrane (red). With some approximation, apical membrane of the epithelial cell reflects axonal membrane of the neuron.*

Therefore it is essential for us to validate our data in neurons where PrP expression is the highest and where PrP plays its physiological role. For the transcytosis assay it is essential to physically separate the media surrounding different membrane compartments. In the classical primary neuronal culture dendrites, soma and axons form the network, were all membranes are exposed to the same media. To overcome this technical problem we decided to use a microfluidic system were soma axons are separated into different compartments not exchanging the media.

III. Preliminary data on PrP transcytosis in neurons.

The purpose of this work is to investigate whether we can reproduce our finding in primary neurons. The experiment is therefore to evaluate if PrP can transcytose from somato-dendritic to axonal membrane, analogous to basolateral to apical transcytosis. In collaboration with JM Peyrin (Université Pierre et Marie Curie) we used a microfluidic system (Fig. C) to detect a passage of PrP bound to the specific antibody from the somatodendritic membrane to the axonal membrane. We therefore incubated somato-dendric compartment of mature cortical neurons plated in a microfluidic device with anti-PrP antibodies.

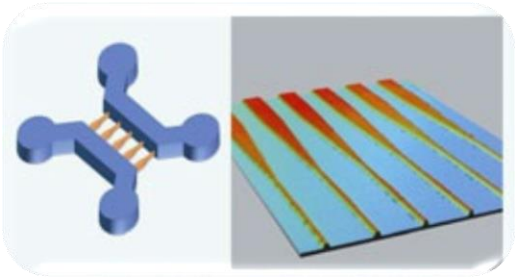

Figure C. Schematics of a microfluidic device. Left – somal and axonal chambers connected by microfluidic channels. Microfluidic channels are depicted on the right.

24 hours later whole microfluidic device was fixed with 4% PFA and subjected to the classical IF as a positive control (Fig. D) or immunostained with secondary antibodies only to visualize transcytosis of PrP bound to the primary antibody (Fig E and F).

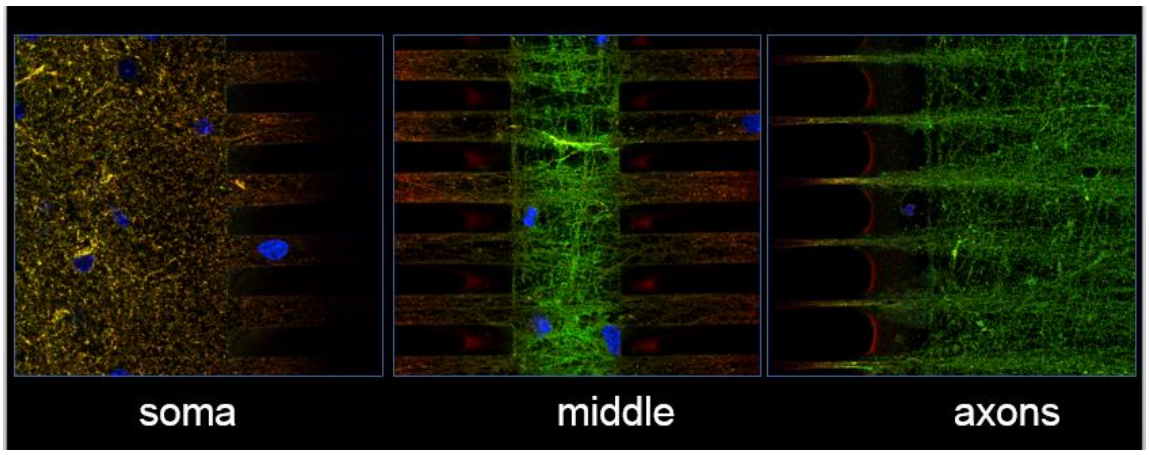

Figure D. Imunnofluorescence of polarized cortical neurons grown in a microfluidic device. Cortical neurons were plated in the somal chamber, grown for 9 days, fixed and immunostained in all compartments. SHA31 is depicted in green, SAF32 in red and DAPI in blue

Note that in classic immunofluorescence SAF32 and SHA31 signals are comparable in the somal chamber, while in axonal chambers SHA31 is stronger than SAF32 (Fig. D). It could indicate that C1 cleavage fragment is prevailing over PrP full-length in the axon; in agreement with *in vivo* data from the sciatic nerve (Bremer et al. 2010).

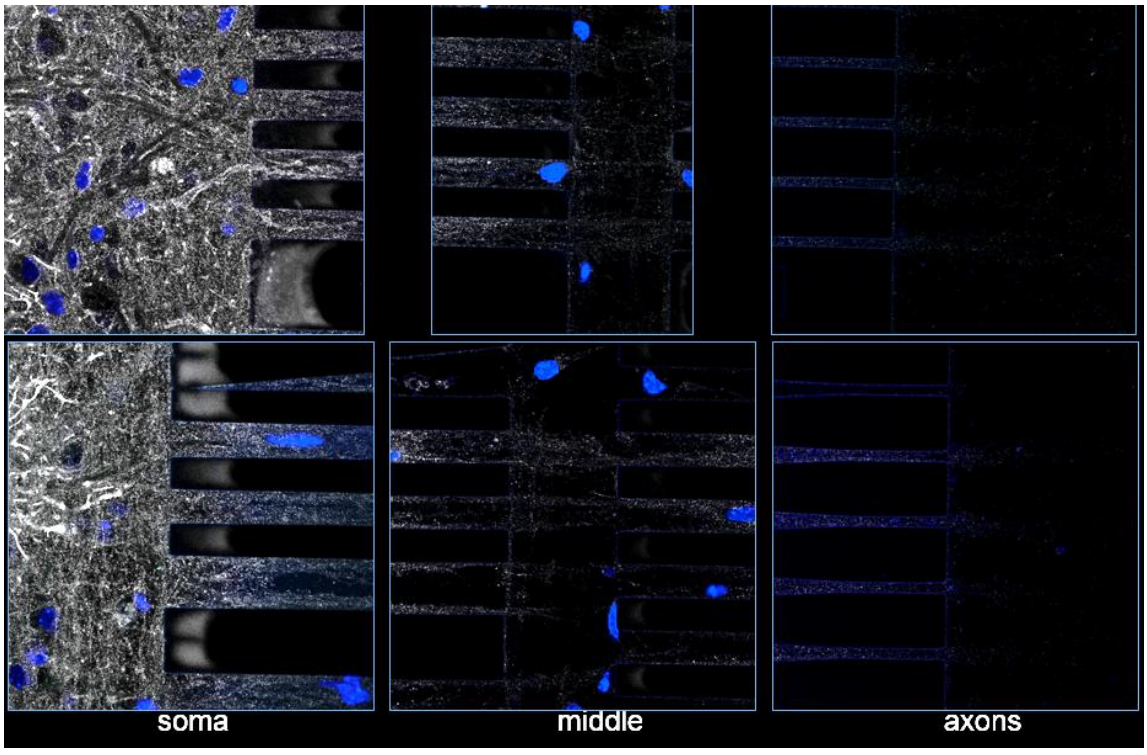

Figure E. Transcytosis assay. Cortical neurons were plated in the somal chamber, grown for 9 days. SAF32 (gray) was add to the somal compartment for 16h, then device was fixed and immunostained in all compartments with secondary antibody only. DAPI is depicted in blue.

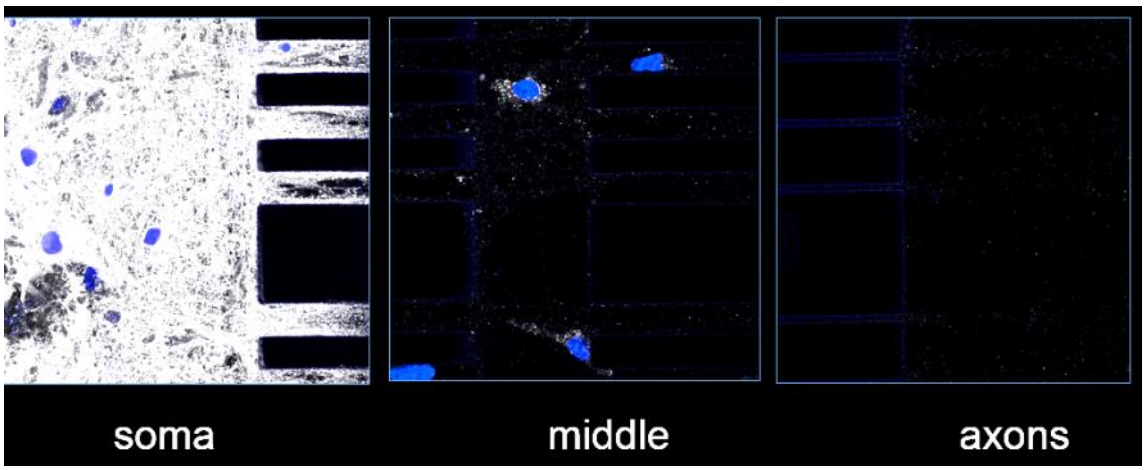

Figure F. Negative control for transcytosis assay. *Cortical neurons were plated in the somal chamber, grown for 9 days, fixed and immunostained with SAF32 (gray) in somal chamber only, while secondary antibody was add in all the compartments. DAPI in blue. Of note few cells scrolling into the axonal chamber are, most likely, microglia, therefore they are stained by secondary anti-mouse antibody.*

As you can see in figures E and F preliminary results are encouraging: at the end of 24h of incubation SAF32 is detectable in axonal compartment. Still, quantity of the signal is small, the increase of the incubation time will, probably, increase the signal (P. Tixador, personal communication).

Transcytosis experiment in neurons has to be repeated with an extended incubation time. If these results are reproducible they will contribute to our understanding of PrP traffic and more importantly infection spreading from the cell body to the axon and distant cells.

Following confirmation of our data in mature neurons can not only increase the impact of this work, but also unravel a contribution of transcytotic mechanisms in prion spreading and prion inhibition by α-cleavage (Westergard et al. 2011). Westergard and colleagues have shown that Tg(C1) mice co-expressing C1 cleavage fragment along with wild-type PrP dramatically delayed time course compared with mice lacking C1. As in MDCK transcytosis and α-cleavage are coupled, stimulation of PrP transcytosis in neuron could potentially lead to the increase of α-cleavage and accumulation of non-convertible C1 fragment.

References

Abounit, S. & Zurzolo, C., 2012. Wiring through tunneling nanotubes--from electrical signals to organelle transfer. *Journal of cell science*, 125(Pt 5), pp.1089–98.

Aguzzi, A. & Calella, A.M., 2009. Prions: protein aggregation and infectious diseases. *Physiological reviews*, 89(4), pp.1105–1152.

Aguzzi, A. & Falsig, J., 2012. Prion propagation, toxicity and degradation. *Nature neuroscience*, 15(7), pp.936–939.

Aguzzi, A. & Miele, G., 2004. Recent advances in prion biology. *Current opinion in neurology*, 17(3), pp.337–342.

Alfalah, M. et al., 1999. O-linked glycans mediate apical sorting of human intestinal sucrase-isomaltase through association with lipid rafts. *Current biology : CB*, 9(11), pp.593–6.

Altmeppen, H.C. et al., 2011. Lack of a-disintegrin-and-metalloproteinase ADAM10 leads to intracellular accumulation and loss of shedding of the cellular prion protein in vivo. *Molecular neurodegeneration*, 6, p.36.

Altmeppen, H.C. et al., 2013. Roles of endoproteolytic alpha-cleavage and shedding of the prion protein in neurodegeneration. *The FEBS journal*, 280(18), pp.4338–4347.

Altmeppen, H.C. et al., 2015. The sheddase ADAM10 is a potent modulator of prion disease. *eLife*, 4, p.e04260.

Americo, T. a., Chiarini, L.B. & Linden, R., 2007. Signaling induced by hop/STI-1 depends on endocytosis. *Biochemical and Biophysical Research Communications*, 358(2), pp.620–625.

Ang, A.L. et al., 2004. Recycling endosomes can serve as intermediates during transport from the Golgi to the plasma membrane of MDCK cells. *The Journal of cell biology*, 167(3), pp.531–43.

Aparicio, L.A. et al., 2015. Clinical implications of epithelial cell plasticity in cancer progression. *Cancer Letters*, 366(1), pp.1–10.

Apodaca, G., Gallo, L.I. & Bryant, D.M., 2012. Role of membrane traffic in the generation of epithelial cell asymmetry. *Nature cell biology*, 14(12), pp.1235–43.

Apodaca, G., Katz, L.A. & Mostov, K.E., 1994. Receptor-mediated transcytosis of IgA in MDCK cells is via apical recycling endosomes. *The Journal of cell biology*, 125(1), pp.67–86.

Aroeti, B. & Mostov, K.E., 1994. Polarized sorting of the polymeric immunoglobulin receptor in the exocytotic and endocytotic pathways is controlled by the same amino acids. *The EMBO journal*, 13(10), pp.2297–304.

Arruda-Carvalho, M. et al., 2007. Hop/STI1 modulates retinal proliferation and cell death independent of PrPC. *Biochemical and Biophysical Research Communications*, 361(2), pp.474–480.

Assemat, E. et al., 2008. Polarity complex proteins. *Biochimica et biophysica acta*, 1778(3), pp.614–630.

Balaji, K. et al., 2012. RIN1 orchestrates the activation of RAB5 GTPases and ABL tyrosine kinases to determine the fate of EGFR. *Journal of cell science*, 125(Pt 23), pp.5887–96.

Barman, S. & Nayak, D.P., 2000. Analysis of the transmembrane domain of influenza virus neuraminidase, a type II transmembrane glycoprotein, for apical sorting and raft association. *Journal of virology*, 74(14), pp.6538–45.

Basler, K. et al., 1986. Scrapie and cellular PrP isoforms are encoded by the same chromosomal gene. *Cell*, 46(3), pp.417–28.

Bate, C. & Williams, A., 2012. Neurodegeneration induced by clustering of sialylated glycosylphosphatidylinositols of prion proteins. *Journal of Biological Chemistry*, 287(11), pp.7935–7944.

Baumann, F. et al., 2007. Lethal recessive myelin toxicity of prion protein lacking its central domain. *The EMBO journal*, 26(2), pp.538–47.

Béland, M. et al., 2014. Aβ induces its own prion protein N-terminal fragment (PrPN1)–mediated neutralization in amorphous aggregates. *Neurobiology of Aging*, 35(7), pp.1537–1548.

Benetti, F. & Legname, G., 2009. De novo mammalian prion synthesis. *Prion*, 3(4), pp.213–219.

Benting, J. et al., 1999. Acyl and alkyl chain length of GPI-anchors is critical for raft association in vitro. *FEBS letters*, 462(1-2), pp.47–50.

Benting, J.H., Rietveld, A.G. & Simons, K., 1999. N-Glycans mediate the apical sorting of a GPI-anchored, raft-associated protein in Madin-Darby canine kidney cells. *The Journal of cell biology*, 146(2), pp.313–20.

Beraldo, F.H. et al., 2011. Metabotropic glutamate receptors transduce signals for neurite outgrowth after binding of the prion protein to laminin γ1 chain. *The FASEB journal : official publication of the Federation of American Societies for Experimental Biology*, 25(1), pp.265–279.

Beranger, F. et al., 2001. Cell culture models of transmissible spongiform encephalopathies. *Biochemical and biophysical research communications*, 289(2), pp.311–316.

Beringue, V., 2003. Regional heterogeneity of cellular prion protein isoforms in the mouse brain. *Brain*, 126(9), pp.2065–2073.

Le Bivic, A. et al., 1990. Vectorial targeting of an endogenous apical membrane sialoglycoprotein and uvomorulin in MDCK cells. *The Journal of cell biology*, 110(5), pp.1533–9.

Le Bivic, A., Garcia, M. & Rodriguez-Boulan, E., 1993a. Ricin-resistant Madin-Darby canine kidney cells missort a major endogenous apical sialoglycoprotein. *The Journal of biological chemistry*, 268(10), pp.6909–6916.

Le Bivic, A., Garcia, M. & Rodriguez-Boulan, E., 1993b. Ricin-resistant Madin-Darby canine kidney cells missort a major endogenous apical sialoglycoprotein. *The Journal of biological chemistry*, 268(10), pp.6909–16.

Blattler, T., 2002. Transmission of prion disease. *APMIS : acta pathologica, microbiologica, et immunologica Scandinavica*, 110(1), pp.71–78.

Bodrikov, V., Solis, G.P. & Stuermer, C.A.O., 2011. Prion protein promotes growth cone development through reggie/flotillin-dependent N-cadherin trafficking. *The Journal of neuroscience : the official journal of the Society for Neuroscience*, 31(49), pp.18013–25.

Bonifacino, J.S., 2014. Adaptor proteins involved in polarized sorting. *The Journal of Cell Biology*, 204(1), pp.7–17.

Bonifacino, J.S. & Traub, L.M., 2003. Signals for sorting of transmembrane proteins to endosomes and lysosomes. *Annual review of biochemistry*, 72, pp.395–447.

Borchelt, D.R. et al., 1993. Release of the cellular prion protein from cultured cells after loss of its glycoinositol phospholipid anchor. *Glycobiology*, 3(4), pp.319–29.

Borchelt, D.R., 1990. Scrapie and cellular prion proteins differ in their kinetics of synthesis and topology in cultured cells. *The Journal of Cell Biology*, 110(3), pp.743–752.

Bradke, F. & Dotti, C.G., 1998. Membrane traffic in polarized neurons. *Biochimica et Biophysica Acta (BBA) - Molecular Cell Research*, 1404(1-2), pp.245–258.

Bremer, J. et al., 2010. Axonal prion protein is required for peripheral myelin maintenance. *Nature neuroscience*, 13(3), pp.310–8.

Brewer, C.B. & Roth, M.G., 1991. A single amino acid change in the cytoplasmic domain alters the polarized delivery of influenza virus hemagglutinin. *The Journal of cell biology*, 114(3), pp.413–21.

Brewis, I.A. et al., 1995. Structures of the glycosyl-phosphatidylinositol anchors of porcine and human renal membrane dipeptidase. Comprehensive structural studies on the porcine anchor and interspecies comparison of the glycan core structures. *The Journal of biological chemistry*, 270(39), pp.22946–56.

Brock, S.C. et al., 2005. The transmembrane domain of the respiratory syncytial virus F protein is an orientation-independent apical plasma membrane sorting sequence. *Journal of virology*, 79(19), pp.12528–35.

Brown, D.A., 2006. Lipid rafts, detergent-resistant membranes, and raft targeting signals. *Physiology (Bethesda,*

Md.), 21(6), pp.430–9.

Brown, D.A., Crise, B. & Rose, J.K., 1989. Mechanism of membrane anchoring affects polarized expression of two proteins in MDCK cells. *Science (New York, N.Y.)*, 245(4925), pp.1499–501.

Brown, D.A. & Rose, J.K., 1992. Sorting of GPI-anchored proteins to glycolipid-enriched membrane subdomains during transport to the apical cell surface. *Cell*, 68(3), pp.533–544.

Brown, D.A. & Rose, J.K., 1992. Sorting of GPI-anchored proteins to glycolipid-enriched membrane subdomains during transport to the apical cell surface. *Cell*, 68(3), pp.533–44.

Brown, G. et al., 2004. Analysis of the interaction between respiratory syncytial virus and lipid-rafts in Hep2 cells during infection. *Virology*, 327(2), pp.175–85.

Brown, L.R. & Harris, D.A., 2003. Copper and zinc cause delivery of the prion protein from the plasma membrane to a subset of early endosomes and the Golgi. *Journal of neurochemistry*, 87(2), pp.353–63.

Bryant, D.M. & Mostov, K.E., 2008. From cells to organs: building polarized tissue. *Nature reviews. Molecular cell biology*, 9(11), pp.887–901.

Büeler, H. et al., 1992. Normal development and behaviour of mice lacking the neuronal cell-surface PrP protein. *Nature*, 356(6370), pp.577–82.

Caetano, F. a. et al., 2011. Amyloid-beta oligomers increase the localization of prion protein at the cell surface. *Journal of Neurochemistry*, 117(3), pp.538–553.

Campana, V. et al., 2007. Characterization of the properties and trafficking of an anchorless form of the prion protein. *The Journal of biological chemistry*, 282(31), pp.22747–56.

Campana, V., Sarnataro, D. & Zurzolo, C., 2005. The highways and byways of prion protein trafficking. *Trends in cell biology*, 15(2), pp.102–11.

Cancellotti, E. et al., 2005. Altered glycosylated PrP proteins can have different neuronal trafficking in brain but do not acquire scrapie-like properties. *The Journal of biological chemistry*, 280(52), pp.42909–18.

Cancino, J. et al., 2007. Antibody to AP1B adaptor blocks biosynthetic and recycling routes of basolateral proteins at recycling endosomes. *Molecular biology of the cell*, 18(12), pp.4872–4884.

Cao, X., Surma, M.A. & Simons, K., 2012. Polarized sorting and trafficking in epithelial cells. *Cell research*, 22(5), pp.793–805.

Carlson, G.A. et al., 1994. Genetics of prion diseases and prion diversity in mice. *Philosophical transactions of the Royal Society of London. Series B, Biological sciences*, 343(1306), pp.363–369.

Casanova, J.E. et al., 1999. Association of Rab25 and Rab11a with the apical recycling system of polarized Madin-Darby canine kidney cells. *MOLECULAR BIOLOGY OF THE CELL*, 10(1), pp.47–61.

Caughey, B., 1991. In vitro expression and biosynthesis of prion protein. *Current topics in microbiology and immunology*, 172, pp.93–107.

Caughey, B. et al., 1989. Prion protein biosynthesis in scrapie-infected and uninfected neuroblastoma cells. *Journal of virology*, 63(1), pp.175–81.

Chatigny, M.A. & Prusiner, S.B., 1980. Biohazards of investigations on the transmissible spongiform encephalopathies. *Reviews of infectious diseases*, 2(5), pp.713–724.

Chatterjee, S., 2001. GPI anchoring leads to sphingolipid-dependent retention of endocytosed proteins in the recycling endosomal compartment. *The EMBO Journal*, 20(7), pp.1583–1592.

Chatterjee, S. & Mayor, S., 2001. The GPI-anchor and protein sorting. *Cellular and molecular life sciences : CMLS*, 58(14), pp.1969–1987.

Chen, S., Yadav, S.P. & Surewicz, W.K., 2010. Interaction between human prion protein and amyloid-beta (Abeta) oligomers: role OF N-terminal residues. *The Journal of biological chemistry*, 285(34), pp.26377–83.

Chen, S.G. et al., 1995. Truncated forms of the human prion protein in normal brain and in prion diseases. *The*

Journal of biological chemistry, 270(32), pp.19173–80.

Cheong, K.H. et al., 1999. VIP17/MAL, a lipid raft-associated protein, is involved in apical transport in MDCK cells. *Proceedings of the National Academy of Sciences*, 96(11), pp.6241–6248.

Chesebro, B. et al., 2005. Anchorless prion protein results in infectious amyloid disease without clinical scrapie. *Science (New York, N.Y.)*, 308(5727), pp.1435–9.

Chiarini, L.B. et al., 2002. Cellular prion protein transduces neuroprotective signals. *EMBO Journal*, 21(13), pp.3317–3326.

Chivet, M. et al., 2014. Exosomes secreted by cortical neurons upon glutamatergic synapse activation specifically interact with neurons. *Journal of Extracellular Vesicles*, 3.

Choi, S. ed., 2012. *Encyclopedia of Signaling Molecules*, New York, NY: Springer New York.

Christensen, H.M. & Harris, D.A., 2009. A deleted prion protein that is neurotoxic in vivo is localized normally in cultured cells. *Journal of Neurochemistry*, 108(1), pp.44–56.

Chuang, J.Z. & Sung, C.H., 1998. The cytoplasmic tail of rhodopsin acts as a novel apical sorting signal in polarized MDCK cells. *The Journal of cell biology*, 142(5), pp.1245–56.

Cissé, M.A. et al., 2005. The disintegrin ADAM9 indirectly contributes to the physiological processing of cellular prion by modulating ADAM10 activity. *The Journal of biological chemistry*, 280(49), pp.40624–31.

Citi, S. et al., 2014. Epithelial junctions and Rho family GTPases: the zonular signalosome. *Small GTPases*, 5(4), pp.1–15.

Collinge, J. et al., 1994. Prion protein is necessary for normal synaptic function. *Nature*, 370(6487), pp.295–7.

Costanzo, M. et al., 2013. Transfer of polyglutamine aggregates in neuronal cells occurs in tunneling nanotubes. *Journal of Cell Science*, 126(16), pp.3678–3685.

Costanzo, M. & Zurzolo, C., 2013. The cell biology of prion-like spread of protein aggregates: mechanisms and implication in neurodegeneration. *The Biochemical journal*, 452(1), pp.1–17.

Cresawn, K.O. et al., 2007. Differential involvement of endocytic compartments in the biosynthetic traffic of apical proteins. *The EMBO journal*, 26(16), pp.3737–48.

Davis, E.M. et al., 2015. Comparative Haploid Genetic Screens Reveal Divergent Pathways in the Biogenesis and Trafficking of Glycophosphatidylinositol-Anchored Proteins. *Cell reports*, 11(11), pp.1727–36.

Debnath, J. & Brugge, J.S., 2005. Modelling glandular epithelial cancers in three-dimensional cultures. *Nature reviews. Cancer*, 5(9), pp.675–88.

Deeg, M.A. et al., 1992. Glycan components in the glycoinositol phospholipid anchor of human erythrocyte acetylcholinesterase. Novel fragments produced by trifluoroacetic acid. *The Journal of biological chemistry*, 267(26), pp.18573–80.

Delacour, D. et al., 2006. Requirement for galectin-3 in apical protein sorting. *Current biology : CB*, 16(4), pp.408–414.

Dempsey, P.J., Meise, K.S. & Coffey, R.J., 2003. Basolateral sorting of transforming growth factor-alpha precursor in polarized epithelial cells: characterization of cytoplasmic domain determinants. *Experimental cell research*, 285(2), pp.159–74.

Deora, A. et al., 2006. *Cell Biology*, Elsevier.

Deora, A.A. et al., 2005. Mechanisms regulating tissue-specific polarity of monocarboxylate transporters and their chaperone CD147 in kidney and retinal epithelia. *Proceedings of the National Academy of Sciences of the United States of America*, 102(45), pp.16245–16250.

Deora, A.A. et al., 2004. The basolateral targeting signal of CD147 (EMMPRIN) consists of a single leucine and is not recognized by retinal pigment epithelium. *Molecular biology of the cell*, 15(9), pp.4148–4165.

Derby, M.C. et al., 2007. The trans-Golgi Network Golgin, GCC185, is Required for Endosome-to-Golgi Transport

and Maintenance of Golgi Structure. *Traffic*, 8(6), pp.758–773.

Dillon, C. et al., 2002. Basolateral targeting of ERBB2 is dependent on a novel bipartite juxtamembrane sorting signal but independent of the C-terminal ERBIN-binding domain. *Molecular and cellular biology*, 22(18), pp.6553–63.

Distel, B. et al., 1998. Basolateral sorting of the cation-dependent mannose 6-phosphate receptor in Madin-Darby canine kidney cells. Identification of a basolateral determinant unrelated to clathrin-coated pit localization signals. *The Journal of biological chemistry*, 273(1), pp.186–93.

Dotti, C.G., Parton, R.G. & Simons, K., 1991. Polarized sorting of glypiated proteins in hippocampal neurons. *Nature*, 349(6305), pp.158–61.

Dotti, C.G. & Simons, K., 1990. Polarized sorting of viral glycoproteins to the axon and dendrites of hippocampal neurons in culture. *Cell*, 62(1), pp.63–72.

Dron, M. et al., 2010. Endogenous proteolytic cleavage of disease-associated prion protein to produce C2 fragments is strongly cell- and tissue-dependent. *The Journal of biological chemistry*, 285(14), pp.10252–64.

Dunbar, L.A., Aronson, P. & Caplan, M.J., 2000. A transmembrane segment determines the steady-state localization of an ion-transporting adenosine triphosphatase. *The Journal of cell biology*, 148(4), pp.769–78.

Edeling, M.A., Smith, C. & Owen, D., 2006. Life of a clathrin coat: insights from clathrin and AP structures. *Nature reviews. Molecular cell biology*, 7(1), pp.32–44.

Endres, K. et al., 2009. Influence of ADAM10 on prion protein processing and scrapie infectiosity in vivo. *Neurobiology of disease*, 36(2), pp.233–41.

Fan, S. et al., 2004. Polarity Proteins Control Ciliogenesis via Kinesin Motor Interactions. *Current Biology*, 14(16), pp.1451–1461.

Ferguson, M.A. et al., 1988. Glycosyl-phosphatidylinositol moiety that anchors Trypanosoma brucei variant surface glycoprotein to the membrane. *Science (New York, N.Y.)*, 239(4841 Pt 1), pp.753–9.

Ferguson, M.A., 1999. The structure, biosynthesis and functions of glycosylphosphatidylinositol anchors, and the contributions of trypanosome research. *Journal of cell science*, 112 (Pt 1, pp.2799–809.

Ferguson, M.A., Kinoshita, T. & Hart, G.W., 2009. Glycosylphosphatidylinositol Anchors.

Ferguson, M.A., Low, M.G. & Cross, G.A., 1985. Glycosyl-sn-1,2-dimyristylphosphatidylinositol is covalently linked to Trypanosoma brucei variant surface glycoprotein. *The Journal of biological chemistry*, 260(27), pp.14547–55.

Fevrier, B. et al., 2004. Cells release prions in association with exosomes. *Proceedings of the National Academy of Sciences*, 101(26), pp.9683–9688.

Fevrier, B. et al., 2005. Exosomes: a bubble ride for prions? *Traffic (Copenhagen, Denmark)*, 6(1), pp.10–17.

Fivaz, M. et al., 2002. Differential sorting and fate of endocytosed GPI-anchored proteins. *The EMBO journal*, 21(15), pp.3989–4000.

Fluharty, B.R. et al., 2013. An N-terminal fragment of the prion protein binds to amyloid-beta oligomers and inhibits their neurotoxicity in vivo. *J Biol Chem*, 288(11), pp.7857–7866.

Folsch, H. et al., 1999. A novel clathrin adaptor complex mediates basolateral targeting in polarized epithelial cells. *CELL*, 99(2), pp.189–198.

Folsch, H., 2003. The AP-1A and AP-1B clathrin adaptor complexes define biochemically and functionally distinct membrane domains. *The Journal of Cell Biology*, 163(2), pp.351–362.

Fontaine, T. et al., 2003. Structures of the glycosylphosphatidylinositol membrane anchors from Aspergillus fumigatus membrane proteins. *Glycobiology*, 13(3), pp.169–77.

Ford, M.J. et al., 2002. Selective expression of prion protein in peripheral tissues of the adult mouse. *Neuroscience*, 113(1), pp.177–92.

Fujita, M. & Kinoshita, T., 2012a. GPI-anchor remodeling: potential functions of GPI-anchors in intracellular trafficking and membrane dynamics. *Biochimica et biophysica acta*, 1821(8), pp.1050–1058.

Fujita, M. & Kinoshita, T., 2012b. GPI-anchor remodeling: potential functions of GPI-anchors in intracellular trafficking and membrane dynamics. *Biochimica et biophysica acta*, 1821(8), pp.1050–8.

Fuller, S.D., Bravo, R. & Simons, K., 1985. An enzymatic assay reveals that proteins destined for the apical or basolateral domains of an epithelial cell line share the same late Golgi compartments. *The EMBO journal*, 4(2), pp.297–307.

Fuller, S.D. & Simons, K., 1986. Transferrin receptor polarity and recycling accuracy in "tight" and "leaky" strains of Madin-Darby canine kidney cells. *The Journal of cell biology*, 103(5), pp.1767–79.

Le Gall, A.H. et al., 1997. The neural cell adhesion molecule expresses a tyrosine-independent basolateral sorting signal. *The Journal of biological chemistry*, 272(7), pp.4559–4567.

Galvan, C. et al., 2005. Proper axonal distribution of PrP(C) depends on cholesterol-sphingomyelin-enriched membrane domains and is developmentally regulated in hippocampal neurons. *Molecular and cellular neurosciences*, 30(3), pp.304–15.

Gan, Y., McGraw, T.E. & Rodriguez-Boulan, E., 2002. The epithelial-specific adaptor AP1B mediates post-endocytic recycling to the basolateral membrane. *Nature cell biology*, 4(8), pp.605–609.

Gassama-Diagne, A. et al., 2006. Phosphatidylinositol-3,4,5-trisphosphate regulates the formation of the basolateral plasma membrane in epithelial cells. *Nature cell biology*, 8(9), pp.963–70.

Gassama-Diagne, A. & Payrastre, B., 2009. Phosphoinositide signaling pathways: promising role as builders of epithelial cell polarity. *International review of cell and molecular biology*, 273, pp.313–43.

Gauczynski, S. et al., 2006. The 37-kDa/67-kDa laminin receptor acts as a receptor for infectious prions and is inhibited by polysulfated glycanes. *The Journal of infectious diseases*, 194(5), pp.702–9.

Gauczynski, S. et al., 2001. The 37-kDa/67-kDa laminin receptor acts as the cell-surface receptor for the cellular prion protein. *The EMBO journal*, 20(21), pp.5863–75.

Gaush, C.R., Hard, W.L. & Smith, T.F., 1966. Characterization of an Established Line of Canine Kidney Cells (MDCK). *Experimental Biology and Medicine*, 122(3), pp.931–935.

Gephart, J.D. et al., 2011. Identification of a novel mono-leucine basolateral sorting motif within the cytoplasmic domain of amphiregulin. *Traffic (Copenhagen, Denmark)*, 12(12), pp.1793–804.

Giffroy, D. et al., 1998. In vivo stimulation of polymeric Ig receptor transcytosis by circulating polymeric IgA in rat liver. *INTERNATIONAL IMMUNOLOGY*, 10(3), pp.347–354.

Godsave, S.F. et al., 2013. Plasma membrane invaginations containing clusters of full-length PrPSc are an early form of prion-associated neuropathology in vivo. *Neurobiology of aging*, 34(6), pp.1621–31.

Goh, L.K. et al., 2010. Multiple mechanisms collectively regulate clathrin-mediated endocytosis of the epidermal growth factor receptor. *The Journal of Cell Biology*, 189(5), pp.871–883.

Goldenring, J.R., 2013. A central role for vesicle trafficking in epithelial neoplasia: intracellular highways to carcinogenesis. *Nature Reviews Cancer*, 13(11), pp.813–820.

Goldfarb, L.G. et al., 1991. Creutzfeldt-Jacob disease associated with the PRNP codon 200Lys mutation: an analysis of 45 families. *European journal of epidemiology*, 7(5), pp.477–86.

Gonzalez, A. & Rodriguez-Boulan, E., 2009. Clathrin and AP1B: key roles in basolateral trafficking through trans-endosomal routes. *FEBS letters*, 583(23), pp.3784–3795.

Goold, R. et al., 2013. Alternative fates of newly formed PrPSc upon prion conversion on the plasma membrane. *Journal of cell science*, 126(Pt 16), pp.3552–62.

Goold, R. et al., 2011. Rapid cell-surface prion protein conversion revealed using a novel cell system. *Nature communications*, 2, p.281.

Gousset, K. et al., 2009. Prions hijack tunnelling nanotubes for intercellular spread. *Nature cell biology*, 11(3), pp.328–36.

Gousset, K. & Zurzolo, C., 2009. Tunnelling nanotubes: a highway for prion spreading? *Prion*, 3(2), pp.94–98.

Graichen, R. et al., 1996. Glycolipid-independent sorting of a secretory glycoprotein to the apical surface of polarized epithelial cells. *The Journal of biological chemistry*, 271(27), pp.15854–7.

Gravotta, D. et al., 2007. AP1B sorts basolateral proteins in recycling and biosynthetic routes of MDCK cells. *Proceedings of the National Academy of Sciences of the United States of America*, 104(5), pp.1564–1569.

Griffiths, G. & Simons, K., 1986. The trans Golgi network: sorting at the exit site of the Golgi complex. *Science (New York, N.Y.)*, 234(4775), pp.438–43.

Guerriero, C., Lai, Y. & Weisz, O., 2008. Differential sorting and Golgi export requirements for raft-associated and raft-independent apical proteins along the biosynthetic pathway. *Journal of Biological Chemistry*.

Guillot-Sestier, M.V. et al., 2009. The α-secretase-derived N-terminal product of cellular prion, N1, displays neuroprotective function in vitro and in vivo. *Journal of Biological Chemistry*, 284(51), pp.35973–35986.

Guillot-Sestier, M.V. et al., 2012. α-secretase-derived fragment of cellular prion, N1, protects against monomeric and oligomeric amyloid β(Aβ)-associated cell death. *Journal of Biological Chemistry*, 287(7), pp.5021–5032.

Guillot-Sestier, M.-V. & Checler, F., 2012. α-Secretase-derived cleavage of cellular prion yields biologically active catabolites with distinct functions. *Neuro-degenerative diseases*, 10(1-4), pp.294–7.

Guizzunti, G. & Zurzolo, C., 2014. The fate of PrP GPI-anchor signal peptide is modulated by P238S pathogenic mutation. *Traffic (Copenhagen, Denmark)*, 15(1), pp.78–93.

Hanzel, D. et al., 1991. New techniques lead to advances in epithelial cell polarity. *Seminars in cell biology*, 2(6), pp.341–53.

Harder, T. & Sangani, D., 2009. Plasma membrane rafts engaged in T cell signalling: new developments in an old concept. *Cell Communication and Signaling*, 7(1), p.21.

Harper, J.D. & Lansbury, P.T.J., 1997. Models of amyloid seeding in Alzheimer's disease and scrapie: mechanistic truths and physiological consequences of the time-dependent solubility of amyloid proteins. *Annual review of biochemistry*, 66, pp.385–407.

Harris, D.A. et al., 1993. Processing of a cellular prion protein: identification of N- and C-terminal cleavage sites. *Biochemistry*, 32(4), pp.1009–16.

Harris, D.A. & True, H.L., 2006. New insights into prion structure and toxicity. *Neuron*, 50(3), pp.353–357.

He, C. et al., 2002. The epidermal growth factor receptor juxtamembrane domain has multiple basolateral plasma membrane localization determinants, including a dominant signal with a polyproline core. *The Journal of biological chemistry*, 277(41), pp.38284–93.

Hegde, R.S. et al., 1998. A transmembrane form of the prion protein in neurodegenerative disease. *Science (New York, N.Y.)*, 279(5352), pp.827–34.

Heiseke, A. et al., 2008. The novel sorting nexin SNX33 interferes with cellular PrP formation by modulation of PrP shedding. *Traffic (Copenhagen, Denmark)*, 9(7), pp.1116–29.

Heppner, F.L. et al., 2001. Transepithelial prion transport by M cells. *Nature medicine*, 7(9), pp.976–7.

Homans, S.W. et al., 1988. Complete structure of the glycosyl phosphatidylinositol membrane anchor of rat brain Thy-1 glycoprotein. *Nature*, 333(6170), pp.269–72.

Hooper, N.M., Taylor, D.R. & Watt, N.T., 2008. Mechanism of the metal-mediated endocytosis of the prion protein. *Biochemical Society transactions*, 36(Pt 6), pp.1272–1276.

Hoque, M.Z. et al., 1996. Mutation in the prion protein gene at codon 232 in Japanese patients with Creutzfeldt-Jakob disease: a clinicopathological, immunohistochemical and transmission study. *Acta neuropathologica*, 92(5), pp.441–6.

Horton, A.C. & Ehlers, M.D., 2003. Neuronal polarity and trafficking. *Neuron*, 40(2), pp.277–95.

Howes, M.T., Mayor, S. & Parton, R.G., 2010. Molecules, mechanisms, and cellular roles of clathrin-independent endocytosis. *Current opinion in cell biology*, 22(4), pp.519–27.

Hsiao, K. & Prusiner, S.B., 1991. Molecular genetics and transgenic model of Gertsmann-Straussler-Scheinker disease. *Alzheimer disease and associated disorders*, 5(3), pp.155–162.

Hua, W. et al., 2006. Vectorial insertion of apical and basolateral membrane proteins in polarized epithelial cells revealed by quantitative 3D live cell imaging. *The Journal of cell biology*, 172(7), pp.1035–44.

Huet, G. et al., 1998. GalNAc-alpha-O-benzyl inhibits NeuAcalpha2-3 glycosylation and blocks the intracellular transport of apical glycoproteins and mucus in differentiated HT-29 cells. *The Journal of cell biology*, 141(6), pp.1311–22.

Hunziker, W. et al., 1991. Basolateral sorting in MDCK cells requires a distinct cytoplasmic domain determinant. *Cell*, 66(5), pp.907–20.

Hunziker, W. & Fumey, C., 1994. A di-leucine motif mediates endocytosis and basolateral sorting of macrophage IgG Fc receptors in MDCK cells. *The EMBO journal*, 13(13), pp.2963–9.

Hurley, J.H., 2015. ESCRTs are everywhere. *The EMBO journal*.

Huttner, W.B. & Zimmerberg, J., 2001. Implications of lipid microdomains for membrane curvature, budding and fission. *Current opinion in cell biology*, 13(4), pp.478–84.

Iden, S. & Collard, J.G., 2008. Crosstalk between small GTPases and polarity proteins in cell polarization. *Nature reviews. Molecular cell biology*, 9(11), pp.846–59.

Ihrke, G. et al., 2001. Competing sorting signals guide endolyn along a novel route to lysosomes in MDCK cells. *The EMBO journal*, 20(22), pp.6256–64.

van IJzendoorn, S.C.D. et al., 2002. Direct interaction between rab3b and the polymeric immunoglobulin receptor controls ligand-stimulated transcytosis in epithelial cells. *DEVELOPMENTAL CELL*, 2(2), pp.219–228.

Ikezawa, H., 2002. Glycosylphosphatidylinositol (GPI)-anchored proteins. *Biological & pharmaceutical bulletin*, 25(4), pp.409–17.

Imjeti, N.S. et al., 2011a. N-Glycosylation instead of cholesterol mediates oligomerization and apical sorting of GPI-APs in FRT cells. *Molecular biology of the cell*, 22(23), pp.4621–34.

Imjeti, N.S. et al., 2011b. N-Glycosylation instead of cholesterol mediates oligomerization and apical sorting of GPI-APs in FRT cells. *Molecular biology of the cell*, 22(23), pp.4621–34.

Jacob, R. et al., 2000. Structural determinants required for apical sorting of an intestinal brush-border membrane protein. *The Journal of biological chemistry*, 275(9), pp.6566–72.

Jiménez-Huete, A. et al., 1998. Endogenous proteolytic cleavage of normal and disease-associated isoforms of the human prion protein in neural and non-neural tissues. *The American journal of pathology*, 153(5), pp.1561–72.

Johnson, K.F. & Kornfeld, S., 1992. A His-Leu-Leu sequence near the carboxyl terminus of the cytoplasmic domain of the cation-dependent mannose 6-phosphate receptor is necessary for the lysosomal enzyme sorting function. *The Journal of biological chemistry*, 267(24), pp.17110–5.

Jung, J.-J. et al., 2013. Syntaxin 16 regulates lumen formation during epithelial morphogenesis. *PloS one*, 8(4), p.e61857.

Kadir, S. et al., 2011. Microtubule remodelling is required for the front-rear polarity switch during contact inhibition of locomotion. *Journal of cell science*, 124(Pt 15), pp.2642–53.

Keller, P. et al., 2001. Multicolour imaging of post-Golgi sorting and trafficking in live cells. *Nature cell biology*, 3(2), pp.140–9.

Kellermann, O. et al., 2002. From stem cells to prion signalling. *Comptes rendus biologies*, 325(1), pp.9–15.

De Keukeleire, B. et al., 2007. Human cellular prion protein hPrPC is sorted to the apical membrane of epithelial cells. *Biochemical and biophysical research communications*, 354(4), pp.949–54.

Kinlough, C.L. et al., 2006. Recycling of MUC1 is dependent on its palmitoylation. *The Journal of biological chemistry*, 281(17), pp.12112–22.

Kitagawa, Y. et al., 1994. N-glycosylation of erythropoietin is critical for apical secretion by Madin-Darby canine kidney cells. *Experimental cell research*, 213(2), pp.449–57.

Kocisko, D.A. et al., 1994. Cell-free formation of protease-resistant prion protein. *Nature*, 370(6489), pp.471–4.

Kojima, A., Konishi, M. & Akizawa, T., 2014. Prion fragment peptides are digested with membrane type matrix metalloproteinases and acquire enzyme resistance through Cu^{2+}-binding. *Biomolecules*, 4(2), pp.510–26.

Kostaras, E. et al., 2012. SARA and RNF11 interact with each other and ESCRT-0 core proteins and regulate degradative EGFR trafficking. *Oncogene*, 32(44), pp.5220–5232.

Kreitzer, G. et al., 2003. Three-dimensional analysis of post-Golgi carrier exocytosis in epithelial cells. *Nature cell biology*, 5(2), pp.126–136.

Kretzschmar, H. & Tatzelt, J., 2013. Prion disease: a tale of folds and strains. *Brain pathology (Zurich, Switzerland)*, 23(3), pp.321–32.

Kretzschmar, H.A. et al., 1986. Molecular cloning of a human prion protein cDNA. *DNA (Mary Ann Liebert, Inc.)*, 5(4), pp.315–24.

Kujala, P. et al., 2011. Prion uptake in the gut: identification of the first uptake and replication sites. *PLoS pathogens*, 7(12), p.e1002449.

Kumari, S. & Mayor, S., 2008. ARF1 is directly involved in dynamin-independent endocytosis. *Nature cell biology*, 10(1), pp.30–41.

Kundu, A. et al., 1996. Transmembrane domain of influenza virus neuraminidase, a type II protein, possesses an apical sorting signal in polarized MDCK cells. *Journal of virology*, 70(9), pp.6508–15.

Kuzmin, P.I. et al., 2005. Line Tension and Interaction Energies of Membrane Rafts Calculated from Lipid Splay and Tilt. *Biophysical Journal*, 88(2), pp.1120–1133.

Laffont-Proust, I. et al., 2005. The N-terminal cleavage of cellular prion protein in the human brain. *FEBS letters*, 579(28), pp.6333–7.

Lakhan, S.E., Sabharanjak, S. & De, A., 2009a. Endocytosis of glycosylphosphatidylinositol-anchored proteins. *Journal of biomedical science*, 16, p.93.

Lakhan, S.E., Sabharanjak, S. & De, A., 2009b. Endocytosis of glycosylphosphatidylinositol-anchored proteins. *Journal of biomedical science*, 16, p.93.

Larson, M. et al., 2012. The complex PrP(c)-Fyn couples human oligomeric Aβ with pathological tau changes in Alzheimer's disease. *The Journal of neuroscience : the official journal of the Society for Neuroscience*, 32(47), pp.16857–71a.

Laurén, J. et al., 2009. Cellular prion protein mediates impairment of synaptic plasticity by amyloid-β oligomers. *Nature*, 457(7233), pp.1128–1132.

Lebreton, S., Paladino, S. & Zurzolo, C., 2008. Selective Roles for Cholesterol and Actin in Compartmentalization of Different Proteins in the Golgi and Plasma Membrane of Polarized Cells. *Journal of Biological Chemistry*, 283(43), pp.29545–29553.

Lee, K.S. et al., 2001. Internalization of mammalian fluorescent cellular prion protein and N-terminal deletion mutants in living cells. *Journal of neurochemistry*, 79(1), pp.79–87.

Legname, G. et al., 2004. Synthetic mammalian prions. *Science (New York, N.Y.)*, 305(5684), pp.673–6.

Leighton, J. et al., 1970. A cell line derived from normal dog kidney (MDCK) exhibiting qualities of papillary adenocarcinoma and of renal tubular epithelium. *Cancer*, 26(5), pp.1022–1028.

Lewis, V. et al., 2015. Prion protein "gamma-cleavage": characterizing a novel endoproteolytic processing event. *Cellular and molecular life sciences : CMLS*.

Li, A. et al., 2007. N-terminally deleted forms of the prion protein activate both Bax-dependent and Bax-independent neurotoxic pathways. *The Journal of neuroscience : the official journal of the Society for Neuroscience*, 27(4), pp.852–9.

Li, R. et al., 2003. On the same cell type GPI-anchored normal cellular prion and DAF protein exhibit different biological properties. *Biochemical and biophysical research communications*, 303(2), pp.446–51.

Liang, J. et al., 2012. Cellular prion protein regulates its own α-cleavage through ADAM8 in skeletal muscle. *The Journal of biological chemistry*, 287(20), pp.16510–20.

Liang, J. & Kong, Q., 2012. α-Cleavage of cellular prion protein. *Prion*, 6(5), pp.453–60.

Lin, S. et al., 1998. Mutations in the middle of the transmembrane domain reverse the polarity of transport of the influenza virus hemagglutinin in MDCK epithelial cells. *The Journal of cell biology*, 142(1), pp.51–7.

Linden, R. et al., 2008. Physiology of the prion protein. *Physiological reviews*, 88(2), pp.673–728.

Linden, R., Cordeiro, Y. & Lima, L.M.T.R., 2012. Allosteric function and dysfunction of the prion protein. *Cellular and Molecular Life Sciences*, 69(7), pp.1105–1124.

Lingwood, D. & Simons, K., 2010. Lipid rafts as a membrane-organizing principle. *Science (New York, N.Y.)*, 327(5961), pp.46–50.

Lisanti, M.P. et al., 1989a. A glycophospholipid membrane anchor acts as an apical targeting signal in polarized epithelial cells. *The Journal of cell biology*, 109(5), pp.2145–56.

Lisanti, M.P. et al., 1989b. A glycophospholipid membrane anchor acts as an apical targeting signal in polarized epithelial cells. *The Journal of cell biology*, 109(5), pp.2145–2156.

Lisanti, M.P. et al., 1988. Polarized apical distribution of glycosyl-phosphatidylinositol-anchored proteins in a renal epithelial cell line. *Proceedings of the National Academy of Sciences of the United States of America*, 85(24), pp.9557–9561.

Lisanti, M.P. et al., 1990. Preferred apical distribution of glycosyl-phosphatidylinositol (GPI) anchored proteins: a highly conserved feature of the polarized epithelial cell phenotype. *The Journal of membrane biology*, 113(2), pp.155–67.

Lisanti, M.P. et al., 1990. Vectorial apical delivery and slow endocytosis of a glycolipid-anchored fusion protein in transfected MDCK cells. *Proceedings of the National Academy of Sciences*, 87(19), pp.7419–7423.

Liu, T. et al., 2001. Differential expression of cellular prion protein in mouse brain as detected with multiple anti-PrP monoclonal antibodies. *Brain research*, 896(1-2), pp.118–29.

Lock, J.G., 2005. Rab11 in Recycling Endosomes Regulates the Sorting and Basolateral Transport of E-Cadherin. *Molecular Biology of the Cell*, 16(4), pp.1744–1755.

Loubet, D. et al., 2012. Neuritogenesis: the prion protein controls β1 integrin signaling activity. *FASEB journal : official publication of the Federation of American Societies for Experimental Biology*, 26(2), pp.678–90.

Low, M.G., 1989. Glycosyl-phosphatidylinositol: a versatile anchor for cell surface proteins. *FASEB journal : official publication of the Federation of American Societies for Experimental Biology*, 3(5), pp.1600–1608.

Low, M.G. & Saltiel, A.R., 1988. Structural and functional roles of glycosyl-phosphatidylinositol in membranes. *Science (New York, N.Y.)*, 239(4837), pp.268–75.

Luini, A. et al., 2005. Large pleiomorphic traffic intermediates in the secretory pathway. *Current opinion in cell biology*, 17(4), pp.353–61.

Lundmark, R. et al., 2008. The GTPase-activating protein GRAF1 regulates the CLIC/GEEC endocytic pathway. *Current biology : CB*, 18(22), pp.1802–8.

Luton, F. et al., 1999. The SRC family protein tyrosine kinase p62(yes) controls polymeric IgA transcytosis in vivo.

MOLECULAR CELL, 4(4), pp.627–632.

MacGregor, I. et al., 1999. Application of a time-resolved fluoroimmunoassay for the analysis of normal prion protein in human blood and its components. *Vox sanguinis*, 77(2), pp.88–96.

Macrae, J.I. et al., 2005. Structural characterization of NETNES, a novel glycoconjugate in Trypanosoma cruzi epimastigotes. *The Journal of biological chemistry*, 280(13), pp.12201–11.

Maeda, Y. et al., 2007. Fatty acid remodeling of GPI-anchored proteins is required for their raft association. *Molecular biology of the cell*, 18(4), pp.1497–506.

Maeda, Y. & Kinoshita, T., 2011. Structural remodeling, trafficking and functions of glycosylphosphatidylinositol-anchored proteins. *Progress in lipid research*, 50(4), pp.411–24.

Magalhães, A.C. et al., 2002. Endocytic intermediates involved with the intracellular trafficking of a fluorescent cellular prion protein. *The Journal of biological chemistry*, 277(36), pp.33311–8.

Málaga-Trillo, E. et al., 2009. Regulation of embryonic cell adhesion by the prion protein. *PLoS biology*, 7(3), p.e55.

Malaga-Trillo, E. & Sempou, E., 2009. PrPs: Proteins with a purpose: Lessons from the zebrafish. *Prion*, 3(3), pp.129–133.

Mallucci, G. et al., 2003. Depleting neuronal PrP in prion infection prevents disease and reverses spongiosis. *Science (New York, N.Y.)*, 302(5646), pp.871–4.

Mallucci, G.R. et al., 2002. Post-natal knockout of prion protein alters hippocampal CA1 properties, but does not result in neurodegeneration. *The EMBO journal*, 21(3), pp.202–10.

Mangé, A. et al., 2004. Alpha- and beta- cleavages of the amino-terminus of the cellular prion protein. *Biology of the cell / under the auspices of the European Cell Biology Organization*, 96(2), pp.125–32.

Manninen, A., 2015. Epithelial polarity--generating and integrating signals from the ECM with integrins. *Experimental cell research*, 334(2), pp.337–49.

Marijanovic, Z. et al., 2009. Identification of an intracellular site of prion conversion. *PLoS Pathogens*, 5(5), p.e1000426.

Martin-Belmonte, F. et al., 2000. The MAL Proteolipid Is Necessary for the Overall Apical Delivery of Membrane Proteins in the Polarized Epithelial Madin-Darby Canine Kidney and Fischer Rat Thyroid Cell Lines. *Molecular Biology of the Cell*, 11(6), pp.2033–2045.

Martínez-Maza, R. et al., 2001. The role of N-glycosylation in transport to the plasma membrane and sorting of the neuronal glycine transporter GLYT2. *The Journal of biological chemistry*, 276(3), pp.2168–73.

Martins, V.R. et al., 2010. Prion protein: orchestrating neurotrophic activities. *Current issues in molecular biology*, 12(2), pp.63–86.

Maruyama, M. et al., 2005. Cholesterol is required for the polarized secretion of erythropoietin in Madin-Darby canine kidney cells. *Archives of biochemistry and biophysics*, 438(2), pp.174–81.

Marzolo, M.-P. et al., 2003. Differential distribution of low-density lipoprotein-receptor-related protein (LRP) and megalin in polarized epithelial cells is determined by their cytoplasmic domains. *Traffic (Copenhagen, Denmark)*, 4(4), pp.273–88.

Marzolo, M.P., Bull, P. & González, A., 1997. Apical sorting of hepatitis B surface antigen (HBsAg) is independent of N-glycosylation and glycosylphosphatidylinositol-anchored protein segregation. *Proceedings of the National Academy of Sciences of the United States of America*, 94(5), pp.1834–9.

Mastrianni, J.A., 2010. The genetics of prion diseases. *Genetics in medicine : official journal of the American College of Medical Genetics*, 12(4), pp.187–195.

MATLIN, K.S. & SIMONS, K., 1984. SORTING OF AN APICAL PLASMA-MEMBRANE GLYCOPROTEIN OCCURS BEFORE IT REACHES THE CELL-SURFACE IN CULTURED EPITHELIAL-CELLS. *JOURNAL OF CELL BIOLOGY*, 99(6), pp.2131–2139.

Matter, K. et al., 1993. Common signals control low density lipoprotein receptor sorting in endosomes and the Golgi complex of MDCK cells. *Cell*, 74(6), pp.1053–64.

Matter, K., Hunziker, W. & Mellman, I., 1992. Basolateral sorting of LDL receptor in MDCK cells: the cytoplasmic domain contains two tyrosine-dependent targeting determinants. *Cell*, 71(5), pp.741–53.

Matter, K. & Mellman, I., 1994. Mechanisms of cell polarity: sorting and transport in epithelial cells. *Current opinion in cell biology*, 6(4), pp.545–54.

Matter, K., Yamamoto, E.M. & Mellman, I., 1994. Structural requirements and sequence motifs for polarized sorting and endocytosis of LDL and Fc receptors in MDCK cells. *The Journal of cell biology*, 126(4), pp.991–1004.

Mattila, P.E. et al., 2009. MUC1 traverses apical recycling endosomes along the biosynthetic pathway in polarized MDCK cells. *Biological chemistry*, 390(7), pp.551–6.

Mayor, S., Sabharanjak, S. & Maxfield, F.R., 1998. Cholesterol-dependent retention of GPI-anchored proteins in endosomes. *The EMBO journal*, 17(16), pp.4626–38.

McConville, M.J. & Ferguson, M.A., 1993. The structure, biosynthesis and function of glycosylated phosphatidylinositols in the parasitic protozoa and higher eukaryotes. *The Biochemical journal*, 294 (Pt 2, pp.305–24.

McDonald, A.J. et al., 2014. A new paradigm for enzymatic control of α-cleavage and β-cleavage of the prion protein. *The Journal of biological chemistry*, 289(2), pp.803–13.

McDonald, A.J. & Millhauser, G.L., PrP overdrive: does inhibition of α-cleavage contribute to PrP(C) toxicity and prion disease? *Prion*, 8(2).

McMahon, H.E. et al., 2001. Cleavage of the amino terminus of the prion protein by reactive oxygen species. *The Journal of biological chemistry*, 276(3), pp.2286–91.

McMahon, H.T. & Gallop, J.L., 2005. Membrane curvature and mechanisms of dynamic cell membrane remodelling. *Nature*, 438(7068), pp.590–6.

van Meer, G. & Simons, K., 1988. Lipid polarity and sorting in epithelial cells. *Journal of cellular biochemistry*, 36(1), pp.51–58.

van Meer, G. & Vaz, W.L.C., 2005. Membrane curvature sorts lipids. *EMBO reports*, 6(5), pp.418–419.

Mellman, I. & Nelson, W.J., 2008a. Coordinated protein sorting, targeting and distribution in polarized cells. *Nature reviews. Molecular cell biology*, 9(11), pp.833–45.

Mellman, I. & Nelson, W.J., 2008b. Coordinated protein sorting, targeting and distribution in polarized cells. *Nature reviews. Molecular cell biology*, 9(11), pp.833–45.

Milane, L. et al., 2015. Exosome Mediated Communication within the Tumor Microenvironment. *Journal of Controlled Release*.

Miranda, K.C. et al., 2001. A dileucine motif targets E-cadherin to the basolateral cell surface in Madin-Darby canine kidney and LLC-PK1 epithelial cells. *The Journal of biological chemistry*, 276(25), pp.22565–72.

Misek, D.E., Bard, E. & Rodriguez-Boulan, E., 1984. Biogenesis of epithelial cell polarity: intracellular sorting and vectorial exocytosis of an apical plasma membrane glycoprotein. *Cell*, 39(3 Pt 2), pp.537–546.

Misfeldt, D.S., Hamamoto, S.T. & Pitelka, D.R., 1976. Transepithelial transport in cell culture. *Proceedings of the National Academy of Sciences of the United States of America*, 73(4), pp.1212–1216.

Miyazawa, K. et al., 2010. Transcytosis of murine-adapted bovine spongiform encephalopathy agents in an in vitro bovine M cell model. *Journal of virology*, 84(23), pp.12285–91.

Montesano, R., Matsumoto, K., et al., 1991. Identification of a fibroblast-derived epithelial morphogen as hepatocyte growth factor. *Cell*, 67(5), pp.901–8.

Montesano, R., Schaller, G. & Orci, L., 1991. Induction of epithelial tubular morphogenesis in vitro by fibroblast-

derived soluble factors. *Cell*, 66(4), pp.697–711.

Morel, E. et al., 2004. The cellular prion protein PrPc is expressed in human enterocytes in cell-cell junctional domains. *The Journal of biological chemistry*, 279(2), pp.1499–505.

Mostov, K., Su, T. & ter Beest, M., 2003. Polarized epithelial membrane traffic: conservation and plasticity. *Nature cell biology*, 5(4), pp.287–93.

Mostov, K.E., 2003. Epithelial polarity and morphogenesis. *Methods (San Diego, Calif.)*, 30(3), pp.189–90.

Mostov, K.E. & Cardone, M.H., 1995. Regulation of protein traffic in polarized epithelial cells. *BioEssays : news and reviews in molecular, cellular and developmental biology*, 17(2), pp.129–38.

Mostov, K.E., Verges, M. & Altschuler, Y., 2000. Membrane traffic in polarized epithelial cells. *CURRENT OPINION IN CELL BIOLOGY*, 12(4), pp.483–490.

Mouillet-Richard, S. et al., 2005. Modulation of serotonergic receptor signaling and cross-talk by prion protein. *Journal of Biological Chemistry*, 280(6), pp.4592–4601.

Mukasa, R. et al., 1995. Characterization of glycosylphosphatidylinositol (GPI)-anchored NCAM on mouse skeletal muscle cell line C2C12: the structure of the GPI glycan and release during myogenesis. *Archives of biochemistry and biophysics*, 318(1), pp.182–90.

Muñiz, M. & Zurzolo, C., 2014. Sorting of GPI-anchored proteins from yeast to mammals--common pathways at different sites? *Journal of cell science*, 127(Pt 13), pp.2793–801.

Musch, A. et al., 1996. Transport of vesicular stomatitis virus G protein to the cell surface is signal mediated in polarized and nonpolarized cells. *The Journal of cell biology*, 133(3), pp.543–558.

Naim, H.Y. et al., 1999. Temporal association of the N- and O-linked glycosylation events and their implication in the polarized sorting of intestinal brush border sucrase-isomaltase, aminopeptidase N, and dipeptidyl peptidase IV. *The Journal of biological chemistry*, 274(25), pp.17961–7.

Nakano, Y. et al., 1994. Structural study on the glycosyl-phosphatidylinositol anchor and the asparagine-linked sugar chain of a soluble form of CD59 in human urine. *Archives of biochemistry and biophysics*, 311(1), pp.117–26.

Nakato, G. et al., 2012. Cutting Edge: Brucella abortus exploits a cellular prion protein on intestinal M cells as an invasive receptor. *Journal of immunology (Baltimore, Md. : 1950)*, 189(4), pp.1540–4.

Nakatsu, F., Hase, K. & Ohno, H., 2014. The Role of the Clathrin Adaptor AP-1: Polarized Sorting and Beyond. *Membranes*, 4(4), pp.747–763.

Nazer, B., Hong, S. & Selkoe, D.J., 2008. LRP promotes endocytosis and degradation, but not transcytosis, of the amyloid-β peptide in a blood–brain barrier in vitro model. *Neurobiology of Disease*, 30(1), pp.94–102.

Nelson, W.J., 2009. Remodeling epithelial cell organization: transitions between front-rear and apical-basal polarity. *Cold Spring Harbor perspectives in biology*, 1(1), p.a000513.

Neumüller, R.A. & Knoblich, J.A., 2009. Dividing cellular asymmetry: asymmetric cell division and its implications for stem cells and cancer. *Genes & development*, 23(23), pp.2675–99.

Nichols, B.J. et al., 2001. Rapid cycling of lipid raft markers between the cell surface and Golgi complex. *The Journal of cell biology*, 153(3), pp.529–41.

Nosjean, O., Briolay, A. & Roux, B., 1997. Mammalian GPI proteins: sorting, membrane residence and functions. *Biochimica et biophysica acta*, 1331(2), pp.153–186.

Nourizadeh-Lillabadi, R. et al., 2010. Early embryonic gene expression profiling of zebrafish prion protein (Prp2) morphants. *PloS one*, 5(10), p.e13573.

Nunziante, M., Gilch, S. & Schätzl, H.M., 2003. Essential role of the prion protein N terminus in subcellular trafficking and half-life of cellular prion protein. *The Journal of biological chemistry*, 278(6), pp.3726–34.

O'Brien, L.E., Zegers, M.M.P. & Mostov, K.E., 2002. Opinion: Building epithelial architecture: insights from three-

dimensional culture models. *Nature reviews. Molecular cell biology*, 3(7), pp.531–7.

Odorizzi, G. & Trowbridge, I.S., 1997. Structural requirements for basolateral sorting of the human transferrin receptor in the biosynthetic and endocytic pathways of Madin-Darby canine kidney cells. *The Journal of cell biology*, 137(6), pp.1255–64.

Ohno, H. et al., 1999. Mu1B, a novel adaptor medium chain expressed in polarized epithelial cells. *FEBS letters*, 449(2-3), pp.215–20.

Oliveira-Martins, J.B. et al., 2010. Unexpected tolerance of alpha-cleavage of the prion protein to sequence variations. *PloS one*, 5(2), p.e9107.

Overath, P. & Engstler, M., 2004. Endocytosis, membrane recycling and sorting of GPI-anchored proteins: Trypanosoma brucei as a model system. *Molecular microbiology*, 53(3), pp.735–744.

Overeem, A.W., Bryant, D.M. & van IJzendoorn, S.C.D., 2015. Mechanisms of apical-basal axis orientation and epithelial lumen positioning. *Trends in cell biology*, 25(8), pp.476–85.

Oxley, D. & Bacic, A., 1999. Structure of the glycosylphosphatidylinositol anchor of an arabinogalactan protein from Pyrus communis suspension-cultured cells. *Proceedings of the National Academy of Sciences of the United States of America*, 96(25), pp.14246–51.

Paladino, S. et al., 2008. Different GPI-attachment signals affect the oligomerisation of GPI-anchored proteins and their apical sorting. *Journal of cell science*, 121(Pt 24), pp.4001–7.

Paladino, S. et al., 2014. Golgi sorting regulates organization and activity of GPI proteins at apical membranes. *Nature chemical biology*, 10(5), pp.350–7.

Paladino, S. et al., 2006a. GPI-anchored proteins are directly targeted to the apical surface in fully polarized MDCK cells. *The Journal of cell biology*, 172(7), pp.1023–34.

Paladino, S. et al., 2006b. GPI-anchored proteins are directly targeted to the apical surface in fully polarized MDCK cells. *The Journal of cell biology*, 172(7), pp.1023–34.

Paladino, S. et al., 2007. Oligomerization is a specific requirement for apical sorting of glycosyl-phosphatidylinositol-anchored proteins but not for non-raft-associated apical proteins. *Traffic (Copenhagen, Denmark)*, 8(3), pp.251–8.

Paladino, S. et al., 2004. Protein oligomerization modulates raft partitioning and apical sorting of GPI-anchored proteins. *The Journal of cell biology*, 167(4), pp.699–709.

Paladino, S., Lebreton, S. & Zurzolo, C., 2015. Trafficking and Membrane Organization of GPI-Anchored Proteins in Health and Diseases. *Current topics in membranes*, 75, pp.269–303.

Paladino, S., Sarnataro, D. & Zurzolo, C., 2002. Detergent-resistant membrane microdomains and apical sorting of GPI-anchored proteins in polarized epithelial cells. *International journal of medical microbiology : IJMM*, 291(6-7), pp.439–445.

Pan, K.M., Stahl, N. & Prusiner, S.B., 1992. Purification and properties of the cellular prion protein from Syrian hamster brain. *Protein science : a publication of the Protein Society*, 1(10), pp.1343–52.

Pang, S., Urquhart, P. & Hooper, N.M., 2004. N-glycans, not the GPI anchor, mediate the apical targeting of a naturally glycosylated, GPI-anchored protein in polarised epithelial cells. *Journal of cell science*, 117(Pt 21), pp.5079–86.

Pantera, B. et al., 2009. PrP c activation induces neurite outgrowth and differentiation in PC12 cells: role for caveolin-1 in the signal transduction pathway. *Journal of Neurochemistry*, 110(1), pp.194–207.

Paquet, S. et al., 2004. Prion infection of epithelial Rov cells is a polarized event. *Journal of virology*, 78(13), pp.7148–52.

Parizek, P. et al., 2001. Similar turnover and shedding of the cellular prion protein in primary lymphoid and neuronal cells. *The Journal of biological chemistry*, 276(48), pp.44627–32.

Park, S.Y. & Guo, X., 2014. Adaptor protein complexes and intracellular transport. *Bioscience Reports*, 34(4),

pp.381–390.

Parkin, E.T. et al., 2004. Dual mechanisms for shedding of the cellular prion protein. *The Journal of biological chemistry*, 279(12), pp.11170–8.

Parton, R.G. & Richards, A.A., 2003. Lipid Rafts and Caveolae as Portals for Endocytosis: New Insights and Common Mechanisms. *Traffic*, 4(11), pp.724–738.

Paulick, M.G. & Bertozzi, C.R., 2008. The glycosylphosphatidylinositol anchor: a complex membrane-anchoring structure for proteins. *Biochemistry*, 47(27), pp.6991–7000.

Pauly, P.C. & Harris, D.A., 1998. Copper stimulates endocytosis of the prion protein. *The Journal of biological chemistry*, 273(50), pp.33107–10.

Perini, F. et al., 1996. PrP27-30 is a normal soluble prion protein fragment released by human platelets. *Biochemical and biophysical research communications*, 223(3), pp.572–7.

Petit, C.S. V et al., 2012. Requirement of cellular prion protein for intestinal barrier function and mislocalization in patients with inflammatory bowel disease. *Gastroenterology*, 143(1), pp.122–32.e15.

Petit, C.S. V et al., 2013. Roles of the cellular prion protein in the regulation of cell-cell junctions and barrier function. *Tissue barriers*, 1(2), p.e24377.

Pflanzner, T. et al., 2012. Cellular prion protein participates in amyloid-β transcytosis across the blood-brain barrier. *Journal of cerebral blood flow and metabolism : official journal of the International Society of Cerebral Blood Flow and Metabolism*, 32(4), pp.628–32.

Le Pichon, C.E. et al., 2009. Olfactory behavior and physiology are disrupted in prion protein knockout mice. *Nature neuroscience*, 12(1), pp.60–9.

Pietri, M. et al., 2006. Overstimulation of PrPC signaling pathways by prion peptide 106-126 causes oxidative injury of bioaminergic neuronal cells. *Journal of Biological Chemistry*, 281(38), pp.28470–28479.

Pietrini, G. et al., 1994. The axonal gamma-aminobutyric acid transporter GAT-1 is sorted to the apical membranes of polarized epithelial cells. *The Journal of biological chemistry*, 269(6), pp.4668–74.

Pike, L.J., 2003. Lipid rafts: bringing order to chaos. *Journal of lipid research*, 44(4), pp.655–67.

Polishchuk, R., Di Pentima, A. & Lippincott-Schwartz, J., 2004. Delivery of raft-associated, GPI-anchored proteins to the apical surface of polarized MDCK cells by a transcytotic pathway. *Nature cell biology*, 6(4), pp.297–307.

Polymenidou, M. et al., 2008. Canine MDCK cell lines are refractory to infection with human and mouse prions. *Vaccine*, 26(21), pp.2601–14.

Pradines, E. et al., 2013. Pathogenic prions deviate PrP(C) signaling in neuronal cells and impair A-beta clearance. *Cell death & disease*, 4(1), p.e456.

Prusiner, S.B., 1994. Molecular biology and genetics of prion diseases. *Philosophical transactions of the Royal Society of London. Series B, Biological sciences*, 343(1306), pp.447–463.

Prusiner, S.B., 1998. Nobel Lecture: Prions. *Proceedings of the National Academy of Sciences*, 95(23), pp.13363–13383.

Prusiner, S.B., 1998. Prions. *Proceedings of the National Academy of Sciences of the United States of America*, 95(23), pp.13363–13383.

Prusiner, S.B., Stahl, N. & DeArmond, S.J., 1988. Novel mechanisms of degeneration of the central nervous system--prion structure and biology. *Ciba Foundation symposium*, 135, pp.239–260.

Puckett, C. et al., 1991. Genomic structure of the human prion protein gene. *American journal of human genetics*, 49(2), pp.320–9.

Puig, B. et al., 2011. N-glycans and glycosylphosphatidylinositol-anchor act on polarized sorting of mouse PrP(C) in Madin-Darby canine kidney cells. *PloS one*, 6(9), p.e24624.

Rajendran, L. & Simons, K., 2005. Lipid rafts and membrane dynamics. *Journal of cell science*, 118(Pt 6), pp.1099–102.

Ravi, M. et al., 2015. 3D cell culture systems: advantages and applications. *Journal of cellular physiology*, 230(1), pp.16–26.

Richardson, D.D. & Fernandez-Borja, M., 2016. Leukocyte adhesion and polarization: role of glycosylphosphatidylinositol-anchored proteins. *BioArchitecture*, pp.00–00.

Rindler, M.J. et al., 1984. Viral glycoproteins destined for apical or basolateral plasma membrane domains traverse the same Golgi apparatus during their intracellular transport in doubly infected Madin-Darby canine kidney cells. *The Journal of cell biology*, 98(4), pp.1304–1319.

Robertson, C. et al., 2006. Cellular prion protein is released on exosomes from activated platelets. *Blood*, 107(10), pp.3907–11.

Rodríguez, A. et al., 2006. Group I mGluR signaling in BSE-infected bovine-PrP transgenic mice. *Neuroscience letters*, 410(2), pp.115–20.

Rodriguez Boulan, E. & Pendergast, M., 1980. Polarized distribution of viral envelope proteins in the plasma membrane of infected epithelial cells. *Cell*, 20(1), pp.45–54.

Rodriguez Boulan, E. & Sabatini, D.D., 1978. Asymmetric budding of viruses in epithelial monlayers: a model system for study of epithelial polarity. *Proceedings of the National Academy of Sciences of the United States of America*, 75(10), pp.5071–5075.

Rodriguez-Boulan, E., Kreitzer, G. & Musch, A., 2005. Organization of vesicular trafficking in epithelia. *Nature reviews. Molecular cell biology*, 6(3), pp.233–247.

Rodriguez-Boulan, E., Kreitzer, G. & Müsch, A., 2005. Organization of vesicular trafficking in epithelia. *Nature Reviews Molecular Cell Biology*, 6(3), pp.233–247.

Rodriguez-Boulan, E. & Macara, I.G., 2014a. Organization and execution of the epithelial polarity programme. *Nature reviews. Molecular cell biology*, 15(4), pp.225–42.

Rodriguez-Boulan, E. & Macara, I.G., 2014b. Organization and execution of the epithelial polarity programme. *Nature reviews. Molecular cell biology*, 15(4), pp.225–42.

Rodriguez-Boulan, E. & Powell, S.K., 1992. Polarity of epithelial and neuronal cells. *Annual review of cell biology*, 8, pp.395–427.

Rojas, R. & Apodaca, G., 2002. Immunoglobulin transport across polarized epithelial cells. *Nature Reviews Molecular Cell Biology*, 3(12), pp.944–956.

Roucou, X. et al., 2003. Cytosolic prion protein is not toxic and protects against Bax-mediated cell death in human primary neurons. *The Journal of biological chemistry*, 278(42), pp.40877–81.

Roush, D.L. et al., 1998. Tyrosine-based membrane protein sorting signals are differentially interpreted by polarized Madin-Darby canine kidney and LLC-PK1 epithelial cells. *The Journal of biological chemistry*, 273(41), pp.26862–9.

Rouvinski, A. et al., 2014. Live imaging of prions reveals nascent PrPSc in cell-surface, raft-associated amyloid strings and webs. *The Journal of Cell Biology*, 204(3), pp.423–441.

Rudd, P.M. et al., 2001. Prion glycoprotein: Structure, dynamics, and roles for the sugars. *Biochemistry*, 40(13), pp.3759–3766.

Rushworth, J. V. et al., 2013. Prion protein-mediated toxicity of amyloid-?? oligomers requires lipid rafts and the transmembrane LRP1. *Journal of Biological Chemistry*, 288(13), pp.8935–8951.

Russelakis-Carneiro, M. et al., 2002. Changes in the glycosylation pattern of prion protein in murine scrapie. Implications for the mechanism of neurodegeneration in prion diseases. *The Journal of biological chemistry*, 277(39), pp.36872–7.

Ryou, C. & Mays, C.E., 2008. Prion propagation in vitro: are we there yet? *International journal of medical sciences*,

5(6), pp.347–353.

Sabharanjak, S. et al., 2002. GPI-Anchored Proteins Are Delivered to Recycling Endosomes via a Distinct cdc42-Regulated, Clathrin-Independent Pinocytic Pathway. *Developmental Cell*, 2(4), pp.411–423.

Salamat, M.K. et al., 2013. Mammalian prions: tolerance to sequence changes-how far? *Prion*, 7(2), pp.131–135.

Sandberg, M.K. et al., 2011. Prion propagation and toxicity in vivo occur in two distinct mechanistic phases. *Nature*, 470(7335), pp.540–2.

Santos, T.G. et al., 2013. Laminin-γ1 chain and stress inducible protein 1 synergistically mediate PrPC-dependent axonal growth via Ca2+ mobilization in dorsal root ganglia neurons. *Journal of Neurochemistry*, 124(2), pp.210–223.

Santuccione, A. et al., 2005. Prion protein recruits its neuronal receptor NCAM to lipid rafts to activate p59fyn and to enhance neurite outgrowth. *Journal of Cell Biology*, 169(2), pp.341–354.

Sarnataro, D. et al., 2002. PrPC Is Sorted to the Basolateral Membrane of Epithelial Cells Independently of its Association with Rafts. *Traffic*, 3(11), pp.810–821.

Satir, P., Pedersen, L.B. & Christensen, S.T., 2010. The primary cilium at a glance. *Journal of cell science*, 123(Pt 4), pp.499–503.

Schätzl, H.M. et al., 1995. Prion protein gene variation among primates. *Journal of molecular biology*, 245(4), pp.362–74.

Scheiffele, P., Peränen, J. & Simons, K., 1995. N-glycans as apical sorting signals in epithelial cells. *Nature*, 378(6552), pp.96–8.

Scheiffele, P., Roth, M.G. & Simons, K., 1997. Interaction of influenza virus haemagglutinin with sphingolipid-cholesterol membrane domains via its transmembrane domain. *The EMBO journal*, 16(18), pp.5501–8.

Schiff, E. et al., 2008. Coexpression of wild-type and mutant prion proteins alters their cellular localization and partitioning into detergent-resistant membranes. *Traffic (Copenhagen, Denmark)*, 9(7), pp.1101–15.

Schmalbruch, H., 1986. Fiber composition of the rat sciatic nerve. *The Anatomical record*, 215(1), pp.71–81.

Schneider, A. & Simons, M., 2013. Exosomes: vesicular carriers for intercellular communication in neurodegenerative disorders. *Cell and tissue research*, 352(1), pp.33–47.

Schneider, C.A., Rasband, W.S. & Eliceiri, K.W., 2012. NIH Image to ImageJ: 25 years of image analysis. *Nature Methods*, 9(7), pp.671–675.

Schor, I.E. et al., 2013. Intragenic epigenetic changes modulate NCAM alternative splicing in neuronal differentiation. *The EMBO journal*, 32(16), pp.2264–74.

Schrock, Y., Solis, G.P. & Stuermer, C.A.O., 2009. Regulation of focal adhesion formation and filopodia extension by the cellular prion protein (PrPC). *FEBS letters*, 583(2), pp.389–93.

Schuck, S. & Simons, K., 2006. Controversy fuels trafficking of GPI-anchored proteins. *The Journal of cell biology*, 172(7), pp.963–5.

Schuck, S. & Simons, K., 2004. Polarized sorting in epithelial cells: raft clustering and the biogenesis of the apical membrane. *Journal of cell science*, 117(Pt 25), pp.5955–64.

Senatore, A., Restelli, E. & Chiesa, R., 2013. Synaptic dysfunction in prion diseases: a trafficking problem? *International journal of cell biology*, 2013, p.543803.

Sfakianos, J. et al., 2007. Par3 functions in the biogenesis of the primary cilium in polarized epithelial cells. *The Journal of Cell Biology*, 179(6), pp.1133–1140.

Sharma, P., Sabharanjak, S. & Mayor, S., 2002. Endocytosis of lipid rafts: an identity crisis. *Seminars in Cell & Developmental Biology*, 13(3), pp.205–214.

Shyng, S.L. et al., 1995. The N-terminal domain of a glycolipid-anchored prion protein is essential for its endocytosis via clathrin-coated pits. *The Journal of biological chemistry*, 270(24), pp.14793–800.

Shyng, S.L., Huber, M.T. & Harris, D.A., 1993. A prion protein cycles between the cell surface and an endocytic compartment in cultured neuroblastoma cells. *The Journal of biological chemistry*, 268(21), pp.15922–8.

Silverman, M.A. et al., 2005. Motifs that mediate dendritic targeting in hippocampal neurons: a comparison with basolateral targeting signals. *Molecular and cellular neurosciences*, 29(2), pp.173–80.

Simmen, T. et al., 2002. AP-4 binds basolateral signals and participates in basolateral sorting in epithelial MDCK cells. *Nature cell biology*, 4(2), pp.154–9.

Simons, K. & Gerl, M.J., 2010. Revitalizing membrane rafts: new tools and insights. *Nature reviews. Molecular cell biology*, 11(10), pp.688–99.

Simons, K. & Ikonen, E., 1997. Functional rafts in cell membranes. *Nature*, 387(6633), pp.569–72.

Simons, K. & Toomre, D., 2000. Lipid rafts and signal transduction. *Nature reviews. Molecular cell biology*, 1(1), pp.31–9.

Simons, K. & Wandinger-Ness, A., 1990. Polarized sorting in epithelia. *Cell*, 62(2), pp.207–10.

Slimane, T.A. et al., 2000. Apical secretion and sialylation of soluble dipeptidyl peptidase IV are two related events. *Experimental cell research*, 258(1), pp.184–94.

Solis, G.P. et al., 2012. Reggies/flotillins regulate E-cadherin-mediated cell contact formation by affecting EGFR trafficking. *Molecular Biology of the Cell*, 23(10), pp.1812–1825.

Solomon, I.H. et al., 2011. An N-terminal polybasic domain and cell surface localization are required for mutant prion protein toxicity. *The Journal of biological chemistry*, 286(16), pp.14724–36.

Sonnino, S. & Prinetti, A., 2013. Membrane domains and the "lipid raft" concept. *Current medicinal chemistry*, 20(1), pp.4–21.

Soza, A. et al., 2004. Sorting competition with membrane-permeable peptides in intact epithelial cells revealed discrimination of transmembrane proteins not only at the trans-Golgi network but also at pre-Golgi stages. *The Journal of biological chemistry*, 279(17), pp.17376–83.

Spudich, A. et al., 2005. Aggravation of ischemic brain injury by prion protein deficiency: Role of ERK-1/-2 and STAT-1. *Neurobiology of Disease*, 20(2), pp.442–449.

Stahl, N. et al., 1992. Glycosylinositol phospholipid anchors of the scrapie and cellular prion proteins contain sialic acid. *Biochemistry*, 31(21), pp.5043–53.

Steele, A.D. et al., 2006. Prion protein (PrPc) positively regulates neural precursor proliferation during developmental and adult mammalian neurogenesis. *Proceedings of the National Academy of Sciences of the United States of America*, 103(9), pp.3416–21.

Stephens, D.J. & Banting, G., 1998. Specificity of interaction between adaptor-complex medium chains and the tyrosine-based sorting motifs of TGN38 and lgp120. *The Biochemical journal*, 335 (Pt 3, pp.567–72.

Stewart, R.S. et al., 2005. Neurodegenerative illness in transgenic mice expressing a transmembrane form of the prion protein. *The Journal of neuroscience : the official journal of the Society for Neuroscience*, 25(13), pp.3469–77.

Stoops, E.H. & Caplan, M.J., 2014. Trafficking to the apical and basolateral membranes in polarized epithelial cells. *Journal of the American Society of Nephrology : JASN*, 25(7), pp.1375–86.

Sun, A.Q. et al., 1998. Sorting of rat liver and ileal sodium-dependent bile acid transporters in polarized epithelial cells. *The American journal of physiology*, 275(5 Pt 1), pp.G1045–55.

Sunyach, C. et al., 2007. The C-terminal products of cellular prion protein processing, C1 and C2, exert distinct influence on p53-dependent staurosporine-induced caspase-3 activation. *The Journal of biological chemistry*, 282(3), pp.1956–63.

Sunyach, C. et al., 2003. The mechanism of internalization of glycosylphosphatidylinositol-anchored prion protein. *The EMBO journal*, 22(14), pp.3591–601.

Tahirovic, S. & Bradke, F., 2009. Neuronal Polarity. *Cold Spring Harbor Perspectives in Biology*, 1(3), pp.a001644–a001644.

Tai, A.W., Chuang, J.Z. & Sung, C.H., 2001. Cytoplasmic dynein regulation by subunit heterogeneity and its role in apical transport. *JOURNAL OF CELL BIOLOGY*, 153(7), pp.1499–1509.

Takano, T. et al., 2015. Neuronal polarization. *Development (Cambridge, England)*, 142(12), pp.2088–93.

Takeda, T., Yamazaki, H. & Farquhar, M.G., 2003. Identification of an apical sorting determinant in the cytoplasmic tail of megalin. *AJP: Cell Physiology*, 284(5), pp.C1105–C1113.

Taraboulos, A. et al., 1992. Synthesis and trafficking of prion proteins in cultured cells. *Molecular biology of the cell*, 3(8), pp.851–63.

Taylor, D.R., 2005. Assigning functions to distinct regions of the N-terminus of the prion protein that are involved in its copper-stimulated, clathrin-dependent endocytosis. *Journal of Cell Science*, 118(21), pp.5141–5153.

Taylor, D.R. et al., 2009. Role of ADAMs in the ectodomain shedding and conformational conversion of the prion protein. *The Journal of biological chemistry*, 284(34), pp.22590–600.

Taylor, D.R. & Hooper, N.M., 2007. The low-density lipoprotein receptor-related protein 1 (LRP1) mediates the endocytosis of the cellular prion protein. *The Biochemical journal*, 402(1), pp.17–23.

Taylor, D.R. & Hooper, N.M., 2006. The prion protein and lipid rafts. *Molecular membrane biology*, 23(1), pp.89–99.

Thomas, D.C., Brewer, C.B. & Roth, M.G., 1993. Vesicular stomatitis virus glycoprotein contains a dominant cytoplasmic basolateral sorting signal critically dependent upon a tyrosine. *The Journal of biological chemistry*, 268(5), pp.3313–20.

Tian, A. & Baumgart, T., 2009. Sorting of Lipids and Proteins in Membrane Curvature Gradients. *Biophysical Journal*, 96(7), pp.2676–2688.

Tobler, I. et al., 1996. Altered circadian activity rhythms and sleep in mice devoid of prion protein. *Nature*, 380(6575), pp.639–642.

Trischler, M., Koch-Brandt, C. & Ullrich, O., 2001. Apical transport of osteopontin is independent of N-glycosylation and sialylation. *Molecular membrane biology*, 18(4), pp.275–81.

Tuma, P.L. & Hubbard, A.L., 2003. Transcytosis: crossing cellular barriers. *Physiological reviews*, 83(3), pp.871–932.

Turnbaugh, J.A. et al., 2011. The N-Terminal, Polybasic Region Is Critical for Prion Protein Neuroprotective Activity A. F. Hill, ed. *PLoS ONE*, 6(9), p.e25675.

Tveit, H. et al., 2005. Proteolytic processing of the ovine prion protein in cell cultures. *Biochemical and biophysical research communications*, 337(1), pp.232–40.

Tzaban, S. et al., 2009. The recycling and transcytotic pathways for IgG transport by FcRn are distinct and display an inherent polarity. *The Journal of cell biology*, 185(4), pp.673–84.

Uelhoff, A. et al., 2005. A pathogenic PrP mutation and doppel interfere with polarized sorting of the prion protein. *The Journal of biological chemistry*, 280(7), pp.5137–40.

Um, J.W. et al., 2012. Alzheimer amyloid-β oligomer bound to postsynaptic prion protein activates Fyn to impair neurons. *Nature Neuroscience*, 15(9), pp.1227–1235.

Urban, J. et al., 1987. Constitutive apical secretion of an 80-kD sulfated glycoprotein complex in the polarized epithelial Madin-Darby canine kidney cell line. *The Journal of cell biology*, 105(6 Pt 1), pp.2735–43.

Vella, L.J. et al., 2007. Packaging of prions into exosomes is associated with a novel pathway of PrP processing. *The Journal of pathology*, 211(5), pp.582–90.

Viegas, P. et al., 2006. Junctional expression of the prion protein PrPC by brain endothelial cells: a role in trans-endothelial migration of human monocytes. *Journal of cell science*, 119(Pt 22), pp.4634–43.

Vincent, B. et al., 2001. The disintegrins ADAM10 and TACE contribute to the constitutive and phorbol ester-

regulated normal cleavage of the cellular prion protein. *The Journal of biological chemistry*, 276(41), pp.37743–6.

Vinci, M. et al., 2012. Advances in establishment and analysis of three-dimensional tumor spheroid-based functional assays for target validation and drug evaluation. *BMC biology*, 10, p.29.

Wang, E.I. et al., 2000. Apical and basolateral endocytic pathways of MDCK cells meet in acidic common endosomes distinct from a nearly-neutral apical recycling endosome. *TRAFFIC*, 1(6), pp.480–493.

Watarai, M. et al., 2003. Cellular prion protein promotes Brucella infection into macrophages. *The Journal of experimental medicine*, 198(1), pp.5–17.

Watt, N.T. et al., 2005. Reactive oxygen species-mediated beta-cleavage of the prion protein in the cellular response to oxidative stress. *The Journal of biological chemistry*, 280(43), pp.35914–21.

Wehrle-Haller, B. & Imhof, B.A., 2001. Stem cell factor presentation to c-Kit. Identification of a basolateral targeting domain. *The Journal of biological chemistry*, 276(16), pp.12667–74.

Weise, C. et al., 2010. Tyrosine residues in the cytoplasmic domains affect sorting and fusion activity of the Nipah virus glycoproteins in polarized epithelial cells. *Journal of virology*, 84(15), pp.7634–41.

Weisz, O.A. & Rodriguez-Boulan, E., 2009a. Apical trafficking in epithelial cells: signals, clusters and motors. *Journal of cell science*, 122(Pt 23), pp.4253–66.

Weisz, O.A. & Rodriguez-Boulan, E., 2009b. Apical trafficking in epithelial cells: signals, clusters and motors. *Journal of cell science*, 122(Pt 23), pp.4253–66.

Westergard, L., Turnbaugh, J.A. & Harris, D.A., 2011. A naturally occurring C-terminal fragment of the prion protein (PrP) delays disease and acts as a dominant-negative inhibitor of PrPSc formation. *The Journal of biological chemistry*, 286(51), pp.44234–42.

Wik, L. et al., 2012. Separate mechanisms act concurrently to shed and release the prion protein from the cell. *Prion*, 6(5), pp.498–509.

Wild-Bode, C. et al., 2006. A basolateral sorting signal directs ADAM10 to adherens junctions and is required for its function in cell migration. *The Journal of biological chemistry*, 281(33), pp.23824–9.

Wille, H. et al., 2002. Structural studies of the scrapie prion protein by electron crystallography. *Proceedings of the National Academy of Sciences of the United States of America*, 99(6), pp.3563–8.

Winckler, B., Forscher, P. & Mellman, I., 1999. A diffusion barrier maintains distribution of membrane proteins in polarized neurons. *Nature*, 397(6721), pp.698–701.

Winckler, B. & Mellman, I., 1999. Neuronal polarity: controlling the sorting and diffusion of membrane components. *Neuron*, 23(4), pp.637–40.

Windl, O. et al., 1999. Molecular genetics of human prion diseases in Germany. *Human genetics*, 105(3), pp.244–52.

Wopfner, F. et al., 1999. Analysis of 27 mammalian and 9 avian PrPs reveals high conservation of flexible regions of the prion protein. *Journal of molecular biology*, 289(5), pp.1163–78.

Yadavalli, R. et al., 2004. Calpain-dependent endoproteolytic cleavage of PrPSc modulates scrapie prion propagation. *The Journal of biological chemistry*, 279(21), pp.21948–56.

Yeaman, C., 1997. The O-glycosylated Stalk Domain Is Required for Apical Sorting of Neurotrophin Receptors in Polarized MDCK Cells. *The Journal of Cell Biology*, 139(4), pp.929–940.

Yeaman, C. et al., 1997. The O-glycosylated stalk domain is required for apical sorting of neurotrophin receptors in polarized MDCK cells. *The Journal of cell biology*, 139(4), pp.929–40.

Yeaman, C., Grindstaff, K.K. & Nelson, W.J., 1999. New perspectives on mechanisms involved in generating epithelial cell polarity. *Physiological reviews*, 79(1), pp.73–98.

Yim, Y.-I. et al., 2015. The multivesicular body is the major internal site of prion conversion. *Journal of cell science*,

128(7), pp.1434–43.

Yu, C.-Y. et al., 2007. A bipartite signal regulates the faithful delivery of apical domain marker podocalyxin/Gp135. *Molecular biology of the cell*, 18(5), pp.1710–22.

Zanata, S.M. et al., 2002. Stress-inducible protein 1 is a cell surface ligand for cellular prion that triggers neuroprotection. *EMBO Journal*, 21(13), pp.3307–3316.

Zhang, C.C. et al., 2006. Prion protein is expressed on long-term repopulating hematopoietic stem cells and is important for their self-renewal. *Proceedings of the National Academy of Sciences of the United States of America*, 103(7), pp.2184–9.

Zhao, H. et al., 2006. Proteolytic cleavage and shedding of the bovine prion protein in two cell culture systems. *Virus research*, 115(1), pp.43–55.

Zhao, Z. et al., 2015. Central role for PICALM in amyloid-β blood-brain barrier transcytosis and clearance. *Nature neuroscience*, 18(7), pp.978–987.

Zurzolo, C. et al., 1994. Glycosphingolipid clusters and the sorting of GPI-anchored proteins in epithelial cells. *Brazilian journal of medical and biological research = Revista brasileira de pesquisas medicas e biologicas / Sociedade Brasileira de Biofisica ... [et al.]*, 27(2), pp.317–322.

Zurzolo, C. et al., 1993. Glycosylphosphatidylinositol-anchored proteins are preferentially targeted to the basolateral surface in Fischer rat thyroid epithelial cells. *The Journal of cell biology*, 121(5), pp.1031–1039.

Zurzolo, C. et al., 1992. Modulation of transcytotic and direct targeting pathways in a polarized thyroid cell line. *The EMBO journal*, 11(6), pp.2337–44.

Appendix: « Astrocyte-to-neuron intercellular prion transfer is mediated by cell-cell contact»

General introduction

The intracellular transfer of prion and prion-like aggregates is one of the strongest features of our laboratory. In 2009 Edwin Shiff, has shown that infectious prion protein can use Tunneling NanoTubes (TNT) as the highway to invade the neighboring cell (Gousset et al., 2009). What is a TNT or a TNT-like structure? It is a new type of cell-to-cell connection, thin actin-containing intercellular bridges that connect distant cells of the same type or heterologous cells such as neuronal cells and bone marrow dendritic cells or neurons and astrocytes (Abounit & Zurzolo 2012; Gousset & Zurzolo 2009). Some prion-like proteins were shown to travel through TNT (Costanzo et al. 2013; Costanzo & Zurzolo 2013). Aforementioned articles used mostly cell lines and an important question is whether TNT mediated transfer occurs *in vivo*, in the infected brain or TNT are a restricted feature of cultured cells?

In present article we made a step forward towards the *in vivo* brain context as we were able to show that primary astrocytes transfer prion infection to primary neurons via TNT-like structures.

Summary of results

In this article we have shown that astrocytes are capable to transfer infectious prion to neuronal cells and primary neurons. Astrocyte can uptake prion aggregates from infected neuronal cells and can also transfer prions to both neuronal cells and primary neurons. We have further shown that cell-to-cell contact is greatly contributing to prion transfer from astrocytes to primary neurons. Free PrP^{Sc} aggregates in the media are infectious, but astrocyte secretion of PrP^{Sc}, is not effective in transferring infection to primary neurons. Intercellular transfer was highly enhanced upon cell-to-cell contact. Additionally, PrP^{Sc} is found to colocalize with endo-lysosomal vesicles in TNT, thus pointing to TNTs as a cell connection mediating prion transfer.

Personal contribution

Because of my interest in the physiological models and experimental condition that are close to the *in vivo* systems I was delighted to work with Soraya Victoria, who is the postdoc leading this project. During my PhD I have mastered brain dissections and primary cultures. My contribution to this project was in providing primary cerebellar neuronal and primary astrocytic cultures; I also performed biochemical assays on culture media, and contributed in the finding of TNT between different cell types in the mixed cultures. Finally I contributed to the image analysis and composition of supplementary figures.

Astrocyte-to-neuron intercellular prion transfer is mediated by cell-cell contact.

Running title: prion transfer between astrocytes and neurons.

Guiliana Soraya Victoria, Alexander Arkhipenkho, Seng Zhu, Sylvie Syan and Chiara Zurzolo*

Unité Trafic Membranaire et Pathogenèse, Institut Pasteur, 25-28 Rue du Docteur Roux, 75724 Paris CEDEX 15

*Corresponding author: zurzolo@pasteur.fr, Tel: +33 1 40 61 30 62)

Abstract: Astrocytes are one of the predominant cell types in the brain and have been shown to be one of the earliest sites of prion accumulation in the brain. A fundamental question arising from this observation is whether these cells are involved in intercellular prion transfer and thereby disease propagation. Using primary mouse cerebellar astrocytes and granule neurons, in this study we show that astrocytes are capable of taking up prion from infected neuronal cells as well as transferring prion to both neuronal cells and primary neurons, supporting their implication in disease progression. Interestingly, while astrocytes are capable of secretion of PrP, this was an inefficient method of transferring prion infectivity to neurons. Intercellular transfer was highly enhanced upon co-culturing suggesting that the predominant mechanism of PrP^{Sc} transfer between primary astrocytes and neurons is mediated by cell-to-cell contact. Additionally, PrP^{Sc} is found colocalized with endolysosomal vesicles in tunneling nanotubes between astrocytes, thus pointing to TNTs as a mechanism of transfer.

Introduction: The conversion of the cellular prion protein PrP^{C} to a misfolded β-rich conformer called PrP^{Sc} underlies a group of neurodegenerative diseases known as transmissible spongiform encephalopathies (TSEs). PrP^{Sc} is self-propagating, i.e, capable of inducing the conversion of naïve PrP^{C} molecules to the misfolded conformation (1) and the accumulation of sufficient levels of PrP^{Sc} results in the formation of oligomers and higher-order fibrillar aggregates. These aggregates may be responsible for seeding the propagation of PrP^{Sc} misfolding between cells following their transfer from one cell to another. The accretion and deposition of prion aggregates in neuronal plaques in diseased brains (2) results in inexorable

and fatal neurodegeneration; however, how these are related is not clear since PrP^{Sc} formation and prion toxicity have been shown to be distinct from each other (3,4,5).

Furthermore, while neuronal damage and death are well documented in prion diseases (6,7), the role of other cell types in the brain such as microglia and astrocytes are less understood. We decided to address the role of astrocytes in intercellular PrP^{Sc} transfer and disease propagation for many reasons. Firstly, astrocytes play a major role in the homeostasis of the brain. Astrocytes can modulate neuronal activity by releasing gliotransmitters and scavenging glutamate, are involved in synaptic support and formation and physically contact and connect large numbers of neurons (8,9,10). More interestingly, astrocytes are migrating cells (11) and also bridge structures like neurons and vasculature that otherwise cannot communicate (12), thus inviting the question of whether they could be the key to understanding how prion infectivity crosses the brain-blood barrier. The large numbers of tasks they carry out make them indispensable for normal brain functioning and it is important to understand whether these roles are subverted in the course of neurodegenerative disease and perhaps exploited to transfer infectivity. Interestingly, in neurodegenerative diseases, one well-marked phenotype has been reactive gliosis, including a strong astrocyte response marked by cleavage and upregulation of the astrocyte-specific intermediate filament GFAP. The implications of this reactivity are unclear and may indicate a protective response that in turn could be used to transfer infectivity.

Secondly, there are several indications that astrocytes may be involved in prion propagation. Earlier studies have shown that one of the earliest sites of scrapie accumulation in mice appears to be astrocytes (13) and immunohistochemistry of infected sheep brains shows the accumulation of scrapie in GFAP-positive structures (14). Primary cerebellar astrocyte cultures from transgenic mice expressing hamster PrP^{C} also sustained infection (15) indicating that astrocytes are capable of supporting prion replication and infection. Transgenic mice expressing hamster PrP^{C} only in astrocytes developed prion disease upon challenge with an inoculum of hamster scrapie strain 263K (16). The infection of transgenic-hamster PrP^{C} -expressing astrocytes also resulted in the damage of adjacent neurons that did not express hamster PrP, (17) though those neurons were not capable of replicating prion. Thus, astrocyte infection clearly is deleterious to the brain. However, the fundamental question of whether astrocytes are capable of transferring prion infectivity has yet to be answered.

In this study we investigate this question. Using primary cultures of astrocytes and cerebellar granular neurons (CGNs), we first characterize the relative susceptibility of neurons and astrocytes to infection and show that astrocytes from wild type mice are intrinsically infectable and interestingly, appear to be more prone than neurons to prion replication and accumulation of aggregated PrP^{Sc}. We then investigate whether there is PrP^{Sc} transfer between neurons and astrocytes by developing a co-culture system between neuronal cells and astrocytes. We determine that cerebellar astrocytes can take up PrP^{Sc} from infected neuronal CAD cells in a cell-contact dependent manner. Furthermore, infected astrocytes can efficiently transfer PrP^{Sc} to primary cerebellar granule neurons. Interestingly we find that while astrocytes appeared to secrete PrP into the medium, this did not result in efficient prion transfer to primary neurons, suggesting that transfer in primary cultures relies primarily on cell-cell contact.

Results:

Primary cerebellar astrocytes and neurons are infected with 22L prion: In order to assess and compare prion replication in neurons and astrocytes, primary mixed cultures of mouse cerebellar granular neurons containing astrocytes were prepared. Since the cerebellum is post-natally developed, cultures often contain around 10-15% of astrocytes at early time-points (7 days in vitro, DIV) of the culture; proliferation of astrocytes occurs over time and after 21 days in culture we routinely observe ~ 30-40%. The mixed cultures were left to differentiate for 5 days before inoculation with 22L prion-infected mouse brain homogenate. Replication of mouse scrapie was monitored by western blot and immunofluorescence at 7, 14 and 21 days post infection (dpi). Western blots (Fig 1a) revealed a gradual increase of the characteristic proteinase-K resistant PrP (PrP^{Res}) over the time course of the experiment indicating that the CGN cultures were succesfully infected with 22L prion. β3-tubulin signal did not significantly decrease in comparison to the mock-infected cultures (treated with 0.01% brain homogenate from non-infected mice). This suggested there was no major neuronal loss induced by prion infection over this time point. Immunofluorescence studies of these cultures after GdnTCN treatment revealed that PrP^{Sc} aggregates could be found in both astrocytes and neurons (Fig 1B). Interestingly, the majority of the PrP^{Sc} puncta were found within GFAP-positive cells (Fig 1B and C), suggesting that either astrocytes were taking up the aggregates from neurons (in a possibly protective role) or that they themselves were more apt to replicate prions. Closer

inspection of PrP^{Sc} distribution revealed that between 40-50% of the aggregates were within astrocytes compared to approximately 20% in neurons. A large percentage of aggregates (~ 30%) were unable to be colocalized positively with either type of cell. We hypothesize that this might be extracellular prion aggregate as is frequently reported to occur in infected brain tissue (2, 17) although we cannot rule out difficulties in co-labelling.

To confirm that the astrocytes in our cultures do indeed propagate 22L-prion and that the PrP^{Sc} aggregates within them are the result of *de novo* infection following uptake of the infectious seeds, pure cerebellar astrocytes were isolated and exposed to 22L mouse brain homogenate using the same protocol as for the mixed CGN cultures. Infection was determined as before, by both western blot detection of PrPRes, and immunofluorescence. Fig 1D shows the gradual increase of PrPRes, typical of an infection. Immunofluorescence following guanidium denaturation also showed the canonical punctate distribution of PrP^{Sc} (Fig 1E), indicating that CA cultures are infected. This is similar to the report by Cronier et al., 2004 (15) where pure cerebellar astrocytes over-expressing transgenic hamster PrP were shown capable of sustaining and propagating hamster scrapie infection. The results suggest that mouse scrapie 22L brain homogenate infects both neurons and astrocytes expressing endogenous levels of PrP^{C}. They also suggest that cerebellar astrocytes are more susceptible to prion accumulation than cerebellar granule neurons. A very recent report (18) demonstrated that cortical astrocytes from adult hamster brains were much more efficient than neurons at uptake of exogenous prion, and we speculate that this might promote increased susceptibility of astrocytes to infection.

Subcellular compartmentalization of PrP^{Sc}: Studies in immortalized neuronal cell lines (19, 20) have shown that PrP^{Sc} is associated with markers of the endo-lysosomal pathway. Furthermore, PrP intracellular trafficking was shown to be important both for prion conversion (19) as well as in intercellular spreading (21). Since in our culture system 22L infection affected neurons and astrocytes, we determined the subcellular localization of PrP^{Sc} at the midpoint of infection (14dpi) in both cell types by using specific neuron and astrocyte markers. In primary mixed cultures, we observed colocalization of PrP^{Sc} with markers of the plasma membrane, lysosomes and lipid droplets (Fig 2).

PrP^{Sc} could be found associated with WGA, a common plasma membrane marker, in both astrocytes and neurons (Fig 2). This suggested that PrP^{Sc} was in close association with the plasma membrane in both cell types. Additionally we noted that this association in neurons occurred quite often along the neurite networks, in string-like patterns that have recently been reported to occur in the neuronal cell line ScGT1 (22). Interestingly, we observed a frequent colocalization of PrP^{Sc} with lysosome markers (LamP1) in astrocytes, but not in neurons (Fig 2). These data are consistent with the localization that has been observed *in vivo* in infected murine hippocampi whereby using EM, PrP^{Sc} clusters have been noted on the plasma membrane and in lysosomes of astrocytes in infected neuropil but not in neuronal lysosomes (2, 17). Our corroborative results indicate that primary cultures are a physiologically relevant model in which to study prion infections in vitro. In addition, we also observed localization of PrP^{Sc} with FL-BODIPY -positive structures in both neurons and astrocytes. As this is a common marker of lipid droplets (23) this suggests that PrP^{Sc} might associate with cholesterol-rich lipid droplets. We confirmed the subcellular localization of PrP^{Sc} aggregates in pure cerebellar astrocyte cultures wherein we found a large percentage of PrP^{Sc} in lysosomes, consistent with it being degraded, as well as with WGA- and Bodipy-positive structures, similar to the mixed cultures (Fig 3). PrP^{Sc} was also found in Vamp3-positive compartments. Vamp3 is a marker of the endocytic recycling compartment (ERC), which has previously been shown to be involved in prion conversion (19). While we could colocalize PrP^{Sc} to EEA1, the percentage of this colocalization was almost negligible (~3%) and therefore considered insignificant. Of note, we also observed that the lysosomes appeared to be slightly smaller than those in the mixed cultures. Upon quantification of lysosomal size in astrocytes from mixed versus pure infected cultures using ICY software (24), we noted that the median lysosome size was significantly increased in mixed cultures (Supplementary fig 1). One possible explanation is that astrocytes within the mixed culture phagocytose portions of infected dying neurons or larger external aggregates and the large lysosomes we see might be phagolysosomes resulting from the phagocytic clearance of PrP^{Sc} aggregates

PrP^{Sc} aggregates transfer between astrocytes and neuronal cells: The above results show that propagation of PrP^{Sc} could occur in both mixed CGN cultures and astrocyte cultures upon the exogenous application of a PrP^{Sc} source. This mode of infection presumably occurs by endocytosis of the infectious seed by both cell types followed by replication of the misfolded

protein inside the cells. We were interested however, in determining if PrP^{Sc} aggregates, once internalized and replicated in one cell type could transfer between astrocytes and neurons and whether this transfer would contribute to the propagation of prions in the culture.

In order to address whether transfer of PrP^{Sc} could occur from neurons to astrocytes, we set up co-culture experiments between the chronically prion-infected donor neuronal cell line ScCAD and naïve acceptor cerebellar astrocytes. ScCAD was chosen as a "neuron" donor instead of primary cerebellar neurons due to the difficulty in completely eliminating astrocytes from primary CGN cultures, even in the presence of mitotic inhibitors such as FdU. The use of a pure ScCAD culture thus excluded the possibility that any observed transfer to astrocytes resulted from an infected astrocyte within mixed culture donors rather than from neurons. Naïve acceptor cerebellar astrocytes were co-cultured with ScCAD for 24 hours as described in the methods. Immunofluorescence to detect the presence of PrP^{Sc} aggregates in astrocytes revealed aggregates within 37 ± 7.5% of astrocytes (Fig 4B) within the time frame of our experiment. In order to determine whether these aggregates derived from the scCAD donor and did not arise from conversion and aggregation of endogenous PrP^{C} in the acceptor astrocytes from smaller/ soluble PrP^{Sc} after uptake, we repeated the same experiment using $PrP^{-/-}$ astrocytes from knockout mice (25) as acceptors in this co-culture system. We observed PrP^{Sc} aggregates in these PrP-deficient astrocytes as well, which strongly support the fact that PrP aggregates transfer from infected CAD cells to astrocytes; they also suggest that PrP^{C} is not necessary in the acceptor cells (Supplementary Fig 2).

To determine whether transfer was secretion-dependent, we performed experiments wherein conditioned medium from ScCAD cultures were applied on astrocytes for 24h (see Methods). In this case we obtained 12 ±2.6% of cells with detectable aggregates (Fig 4C) suggesting that the transfer of aggregates from ScCAD to astrocytes was much more efficient when there is cell-cell contact.

Next, in order to determine whether astrocytes could transfer PrP^{Sc} to neuronal cells, 22L prion-infected astrocytes (22L-astrocytes) were co-cultured with naïve acceptor CAD cells for 24h. We consistently observed that a large percentage (81 ± 12.66 %, over three independent experiments) of CAD acceptors contained prion aggregates after being co-cultured with 22L-astrocytes (Fig 5A and B). This was not limited to cells in close contact with astrocytes, but was noted even in cells that were relatively further away from astrocytes, though the numbers of

aggregate-positive cells reduced with distance from astrocytes and efficiency of transfer also depended on the confluence level of astrocytes. Additionally, the efficiency of transfer was much higher than that observed from neuronal cells to astrocytes. To determine whether astrocytes were releasing PrP^{Sc} into the medium, CAD cells were incubated with conditioned medium from 22L-astrocytes (see Methods). After 24h, we observed similar levels of aggregate-positive cells (81.67 ± 18.33%, Fig 5B), suggesting that astrocytes were indeed secreting PrP^{Sc} that was in turn up taken by CAD cells. We therefore precipitated proteins in conditioned medium from both cultures of 22L- astrocytes and ScCAD cultures and assayed for the presence of PrP by Western blot. After 24h of conditioning we were able to detect PrP in 22L-astrocyte-conditioned medium but not in ScCAD-conditioned medium (Fig 5C). Since we did not observe any dead cells over this time period in astrocyte cultures, it seems likely that this PrP is either exocytosed or cleaved from the plasma membrane of infected astrocytes (and not of ScCAD), and is not debris resulting from cell death.

However, PK resistance assays did not reveal any detectable amounts of PK-resistant PrP (data not shown). This could imply that the levels of PrP^{Sc} in the medium released from the astrocytes in this time frame were under the detection sensitivity of a Western blot or that secreted PrP^{Sc} is PK-sensitive (26).

In order to support our observation in a more physiologically relevant context, we repeated the co-culture experiments using primary cerebellar granule neurons (CGN) at 5 DIV as acceptors. To this end, astrocytes that had been infected for 7 days were washed thoroughly, trypsinized and added to coverslips containing naïve CGNs. However, after 24h, it proved difficult to clearly distinguish transferred PrP^{Sc} aggregates from the PrP^{C} signal in the cerebellar granular neurons. A possible explanation is that granule neurons, being very small and with fine neurites, take up the smaller aggregates that are difficult to detect. Thus, to eliminate the possibility of false-positive or false-negative results, we co-cultured the infected astrocytes and naïve neurons for 11 days. Since after 7 days we are able to distinguish PrP^{Sc} aggregates in CGNs after challenging with 22L brain homogenate (Fig. 1), we reasoned that if secreted infectious PrP^{Sc} aggregates were internalized by neurons, some percentage of them would replicate the prion and the resultant aggregates that developed could be more easily detected by microscopy. After 11 days co-culturing, we were able to observe the occurrence of prion aggregates (Fig 6) in 32.2 ±10.98 % of neurons suggesting that 22L-infected astrocytes were able to transfer infection to cerebellar neurons. Although remarkable, the efficiency of transfer however was lower

compared to that observed in the CAD cells. To test for secretion, we performed parallel experiments wherein we conditioned media from 22L-astrocytes for 11 days to approximate the PrP concentrations that might be released over the co-culture time period, and then added this to naïve CGN cultures and incubated for 11 days. Intriguingly, we observed significantly less PrP-aggregate-positive neurons upon incubation with conditioned medium (6.7 ±0.32 %, p=0.041). Additionally, astrocytes that are present in the mixed acceptor CGN culture, which are usually more susceptible to infection (see Fig.1), also displayed a low percentage of transfer (11.3 ± 4.03%). These data indicate that while astrocytes release PrP into the medium, transfer via secretion in primary cells is quite inefficient and relies more on cell-cell contact.

To determine whether astrocytes transfer prion between themselves, we co-cultured 22L-astrocytes with wild-type acceptor astrocytes that had been labeled with Cell-Tracker Green (CTG). After 24h of co-culture, we observed the presence of sharp PrP^{Sc} puncta in the CTG-labelled acceptors (approx. 40 %, Fig 7a and b). Using CTG-labelled PrP $^{-/-}$ astrocytes as acceptors also gave similar results (Supplementary Figure 2), thus these appear to be transferred aggregates. We performed the usual conditioned medium controls in parallel and observed very low numbers of aggregate-positive astrocytes that had been exposed to 22L-astrocyte conditioned medium for either 24h (8.92%) or 11 days (12.7%). These numbers were not significantly affected by increasing the time of conditioning from 24h to 11 days, suggesting that secretion-and-uptake was not very efficient as a mechanism of prion transfer/ infectivity in primary cells. We also observed that 22L-astrocytes form numerous intercellular connections in which PrP^{Sc} aggregates can be found. While many of these structures do not strictly fall within the current criteria for tunneling nanotubes (TNTs) (see discussion), nevertheless some proportion of truly TNT-like structures was detectable between astrocytes (Fig 7C). We found PrP^{Sc} aggregates colocalized with endolysosmal vesicles within TNT-like structures, which together with the much higher efficiency of transfer when physical contact between astrocytes was allowed, point towards these type of structures to be the predominant method of intercellular PrP^{Sc} transfer.

Discussion: The intercellular transfer of prion remains a matter of significant interest and interlinks the question of which cell types are involved in spreading prion with that of which molecular mechanisms mediate the transfer. There are multiple routes and different cell types

wherein prion is replicated and then transferred from the periphery to the central nervous system (27). Nevertheless, in all cases (acquired, sporadic or genetic) it is the accumulation and spread of prion in cells of the central nervous system which results in the pathology of disease. However, the role of non-neuronal cells such as astrocytes (which comprise the greater part of the brain) in scrapie infections is unclear, and there are contradictory reports on their effect on neuropathology, depending on the strain of scrapie (3, 17). Thus, more detailed research is needed into how cells such as astrocytes influence the course of disease. Additionally, while different mechanisms of prion dissemination have been described and proposed, such as exosomal secretion, tunneling nanotubes, GPI painting or axonal transport (28, 29, 30), it is not yet clear whether these mechanisms are common to all the cell types known to replicate prion or whether different cell types use predominantly one or another form of dissemination depending on their primary functions and physiology. This paper presents evidence to suggest that mouse astrocytes are involved in prion intercellular transfer. Our results confirm previous reports that astrocytes replicate prion (15, 16), and, to the best of our knowledge, is the first study to show that astrocytes can indeed transfer PrP^{Sc} to neurons as well as between themselves. Additionally, our data suggest that while astrocytes can transmit prion infectivity via multiple mechanisms, including secretion, they predominantly use cell-cell contact, such as tunneling nanotubes to mediate transfer. This is likely due to the number of functions astrocytes play: as described in the introduction, they are known to secrete a variety of factors to shape the extracellular matrix and influence neuronal behaviour, however they also rely on direct contact to perform a number of regulatory and protective roles. Thus, these functional roles may be exploited to disseminate infectious PrP^{Sc} to neighbouring neurons.

The colocalization results in the primary mixed cultures show that PrP^{Sc} is differentially localized in astrocytes and neurons with respect to lysosomes. We speculate that this might be related to the functions performed by astrocytes and neurons. Astrocytes may assist certain functions of neurons in order to allow them to focus their cellular energy reserves on their function. For example, astrocytes are responsible for a large percentage of cholesterol production and dissemination in the brain (31) and neurons are believed to uptake cholesterol from lipoproteins released from astrocytes (32, 33). Thus it is possible that astrocytes uptake and degrade protein aggregates from both the extracellular space and from damaged or infected neurons in order to protect them from the deleterious effects of their build-up. Indeed, Chung et al., 2013 (34) demonstrated that astrocytes are capable of phagocytosing parts of neurons.

Importantly, cultured astrocytes from different species have been shown to rapidly internalize prion and be capable of its degradation (18, 35) and a recent report showed that glia in Drosophila brains could phagocytose Huntingtin aggregates from neurons (36). Taken together with the observation that astrocytes can take up PrP^{Sc} aggregate from neuronal cells, these data lend weight to the idea that astrocytes may perform most of the prion degradation in mixed cultures, thus explaining the localization of PrP mainly in lysosomes of astrocytes but not neurons.

Nonetheless it is known that neurodegenerative disease impairs astrocytic functions: in mouse models of Alzheimer's and prion disease, the establishment of disease results in lowered astrocytic degradation capacity (37, 38). Thus this function could be subverted in infected astrocytes: the initial capacity to degrade is overtaken at later stages by prion production and increased intracellular burden, resulting in abnormal physiology and, possibly, dissemination from the infected astrocyte. Our finding that PrP can be detected in medium conditioned by infected astrocytes is in line with this idea and suggests that astrocytes release prion protein. Exosomal secretion is one possibility; however it is unclear how efficient this is as a general method of transfer - while prion transfer occurs via exosomes in cultured cell models, the authors note that the efficiency of this method is highly strain-dependent (39). The authors suggest that this may be due to a strain-dependent size-exclusion effect in packing into exosomes, thereby limiting the efficiency of this method. Interestingly, they observed that the infectivity of 22L prion, which we use in this study, was secreted with one of the lowest efficiencies from cultured cells. Our data with primary astrocytes and neurons suggests that it is equally inefficient as a transfer mechanism in primary cells. Additionally, the size of transferred aggregates in acceptor astrocytes in the co-culture system were far too large to be packaged into exosomes and most likely arise not from short-range secretion but from active transfer of PrP^{Sc} packaged in endolysosomal vesicles or, possibly, phagocytosis from infected cell surfaces. However, in apparent contrast to the data in primary cells we observed efficient transfer of PrP^{Sc} from astrocyte-conditioned medium to CAD cells as detected by the presence of PrP^{Sc} aggregates, despite our inability to detect PrPRes in the conditioned medium. One possible explanation for the difference in transfer efficiency between primary cells and CAD could be that cultured CAD cells endocytose secreted factors more efficiently or are more susceptible to prion conversion/replication than primary cerebellar granule neurons. In the case of primary neurons or astrocytes whose physiology is very different, and wherein cell-cell

contact plays a great role in normal functioning, direct physical contact may be the more efficient mechanism of transfer. It is likely that the interplay of signals between the primary neurons and astrocytes influences and encourages their physical contact in a way that is very different from the co-culture system with CAD cells, enhancing transfer via cell-cell contact. Indeed, we found that astrocytes are found in close apposition to neurons, in direct contact with cell bodies. They also form large numbers of intercellular connections between themselves, including TNT-like structures in which we observe PrP^{Sc} aggregates. These thin actin-containing intercellular bridges can connect distant cells of the same type or heterologous cells such as neuronal cells and bone marrow dendritic cells or neurons and astrocytes (29, 40, 41) and mediate the transfer of small molecules, protein aggregates and organelles (29, 40, 42, 43, 44) which make them interesting candidates as a general transfer mechanism. We have previously demonstrated that prion travels within TNTs between CAD neuronal cells, as well as between dendritic cells and primary neurons and that this transfer occurs in endolysosomal compartments (15, 29, 45). Our similar finding of prion transfer between astrocytes suggests that TNTs might be a conserved mechanism of intercellular prion transfer. While identifying TNTs between astrocytes and neurons in our CGN system is fraught with difficulty due to the lack of a TNT-specific marker that allows clear identification of this structure from other neuronal processes, the need for cell-cell contact upon transfer from astrocytes to neurons combined with the presence of PrP^{Sc} in TNTs, suggests that this could be one transfer mechanism in this case as well. Studies have demonstrated that immature neurons can form TNTs with astrocytes (41) thus evidence exists that such a contact is possible between these cell types, at least during development, prior to axonal/dendritic extension. Intriguingly, it was shown in mature differentiated co-cultures that astrocyte-to-neuron Ca2+-transmission occurred through a synapse-independent, physical intercellular contact that had at least some characteristics of a gap junction (46). Since connexins have been shown to be localized to TNTs (41, 47), this also suggests that TNTs between astrocytes and neurons in developed brains or differentiated primary cultures may exist and be a potent method of intercellular communication. However, in the absence of tools to identify or specifically block TNT formation it is currently difficult to assess the extent to which this mechanism contributes in intercellular prion transfer. Indeed, it is as yet unclear whether the other intercellular connections between astrocytes also represent a different type of TNT or are other structures that mediate transfer and intercellular communication. Further investigation into delineating the exact mechanisms

of transfer of prion between astrocytes and neurons should yield useful insights into the propagation of these neurodegenerative diseases as well as in the field of intercellular communication.

Materials and Methods:

Primary cultures: Cerebellar granular neurons and cerebellar astrocytes (CA) were isolated from 4-6 day-old C57BL/6J pups. Pups were euthanized in accordance with regulations set down by the French Government. Cerebella were isolated, meninges removed and washed twice in PBS. After Trypsin-EDTA treatment for 10 minutes at 37°C followed by trypsin inactivation with FBS, 10^5 units/ml of DNase I (Sigma Aldrich) were added and the solution triturated with a 5 ml pipette until the cell suspension was completely dissociated. After gentle centrifugation (700 rpm, 7 minutes no brake), the supernatant was removed and 5 ml of complete neuronal medium (DMEM-Glutamax, 10% FBS, B27 supplement, N2 supplement, 20mM KCl and 1% Pen-strep) was added to the pellet. Cells were plated at a density of 150000-cells/12 mm. For cerebellar astrocytes, the procedure was identical. The day after plating, CA cultures were vigorously shaken to remove debris and other types of glia. Plating and maintenance was carried out using DMEM-Glutamax, 10% Horse serum and 1% Pen-strep as the culture medium.

Cell culture: The mouse catecholaminergic CAD (cath-a-differentiated) neuronal cell line and its chronically scrapie-infected counterpart ScCAD were grown in OPTI-MEM medium supplemented with 10% FBS +1% Penicillin-Streptomycin.

Infection of primary cultures: 22L-infected mouse brain homogenate was sonicated (2 min, 80% amplitude, 5 sec on/2sec off cycles using a Vibra Cell Bioblock Scientific sonicator) and diluted to a final percentage of 0.01% (v/v) in either neuronal or astrocyte medium before adding to the culture. After 2 days, the medium was either completely replaced with fresh medium in the case of astrocyte cultures or half the volume replaced in the case of CGN cultures. Medium was refreshed every week. Time points of 7, 14 and 21 days post infection (dpi) were used to determine whether scrapie propagation occurred, by both western blot and immunofluorescence.

Proteinase K resistance assays and western blots: For western blots to determine infection of primary cultures, cells were lysed in 25mM Tris pH 7.5 buffer containing 1% TritonX-100 and

1% β-octyl glucoside. 50μg of protein was treated with 3.75 μg/ml of proteinase K at 37°C for 30 minutes and methanol-precipitated prior to resuspension in SDS-loading dye and running on a 12% Tris-Glycine gel. Western blots were carried out with Sha31 antibody (SPIBio, mouse anti-PrP, 1:5000), β3-tubulin (Sigma Aldrich, mouse 1:5000), a-tubulin (Sigma-aldrich, mouse 1:10000), GFAP (Dako, rabbit 1:5000). Peroxidase-conjugated secondary antibodies to mouse or rabbit were used (GE Healthcare) and blots were revealed with ECL Western Blot detection reagent (Amersham).

Immunofluorescence: primary cultures or co-cultures were fixed with 4% paraformaldehyde. After permeabilisation with 0.1% TX-100, PrP^{Sc} epitopes were revealed by 5 minutes of treatment with 3M guanidium thiocyanate (GdnTCN) and PrP^{Sc}/PrP^{C} detected using either Sha31 (Spibio, IgG1, mouse) or ICSM35 (DGen, mouse IgG2bk). Antibodies to different markers were as follows: GFAP to detect astrocytes (Dako, rabbit polyclonal), β3 tubulin to mark neuronal processes (Sigma-Aldrich, mouse IgG2a), Lamp1 for lysosomes (BD Pharmingen, rat clone 1D4B), Vamp3 for endocytic recycling compartment (ERC) (Abcam, rabbit) and EEA1 for early endosomes (a gift from Dr. Marino Zerial, rabbit) were all used at 1:500 dilution in blocking buffer (PBS +10% goat serum). Secondary antibodies were conjugated to Alexa-488 or Alexa-546. BODIPY 490/505 (1:1000 dilution) was used to stain lipid droplets. Alexa488-Wheat Germ agglutinin (Life Technologies) was used to mark the plasma membrane. Coverslips were sealed with Aquapolymount ™. Images were acquired using a Zeiss LSM700 confocal microscope. A 40X oil objective (NA 1.3) was used to acquire images of infection or transfer and a 60X oil objective for colocalization studies.

Colocalization studies: Colocalization of PrP^{Sc} with different organelle markers was performed at 14dpi. After fixation and GdnTCN denaturation, immunofluorescence was performed for PrP^{Sc} and different organelle markers. Secondary antibodies to PrP^{Sc} were conjugated to Alexa-546 and secondary antibodies/dyes to the specific organelles were labeled with Alexa-488 or BODIPY 493/503. Z-stack images were acquired using a Zeiss LSM700 confocal microscope with a 63x oil plan apochromat objective (NA 1.4) to eliminate chromatic aberration. Acquisition parameters were close to Nyquist sampling limits, in order to perform image deconvolution. Deconvolution was performed to reduce the point spread function and improve resolution using Huygens Essential software (Scientific Volume Imaging). Colocalization analysis was performed on deconvolved images using the objects-based colocalization plugin in the image analysis software ICY (de Chaumont et al., 2012) with object sizes set at Scale 2 (4-7 pixels) to

eliminate noise and with a threshold for intensity set to minimize PrP^C signal and only pick up the aggregates, which fluoresce more intensely after denaturation.

Co-culture transfer experiments:

Transfer experiments were carried out using a simple Infected Donor-to-Acceptor co-culture system that was adapted to use either astrocytes or neuronal cells interchangeably as donors or acceptors. The different combinations of donor and acceptor cell types are described briefly below.

Neuronal cells-to-astrocytes: To determine if PrP^{Sc} transfer occurred from the chronically infected neuronal cell line ScCAD to naïve astrocytes, cerebellar astrocytes were plated onto poly-D-lysine-coated coverslips and allowed to attach, and differentiate for 5 days. $1x10^5$ "donor" ScCAD cells/ml were then added and co-cultured with the astrocytes for 24h before fixation, GdnTCN treatment to reveal PrP^{Sc} epitopes and immunofluorescence to detect PrP^{Sc}.

Astrocytes-to-neuronal cells: Astrocyte cultures were infected with 22L prion as described above. At 7dpi they were washed extensively before trypsinising and re-plating on cover slips. After 5 days they were again washed extensively to remove any debris or released PrP^{Sc} before naïve CAD cells were added in Opti-MEM medium at a cell density of $1x10^5$/ ml. 24h post co-culture (dpc) cells were fixed and immunofluorescence carried out to detect PrP^{Sc} in acceptor CAD.

Astrocytes-to-primary neurons: 22L-infected donor astrocytes were washed extensively, trypsinised and re-plated on coverslips containing naïve CGNs. After 11 days of co-culture the cultures were fixed and immunofluorescence performed to detect PrP^{Sc} associated with β3-tubulin-positive structures (neurons).

Astrocyte-to-astrocyte: Naïve acceptor cerebellar astrocytes were plated on PDL-coated cover slips. After 5 days, they were stained with 15 μM Cell-Tracker Green (CTG-CMDA, from Life Technologies) according to the manufacturers instructions and washed several times with serum-free medium before replacing fresh medium. 22L-infected donor astrocytes were then trypsinised and added and at 24h, 3d and 11 days after addition, the co-cultures were fixed and immunofluorescence performed. At each time point the number of CTG-labelled astrocytes with detectable aggregates was counted.

Conditioned medium controls were performed in parallel for all combinations of donor and acceptor. Briefly, infected donor (22L-astrocytes or ScCAD) cultures were washed extensively to remove any cell debris. Fresh medium was replaced and then cells were incubated for 24h (or 11 days when co-cultures were performed for 11 days). The conditioned medium from the donors was then collected and pelleted at 2000 rpm to settle any cell debris. The supernatant was then carefully aspirated and after removing the medium from acceptor cultures, added to the acceptors. In the case of primary neuron acceptors, neuronal supplements were added to the conditioned medium prior to addition to prevent cell death. Cells were fixed at the same time points described for the co-cultures and immunofluorescence performed to detect PrP^{Sc}.

Images were processed using the spot detector plugin on the ICY image analysis software to determine the number of acceptor cells (astrocytes/CAD/neurons) that had detectable aggregates after applying an intensity threshold to correct for the diffuse PrP^{C} signal.

Statistical analyses: All graphs show the mean+ s.e.m. from 3 independent experiments. Student's unpaired t-tests were used to evaluate the significance of all the data presented. *P < 0.05, ** P< 0.01

Acknowledgments: The authors thank Dr. Yuan-ju Wu for critical comments on the manuscript. GSV is a recipient of fellowships from the Fondation Recherche Médicale and the Bourse Pasteur-Roux, Institut Pasteur. AA is supported by a Ph.D fellowship from the Ministère de l'Enseignement Supérieur et de la Recherche. SZ is supported by a PhD fellowship from the Chinese Scholarship Council. This work is supported by research grants from the European Commission FP7 PRIORITY contract number 222887, the MI CARNOT ICSA/PMI, grants from the region Ile-de-France (IDF DIM-MALINF 2013), Agence Nationale de la Recherche (ANR-14-JPCD-0002-01) and Equipe FRM (Fondation Recherche Médicale) 2014 (DEQ20140329557) to CZ.

Figures:

Figure 1

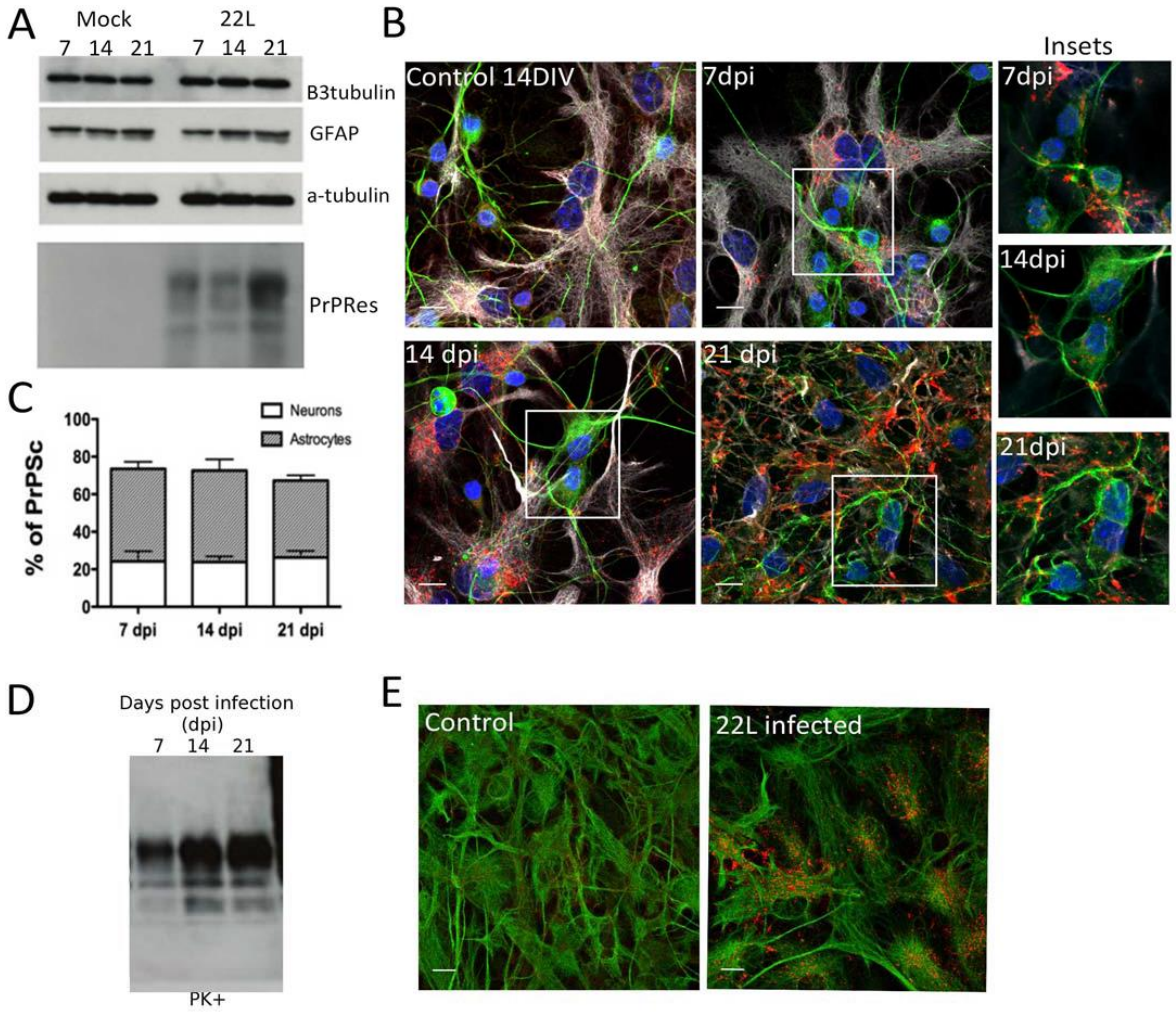

Fig 1: *Infection of primary cerebellar mixed cultures*. (A) Representative western blot of the time course of 22L prion infection. The lowest panel shows the increase of proteinase-K resistant PrP (PrPRes) at 7, 14 and 21 dpi. Other panels depict protein levels of other important protein markers within the culture over the time course of infection: the neuronal marker β3-tubulin signal indicates no apparent loss of neurons, astrocyte-specific GFAP levels are constant. α–tubulin is used as a loading control. (B) Representative immunofluorescence of 22L-infected cultures at 7, 14 and 21 dpi shows that PrP^{Sc} aggregates accumulate over time, mainly in astrocytes. An uninfected CGN culture at 14 DIV shows no aggregation of PrP. DAPI (blue), β3-tubulin (green), PrP^{Sc} (red) and GFAP (white). Insets depict close-ups of neurons at different timepoints of infection to highlight the presence of PrP^{Sc} aggregates within. Only the upper z-stacks are taken to reduce the PrP^{Sc} signal from surrounding astrocytes and focus on neuron-

associated PrP^{Sc}. C) Quantification of the percentage of PrP^{Sc} signal associated with either β3-tubulin or GFAP at 7,14 and 21 dpi. (D) Infection of pure cerebellar astrocyte cultures: representative western blot of PrPRes over 21 days of infection. (E) Representative immunofluorescence images of astrocytes (marked with GFAP in green) that are either uninfected or infected with PrP^{Sc} (red) at 14dpi. The astrocytes in both cases are of the same age in culture. Scale bars: 10 μm.

Figure 2

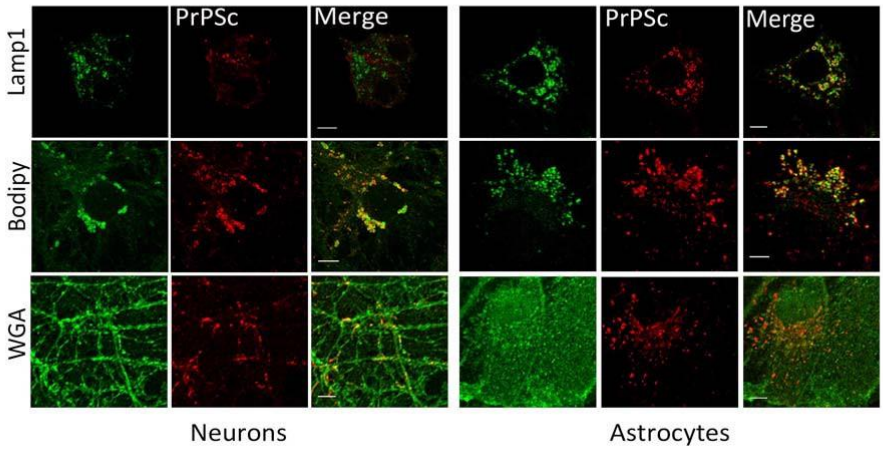

Fig 2: *Subcellular distribution of PrP^{Sc} in primary mixed cerebellar cultures*. Representative images of colocalization of PrP^{Sc} with different organelle markers in granule neurons (left panels) and cerebellar astrocytes (right panels) from a mixed cerebellar culture at 14 dpi. Scale bars: 5 μm.

Figure 3

A

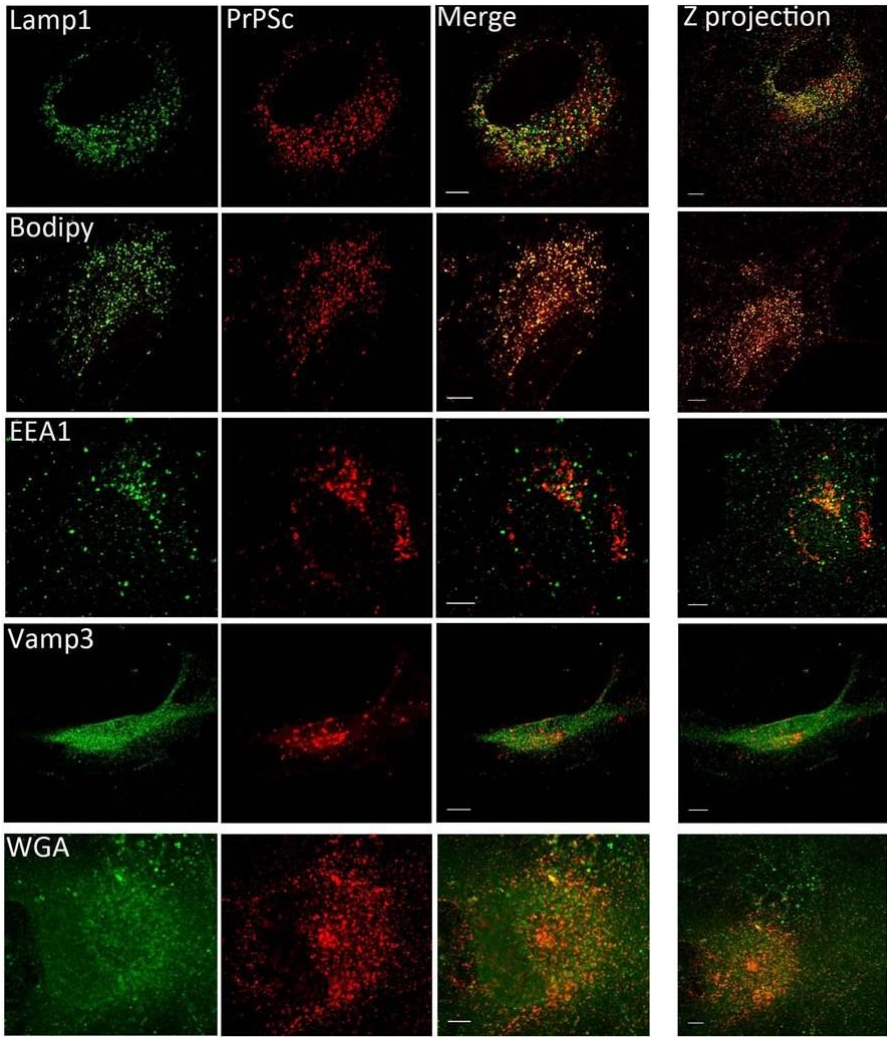

B

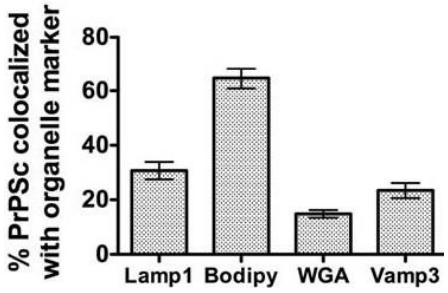

Fig 3: *Colocalization in pure astrocyte cultures*. (A) Representative images of colocalization of PrP^{Sc} with different organelle markers in pure cultures of cerebellar astrocytes at 14 dpi. Single slices are shown for clarity, and the z-projection of the complete cell is shown on the far right. Scale bars: 5 μm (B) Quantification of percentage of colocalization of PrP^{Sc} with respective organelle marker in pure cerebellar astrocytes.

Figure 4

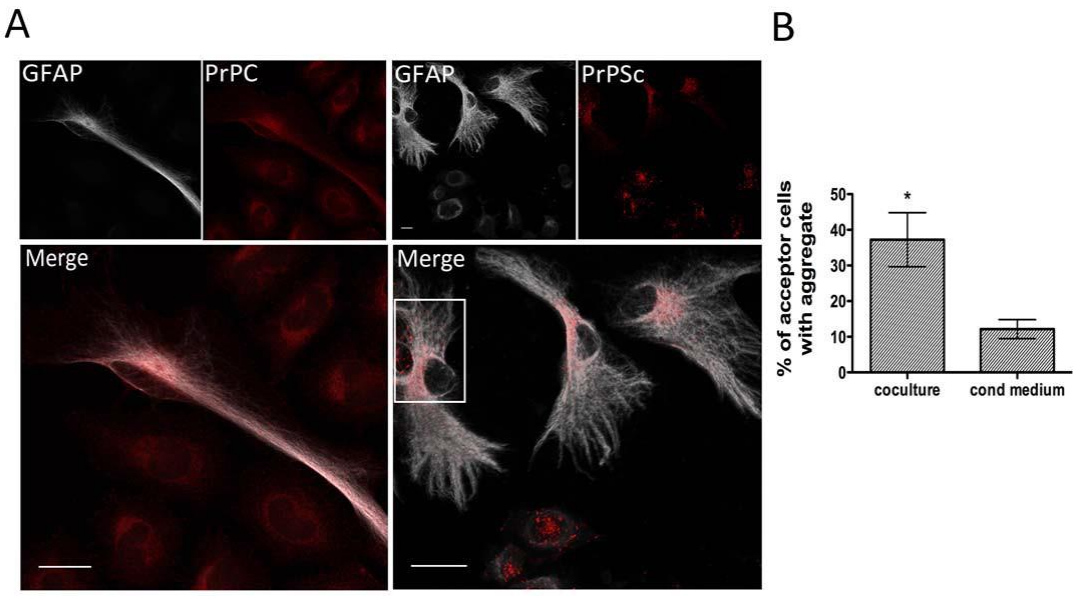

Fig 4: *Transfer of prion from infected neuronal cells to astrocytes*. (A) Left panel: immunofluorescence of 24h co-cultures of uninfected astrocytes and CAD cells to show PrP^{C} distribution. Right panel: immunofluorescence of 24h co-cultures of astrocytes with prion-infected ScCAD. Larger PrP^{Sc} puncta (red) are clearly visible in the astrocyte on the far left (inset). Scale bars: 10 μm. (B) Quantification of the percentage of acceptor astrocytes with PrP^{Sc} puncta after 24h co-culture and treatment with ScCAD-conditioned medium. The results suggest that cell-cell contact is the more efficient method of transfer (*p =0.0174, Students unpaired t-test).

Figure 5

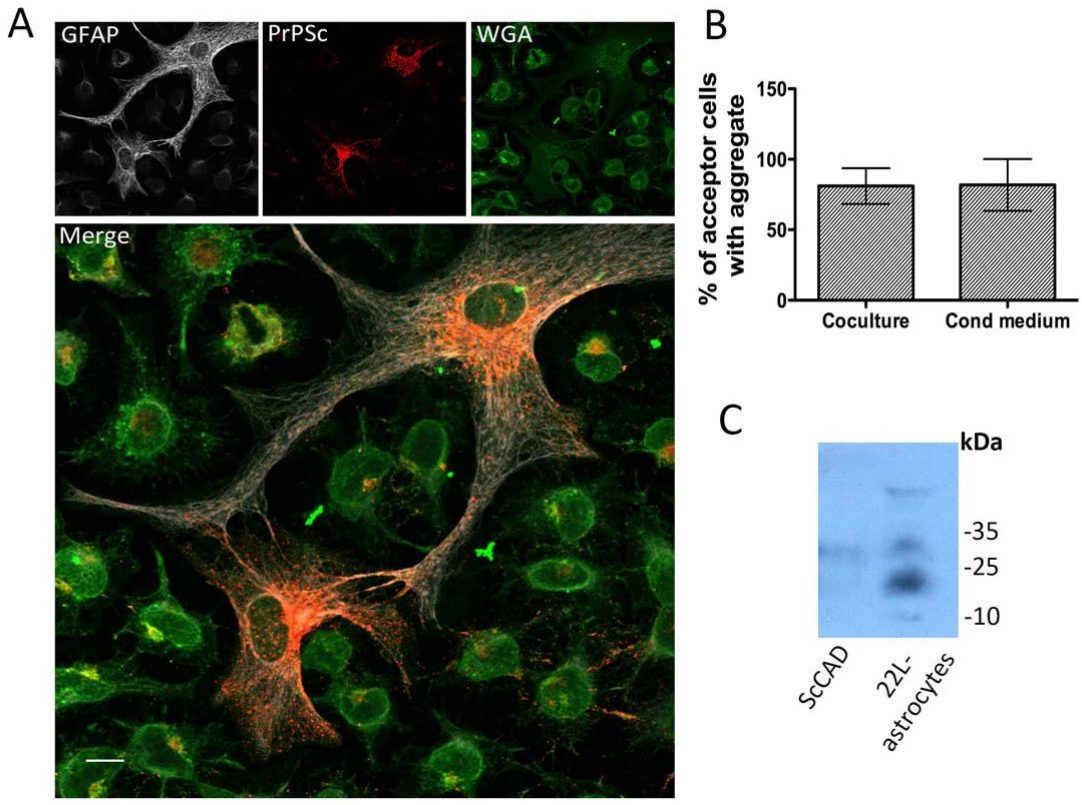

Fig 5: *Transfer of prion from infected astrocytes to neuronal cells*. (A) Immunofluorescence image of 24h-co-cultures between 22L-astrocytes and naïve CAD cells. > 90% of CAD cells have detectable punctate PrP^{Sc} after co-culture. Scale bars: 10 μm. (B) Quantification of percentage transfer after co-culture and after 24h treatment of CAD with infected astrocyte-conditioned medium suggests that transfer is secretion-mediated. (C) Western blot to detect PrP in conditioned medium from either ScCAD or infected astrocytes shows that within the 24h time-point of the co-culture, astrocytes secrete detectable amounts of PrP while ScCAD do not.

Figure 6

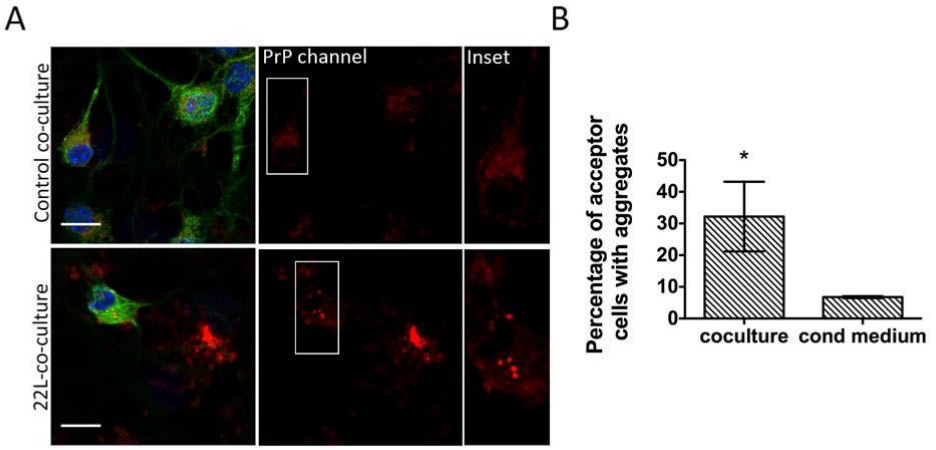

Fig 6: Transfer of prion from infected astrocytes to primary cerebellar granular neurons.

Uninfected (upper panels, control co-culture) or 22L-astrocytes were co-cultured with cerebellar granular neurons (lower panels, 22L-co-culture) for 11 days. Bright PrP^{Sc} puncta (red) were detectable within β3-tubulin-positive neuronal cell bodies (green) suggesting transfer of infectivity could occur in primary culture as well. Only the upper stacks of the image are shown for clarity to demonstrate that infection is within neurons. Insets highlight the presence of aggregates within cell bodies of neurons in the 22L co-cultures compared to the more diffuse PrP^{C} signal in uninfected co-cultures. Scale bars: 10 μm.

Figure 7

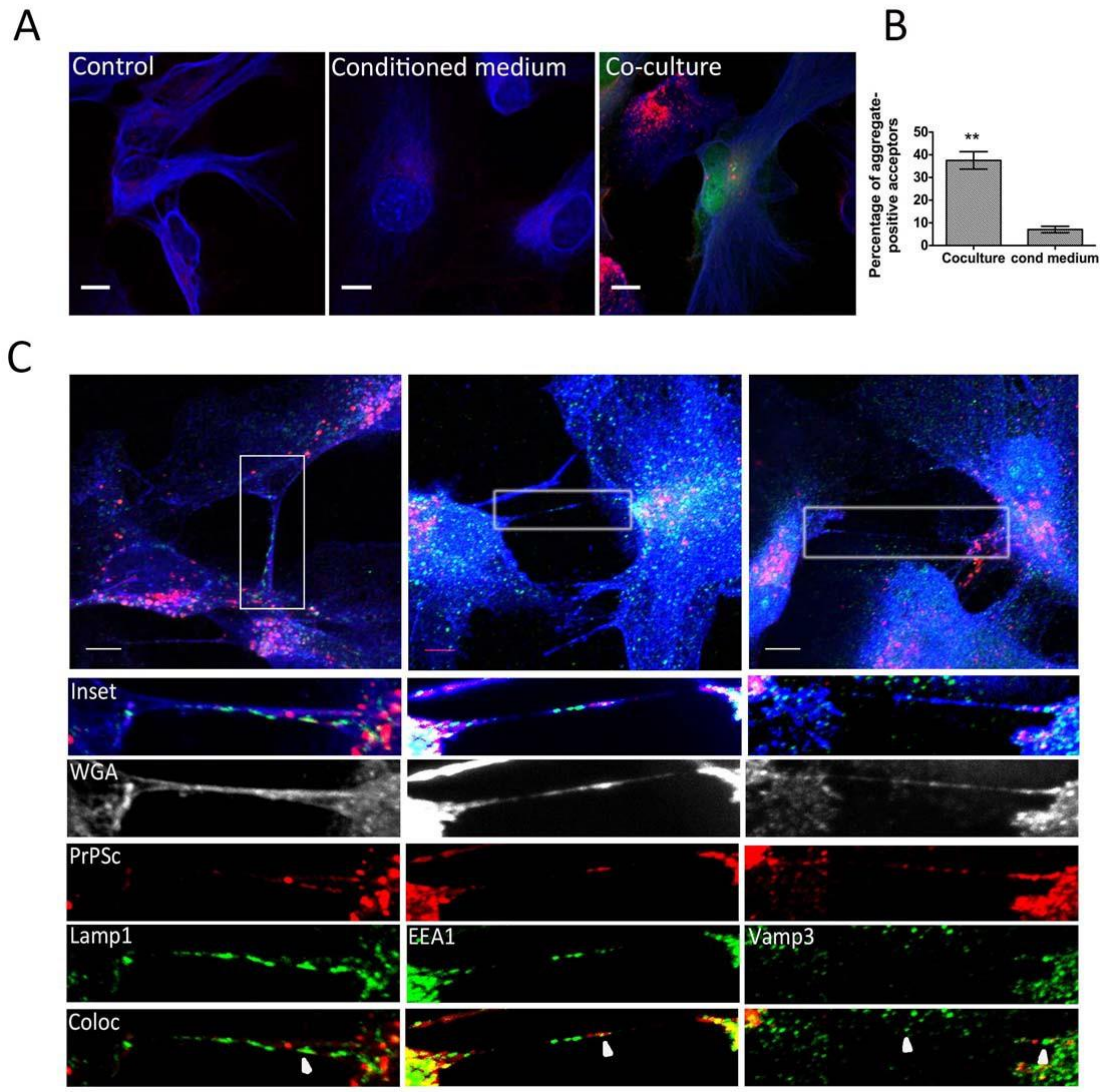

Fig 7: *Transfer of prion between infected astrocytes*. A) PrP^{Sc} aggregates (red) are easily detected in green CTG-acceptor astrocytes after 24-co-culture with unlabeled 22L-astrocytes. Shown for comparison are representative images of uninfected astrocytes (control) and astrocytes that have been cultured for 24h in the presence of 24h 22L-astrocyte conditioned medium (conditioned medium). GFAP is shown in blue. Scale bars: 10 μm. (B) Quantification of the percentage of CTG-astrocytes that contain transferred PrP^{Sc} after overnight co-culturing shows that inter-astrocyte transfer is more efficient in co-culture than in the presence of conditioned medium. (C) Intercellular connections mediating PrP^{Sc} transfer between astrocytes: 22L-infected astrocytes form numerous PrP^{Sc}-containing intercellular connections including TNTs (Insets). PrP^{Sc} aggregates colocalize with endolysosomal vesicles within TNTs (white arrowheads), including lysosomes (Lamp1), early endosomes (EEA1) and endocytic recycling

compartments (Vamp3). Organelle markers are shown in green, PrP^{Sc} in red and WGA to mark the plasma membrane in white. Scale bars: 5 μm.

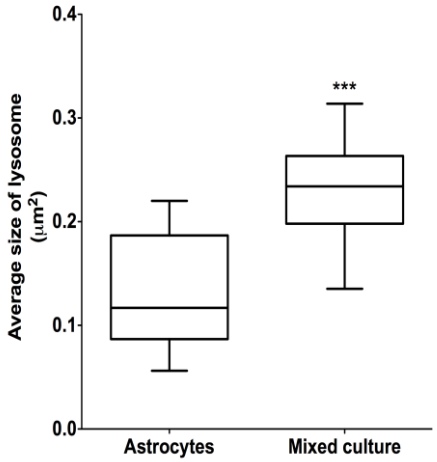

Supplementary Fig 1: Size of lysosomes in astrocytes from 22L-infected pure astrocyte cultures versus in 22L-infected mixed CGN cultures. Lysosomes in mixed infected cultures appear to be bigger than in pure infected primary astrocytes cultures (***p≤0.0001, unpaired Students two-tailed test). Lysosome size was measured using the aggregates detector plugin on the ICY software.

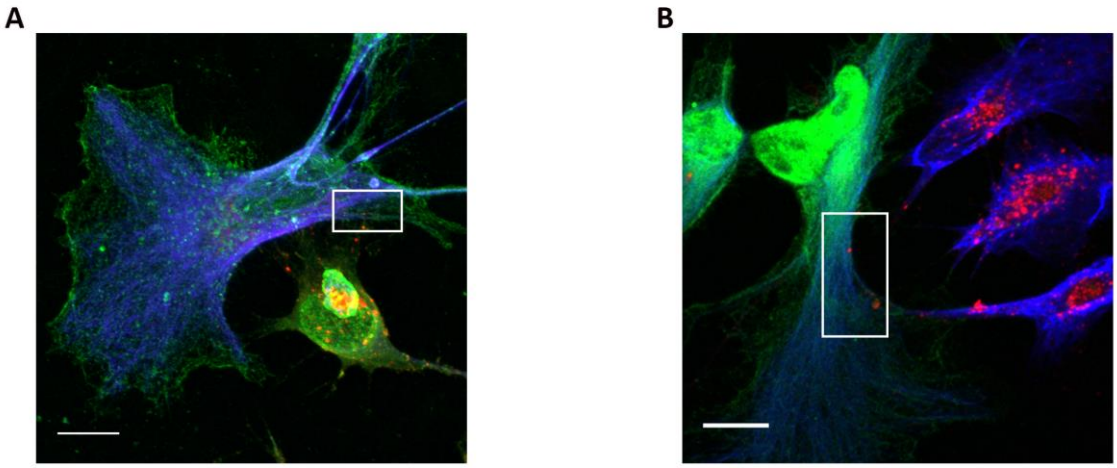

Supplementary Fig 2: Transfer of PrP^{Sc} aggregates (red) from PrP-positive prion-infected cells to PrP-deficient astrocytes. (A) Transfer from chronically infected ScCAD neuronal cell line labelled in green WGA-Alexa488 to $PrP^{-/-}$ astrocytes, marked with GFAP in blue. (B) Transfer from 22L-infected donor astrocytes to CTG-labelled acceptor $PrP^{-/-}$ astrocytes (green). Images

were acquired on a Zeiss LSM700 confocal microscope and Z-projections through the entire cellular volume are shown. Scale bars: 10 um.

References:

1. Aguzzi A, Calella AM. Prions: protein aggregation and infectious diseases. Physiol Rev. 2009 Oct;89(4):1105-52. doi: 10.1152/physrev.00006.2009. Review.
2. Godsave SF, Wille H, Kujala P, Latawiec D, DeArmond SJ, Serban A, Prusiner SB, Peters PJ. Cryo-immunogold electron microscopy for prions: toward identification of a conversion site. J Neurosci 2008;28(47):12489-99. doi: 10.1523/JNEUROSCI.4474-08.2008.
3. Mallucci G, Dickinson A, Linehan J, Klöhn PC, Brandner S, Collinge J. Depleting neuronal PrP in prion infection prevents disease and reverses spongiosis. Science. 2003 Oct 31;302(5646):871-4.PMID:14593181
4. Sandberg MK, Al-Doujaily H, Sharps B, Clarke AR, Collinge J. Prion propagation and toxicity in vivo occur in two distinct mechanistic phases. Nature. 2011 Feb 24;470(7335):540-2. doi: 10.1038/nature09768.
5. Moreno JA, Halliday M, Molloy C, Radford H, Verity N, Axten JM, Ortori CA, Willis AE, Fischer PM, Barrett DA, Mallucci GR. Oral treatment targeting the unfolded protein response prevents neurodegeneration and clinical disease in prion-infected mice. Sci Transl Med. 2013 Oct 9;5(206):206ra138. doi: 10.1126/scitranslmed.3006767.
6. Soto C, Satani N. The intricate mechanisms of neurodegeneration in prion diseases. Trends Mol Med. 2011 Jan;17(1):14-24. doi: 10.1016/j.molmed.2010.09.001.
7. Fuhrmann M, Mitteregger G, Kretzschmar H, Herms J. Dendritic pathology in prion disease starts at the synaptic spine. J Neurosci. 2007 Jun 6;27(23):6224-33.
8. Lalo U, Rasooli-Nejad S, Pankratov Y. Exocytosis of gliotransmitters from cortical astrocytes: implications for synaptic plasticity and aging. Biochem Soc Trans. 2014 Oct;42(5):1275-81.
9. Chung WS, Clarke LE, Wang GX, Stafford BK, Sher A, Chakraborty C, Joung J, Foo LC, Thompson A, Chen C, Smith SJ, Barres BA. Astrocytes mediate synapse elimination through MEGF10 and MERTK pathways. Nature. 2013 Dec 19;504(7480):394-400. doi: 10.1038/nature12776. Epub 2013 Nov 24
10. Filosa A, Paixão S, Honsek SD, Carmona MA, Becker L, Feddersen B, Gaitanos L, Rudhard Y, Schoepfer R, Klopstock T, Kullander K, Rose CR, Pasquale EB, Klein R. Neuron-glia communication via EphA4/ephrin-A3 modulates LTP through glial glutamate transport. Nat Neurosci. 2009 Oct;12(10):1285-92. doi: 10.1038/nn.2394. Epub 2009 Sep 6.

11. Jacobsen CT, Miller RH. Control of astrocyte migration in the developing cerebral cortex. Dev Neurosci. 2003 Mar-Aug;25(2-4):207-16.
12. Zonta M, Angulo MC, Gobbo S, Rosengarten B, Hossmann KA, Pozzan T, Carmignoto G. Neuron-to-astrocyte signaling is central to the dynamic control of brain microcirculation. Nat Neurosci. 2003 Jan;6(1):43-50.
13. Diedrich, J.F., Bendheim, P.E., Kim, Y.S., Carp, R.I., and Haase, A.T. (1991). Scrapie-associated prion protein accumulates in astrocytes during scrapie infection. Proc Natl Acad Sci USA88, 375-379.
14. Hernández RS, Sarasa R, Toledano A, Badiola JJ, Monzón M. Morphological approach to assess the involvement of astrocytes in prion propagation. Cell Tissue Res. 2014
15. Cronier S, Laude H, Peyrin JM. Prions can infect primary cultured neurons and astrocytes and promote neuronal cell death. Proc Natl Acad Sci U S A. 2004 Aug 17;101(33):12271-6. Epub 2004 Aug 9.
16. Raeber AJ, Race RE, Brandner S, Priola SA, Sailer A, Bessen RA, Mucke L, Manson J, Aguzzi A, Oldstone MB, Weissmann C, Chesebro B. Astrocyte-specific expression of hamster prion protein (PrP) renders PrP knockout mice susceptible to hamster scrapie. EMBO J. 1997 Oct 15;16(20):6057-65.
17. Jeffrey M, Goodsir CM, Race RE, Chesebro B (2004) Scrapie-specific neuronal lesions are independent of neuronal PrP expression. Ann Neurol 55:781–792.
18. Hollister JR, Lee KS, Dorward DW, Baron GS. Efficient uptake and dissemination of scrapie prion protein by astrocytes and fibroblasts from adult hamster brain. PLoS One. 2015 Jan 30;10(1):e0115351. doi: 10.1371/journal.pone.0115351.
19. Marijanovic Z, Caputo A, Campana V, Zurzolo C. Identification of an intracellular site of prion conversion. PLoS Pathog. 2009 5(5):e1000426.
20. Uchiyama K, Muramatsu N, Yano M, Usui T, Miyata H, Sakaguchi S. Prions disturb post-Golgi trafficking of membrane proteins. Nat Commun. 2013;4:1846. doi: 10.1038/ncomms2873.
21. Zhu S, Victoria GS, Marzo L, Ghosh R, Zurzolo C. Prion aggregates transfer through tunneling nanotubes in endocytic vesicles. Prion. 2015;9(2):125-35. doi: 10.1080/19336896.2015.1025189. PMID:25996400
22. Rouvinski A, Karniely S, Kounin M, Moussa S, Goldberg MD, Warburg G, Lyakhovetsky R, Papy-Garcia D, Kutzsche J, Korth C, Carlson GA, Godsave SF, Peters PJ, Luhr K,

Kristensson K, Taraboulos A. Live imaging of prions reveals nascent PrPSc in cell-surface, raft-associated amyloid strings and webs. J Cell Biol 2014 204(3):423-41

23. Spangenburg EE, Pratt SJ, Wohlers LM, Lovering RM. Use of BODIPY (493/503) to visualize intramuscular lipid droplets in skeletal muscle. J Biomed Biotechnol. 2011;2011:598358. doi: 10.1155/2011/598358. Epub 2011 Sep 25. PMID: 21960738
24. de Chaumont F, Dallongeville S, Chenouard N, Hervé N, Pop S, Provoost T, Meas-Yedid V, Pankajakshan P, Lecomte T, Le Montagner Y, Lagache T, Dufour A, Olivo-Marin JC. Icy: an open bioimage informatics platform for extended reproducible research. Nat Methods. 2012 Jun 28;9(7):690-6. doi: 10.1038/nmeth.2075. PMID:22743774
25. Büeler H, Fischer M, Lang Y, Bluethmann H, Lipp HP, DeArmond SJ, Prusiner SB, Aguet M, Weissmann C. Normal development and behaviour of mice lacking the neuronal cell-surface PrP protein. Nature. 1992 Apr 16;356(6370):577-82.
26. Pastrana MA, Sajnani G, Onisko B, Castilla J, Morales R, Soto C, Requena JR (2006) Isolation and Characterization of a Proteinase K-Sensitive PrP(Sc) Fraction. Biochemistry 45:15710–15717.
27. Davies GA, Bryant AR, Reynolds JD, Jirik FR, Sharkey KA. Prion diseases and the gastrointestinal tract.Can J Gastroenterol. 2006 Jan;20(1):18-24. Review.PMID:16432555
28. Fevrier B, Vilette D, Archer F, Loew D, Faigle W, Vidal M, Laude H, Raposo G. Cells release prions in association with exosomes. Proc Natl Acad Sci U S A. 2004 Jun 29;101(26):9683-8. Epub 2004 Jun 21.PMID:15210972
29. Gousset K, Schiff E, Langevin C, Marijanovic Z, Caputo A, Browman DT, Chenouard N, de Chaumont F, Martino A, Enninga J, Olivo-Marin JC, Männel D, Zurzolo C. Prions hijack tunnelling nanotubes for intercellular spread. Nat Cell Biol 2009;11(3):328-36. doi: 10.1038/ncb1841
30. Liu T, Li R, Pan T, Liu D, Petersen RB, Wong BS, Gambetti P, Sy MS. Intercellular transfer of the cellular prion protein. J Biol Chem. 2002 Dec 6;277(49):47671-8. Epub 2002 Sep 30.
31. Bjorkhem I, Leoni V, Meaney S. Genetic connections between neurological disorders and cholesterol metabolism. J Lipid Res. 2010;51:2489–2503.

32. Göritz C, Mauch DH, Nägler K, Pfrieger FW. Role of glia-derived cholesterol in synaptogenesis: new revelations in the synapse-glia affair. J Physiol Paris. 2002 Apr-Jun;96(3-4):257-63..
33. Pfrieger FW. Outsourcing in the brain: do neurons depend on cholesterol delivery by astrocytes? Bioessays. 2003 Jan;25(1):72-8.
34. Chung WS, Clarke LE, Wang GX, Stafford BK, Sher A, Chakraborty C, Joung J, Foo LC, Thompson A, Chen C, Smith SJ, Barres BA. Astrocytes mediate synapse elimination through MEGF10 and MERTK pathways. Nature. 2013 Dec 19;504(7480):394-400. doi: 10.1038/nature12776. Epub 2013 Nov 24.
35. Choi YP, Head MW, Ironside JW, Priola SA. Uptake and degradation of protease-sensitive and -resistant forms of abnormal human prion protein aggregates by human astrocytes. Am J Pathol. 2014 Dec;184(12):3299-307. doi: 10.1016/j.ajpath.2014.08.005. Epub 2014 Sep 30.
36. Pearce MM, Spartz EJ, Hong W, Luo L, Kopito RR. Prion-like transmission of neuronal huntingtin aggregates to phagocytic glia in the Drosophila brain. Nat Commun. 2015 Apr 13;6:6768. doi: 10.1038/ncomms7768.
37. Wyss-Coray T, Loike JD, Brionne TC, Lu E, Anankov R, Yan F, Silverstein SC, Husemann J. Adult mouse astrocytes degrade amyloid-beta in vitro and in situ. Nat Med. 2003 Apr;9(4):453-7. Epub 2003 Mar 3. PMID:12612547
38. Jackson WS, Krost C, Borkowski AW, Kaczmarczyk L. Translation of the Prion Protein mRNA Is Robust in Astrocytes but Does Not Amplify during Reactive Astrocytosis in the Mouse Brain. PLoS ONE 2014 9(4): e95958. doi:10.1371/journal.pone.0095958
39. Arellano-Anaya ZE, Huor A, Leblanc P, Lehmann S, Provansal M, Raposo G, Andréoletti O, Vilette D. Prion strains are differentially released through the exosomal pathway. Cell Mol Life Sci 2014. Epub ahead of print
40. Rustom A, Saffrich R, Markovic I, Walther P, Gerdes HH. Nanotubular highways for intercellular organelle transport. Science. 2004;303(5660):1007-10.
41. Wang X, Bukoreshtliev NV, Gerdes HH. Developing neurons form transient nanotubes facilitating electrical coupling and calcium signaling with distant astrocytes. PLoS One. 2012;7(10):e47429. doi: 10.1371/journal.pone.0047429. Epub 2012 Oct 11.

42. Abounit S, Zurzolo C. Wiring through tunneling nanotubes--from electrical signals to organelle transfer. J Cell Sci. 2012 Mar 1;125(Pt 5):1089-98. doi: 10.1242/jcs.083279. Epub 2012 Mar 7. Review. PMID:22399801
43. Marzo L, Gousset K, Zurzolo C. Multifaceted roles of tunneling nanotubes in intercellular communication. Front Physiol. 2012 Apr 10;3:72. doi: 10.3389/fphys.2012.00072. eCollection 2012. PMID: 22514537
44. Costanzo M, Abounit S, Marzo L, Danckaert A, Chamoun Z, Roux P, Zurzolo C. Transfer of polyglutamine aggregates in neuronal cells occurs in tunneling nanotubes. J Cell Sci. 2013 Aug 15;126(Pt 16):3678-85. doi: 10.1242/jcs.126086. Epub 2013 Jun 18. PMID:23781027
45. Langevin C, Gousset K, Costanzo M, Richard-Le Goff O, Zurzolo C. Characterization of the role of dendritic cells in prion transfer to primary neurons. Biochem J. 2010 Oct 15;431(2):189-98. doi: 10.1042/BJ20100698. PMID:20670217
46. Nedergaard M. Direct signaling from astrocytes to neurons in cultures of mammalian brain cells. Science. 1994 Mar 25;263(5154):1768-71.PMID:8134839
47. Wang X, Veruki ML, Bukoreshtliev NV, Hartveit E, Gerdes HH. Animal cells connected by nanotubes can be electrically coupled through interposed gap-junction channels. Proc Natl Acad Sci U S A. 2010 Oct 5;107(40):17194-9. doi: 10.1073/pnas.1006785107. Epub 2010 Sep 20.PMID:20855598

Arkhipenko Alexander: PrP traffic in polarized MDCK cells

Summary

The Prion Protein (PrP) is a ubiquitously expressed glycosylated membrane protein attached to the external leaflet of the plasma membrane via a glycosylphosphatidylinositol anchor (GPI). While the misfolded PrP^{Sc} scrapie isoform is the infectious agent of "prion diseases", the cellular isoform (PrP^{C}) is an enigmatic protein with unclear function. Prion protein has received considerable attention due to its central role in the development of Transmissible Spongiform Encephalopathies (TSEs) known as "prion diseases", in animals and humans. Understanding the trafficking, the processing and degradation of PrP is of fundamental importance in order to unravel the mechanism of PrP^{Sc} mediated pathogenesis, its spreading and cytotoxicity. The available data regarding PrP trafficking are contradictory. To investigate PrP trafficking and sorting we used polarized MDCK cells (two-dimensional and tree-dimensional cultures) where the intracellular traffic of GPI-anchored proteins (GPI-APs) is well characterized. GPI-APs that are sorted in the Trans Golgi Network follow a direct route from the Golgi apparatus to the apical plasma membrane. The exception to direct apical sorting of native GPI-APs in MDCK cells is represented by the Prion Protein. Of interest, PrP localization in polarized MDCK cells is controversial and its mechanism of trafficking is not clear.

We found that full-length PrP and its cleavage fragments are segregated in different domains of the plasma membrane in polarized cells in both 2D and 3D cultures and that the C1/PrP full-length ratio increases upon MDCK polarization. We revealed that differently from other GPI-APs, PrP undergoes basolateral-to-apical transcytosis in fully polarized MDCK cells and is α-cleaved during its transport to the apical surface.

This study not only reconciles and explains the different findings in the previous literature but also provides a better picture of PrP trafficking and processing, which has been shown to have major implications for its role in prion disease.

Résumé en français

La Protéine Prion (PrP) est une glycoprotéine ubiquitaire attachée au feuillet externe de la membrane plasmique par une ancre glycosylphosphatidylinositole (GPI). PrP est l'agent infectieux responsable de la maladie Creutzfeld-Jacob ou « maladie de la vache folle ». Cette protéine existe sous sa forme cellulaire mais également sous sa forme infectieuse, nommée PrP^{Sc} (Scrapie). Alors que la fonction de PrP^{Sc} est établie au cours de la pathogenèse, la fonction de la protéine cellulaire est beaucoup plus énigmatique notamment chez les mammifères. Il est clairement admis que la forme infectieuse découle d'un changement de conformation de la forme cellulaire. Ainsi afin de mieux appréhender le rôle de la protéine prion dans les cellules saines mais également lors de la pathogenèse il apparaît essentiel d'étudier le trafic de cette protéine. La protéine prion est exprimée partout dans le corps et elle est enrichie dans les cellules neuronales qui sont comme les cellules épithéliales des cellules polarisées.

J'ai au cours de ma thèse étudié le trafic de la protéine prion dans les cellules polarisées MDCK. MDCK est la lignée épithéliale sur laquelle nous avons la plus grande connaissance. Dans mon travail j'ai utilisé des cellules MDCK polarisées classiquement en culture bidimensionnelle (2D) mais également en culture tridimensionnelle (3D) où les cellules forment des kystes, structures hautement polarisées, physiologiquement proches de l'épithélium *in vivo*. Il apparaît que dans les cellules MDCK polarisées sur filtre (en 2D) la localisation de la PrP est controversée.

Nous avons trouvé que, contrairement à la majorité des protéines à ancre GPI, la PrP suit la voie de transcytose. La PrP qui se retrouve à la membrane baso-latérale est transcytosée vers la membrane apicale. De plus la PrP envoyée à la surface apicale est clivée (clivage alpha) générant deux fragments distincts : le fragment C1, pourvu de l'ancre GPI qui reste associé à la surface apicale et le fragment soluble N1 qui est sécrété dans le milieu de culture des cellules MDCK cultivées en 2D ou dans le lumen des cellules MDCK cultivées en 3D.

Mon travail permet de mieux comprendre les études réalisées auparavant mais surtout révèle l'existence d'un mécanisme de transcytose de la protéine prion dans les cellules épithéliales. Cette information est essentielle et nous permet de supposer que ce mécanisme pourrait être également utilisé par les cellules neuronales.